



Dipl.-Ing. (FH) Martin Lemmerer, ALM

# **Integrated process development for Leloir glycosyltransferase catalyzed reactions**

## **DISSERTATION**

zur Erlangung des akademischen Grades

Doktor der technischen Wissenschaften

eingereicht an der

**Technischen Universität Graz**

Betreuer

Prof. Dipl.-Ing. Dr.techn. Bernd Nidetzky

Institut für Bioprozesstechnik

## **EIDESSTATTLICHE ERKLÄRUNG**

**Ich erkläre an Eides statt, dass ich die vorliegende Arbeit selbstständig verfasst, andere als die angegebenen Quellen/Hilfsmittel nicht benutzt, und die den benutzten Quellen wörtlich und inhaltlich entnommenen Stellen als solche kenntlich gemacht habe. Das in TUGRAZonline hochgeladene Textdokument ist mit der vorliegenden Dissertation identisch.**

---

Datum

---

Unterschrift

## Dedication

I dedicate my PhD thesis to my family. I have a special feeling of gratitude to my wife Lauren Clark and my loving parents Hildegard and Franz Lemmerer. Their words of encouragement and push for tenacity ring in my ears.

## Acknowledgments

I wish to thank my thesis director Prof. DI Dr. techn. Bernd Nidetzky who was more than generous with his expertise and precious time. Moreover, Prof. Nidetzky's excitement and willingness to provide feedback made the completion of this research an enjoyable experience.

I also would like to thank DI Dr. techn. Katharina Schmölzer for her support throughout the entire thesis process.

A special thanks to my team members in the SuSy Project, DI Dr. techn. Alexander Gutmann and Alexander Lepak MSc, BSc.

I owe my deepest gratitude to Ing. Margaretha Schiller and Karin Longus for their efforts in the lab.

Finally, I want to thank everybody else involved in this project at the Institute for their help and kindness.

This work has been supported by the Federal Ministry of Science, Research and Economy (BMWFW), the Federal Ministry of Traffic, Innovation and Technology (bmvit), the Styrian Business Promotion Agency SFG, the Standortagentur Tirol, the Government of Lower Austria and Business Agency Vienna through the COMET-Funding Program managed by the Austrian Research Promotion Agency FFG. Financial support from the EU FP7 project SuSy (Sucrose Synthase as Effective Mediator of Glycosylation) is gratefully acknowledged.

## Abstract

Leloir glycosyltransferases are handy catalysts for the glycosylation of organic compounds to improve parameters such as water solubility, bioavailability and pharmaceutical potency of target molecules. In the presented study, the focus was the production of UDP-glucose and Nothofagin in gram scale. To surpass chemical synthesis, enzyme catalyzed reactions require integrated process development including optimization of catalyst expression, substrate conversion and product purification.

For improved soluble catalyst expression in *E.coli* we chose two different approaches; either by utilization of a constitutive promoter or by tunable inhibition of *E. coli* RNA polymerase to impair cell growth but enhance target protein expression, both methods yielding in substantially higher amount soluble enzyme per gram cell dry weight compared to reference *E.coli* BL21(DE3). The produced biocatalysts were used as whole cells or in purified form depending on the application.

Conversion of UDP and sucrose into UDP-glucose catalyzed by sucrose synthase whole cells yielded in  $\sim 100 \text{ g}_{\text{UDP-glucose}}/\text{L}$  reaction, a total turnover number of  $103 \text{ g}_{\text{UDP-glucose}}/\text{g}_{\text{cell dry weight}}$  at a space time yield of  $10 \text{ g/L/h}$ . For product isolation, a universally applicable chromatography free downstream processing procedure using (fractional) ethanol precipitation was developed. In a single batch  $\sim 100 \text{ g}$  UDP-glucose with a purity of greater than 90% and an isolated yield of roughly 73% were produced and commercially exploited.

Through a cascade reaction of sucrose synthase and a C-glycosyltransferase we could demonstrate integrated biocatalytic production of Nothofagin at a scale of 100 g. Therefore, the water insoluble substrate Phloretin was solubilized through complexation with a cyclodextrin derivative and the reaction complemented with a sugar donor UDP/UDP-glucose recycling system. Established performance metrics of 97 % yield and  $\sim 50 \text{ g}_{\text{Nothofagin}}/\text{L}$  at a space-time yield of  $3 \text{ g/L/h}$  were achieved, furthermore, UDP-glucose was regenerated  $\sim 220$  times. A scalable downstream process for efficient recovery of Nothofagin ( $\geq 95 \%$  purity;  $\geq 65 \%$  yield) was developed.

In summary, we could show the potential for process intensification utilizing glycosyltransferases by production of much sought after, difficult-to-synthesize compounds.

## Zusammenfassung

Leloir Glykosyltransferasen sind vielseitige Katalysatoren um organische Stoffe zu glykolysieren. Dadurch können Eigenschaften wie Wasserlöslichkeit, Bioverfügbarkeit und pharmakologische Wirkung verbessert werden. Die durchgeführte Studie wurde zielgerichtet auf die Herstellung von jeweils mehreren Gramm UDP-Glukose und Nothofagin ausgelegt. Um die chemische Synthese dieser Stoffe zu übertreffen war es notwendig den vollständigen Prozess zu betrachten und dabei die Enzymexpression, die biokatalytische Reaktion und die Aufreinigung des Endprodukts zu optimieren.

Um eine erhöhte Enzymexpression in *E.coli* zu erzielen haben wir zwei verschiedene Ansätze verwählt. Entweder wurde ein konstitutiver Promoter verwendet oder ein induzierbarer RNA Polymerase Inhibitor, der das Zellwachstum nicht aber die Zielproteinexpression hemmt, verwendet. Beide Verfahren konnten eine erhöhte Expression im Vergleich zum Referenz *E.coli* Stamm BL21(DE3) von löslichem Enzym erzielen. Die dabei hergestellten Biokatalysatoren wurden je nach Verwendung für die Ganzzellsynthese oder in gereinigter Form eingesetzt.

Durch die Umsetzung von UDP und Sucrose zu UDP-Glukose mittels Sucrose Synthase in Ganzzellen konnten  $\sim 100 \text{ g}_{\text{UDP-Glukose}}/\text{L}$  Reaktion hergestellt werden. Weiters wurde eine total turnover number von  $103 \text{ g}_{\text{UDP-Glukose}}/\text{g}_{\text{Zelltrockenmasse}}$  bei einer space-time-yield von  $10 \text{ g/L/h}$  erzielt. Um das Produkt zu isolieren wurde eine universell anwendbare Chromatographie-freie Aufreinigungsmethode entwickelt. Pro Charge konnten somit  $\sim 100 \text{ g}$  UDP-Glukose mit einer Reinheit größer 90 % und einer Ausbeute von 73% hergestellt und kommerziell verwertet werden.

Mittels einer enzymatischen Kaskadenreaktion von Sucrose Synthase und einer C-Glykosyltransferase konnten wir die Herstellung von 100 g Nothofagin realisieren. Das wasserunlösliche Phloretin wurde durch Komplexierung mit einem Cyclodextrinderivat in Lösung gebracht. Weiters enthielt die Reaktion ein UDP/UDP-Glukose Recyclingsystem. So konnten wir  $\sim 50 \text{ g}_{\text{Nothofagin}}/\text{L}$  mit 97% Umsetzung und einer space-time-yield von  $3 \text{ g/L/h}$  erreichen; zusätzlich konnte UDP-Glukose  $\sim 220$ -mal regeneriert werden. Im Anschluss wurde eine skalierbare Aufreinigung von Nothofagin ( $\geq 95$  % Reinheit;  $\geq 65$  % Ausbeute) entwickelt. Zusammenfassend konnten wir Prozessverbesserungen durch die Anwendung von Glykosyltransferasen zeigen und dadurch die Herstellung von schwer synthetisierbaren Feinchemikalien ermöglichen.

## Table of contents

### **Downstream Processing of Nucleoside-Diphospho-Sugars from Sucrose Synthase Reaction Mixtures at Decreased Solvent Consumption**

Martin Lemmerer, Katharina Schmölzer, Alexander Gutmann, Bernd Nidetzky

Advanced Synthesis and Catalysis (2016), 358, 3113. 8

Supporting Information 20

### **Integrated process design for biocatalytic synthesis by a Leloir Glycosyltransferase: UDP-glucose production with sucrose synthase**

Katharina Schmölzer, Martin Lemmerer, Alexander Gutmann, Bernd Nidetzky

Biotechnology and Bioengineering (2017), 114, 924–928. 40

Supporting Information 46

### **Biocatalytic Cascade of Polyphosphate Kinase and Sucrose Synthase for Synthesis of Nucleotide-Activated Derivatives of Glucose**

Sandra Kulmer, Alexander Gutmann, Martin Lemmerer, Bernd Nidetzky

Advanced Synthesis and Catalysis (2017), 359, 292. 60

Supporting Information 71

### **Glycosyltransferase Cascades Made Fit for Chemical Production: Integrated Biocatalytic Process for the Natural Polyphenol C-Glucoside Nothofagin**

Katharina Schmölzer, Martin Lemmerer, Bernd Nidetzky

Biotechnology and Bioengineering (2018), 115, 545–556. 83

Supporting Information 96

### **Decoupling of recombinant protein production from *E. coli* growth enhances functional expression of plant Leloir glycosyltransferases**

Martin Lemmerer, Jürgen Mairhofer, Alexander Lepak, Karin Longus, Rainer Hahn, Bernd Nidetzky

Manuscript in preparation 114

Supporting Information 143

**Scientific record 158**

Downstream Processing of Nucleoside-Diphospho-  
Sugars from Sucrose Synthase Reaction Mixtures  
at Decreased Solvent Consumption



# Downstream Processing of Nucleoside-Diphospho-Sugars from Sucrose Synthase Reaction Mixtures at Decreased Solvent Consumption

Martin Lemmerer,<sup>+a</sup> Katharina Schmölder,<sup>+a</sup> Alexander Gutmann,<sup>b</sup>  
and Bernd Nidetzky<sup>a,b,\*</sup>

<sup>a</sup> Austrian Centre of Industrial Biotechnology, Petersgasse 14, 8010 Graz, Austria

<sup>b</sup> Institute of Biotechnology and Biochemical Engineering, Graz University of Technology, NAWI Graz, Petersgasse 12/I, 8010 Graz, Austria

Fax: (+43)-316-873-8434; phone: (+43)-316-873-8400; e-mail: bernd.nidetzky@tugraz.at

<sup>+</sup> These authors contributed equally to this work.

Received: May 20, 2016; Revised: July 24, 2016; Published online: September 12, 2016



Supporting information for this article can be found under: <http://dx.doi.org/10.1002/adsc.201600540>.

**Abstract:** Nucleoside-diphospho-sugars (NDP-sugars) are highly demanded as specialty chemicals and as substrates for enzymatic glycosylations. Biocatalysis is efficient for their synthesis; however, downstream processing (DSP) is a bottleneck of the overall production. We describe two scalable DSP routes for recovery of NDP-glucose (NDP-glc) from sucrose synthase (SuSy) reaction mixtures. In both routes product precipitation with ethanol replaced size exclusion chromatography (SEC) which, due to high solvent consumption, constitutes the main limiting step of current DSP protocols. We also show that selective phosphomonoester hydrolysis by alkaline phosphatase, characterized in that it did not degrade the phosphodiester linkage in NDP-glc, was a useful alternative to anion-exchange chromatography

(AEC) for capture and initial purification of the product. Based on comprehensive route optimization, we show uridine 5'-diphosphate glucose (UDP-glc) recovery at the  $\geq 0.5$  g scale in a yield of about 80% and in a purity of 86% (phosphatase route) and 95% (AEC route). Solvent savings of up to 38-fold compared to the conventional AEC-SEC route were achieved. There is a clear demand for both new routes, as requirements on DSP regarding purity and costs vary with the field of application. Both DSP routes seem to be applicable to other NDP-sugars and different methods of their synthesis.

**Keywords:** downstream processing; glycobiochemistry; glycosylation; green chemistry; nucleotide sugars

## Introduction

Nucleoside-diphospho-sugars (NDP-sugars) are used as specialty carbohydrates and biochemical reagents.<sup>[1]</sup> As the donor substrates of glycosyltransferases (GTs), they are interesting starting materials for glycoside synthesis.<sup>[2]</sup> GTs catalyze the site- and stereo-selective attachment of sugars to a broad variety of acceptor molecules.<sup>[2c,d,3]</sup> Products with a well-defined glycostructure are in demand for pharmaceutical, cosmetic and food-related applications.<sup>[3a,b,4]</sup> However, high costs and limited availability of the respective NDP-sugar restrict the scale of GT-catalyzed syntheses. Convenient methods of NDP-sugar production at enhanced efficiency are needed. It is often observed

that the downstream processing (DSP) constitutes a critical bottleneck for the overall biocatalytic process development; for the general case see ref.<sup>[5]</sup>; for carbohydrate DSP see ref.<sup>[6]</sup>. Isolation of polar products from aqueous reaction mixtures is a challenging task and is often overlooked.<sup>[5a,7]</sup> In the case of NDP-sugars, the DSP presents a severe problem, the overcoming of which is essential for their cost-effective production at an industrial scale.<sup>[8]</sup>

In contrast to the usually high performance of the upstream part of NDP-sugar production,<sup>[1b,9]</sup> the DSP development is still lagging behind. Scheme 1 shows biocatalytic routes applied to NDP-sugar synthesis at the multigram scale.<sup>[9a,d,10]</sup> In each route, the DSP involves the task of removing sugars or sugar phos-

phates, nucleoside phosphates (nucleotides) as well as inorganic phosphate and other ions from the target product. Current DSP protocols are limited in that one or more chromatographic steps are required.<sup>[1b,d,9c,d,10d,11]</sup> The widespread use of size exclusion chromatography (SEC) for product purification and desalting is problematic in particular. Large-scale application of SEC is severely hampered by limited throughput along with the highly diluted product stream.<sup>[12]</sup> Additionally, limited stability of NDP-sugars at high salt concentration complicates the use of ion exchange chromatography for product capture and purification.<sup>[13]</sup> Therefore, a completely chromatography-free DSP is strongly desired. Note, for DSP without affinity purification the methods applicable are mainly limited by the properties of the target molecule (e.g., hydrophobicity, net charge, size). An efficient assembly of the DSP methods used is thus required for a good process performance.

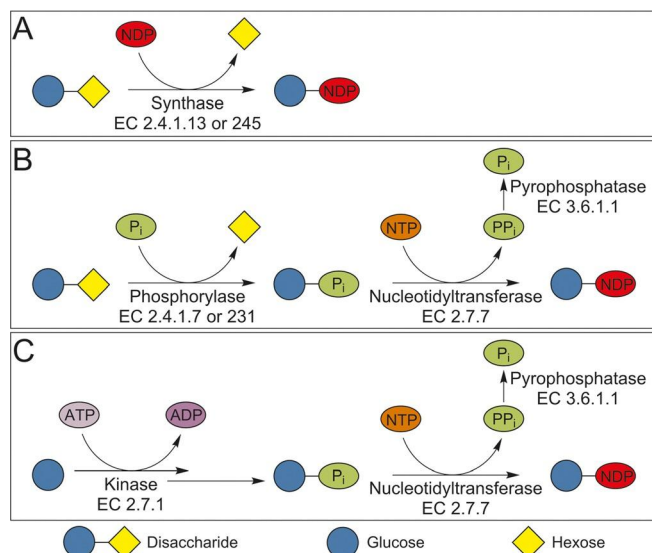
Here we describe the innovative DSP of uridine 5'-diphosphate glucose (UDP-glc) from a sucrose synthase (SuSy; EC 2.4.1.13) reaction mixture *via* two scalable DSP routes B and C (Scheme 2). Both routes feature replacement of SEC by product precipitation with the cosolvent ethanol (EtOH) (B and C). Route C does not use chromatography at all. The DSPs are therefore characterized by an up to 38-fold reduced solvent consumption. This is a substantial improvement in green process metrics. Purification of adenosine 5'-diphosphate glucose (ADP-glc) and UDP-galactose (UDP-gal) *via* chromatography-free DSP (C) is also demonstrated.

## Results and Discussion

### Composition of the Product Mixture and DSP Route Selection

As shown in Scheme 1A, the synthesis of UDP-glc by SuSy involved sucrose and UDP as substrates and fructose as the coproduct of the reaction. For DSP development, a mixture from conversion of 1.5 M sucrose and 0.3 M UDP at pH 5 was used (Scheme 2B and C). The ~5-fold molar excess of sucrose was applied to maximize the UDP utilization in the equilibrium-controlled reaction of SuSy. Task of the DSP was the removal of sugars (255 mM fructose; 1.25 M sucrose) and UDP (43 mM) from the UDP-glc (255 mM). A small amount of uridine 5'-monophosphate (UMP; 2.4 mM) was also present. The target purity was set to  $\geq 85\%$ , in accordance with the UDP-glc currently on the market.

Irrespective of the DSP route used (Scheme 2), the enzyme had to be removed from the reaction mixture first, for which ultrafiltration (10 kDa cut-off) was used. The reaction mixture was highly viscous. A 3-

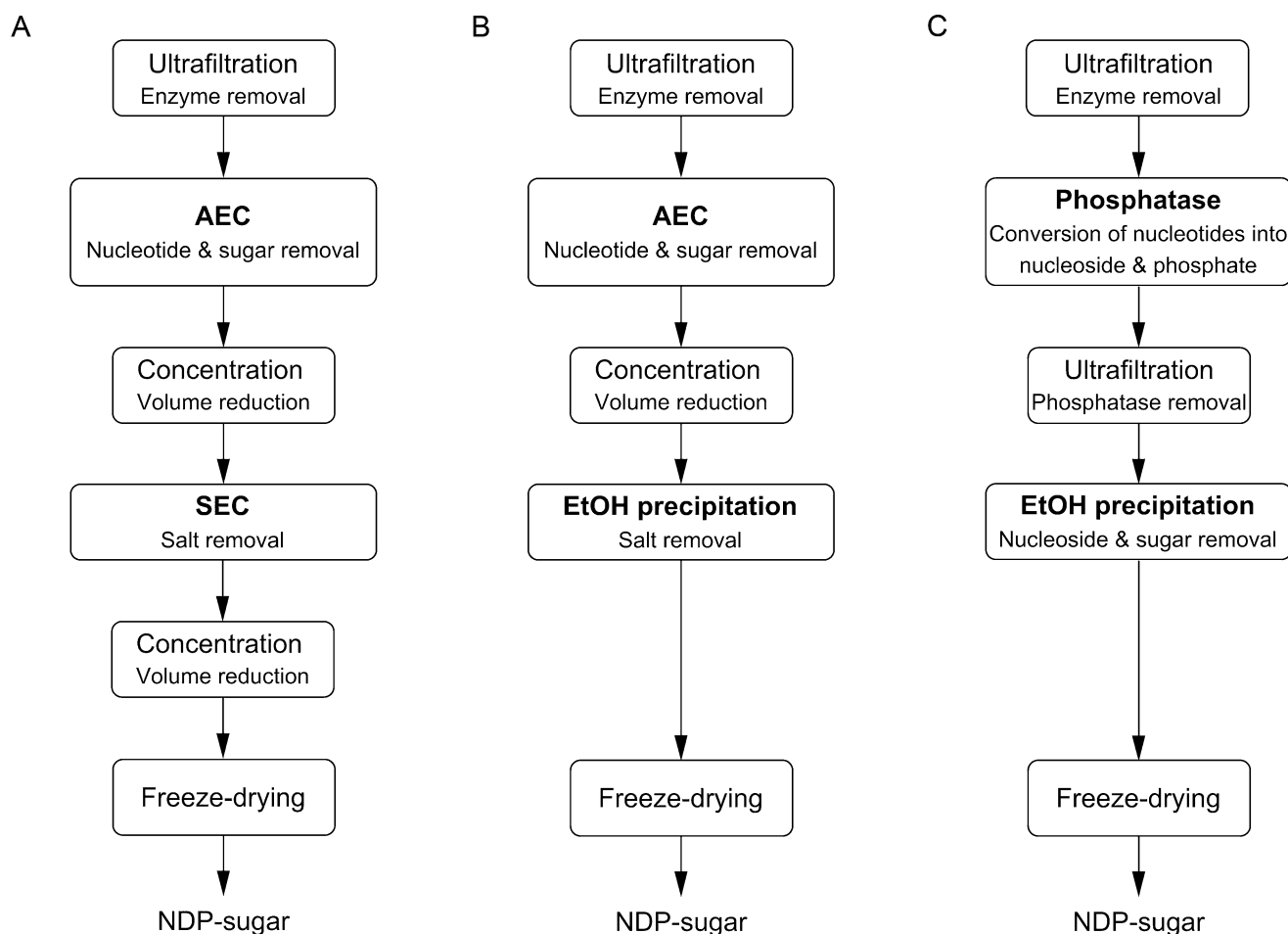


**Scheme 1.** Biocatalytic routes applied to NDP-sugar synthesis, exemplarily shown for NDP-glucose: (A) synthase, (B) phosphorylase and (C) kinase routes. Synthases: sucrose or trehalose synthase; phosphorylases: sucrose or cellobiose phosphorylase; nucleotidyltransferase: UTP-glucose-1-phosphate uridylyltransferase; kinases: depending on the sugar, synthesis of sugar 1-phosphate by direct phosphorylation of C-1 (e.g., galactokinase, *N*-acetylhexosamine 1-kinase) or *via* C-6 (hexokinase) and phosphomutase (EC 5.4.2).

fold dilution presented a compromise between viscosity reduction for improved filterability and final sample volume. The enzyme-free filtrate was used in all experiments. Scheme 2 depicts the DSP routes discussed. The conventional anion-exchange chromatography (AEC)-SEC route served as reference for the DSP development (A). The SEC or both chromatography steps of route A were replaced by alternative unit operations (B and C). Product precipitation by a cosolvent appeared promising to substitute the SEC for desalting. This necessitated a very high separation efficiency in the first DSP step. Thus, an effective AEC was needed (B).

### Improvement of NDP-Sugar Isolation by AEC

Besides applicable flow rate and cost, the main criteria for DSP application of an anion-exchange (AEX) resin are binding capacity, separation efficiency, and solvent consumption. Table S1 in the Supporting Information compares different AEX resins accordingly. Using uridine 5'-triphosphate (UTP) as reference substance, the binding capacities varied in a broad range across the series of resins examined. Dowex 1 $\times$ 8 (Cl<sup>-</sup>-form, 200–400 mesh) is the most effective material. Buffer selection is the key to successful DSP, because it affects not only the AEC but also the following DSP step. Separation efficiency and solvent con-



**Scheme 2.** DSP routes for purification of NDP-sugars from SuSy reaction mixtures: (A) anion-exchange chromatography–size exclusion chromatography (AEC-SEC); (B) anion-exchange chromatography–ethanol precipitation (AEC-EtOH); and (C) phosphatase–ethanol precipitation (CIAP-EtOH) routes.

sumption depend on how effectively the anions of the mobile phase displace the bound substance(s) from the stationary AEX phase.<sup>[14]</sup> Using the Dowex 1×8 resin, different buffers (phosphate, formate, acetate; sodium salts) were screened for their efficiency in separating the compounds of the enzymatic reaction mixture. The tested pH range was 3.5–6.0. Sucrose and fructose are not ionized in the pH range used and were removed in the flow-through.<sup>[15]</sup> AEC-based separation of UDP-glc from UDP and UMP is controlled, among other factors, by the ionic charge (−1 or −2) of the terminal phosphate group in UMP and UDP. The second  $pK_a$  of this group was previously determined to be around 6.0.<sup>[16]</sup> In UDP-glc this phosphate group is glucosylated and has −1 charge, independent of the pH. Under the applied conditions, the best results were obtained with sodium acetate buffer, pH 4.3 (data not shown). Baseline separation of all compounds of the reaction mixture was achieved. Additional benefit of acetate was its high compatibility with a subsequent desalting step by precipitation with an organic cosolvent.

Elution characteristics of the different AEX resins were determined. A linear gradient in sodium acetate (pH 4.3) was applied for elution. Clean separation of UDP-glc from UDP and UMP was required and the amount of solvent needed to achieve this was monitored. Results are summarized in Table S1 of the Supporting Information. They demonstrate that the Toyopearl SuperQ-650M was superior to the other resins examined. Compared to Dowex 1×8, it showed decreased time (~10-fold) and solvent use (~2-fold) for elution of UTP (1 mL columns). Furthermore, a 5-fold increased flow rate was applicable to the separation of UMP, UDP-glc and UDP at a maximum pressure drop of 3 bar. Comparison of the SuperQ-650M to the Dowex 1×8 resin at a preparative scale (~40 mL bed volume) enabled complete separation of about 1 g UDP-glc in a single AEC run. Figure 1 compares the elution profiles in sodium acetate in each case. UDP-glc eluted faster (3.8 h vs. 50 h) at a lower acetate concentration (140 mM vs. 363 mM) and at

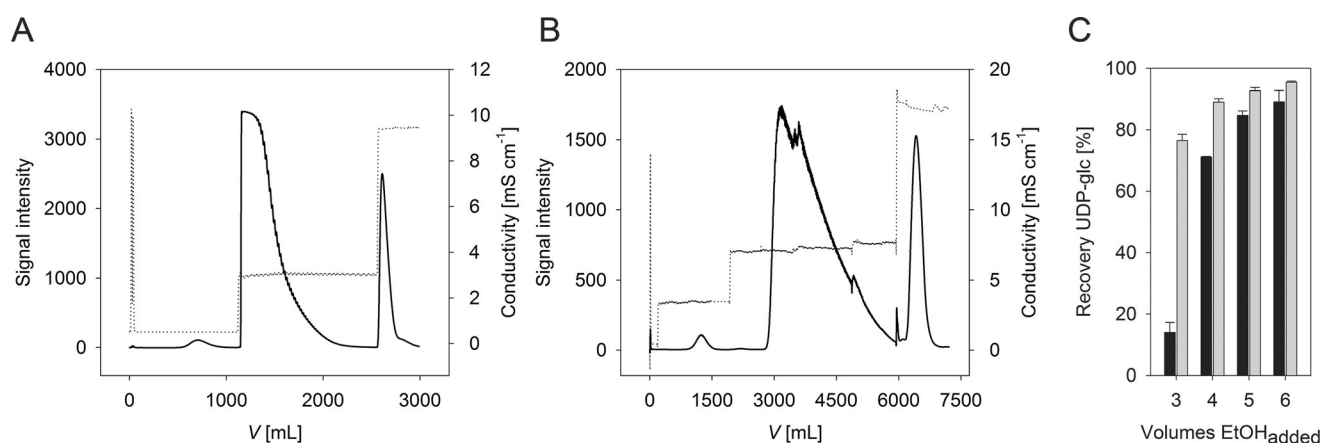


**Figure 1.** SEC-free DSP of UDP-glc (Scheme 2B). Preparative AEC runs on (A) Toyopearl SuperQ-650M and (B) Dowex 1 × 8 (200–400 mesh) 40 mL columns. ~1 g of UDP-glc was loaded. Step gradients in sodium acetate (pH 4.3) were used for elution at (A) 5 cm min<sup>-1</sup> or (B) 1 cm min<sup>-1</sup>. Solid line, UV signal (254 nm); dotted line, conductivity (mS cm<sup>-1</sup>). First peak, UMP; second peak, UDP-glc; last peak, UDP. (C) EtOH precipitation as alternative to SEC. The UDP-glc containing eluate from the Toyopearl SuperQ-650M column was concentrated to ~2M of sodium acetate. Varying volumes of EtOH were added and samples were incubated overnight at different temperatures. Black bars, 4 °C; grey bars, -20 °C.

reduced solvent use (2.3 L vs. 6 L) on SuperQ-650M than on Dowex 1 × 8.

AEC using the SuperQ-650M significantly advances purification of UDP-glc at different levels. Its high separation efficiency at reduced solvent use causes improved step economy compared to other AEX resins. The frequently applied Dowex resins (1 × 2, 1 × 8) suffer from a high solvent consumption.<sup>[11,13b,17]</sup> Q-Sepharose FF has a very low binding capacity (< 5 mg<sub>UTP</sub> mL<sub>resin</sub><sup>-1</sup>).<sup>[9d,18]</sup> The weak AEX DEAE-cellulose was also applied for DSP.<sup>[1d,10d]</sup> However, we observed poor separation efficiency and a high solvent consumption or a low binding capacity for weak AEXs (see the Supporting Information, Table S1). This is the first comprehensive study on AEC for DSP of UDP-glc.

### Replacing the SEC by Precipitation with Ethanol Saves Solvent

In a first step, SEC was used to separate UDP-glc from sodium acetate after the AEC (Scheme 2A). The conditions used for the SEC (stationary phase: Sephadex G-10, eluent: deionized water), represent state of the art DSP with respect to the literature.<sup>[9d,19]</sup> Despite the combination of efficient AEC and SEC unit operations, only ~25 mg UDP-glc could be desalted in one SEC run (see the Supporting Information, Figure S1). Furthermore, ~150 mL of deionized water were required. Table 1 summarizes yields, purities and solvent consumption for each step of UDP-glc DSP *via* the AEC-SEC route (Scheme 2A). Desalting by SEC yields UDP-glc with 99% purity. However, it requires 6 L of deionized water per gram of

purified product, which accounts for two-thirds of the total required solvent. Solvent reduction is a point of reference for DSP improvement.

Another option for desalting is the use of volatile buffer salts (e.g., ammonium formate) and their combined removal with water by lyophilization.<sup>[13b,20]</sup>

**Table 1.** Purification of UDP-glc *via* AEC-SEC route (Scheme 2A).

Step	m <sub>UDP-glc</sub> [mg]	Yield [%]	Purity <sup>[e]</sup> [%]	V <sub>Solvent</sub> <sup>[j]</sup> [L g <sub>UDP-glc</sub> <sup>-1</sup> ]
Start <sup>[a]</sup>	37	100	20 <sup>[f]</sup>	0.015 <sup>[k]</sup>
Filtration	36	97	20 <sup>[f]</sup>	0
AEC <sup>[b]</sup>	33	90	5.6 <sup>[g]</sup>	3 <sup>[l]</sup>
Conc. <sup>[c]</sup>	31	83	16 <sup>[h]</sup>	0
SEC <sup>[d]</sup>	25	68	99 <sup>[i]</sup>	6 <sup>[k]</sup>

<sup>[a]</sup> Sample volume was 0.8 mL.

<sup>[b]</sup> Eluate from SuperQ-650M column, containing 140 mM sodium acetate. Final volume was 37 mL.

<sup>[c]</sup> Pooled UDP-glc containing fractions were 25-fold concentrated under reduced pressure. Final sodium acetate concentration was only ~2M, due to its volatility.

<sup>[d]</sup> Eluate from Sephadex G-10 column (~150 mL; H/D ratio = 62.5). UDP-glc eluted in ~40 mL (see the Supporting Information, Figure S1).

<sup>[e]</sup> Percent by weight.

<sup>[f]</sup> Impurities: 0.2% UMP, 2.5% UDP, 68% sucrose, 6.6% fructose, 2.7% acetate.

<sup>[g]</sup> Impurity was 94% acetate.

<sup>[h]</sup> Impurity was 83% acetate.

<sup>[i]</sup> Impurity was 1% acetate.

<sup>[j]</sup> Solvent consumption calculated for 1 g UDP-glc.

<sup>[k]</sup> Solvent was deionized water.

<sup>[l]</sup> Solvent was sodium acetate buffer (pH 4.3).

However, NDP-sugar decomposition was reported under such conditions.<sup>[13,21]</sup> Product precipitation represents an interesting alternative DSP strategy.<sup>[8,22]</sup> Therefore, we adapted the well-established method of DNA precipitation by EtOH for UDP-glc.<sup>[23]</sup> The basic principle is to shield the phosphate charges of UDP-glc by monovalent cations. EtOH allows the interaction between the phosphate groups and the cations, due to its 3-fold lower dielectric constant than water.<sup>[24]</sup> This causes UDP-glc to precipitate from solution. This method depends on selective product precipitation. The main parameters affecting the recovery of UDP-glc are solvent, solvent volume, salt, incubation temperature and time. Sodium acetate is commonly used for DNA precipitation.<sup>[23]</sup> As NDP-sugars on the market are mostly sodium salts, sodium acetate met our requirements for DSP. EtOH was the most suitable solvent for UDP-glc precipitation for the following reasons: (i) UDP-glc solubility at 20 °C is <math>40 \text{ mg L}^{-1}</math>; (ii) sodium acetate solubility at 20 °C is  $\sim 21 \text{ g L}^{-1}$ ;<sup>[25]</sup> (iii) it is a green solvent.<sup>[26]</sup> Consequently, UDP-glc precipitation had to be optimized with respect to EtOH volume and incubation temperature. The precipitation conditions were only briefly reported.<sup>[8,22]</sup> EtOH precipitation of NDP-sugars has not been integrated in DSP so far.

Before EtOH precipitation, the UDP-glc containing AEC eluate was concentrated to minimize the product loss and to limit the solvent volume needed (Scheme 2B). The eluate was  $\sim 25$ -fold concentrated, in order not to exceed the solubility limit of sodium acetate ( $\sim 4 \text{ M}$  in water at 20 °C). Varying volumes of EtOH were added to this sample and incubated overnight at different temperatures (Figure 1C). The yield depended on the volume of EtOH added and the incubation temperature. At  $-20 \text{ }^\circ\text{C}$  5 volumes of EtOH were sufficient for almost quantitative precipitation of UDP-glc ( $\geq 95\%$ ). Desalting was effective,  $\leq 4\%$  of acetate were detected in the UDP-glc precipitate. No product degradation was observed.

Based on Scheme 2B the AEC-EtOH route was applied to UDP-glc purification on a 0.5-gram scale and results are summarized in Table 2. Progressive reduction of impurities and UDP-glc stability were monitored by HPLC (see the Supporting Information, Figures S2 and S3). UDP-glc was obtained after freeze-drying as a white powder in 81% yield and 95% purity. Product identity was unequivocally confirmed by  $^1\text{H}$  and  $^{13}\text{C}$  NMR spectroscopy (see the Supporting Information, Figures S4 and S5). NMR spectra were in accordance with published data.<sup>[27]</sup> Note, due to formation of a gel during precipitation, the precipitate was resuspended in water before freeze-drying. This gel formation was reported before for the potassium salt of glucose 1-phosphate.<sup>[28]</sup> Freeze-drying is commonly applied for removal of water from aqueous NDP-sugar solutions.<sup>[1d,9d,10d,11]</sup> Desalting by precipita-

**Table 2.** Purification of UDP-glc via AEC-EtOH route (Scheme 2B).

Step	$m_{\text{UDP-glc}}$ [mg]	Yield [%]	Purity [%] <sup>[e]</sup>	$V_{\text{Solvent}}^{\text{[j]}}$ [L $\text{g}_{\text{UDP-glc}}^{-1}$ ]
Start <sup>[a]</sup>	650	100	20 <sup>[f]</sup>	0.015 <sup>[k]</sup>
Filtration	633	97	20 <sup>[f]</sup>	0
AEC <sup>[b]</sup>	588	90	6 <sup>[g]</sup>	3 <sup>[l]</sup>
Conc. <sup>[c]</sup>	538	83	17 <sup>[h]</sup>	0
Precip.; freeze-dry <sup>[d]</sup>	526	81	95 <sup>[i]</sup>	0.2 <sup>[m]</sup> , 0.02 <sup>[k]</sup>

<sup>[a]</sup> Sample volume was 13 mL.

<sup>[b]</sup> Eluate from SuperQ-650M column, containing 140 mM sodium acetate. Final volume was 650 mL.

<sup>[c]</sup> Pooled UDP-glc containing fractions were 25-fold concentrated under reduced pressure. Final volume was 25 mL. Final sodium acetate concentration was  $\sim 2 \text{ M}$ .

<sup>[d]</sup> Product precipitation by 5 volumes EtOH and overnight incubation at  $-20 \text{ }^\circ\text{C}$ . Precipitate was air-dried at room temperature and dissolved in deionized water to  $\sim 50 \text{ mg mL}^{-1}$ .  $\sim 1\%$  product loss during freeze-drying.

<sup>[e]</sup> Percent by weight.

<sup>[f]</sup> Impurities: 0.2% UMP, 2.5% UDP, 68% sucrose, 6.6% fructose, 2.7% acetate.

<sup>[g]</sup> Impurity was 94% acetate.

<sup>[h]</sup> Impurity was 83% acetate.

<sup>[i]</sup> Impurities were 4% acetate and 1% EtOH.

<sup>[j]</sup> Solvent consumption calculated for 1 g UDP-glc.

<sup>[k]</sup> Solvent was deionized water.

<sup>[l]</sup> Solvent was sodium acetate buffer (pH 4.3).

<sup>[m]</sup> Solvent was EtOH.

tion necessitates only 200 mL of EtOH per gram of purified UDP-glc (Scheme 2B). This is a 30-fold saving of solvent compared to SEC (Table 1; Scheme 2A). Moreover, EtOH has a 3-fold lower heat of vaporization than water,<sup>[29]</sup> and could thus be recycled by distillation to save more solvent.

Despite a few scattered reports of NDP-sugar precipitation,<sup>[8,22]</sup> a systematic development for the DSP has been lacking so far. Desalting of thymidine 5'-diphosphate glucose by EtOH/acetone precipitation resulted only in 42.4% yield.<sup>[22]</sup> Precipitation of CMP-N-acetylneuraminic acid using divalent cations required an extra cation exchange chromatography step to obtain the commercial sodium salt.<sup>[8]</sup> EtOH precipitation of glucose 1-phosphate was successfully used for acetate removal, yielding pure product with quantitative recovery.<sup>[28]</sup> We performed for the first time a systematic work-up of UDP-glc precipitation as a functional DSP operation.

### Chromatography-Free DSP of UDP-glc

Based on the good performance of UDP-glc precipitation by EtOH, its applicability in a completely chromatography-free DSP was investigated (Scheme 2C).

Requirement was to prevent co-precipitation of the nucleotides UDP and UMP present in the sample. Selective hydrolysis of the phosphomonoesters into uridine and inorganic phosphate by an alkaline phosphatase appeared as a potent strategy to replace the AEC. In the subsequent precipitation step UDP-glc needs to be separated from sugars (sucrose, fructose), nucleosides (uridine) and phosphate. This is an advancement compared to desalting and other purification strategies described in the literature.<sup>[8,22]</sup> It is a new application in this context.

Selective hydrolysis of nucleotides in the presence of NDP-sugars was demonstrated in several studies.<sup>[1d,9d,30]</sup> Calf intestinal alkaline phosphatase (CIAP) was commonly used. The starting material for CIAP treatment contained 3.3 mM Mg<sup>2+</sup>. The divalent cations were needed to maximize the SuSy activity in the UDP-glc synthesis.<sup>[31]</sup> Note, divalent cations ( $\geq 3$  mM) negatively affect the stability of NDP-glc at pH values  $\geq 7.5$ .<sup>[9d,32]</sup> Thus, the optimum pH for CIAP activity (pH 8) and NDP-sugar stability was not the same and DSP by CIAP had to be optimized accordingly. Figure 2A (see also the Supporting Information, Figure S6) depicts the time course of the CIAP hydrolysis (10 U mL<sup>-1</sup>) at pH 7.0, which presented the best compromise between enzyme activity and UDP-glc stability. Incubation for 24 h resulted in complete degradation of UDP and UMP, whereas only 3% of UDP-glc were hydrolyzed.

The task of the EtOH precipitation was the removal of sugars (85 mM fructose; 417 mM sucrose), uridine (15 mM) and inorganic phosphate (30 mM) from the UDP-glc (85 mM). CIAP had to be removed from the reaction mixture first, for which ultrafiltration (10 kDa cut-off) was used. For precipitation, 200 mM of sodium acetate were added to the resulting enzyme-free filtrate. The EtOH volume was optimized with respect to sugar removal efficiency (sucrose, fructose) and UDP-glc loss. 5 volumes of EtOH were a reasonable compromise. Figure 2B shows that a second precipitation step was needed. UDP-glc purity could be enhanced to ~85% but the recovery decreased (4–11% loss per step). UDP-glc purification on a 0.5-g scale *via* the CIAP-EtOH route (Scheme 2C) is summarized in Table 3 (see the Supporting Information, Figures S7–S11). UDP-glc was obtained in ~80% yield and 86% purity. The residual impurities were 9% sucrose and 5% phosphate. If a higher product purity is required, electro dialysis could be used for selective phosphate removal.<sup>[33]</sup> As no solvent was required for DSP by CIAP, overall savings of ~38- and ~14-fold compared to the AEC-SEC (Table 1; Scheme 2A) and AEC-EtOH routes (Table 2; Scheme 2B) were achieved.

We have shown for the first time a completely chromatography-free DSP of UDP-glc from a complex reaction mixture (Scheme 2C). Product precipitation

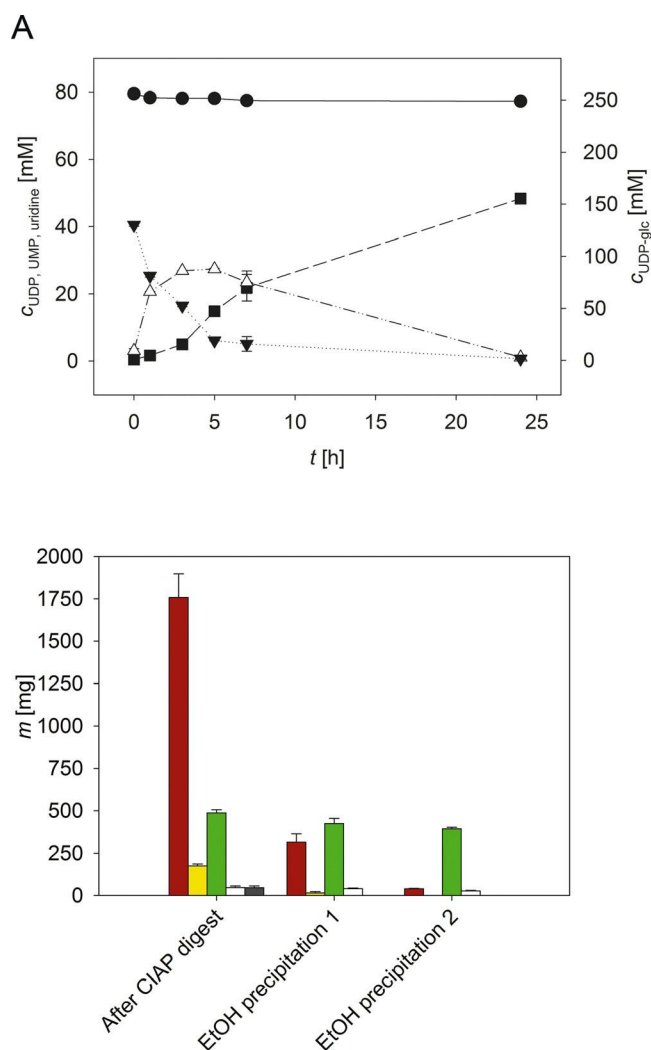


**Figure 2.** Chromatography-free DSP of UDP-glc (Scheme 2C). (A) Time course showing selective hydrolysis of nucleotides by CIAP (10 U mL<sup>-1</sup>) at pH 7.0 and 30°C. UDP-glc, filled circle; uridine, filled square; UMP, open triangle; UDP, closed reverse triangle. (B) Precipitation of UDP-glc by 5 volumes EtOH. Incubation was overnight at -20°C. Red bars, sucrose; yellow bars, fructose; green bars, UDP-glc; white bars, inorganic phosphate; dark grey bars, uridine. ~1% EtOH was detected in air-dried precipitates.

was used for purification instead of desalting.<sup>[22,28]</sup> Hitherto, during the DSP of NDP-sugars alkaline phosphatase treatment was mainly used in combination with AEC or SEC to simplify the chromatographic steps.<sup>[1d,9d,30b,c,34]</sup> Our chromatography-free DSP offers several advantages for scale-up, including that no investment in specialized equipment is required, the avoidance of energy intensive concentration of aqueous AEC and SEC eluates (Scheme 2A and B)<sup>[35]</sup> and a drastically reduced solvent consumption (Table 1, Table 2, and Table 3). The DSP still included freeze-drying, which is energy consuming.

**Table 3.** Purification of UDP-glc *via* CIAP-EtOH route (Scheme 2C).

Step	m <sub>UDP-glc</sub> [mg]	Yield [%]	Purity [%] <sup>[d]</sup>	V <sub>Solvent</sub> <sup>[i]</sup> [L g <sub>UDP-glc</sub> <sup>-1</sup> ]
Start <sup>[a]</sup>	500	100	20 <sup>[e]</sup>	0.015 <sup>[i]</sup>
CIAP <sup>[b]</sup>	474	95	19 <sup>[f]</sup>	0
Filtration	452	90	19 <sup>[f]</sup>	0
Precip. 1 <sup>[c]</sup>	402	80	24 <sup>[g]</sup>	0.1 <sup>[k]</sup> , 0.002 <sup>[l]</sup>
Precip. 2; freeze-dry <sup>[c]</sup>	380	76	86 <sup>[h]</sup>	0.1 <sup>[k]</sup> , 0.02 <sup>[l]</sup>

<sup>[a]</sup> Sample volume was 10 mL.

<sup>[b]</sup> CIAP reaction (10 U mL<sup>-1</sup>) was carried out overnight at 30 °C, pH 7.0.

<sup>[c]</sup> Product precipitation by 5 volumes EtOH and overnight incubation at -20 °C. Precipitate 2 was air-dried at room temperature and dissolved in deionized water to ~40 mg mL<sup>-1</sup>. ~1% product loss during freeze-drying.

<sup>[d]</sup> Percent by weight.

<sup>[e]</sup> Impurities: 0.2% UMP, 2.5% UDP, 68% sucrose, 6.6% fructose, 2.7% acetate.

<sup>[f]</sup> Impurities: 1.7% uridine, 1.7% inorganic phosphate, 68% sucrose, 6.9% fructose, 2.7% acetate.

<sup>[g]</sup> Impurities: 2.5% inorganic phosphate, 17% sucrose, 1.3% fructose, 0.2% acetate, 55% EtOH.

<sup>[h]</sup> Impurities: 5% inorganic phosphate, 9% sucrose.

<sup>[i]</sup> Solvent consumption calculated for 1 g UDP-glc.

<sup>[j]</sup> Solvent was deionized water.

<sup>[k]</sup> Solvent was EtOH.

<sup>[l]</sup> Solvent was sodium acetate buffer (2M, pH 7.0).

However, there is no suitable alternative allowing the removal of impurities (salt, solvent) and ensuring product stability at the same time.

### Chromatography-Free DSP of ADP-glc and UDP-gal

We tested the chromatography-free DSP for purification of other NDP-sugars (Scheme 2C). The known NDP-sugars differ in the sugar or nucleoside moiety. It was not clear how these structural variations affect the DSP. Therefore, UDP-gal and ADP-glc were chosen for DSP.

For DSP of UDP-gal a test solution, containing UDP-gal (16 mM), UDP (7 mM), uridine (1 mM) and MgCl<sub>2</sub> (10 mM), was prepared. For ADP-glc DSP, a mixture from SuSy conversion of 0.5 M sucrose and 50 mM ADP at pH 5 was used. UDP-gal stability was not affected during CIAP treatment (Scheme 2C; see the Supporting Information, Figure S12; 3% product loss). EtOH precipitation caused only ~4% product loss under conditions identical to UDP-glc precipitation. SEC- and chromatography-free DSP of ADP-glc is depicted in Figures S13–S15 in the Supporting Information (see also Scheme 2B and C). 10 mg ADP-glc were isolated using a 1 mL Toyopearl SuperQ column and an optimized step gradient. Alternative

CIAP treatment showed selective hydrolysis of nucleotides. EtOH precipitation under standard conditions caused only ~10% product loss, despite the higher hydrophobicity of the purine-based ADP-glc compared to the pyrimidine-based UDP-sugars.<sup>[36]</sup> Overall, both DSP routes seem to be applicable to other NDP-sugars than UDP-glc after minor adaption of the process conditions.

### Conclusions

The DSP methods used, such as precipitation<sup>[8,22,28]</sup> and phosphatase treatment,<sup>[1d,9d,30b,c,34]</sup> are often found in the literature. However, only their sophisticated combination allowed a completely chromatography-free DSP of UDP-glc from SuSy reaction mixtures (80% yield, 86% purity; Scheme 2C). This yielded solvent savings up to 38-fold compared to the commonly applied AEC-SEC route (Scheme 2A).<sup>[9d,10c,d,11]</sup> The established DSP represents a significant advance for the large-scale syntheses of NDP-sugars using SuSy or related enzymatic methods. There are three major enzymatic routes towards NDP-sugars (Scheme 1). Similar product compositions in all cases suggest the applicability of our DSP. However, the multi-enzyme systems (Scheme 1B and C) cause accumulation of phosphate, requiring extension of the chromatography-free DSP with, for example, electro-dialysis.<sup>[33]</sup>

### Experimental Section

#### Chemicals and Materials

CIAP was from New England Biolabs (Ipswich, MA, USA). UDP (disodium salt), UDP-glc (disodium salt) and UTP (trisodium salt) were from Carbosynth (Compton, Berkshire, U.K.). UDP-gal (disodium salt) was from Roche (Penzberg, Germany). Absolute EtOH was from VWR International (Vienna, Austria). Other chemicals were from Carl Roth (Karlsruhe, Germany). All chemicals were obtained in the highest purity available. ReliSorb DA405/EB, Diaion WA21J and SA10A resins were from Mitsubishi Chemical Corporation (Tokyo, Japan). Dowex 1×8 (Cl<sup>-</sup>-form, 200–400 mesh) and Dowex 1×2 (Cl<sup>-</sup>-form, 50–100 mesh) resins were from Dow Chemical (Midland, MI, USA). Toyopearl GigaCap Q-650M, SuperQ-650M and QAE550C resins were from Tosoh Bioscience (Tokyo, Japan). Sephadex G-10, Q Sepharose FF and HP were from GE Healthcare (Vienna, Austria).

#### Analytical Methods

NDP-sugars, nucleosides, their mono- and diphosphates were analyzed by C18 HPLC using a Kinetex<sup>®</sup> C18 column (5 μm, 100 Å, 50×4.6 mm; Phenomenex, Germany) in reversed phase ion-pairing mode and UV-detection at 262 nm.

Sucrose, fructose, acetate, phosphate and EtOH were analyzed by HPLC using an Aminex HPX-87H column (Biorad, Richmond, CA, USA) and RI detection.<sup>[37]</sup> See the Supporting Information for details.

## DSP Development

**Starting material:** A reaction mixture from the conversion of sucrose and UDP or ADP by SuSy (from *Acidithiobacillus caldus*)<sup>[31a]</sup> was used. The pH of the reaction was controlled at 5.0 using 100% acetic acid. The solution contained 255 mM UDP-glc, 2.4 mM UMP, 43 mM UDP, 1.25 M sucrose, 255 mM fructose and 10 mM MgCl<sub>2</sub>. Alternatively, the solution contained 28 mM ADP-glc, 8 mM AMP, 3 mM ADP, 11 mM adenosine, 472 mM sucrose, 28 mM fructose and 10 mM MgCl<sub>2</sub>. After 3-fold dilution with deionized water to reduce viscosity, the enzyme was removed by Viva-spin concentrators (10 kDa, Sartorius, Germany) at 4000 rpm, 20°C. The ionic strength of the solution was ~4.5 mScm<sup>-1</sup>.

**Anion-exchange chromatography:** All chromatography experiments were performed on an ÄktaPrime plus system (GE Healthcare, Germany) at room temperature. The binding capacity of different AEX resins was determined using self-packed Proteus 1 mL FliQ columns (Generon, U.K.) and sodium succinate buffer (20 mM, pH 4.1). For Q Sepharose FF and HP prepacked 1 mL and 5 mL columns were used. About 5 mg UTP were repeatedly loaded onto the columns at a flow rate of 0.1–0.6 cm min<sup>-1</sup> until breakthrough of UTP was monitored. Different buffers (sodium salts) were tested at different pH values (acetate: pH 4.3, 5.3; formate: pH 4.3; phosphate: pH 3.5, 6.0) for separation of the compounds of the SuSy reaction mixture. The Dowex 1×8 resin (Cl<sup>-</sup>-form, 200–400 mesh, 1 mL column) was used. 0.5 mL of sample were loaded onto the column and eluted with a linear gradient (1 mM salt/column volume) (CV) at a flow rate of 0.6 cm min<sup>-1</sup>. The separation efficiency of all AEX resins was determined with sodium acetate buffer, pH 4.3. A linear gradient (Dowex 1×8, Dowex 1×2: 4.9 mM salt/CV at 0.6 cm min<sup>-1</sup>; all other resins: 10 mM salt/CV at 2.5–3.3 cm min<sup>-1</sup>) was used for elution. For determination of the elution characteristics of the AEX resins, UTP (Dowex 1×8, Dowex 1×2: 120 mg; all other resins: 40 mg) was loaded onto the columns at a flow rate of 0.6 cm min<sup>-1</sup>. The loading buffer was 20 mM sodium acetate, pH 4.3. UTP was eluted with 1 M sodium acetate at 0.6 cm min<sup>-1</sup> (Dowex resins) or 3.3 cm min<sup>-1</sup> (all other resins). CVs for elution of 40 mg UTP were determined. Preparative AEC for isolation of 1 g UDP-glc was performed with self-packed XK 16/20 columns (GE Healthcare, Austria) containing about 40 mL of Dowex 1×8 or Toyopearl SuperQ-650M. Sample was loaded at a flow rate of 0.5 cm min<sup>-1</sup>. Step gradients in sodium acetate (pH 4.3) were used for elution at 5 cm min<sup>-1</sup> (SuperQ-650M) or 1 cm min<sup>-1</sup> (Dowex 1×8). The gradients were as follows: 20 mM 28 CVs, 140 mM 36 CVs, 500 mM 10 CVs (Toyopearl SuperQ-650M); 20 mM 5 CVs, 167 mM 43 CVs, 363 mM 100 CVs, 1000 mM 31 CVs (Dowex 1×8). NDP-sugars, nucleosides, their mono- and diphosphates were detected by UV at 254 nm. UDP-glc containing fractions were pooled.

**Alkaline phosphatase treatment for chromatography-free DSP:** CIAP was used to hydrolyze all phosphomonoesters

(e.g., UDP) in the sample while leaving intact the NDP-sugar, which contains a phosphodiester linkage. Reactions were carried out at 30°C, controlling the pH at 6.0 or 7.0 using 1 M sodium hydroxide. Enzyme was used at 10 U mL<sup>-1</sup>. Samples (5 µL) were taken at certain times and mixed with 95 µL of 1:2 diluted acetonitrile. Precipitated protein was removed by centrifugation (13,000 rpm, 4°C, 30 min). Supernatant was analyzed by reverse phase ion-pair HPLC. Optimum reaction conditions were at pH 7.0 and incubation for 24 h. After the CIAP digest, enzyme was removed by Viva-spin concentrators (10 kDa; 4000 rpm, 20°C).

**Product precipitation with ethanol:** EtOH precipitation was used as alternative for desalting and product purification. The sample used was from AEC or CIAP digestion. The typical AEC sample from SuperQ-650M was ~25-fold concentrated under reduced pressure (40°C, 20 mbar) to yield an ionic strength of about 24 mScm<sup>-1</sup>. The CIAP sample contained 85 mM UDP-glc, 417 mM sucrose, 85 mM fructose, 15 mM uridine and 30 mM inorganic phosphate. The CIAP sample was supplemented with 200 mM sodium acetate to yield an ionic strength of ~12 mScm<sup>-1</sup>. NDP-sugar was precipitated by adding 3–6 volumes of EtOH. Incubation was overnight at –20°C or 4°C. Precipitate was recovered by centrifugation (3320 g, 4°C, 30 min). One (AEC sample) or two (CIAP sample) precipitation steps were performed. The final precipitate was air-dried at room temperature, dissolved in deionized water to a final concentration of 40–50 mg mL<sup>-1</sup>, frozen at –80°C and freeze-dried (Christ Alpha 1–4, B. Braun Biotech International, Melsungen, Germany) for 48 h. Samples were taken at each step and analyzed by HPLC.

## Acknowledgements

*This work was supported by the Federal Ministry of Economy, Family and Youth (BMWFJ), the Federal Ministry of Traffic, Innovation and Technology (BMVIT), the Styrian Business Promotion Agency, SFG, the Standortagentur Tirol and ZIT-Technology Agency of the City of Vienna through the COMET-Funding Programme managed by the Austrian Research Promotion Agency FFG. Financial support from the EU FP7 project SuSy (Sucrose Synthase as Effective Mediator of Glycosylation) is gratefully acknowledged. The authors thank Dr. Hansjörg Weber from the Graz University of Technology for NMR analysis and Prof. Tom Desmet, Ghent University (Belgium), for the SuSyAc-containing plasmid.*

## References

- [1] a) S. Koizumi, H. Kawano, K. Kino, A. Ozaki, U.S. Patent 2004/0166568 A1, **2004**; b) M. M. Muthana, J. Qu, Y. Li, L. Zhang, H. Yu, L. Ding, H. Malekan, X. Chen, *Chem. Commun.* **2012**, 48, 2728–2730; c) D. Warnock, X. Bai, K. Autote, J. Gonzales, K. Kinealy, B. Yan, J. Qian, T. Stevenson, D. Zopf, R. J. Bayer, *Biotechnol. Bioeng.* **2005**, 92, 831–842; d) G. Zhao, W. Guan, L. Cai, P. G. Wang, *Nat. Protoc.* **2010**, 5, 636–646.




- [2] a) T. Bülter, L. Elling, *Glycoconjugate J.* **1999**, *16*, 147–159; b) T. Desmet, W. Soetaert, *Biocatal. Biotransform.* **2011**, *29*, 1–18; c) M. M. Palcic, *Curr. Opin. Chem. Biol.* **2011**, *15*, 226–233; d) C. Zhang, B. R. Griffith, Q. Fu, C. Albermann, X. Fu, I.-K. Lee, L. Li, J. S. Thorson, *Science* **2006**, *313*, 1291–1294; e) J. Seibel, H.-J. Jördening, K. Buchholz, *Biocatal. Biotransform.* **2006**, *24*, 311–342.
- [3] a) F. De Bruyn, J. Maertens, J. Beauprez, W. Soetaert, M. De Mey, *Biotechnol. Adv.* **2015**, *33*, 288–302; b) V. Křen, T. Rezanka, *FEMS Microbiol. Rev.* **2008**, *32*, 858–889; c) D. Bowles, E.-K. Lim, B. Poppenberger, F. E. Vaistij, *Annu. Rev. Plant Biol.* **2006**, *57*, 567–597.
- [4] a) T. Desmet, W. Soetaert, P. Bojarová, V. Křen, L. Dijkhuizen, V. Eastwick-Field, A. Schiller, *Chem. Eur. J.* **2012**, *18*, 10786–10801; b) S. Muthana, H. Cao, X. Chen, *Curr. Opin. Chem. Biol.* **2009**, *13*, 573–581; c) C. A. G. M. Weijers, M. C. R. Franssen, G. M. Visser, *Biotechnol. Adv.* **2008**, *26*, 436–456; d) J. Xiao, T. S. Muzashvili, M. I. Georgiev, *Biotechnol. Adv.* **2014**, *32*, 1145–1156.
- [5] a) J. M. Woodley, *Trends Biotechnol.* **2008**, *26*, 321–327; b) E. M. Buque-Taboada, A. J. J. Straathof, J. J. Heijnen, L. A. M. van der Wielen, *Appl. Microbiol. Biotechnol.* **2006**, *71*, 1–12; c) D. Stark, U. Stockar, *Adv. Biochem. Eng. Biotechnol.* **2003**, *80*, 149–175.
- [6] a) I. E. Baciú, H. J. Jördening, J. Seibel, K. Buchholz, *J. Biotechnol.* **2005**, *116*, 347–357; b) B. M. De Roode, M. C. R. Franssen, A. v. d. Padt, R. M. Boom, *Biotechnol. Prog.* **2003**, *19*, 1391–1402; c) M. Holtkamp, F. A. Erhardt, H. J. Jördening, S. Scholl, *Chem. Eng. Process.* **2009**, *48*, 852–858; d) N. Wagner, A. Bosshart, J. Failmezger, M. Bechtold, S. Panke, *Angew. Chem.* **2015**, *127*, 4256–4260; *Angew. Chem. Int. Ed.* **2015**, *54*, 4182–4186.
- [7] S. Wenda, S. Illner, A. Mell, U. Kragl, *Green Chem.* **2011**, *13*, 3007–3047.
- [8] T. Hamamoto, K. Nagaoka, T. Noguchi, U.S. Patent 8450088 B2, **2013**.
- [9] a) E. Baroja-Fernandez, F. J. Muñoz, J. Pozueta-Romero, M. T. Moran-Zorzano, N. Alonso-Casajus, U.S. Patent 8841514 B2, **2014**; b) H. Kawai, S. Nakajima, M. Okuda, T. Yano, T. Tachiki, T. Tochikura, *J. Ferment. Technol.* **1978**, *56*, 586–592; c) S. Koizumi, T. Endo, K. Tabata, H. Nagano, J. Ohnishi, A. Ozaki, *J. Ind. Microbiol. Biotechnol.* **2000**, *25*, 213–217; d) A. Zervosen, U. Römer, L. Elling, *J. Mol. Catal. B: Enzym.* **1998**, *5*, 25–28.
- [10] a) S.-I. Ryu, J.-E. Kim, E.-J. Kim, S.-K. Chung, S.-B. Lee, *Process Biochem.* **2011**, *46*, 128–134; b) C. Weyler, E. Heinzle, *Appl. Biochem. Biotechnol.* **2015**, *175*, 3729–3736; c) J. Shao, J. Zhang, J. Nahalka, P. G. Wang, *Chem. Commun.* **2002**, 2586–2587; d) Z. Liu, J. Zhang, X. Chen, P. G. Wang, *ChemBioChem* **2002**, *3*, 348–355; e) X. Ma, J. Stöckigt, *Carbohydr. Res.* **2001**, *333*, 159–163.
- [11] J. Oh, S. G. Lee, B. G. Kim, J. K. Sohng, K. Liou, H. C. Lee, *Biotechnol. Bioeng.* **2003**, *84*, 452–458.
- [12] C. Ó'Fágáin, P. M. Cummins, B. F. O'Connor, in: *Protein Chromatography: Methods and Protocols*, Vol. 681, (Eds.: D. Walls, T. S. Loughran), Humana Press, New York, **2011**, pp 25–33.
- [13] a) U. B. Gokhale, O. Hindsgaul, M. M. Palcic, *Can. J. Chem.* **1990**, *68*, 1063–1071; b) K. Marumo, L. Lindqvist, N. Verma, A. Weintraub, P. R. Reeves, A. A. Lindberg, *Eur. J. Biochem.* **1992**, *204*, 539–545.
- [14] A. Shourie, S. S. Chapadgaonkar, in: *Bioanalytical Techniques*, The Energy and Resources Institute, New Delhi, **2005**, pp 125–180.
- [15] R. D. Rocklin, C. A. Pohl, *J. Liq. Chromatogr.* **1983**, *6*, 1577–1590.
- [16] a) A. Gutmann, C. Krump, L. Bungaruang, B. Nidetzky, *Chem. Commun.* **2014**, *50*, 5465–5468; b) R. M. C. Dawson, D. C. Elliott, W. H. Elliott, K. M. Jones, in: *Data for Biochemical Research*, 3<sup>rd</sup> edn., Clarendon Press, Oxford, **1989**, pp 103–114.
- [17] a) L. Elling, M. R. Kula, J. E. Ritter, S. Verseck, WO Patent 1996/027670 A2, **1996**; b) A. Stein, M. R. Kula, L. Elling, *Glycoconjugate J.* **1998**, *15*, 139–145.
- [18] A. Zervosen, A. Stein, H. Adrian, L. Elling, *Tetrahedron* **1996**, *52*, 2395–2404.
- [19] T. Eixelsberger, B. Nidetzky, *Adv. Synth. Catal.* **2014**, *356*, 3575–3584.
- [20] J. C. Errey, B. Mukhopadhyay, K. P. R. Kartha, R. A. Field, *Chem. Commun.* **2004**, 2706–2707.
- [21] J. White-Phillip, C. J. Thibodeaux, H.-w. Liu, *Methods Enzymol.* **2009**, *459*, 521–544.
- [22] A. Zervosen, L. Elling, M. R. Kula, *Angew. Chem.* **1994**, *106*, 592–593; *Angew. Chem. Int. Ed.* **1994**, *33*, 571–572.
- [23] J. Crouse, D. Amorese, *Focus* **1987**, *19*, 13–16.
- [24] M. Mohsen-Nia, H. Amiri, B. Jazi, *J. Solution Chem.* **2010**, *39*, 701–708.
- [25] W. J. Steele, N. Okamura, H. Busch, *Biochim. Biophys. Acta* **1964**, *87*, 490–492.
- [26] C. Capello, U. Fischer, K. Hungerbühler, *Green Chem.* **2007**, *9*, 927–934.
- [27] S. Hanessian, P.-P. Lu, H. Ishida, *J. Am. Chem. Soc.* **1998**, *120*, 13296–13300.
- [28] J. Van der Borght, T. Desmet, W. Soetaert, *Biotechnol. J.* **2010**, *5*, 986–993.
- [29] J. Polák, G. C. Benson, *J. Chem. Thermodyn.* **1971**, *3*, 235–242.
- [30] a) H. Tanaka, Y. Yoshimura, M. R. Jørgensen, J. A. Cuesta-Seijo, O. Hindsgaul, *Angew. Chem.* **2012**, *124*, 11699–11702; *Angew. Chem. Int. Ed.* **2012**, *51*, 11531–11534; b) S. Amann, G. Dräger, C. Rupprath, A. Kirschning, L. Elling, *Carbohydr. Res.* **2001**, *335*, 23–32; c) Y. Zhai, M. Liang, J. Fang, X. Wang, W. Guan, X.-w. Liu, P. Wang, F. Wang, *Biotechnol. Lett.* **2012**, *34*, 1321–1326; d) R. Marquardt, B. Hoersch, A. Seiffert-Stoeriko, A. Stein, A. Zervosen, L. Elling, M. R. Kula, S. Verseck, J. Distler, W. Piepersberg, U.S. Patent 5866378 A, **1999**.
- [31] a) M. Diricks, F. De Bruyn, P. Van Daele, M. Walmagh, T. Desmet, *Appl. Microbiol. Biotechnol.* **2015**, *99*, 8465–8474; b) M. Morell, L. Copeland, *Plant Physiol.* **1985**, *78*, 149–154.
- [32] E. Baroja-Fernández, F. J. Muñoz, J. Li, A. Bahaji, G. Almagro, M. Montero, E. Etxeberria, M. Hidalgo, M. T. Sesma, J. Pozueta-Romero, *Proc. Natl. Acad. Sci. USA* **2012**, *109*, 321–326.
- [33] a) M. Suzuki, K. Kaneda, Y. Nakai, M. Kitaoka, H. Taniuchi, *New Biotechnol.* **2009**, *26*, 137–142; b) Y. Liu,

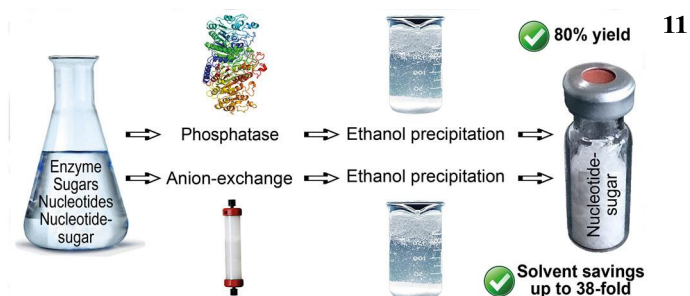
- M. Nishimoto, M. Kitaoka, *Carbohydr. Res.* **2015**, *401*, 1–4.
- [34] L. Elling, C. Rupprath, N. Günther, U. Römer, S. Verseck, P. Weingarten, G. Dräger, A. Kirschning, W. Piersberg, *ChemBioChem* **2005**, *6*, 1423–1430.
- [35] R. A. Sheldon, *Chem. Soc. Rev.* **2012**, *41*, 1437–1451.
- [36] A. P. Cheung, D. Kenney, *J. Chromatogr. A* **1990**, *506*, 119–131.
- [37] B. Petschacher, B. Nidetzky, *Microb. Cell Fact.* **2008**, *7*, 9.
-


FULL PAPERS

Downstream Processing of Nucleoside-Diphospho-Sugars  
from Sucrose Synthase Reaction Mixtures at Decreased  
Solvent Consumption

*Adv. Synth. Catal.* **2016**, 358, 1–11

 Martin Lemmerer, Katharina Schmölder,  
Alexander Gutmann, Bernd Nidetzky\*



*Advanced*   
**Synthesis &  
Catalysis**

Supporting Information

## Supporting Information

### Downstream Processing of Nucleoside-Diphospho-Sugars from Sucrose Synthase Reaction Mixtures at Decreased Solvent Consumption

Martin Lemmerer,<sup>+a</sup> Katharina Schmörlzer,<sup>+a</sup> Alexander Gutmann,<sup>b</sup> and Bernd Nidetzky<sup>a,b\*</sup>

<sup>a</sup>Austrian Centre of Industrial Biotechnology, Petersgasse 14, 8010 Graz, Austria

<sup>b</sup>Institute of Biotechnology and Biochemical Engineering, Graz University of Technology,  
NAWI Graz, Petersgasse 12/I, 8010 Graz, Austria

<sup>+</sup>These authors contributed equally to this work.

\* **Corresponding author:** [bernd.nidetzky@tugraz.at](mailto:bernd.nidetzky@tugraz.at); Phone: +43 316 873 8400; FAX: +43  
316 873 8434

Proofs and reprints should be addressed to Bernd Nidetzky.

#### Table of contents

Analytical methods	S3
Protein expression and purification	S3
Preparative SEC	S3
Solubility measurement of UDP-glc in EtOH	S4
<sup>1</sup> H and <sup>13</sup> C NMR measurements	S4
Preparative AEC for isolation of ADP-glc from SuSy reaction mixture	S5

Table S1. Comparison of binding capacity, separation efficiency and elution characteristics of different AEX resins	S6
Figure S1. Desalting of UDP-glc by SEC	S7
Figure S2. SEC-free DSP of UDP-glc (ion-pair reversed phase HPLC)	S8
Figure S3 SEC-free DSP of UDP-glc (ion exchange HPLC)	S8
Figure S4. <sup>1</sup> H NMR spectrum of UDP-glc after SEC-free DSP	S9
Figure S5. <sup>13</sup> C NMR spectrum of UDP-glc after SEC-free DSP	S10
Figure S6. CIAP treatment for chromatography-free DSP of UDP-glc	S11
Figure S7. Chromatography-free DSP of UDP-glc (ion-pair reversed phase HPLC)	S12
Figure S8. Chromatography-free DSP of UDP-glc (ion exchange HPLC)	S12
Figure S9. Purities of UDP-glc after the SEC-free DSP <i>versus</i> the chromatography-free DSP	S13
Figure S10. <sup>1</sup> H NMR spectrum of UDP-glc after chromatography-free DSP	S14
Figure S11. <sup>13</sup> C NMR spectrum of UDP-glc after chromatography-free DSP	S15
Figure S12. CIAP treatment for chromatography-free DSP of UDP-gal	S16
Figure S13. DSP of ADP-glc by AEC on a Toyopearl SuperQ-650M 1 mL column	S17
Figure S14. SEC-free DSP of ADP-glc	S18
Figure S15. Chromatography-free DSP of ADP-glc	S18
References for Supporting Information	S19

## Methods

### Analytical methods

Uridine-derivates (UMP, UDP and UDP-glucose) were analyzed by reversed phase HPLC using a Kinetex<sup>®</sup> C18 column (5  $\mu\text{m}$ , 100  $\text{\AA}$ , 50 x 4.6 mm; Phenomenex, Germany) in reversed phase ion-pairing mode. HPLC analysis was performed at 35°C with a mobile phase of 87.5% 20 mM potassium phosphate buffer, pH 5.9 containing 40 mM tetra-n-butylammonium bromide (TBAB) and 12.5% acetonitrile at an isocratic flow rate of 2 mL min<sup>-1</sup>. Uridine derivates were monitored by UV-detection at 262 nm.

Sucrose, fructose, acetate, phosphate and ethanol (EtOH) were analyzed by HPLC as described by Petschacher et al.<sup>[1]</sup> A Merck-Hitachi LaChrome HPLC System equipped with an Aminex HPX-87H (Biorad, Richmond, CA, USA) column, a Merck-Hitachi LaChrome L-7250 autosampler and a Merck L-7490 RI detector was used. The system was operated at 65°C, using a flow rate of 0.6 mL min<sup>-1</sup> for the eluent (5 mM sulfuric acid). Applied conditions caused hydrolysis of sucrose into equimolar concentrations of fructose and glucose. The difference of glucose and fructose gave the remaining fructose.

Authentic standards were used for calibration.

### Protein expression and purification

SuSyAc was expressed in *E.coli* BL21 (DE3) and purified as previously described.<sup>[2]</sup> SDS PAGE was used to confirm purity of enzyme preparations.

### Preparative SEC

Among other things, the resolution of SEC depends on the ratio of sample to bed volume.<sup>[3]</sup> Thus, the typical AEC sample from SuperQ-650M was ~25-fold concentrated under reduced pressure (40°C, 20 mbar) to yield an ionic strength of about 24 mS cm<sup>-1</sup>. Note, the eluate was

25-fold concentrated, due to the solubility limit of sodium acetate (~ 4 M in water at 20°C). Acetate was removed from UDP-glc on an ÄktaPrime plus system (GE Healthcare, Germany) with a self-packed XK 16/100 column (H/D ratio = 62.5, GE Healthcare, Austria) containing about 150 mL Sephadex G-10 (exclusion limit = 700 Da; GE Healthcare). 1 mL of sample containing ~ 30 mg UDP-glc was loaded onto the column. Elution was performed with deionized water at a flow rate of 1 cm min<sup>-1</sup>. UDP-glc was detected by UV absorption ( $\lambda$  = 254 nm), while conductivity measurement was used for acetate detection. Automated fraction collection was used to collect 40 mL of pure UDP-glc solution. UDP-glc was not processed further.

#### **Solubility measurement of UDP-glc in EtOH**

20 mg of UDP-glc were dissolved in 1 mL of EtOH. The solution was incubated at 25°C and an agitation rate of 200 rpm using a Thermomixer comfort (Eppendorf, Germany). Samples were taken at certain times. After centrifugation for 5 min at 13,200 rpm, the concentration of UDP-glc in the supernatant was measured with a DeNovix SA-11+ spectrophotometer (DeNovix Inc, US) at 262 nm.

#### **<sup>1</sup>H and <sup>13</sup>C NMR measurements**

~10 mg of UDP-glc were dissolved in 600  $\mu$ L D<sub>2</sub>O. A Varian (Agilent) INOVA 500-MHz NMR spectrometer (Agilent Technologies, Santa Clara, California, USA) and the VNMRJ 2.2D software were used for all measurements. <sup>1</sup>H NMR spectra (499.98 MHz) were measured on a 5 mm indirect detection PFG-probe, while a 5 mm dual direct detection probe with z-gradients was used for <sup>13</sup>C NMR spectra (125.71 MHz). Standard pre-saturation sequence was used: relaxation delay 2 s; 90° proton pulse; 2.048 s acquisition time; spectral width 8 kHz; number of points 32 k. <sup>13</sup>C NMR spectra were recorded with the following pulse sequence: standard <sup>13</sup>C pulse sequence with 45° carbon pulse, relaxation delay 2 s,



Waltz decoupling during acquisition, 2 s acquisition time. ACD/NMR Processor Academic Edition 12.0 (Advanced Chemistry Development Inc.) was used for evaluation of spectra.

### **Preparative AEC for isolation of ADP-glc from SuSy reaction mixture**

AEC was performed using an ÄktaPrime plus system (GE Healthcare, Germany) equipped with a self-packed Proteus FliQ column (Generon, UK) containing about 1 mL of Toyopearl SuperQ-650M. Equilibration with 20 mM sodium acetate buffer pH 4.3 (10 CVs) and loading of sample, containing ~10 mg ADP-glc, were performed at a flow rate of 3.3 cm min<sup>-1</sup>. An optimized step gradient in sodium acetate was used for elution of compounds: adenosine, 20 mM; AMP, 147 mM; ADP-glc, 245 mM; ADP, 363 mM.

**Table S1.** Comparison of binding capacity, separation efficiency and elution characteristics of different AEX resins.

Resin	Particle size <sup>[d]</sup> [ $\mu\text{m}$ ]	AEX	Binding capacity <sup>[h]</sup> [ $\text{mg}_{\text{UTP}} \text{mL}_{\text{resin}}^{-1}$ ]	Separation <sup>[i],[l]</sup>	CVs/40 $\text{mg}_{\text{UTP}}$ <sup>[m]</sup>
Q Sepharose FF <sup>[a]</sup>	45 – 165 <sup>[e]</sup>	strong	<10	+ <sup>[j]</sup>	n.d.
Q Sepharose HP <sup>[b]</sup>	24 – 44 <sup>[e]</sup>	strong	<10	+ <sup>[j]</sup>	n.d.
Diaion WA21J <sup>[c]</sup>	300 – 1180 <sup>[f]</sup>	weak	<5	n.d.	n.d.
Diaion SA10A <sup>[c]</sup>	300 – 1180 <sup>[f]</sup>	strong	70	- <sup>[j]</sup>	65
ReliSorb DA405 <sup>[c]</sup>	200 – 500 <sup>[g]</sup>	weak	35	- <sup>[j]</sup>	190
Dowex 1 $\times$ 8 200 - 400 mesh <sup>[c]</sup>	37- 74 <sup>[f]</sup>	strong	150	+ <sup>[k]</sup>	37 <sup>[n]</sup>
Dowex 1 $\times$ 2 50 - 100 mesh <sup>[c]</sup>	149 – 297 <sup>[f]</sup>	strong	130	+ <sup>[k]</sup>	32 <sup>[n]</sup>
Toyopearl GigaCap Q-650M <sup>[c]</sup>	50 – 100 <sup>[g]</sup>	strong	30	- <sup>[j]</sup>	22 <sup>[o]</sup>
Toyopearl SuperQ-650M <sup>[c]</sup>	40 – 90 <sup>[g]</sup>	strong	40	+ <sup>[j]</sup>	20
Toyopearl QAE550C <sup>[c]</sup>	50 – 150 <sup>[g]</sup>	strong	60	+ <sup>[j]</sup>	190

n.d. not determined; CVs, column volumes.

<sup>[a]</sup>Prepacked 1 mL column (inner diameter 7 mm).

<sup>[b]</sup>Prepacked 5 mL column (inner diameter 16 mm).

<sup>[c]</sup>Self-packed 1 mL FliQ column (inner diameter 6.2 mm).

<sup>[d]</sup>Data from supplier. Matrix: <sup>[e]</sup> 6% cross-linked agarose; <sup>[f]</sup> styrene-divinylbenzene polymer; <sup>[g]</sup> methacrylic polymer.

<sup>[h]</sup>Flow rate was 0.6  $\text{cm min}^{-1}$ , except for Q Sepharose (FF: 0.5  $\text{cm min}^{-1}$ ; HP: 0.1  $\text{cm min}^{-1}$ ) resins.

<sup>[i]</sup>Separation of UMP, UDP-glc and UDP. 0.5 mL of sample were loaded. Elution with a linear gradient of sodium acetate buffer, pH 4.3: <sup>[j]</sup> 10  $\text{mM}_{\text{acetate}}/\text{CV}$  or <sup>[k]</sup> 4.9  $\text{mM}_{\text{acetate}}/\text{CV}$ .

<sup>[l]</sup>Flow rate was 3.3  $\text{cm min}^{-1}$ , except for Dowex (0.6  $\text{cm min}^{-1}$ ) and Q Sepharose (2.5  $\text{cm min}^{-1}$ ) resins.

<sup>[m]</sup>Flow rate was 3.3  $\text{cm min}^{-1}$ , except for Dowex resins (0.6  $\text{cm min}^{-1}$ ).

<sup>[n]</sup>120 mg of UTP had to be loaded, due to high sample dilution. CVs for 40 mg UTP were back-calculated.

<sup>[o]</sup>CVs pro ~30  $\text{mg}_{\text{UTP}}$ , due to limited binding capacity of the resin.

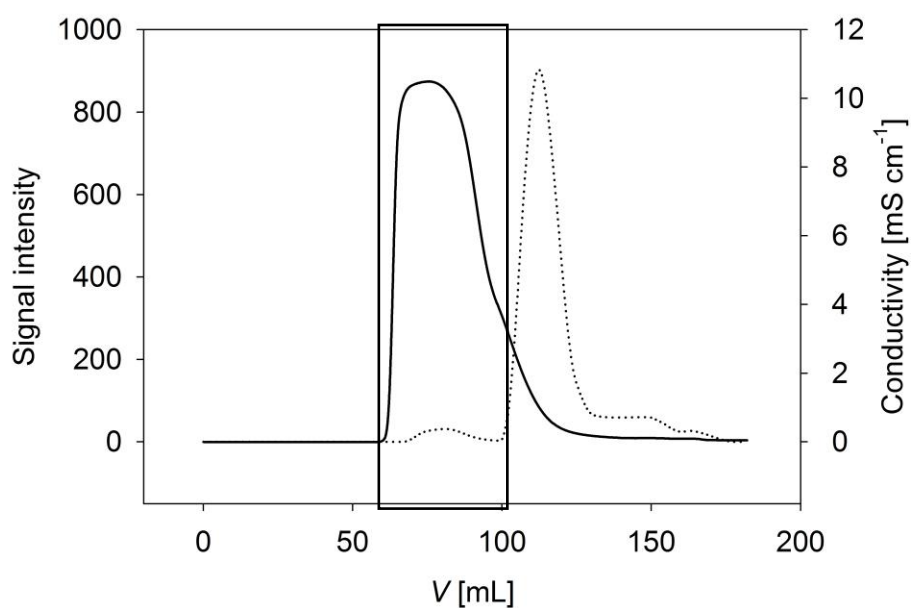


Figure S1. Desalting of UDP-glc by SEC with a self-packed XK 16/100 column (H/D ratio = 62.5) containing about 150 mL Sephadex G-10 (exclusion limit = 700 Da). 1 mL of sample containing ~ 30 mg UDP-glc was loaded. Sodium acetate concentration of the sample was ~2 M. Elution with deionized water at a flow rate of 1 cm min<sup>-1</sup> led to ~ 25 mg pure UDP-glc (black box). Solid line, UV signal ( $\lambda = 254$  nm); dotted line, conductivity (mS cm<sup>-1</sup>).

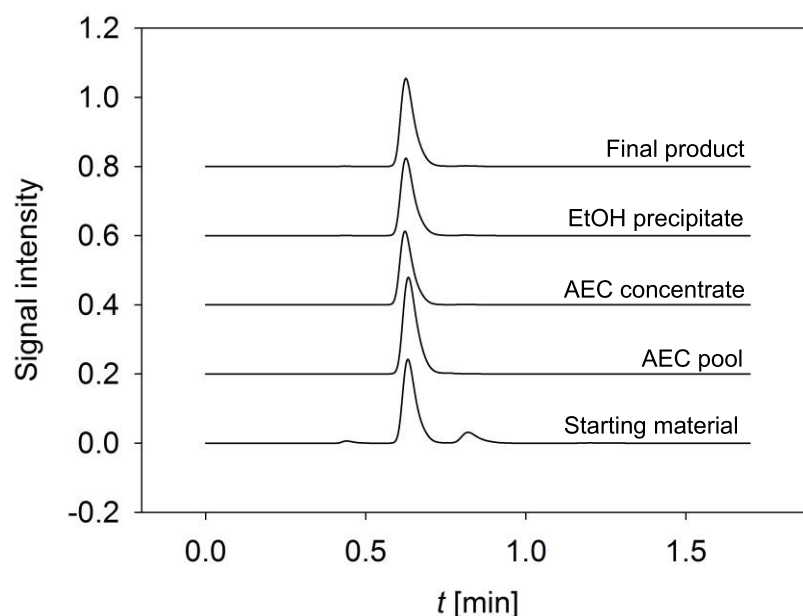


Figure S2. SEC-free DSP of UDP-glc (Scheme 2B). Superposition of ion-pair reversed phase HPLC elution profiles of samples from each process step. Authentic UDP-glc elutes with a retention time of 0.63 min. Retention times of impurities are 0.45 min (UMP) and 0.82 min (UDP). UV detection at 262 nm was used.

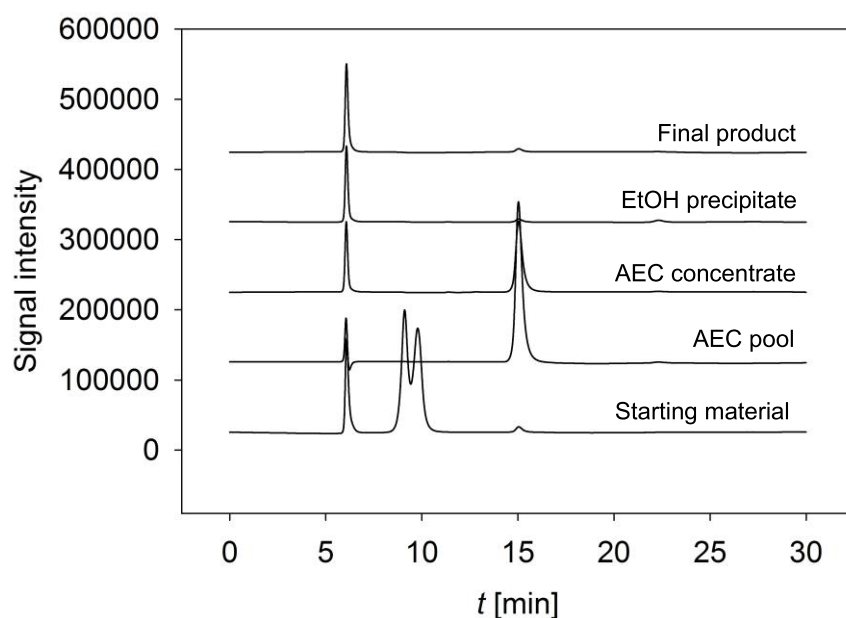


Figure S3. SEC-free DSP of UDP-glc (Scheme 2B). Superposition of ion exchange HPLC elution profiles of samples from each process step. Authentic UDP-glc elutes with a retention time of 6.1 min. Retention times of impurities are 9.1 min (glucose), 9.8 min (fructose), 15.1 min (acetate) and 22.5 min (EtOH). RI detection was used.

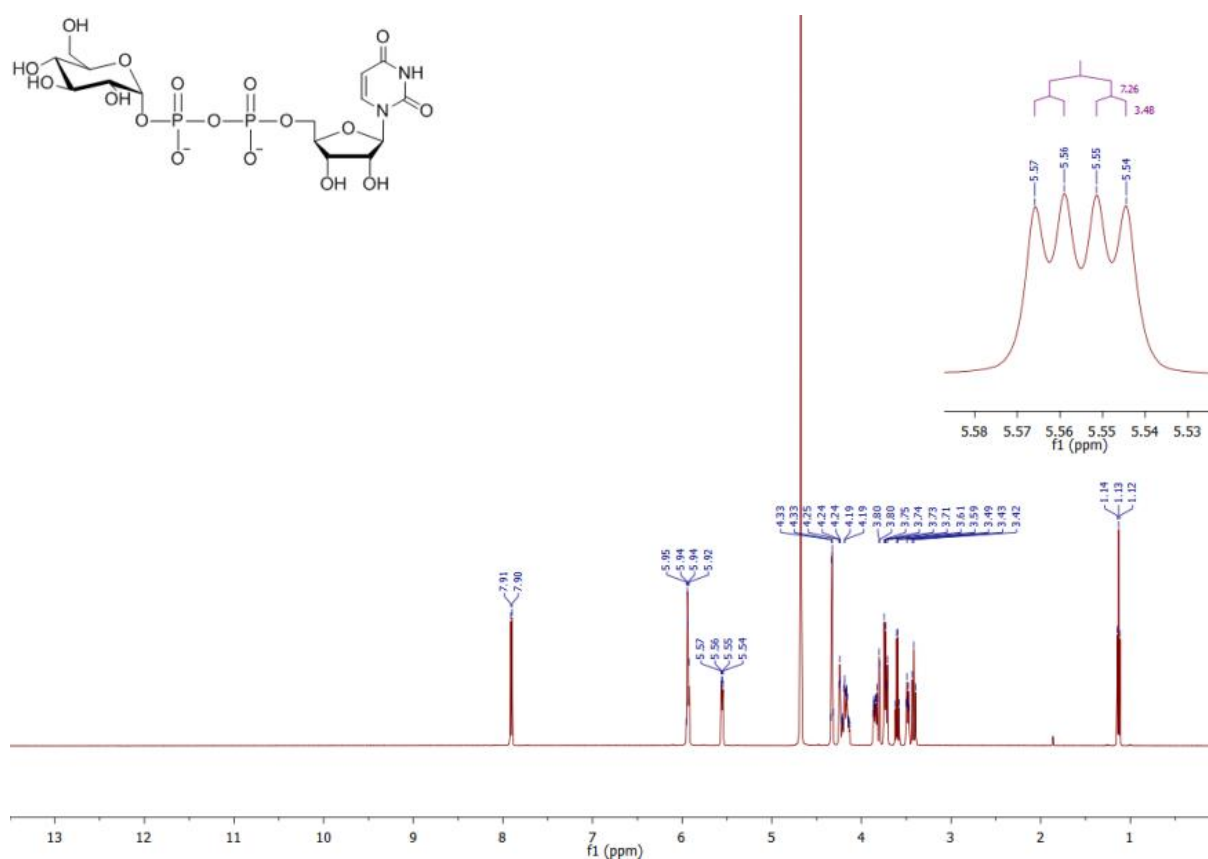


Figure S4. <sup>1</sup>H NMR spectrum of UDP-glc after SEC-free DSP (Scheme 2B). UDP-glc was dissolved in D<sub>2</sub>O. Spectrum is in accordance with previously published data.<sup>[4]</sup>

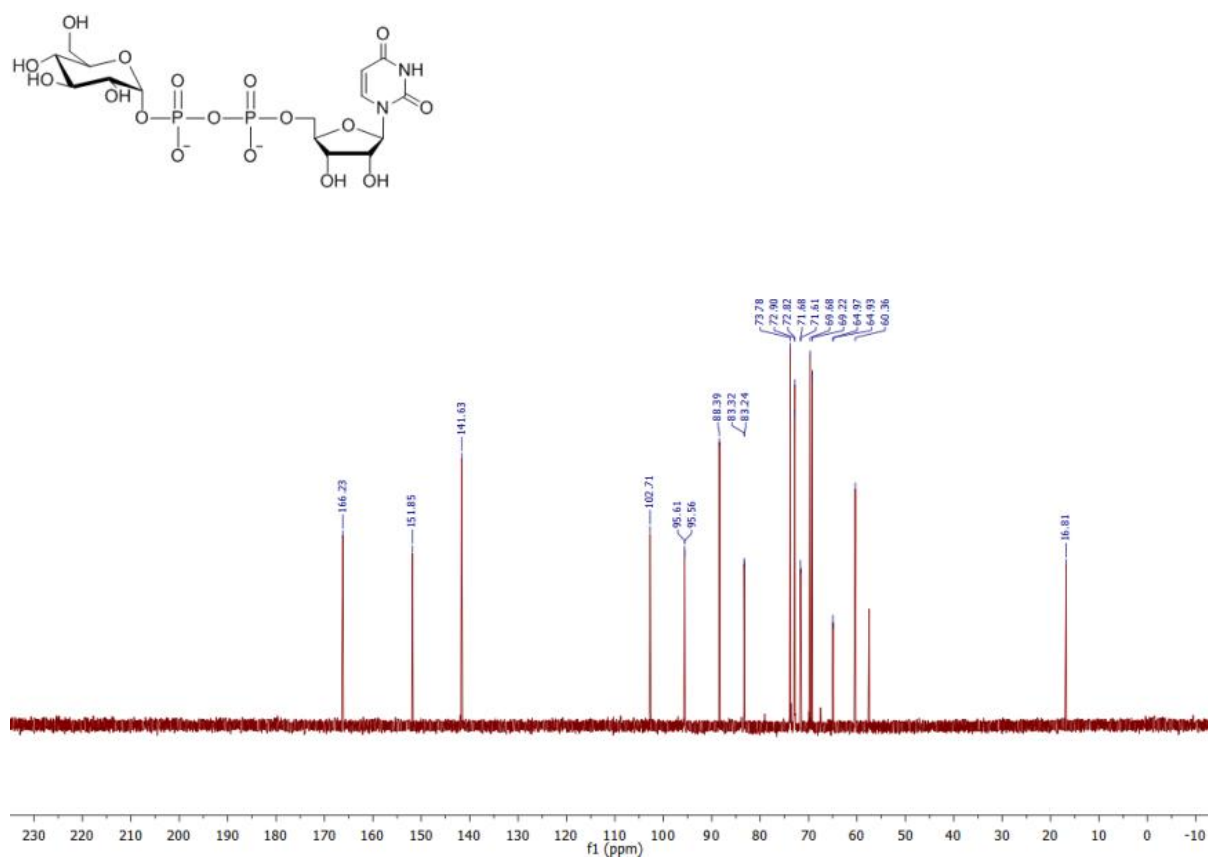


Figure S5. <sup>13</sup>C NMR spectrum of UDP-glc after SEC-free DSP (Scheme 2B). UDP-glc was dissolved in D<sub>2</sub>O. Spectrum is in accordance with previously published data.<sup>[4]</sup>

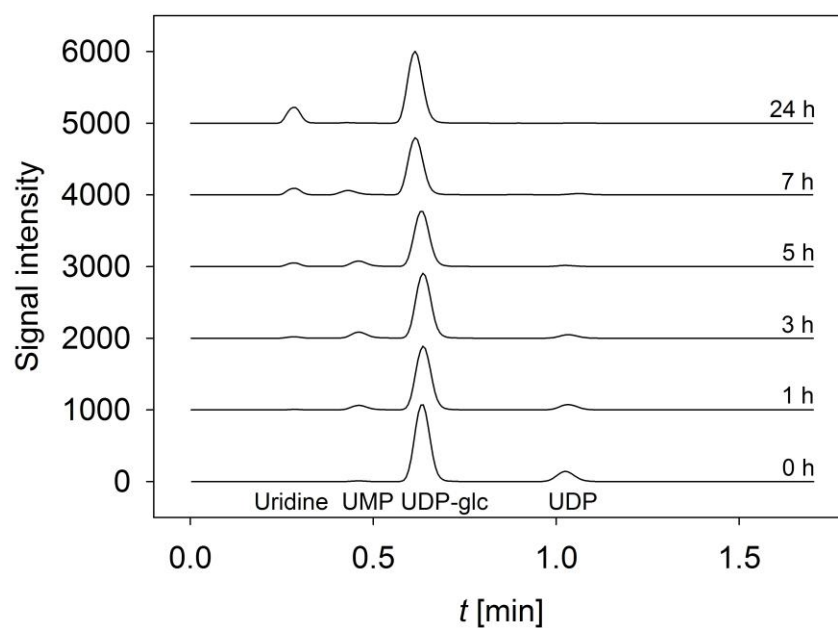


Figure S6. CIAP treatment for chromatography-free DSP (Scheme 2C) of UDP-glc. Reversed-phase ion pairing HPLC analysis showing selective hydrolysis of nucleotides by CIAP ( $10 \text{ U mL}^{-1}$ ) at pH 7.0 and  $30^\circ\text{C}$ . UV-detection at 262 nm was used.

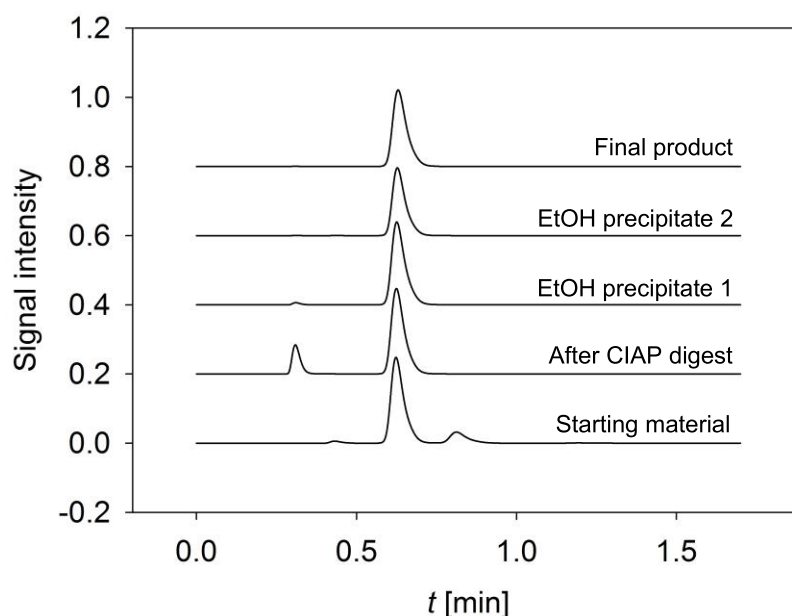


Figure S7. Chromatography-free DSP of UDP-glc (Scheme 2C). Superposition of ion-pair reversed phase HPLC elution profiles of samples from each process step. Authentic UDP-glc elutes with a retention time of 0.63 min. Retention times of impurities are 0.3 min (uridine), 0.45 min (UMP) and 0.82 min (UDP). UV detection at 262 nm was used.

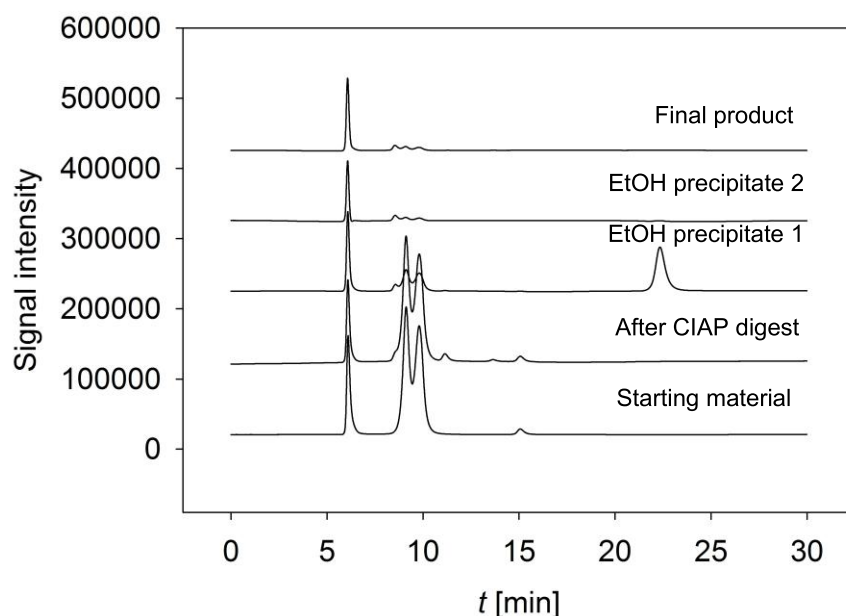
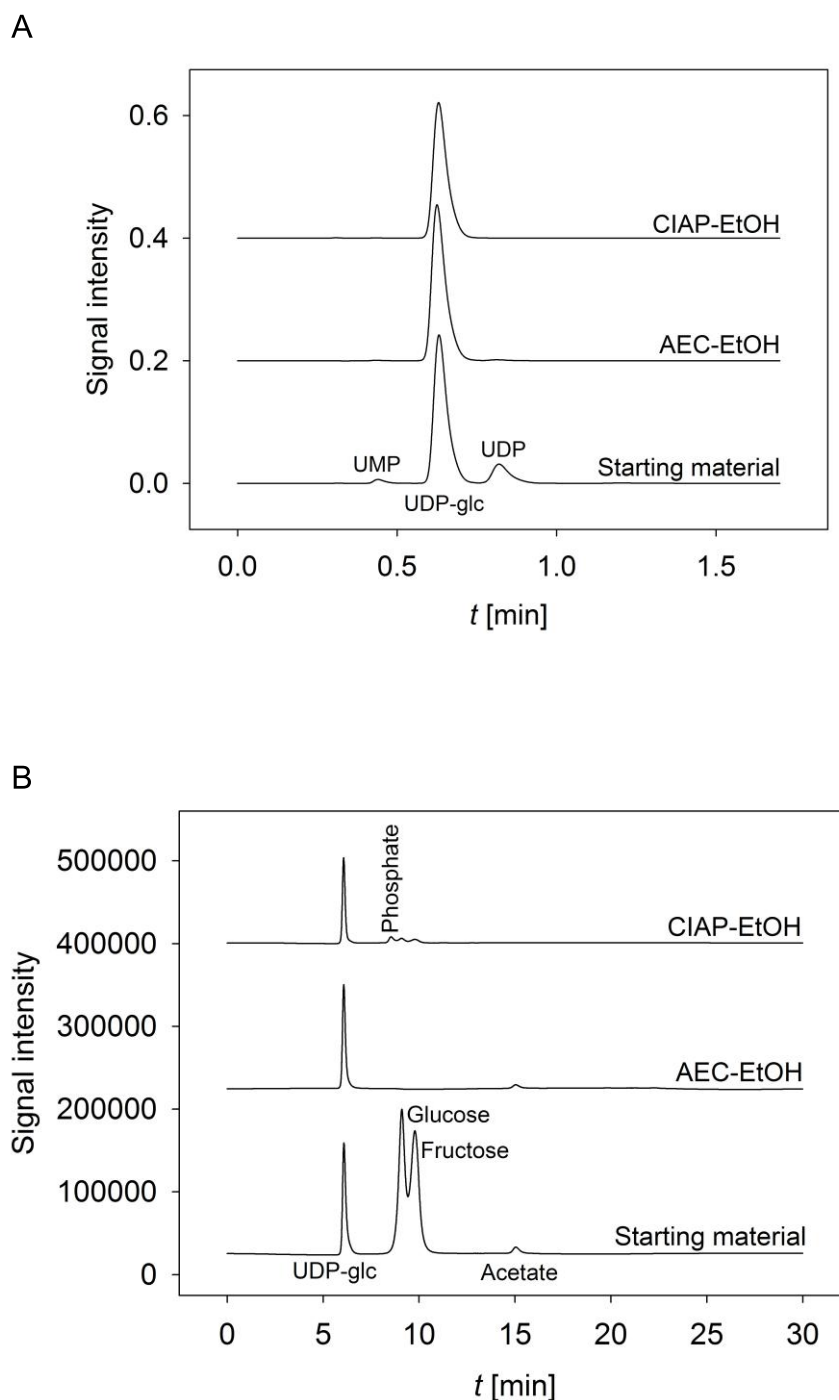


Figure S8. Chromatography-free DSP of UDP-glc (Scheme 2C). Superposition of ion exchange HPLC elution profiles of samples from each process step. Authentic UDP-glc elutes with a retention time of 6.1 min. Retention times of impurities are 8.5 min (inorganic phosphate), 9.1 min (glucose), 9.8 min (fructose), 15.1 min (acetate) and 22.5 min (EtOH). RI detection was used.





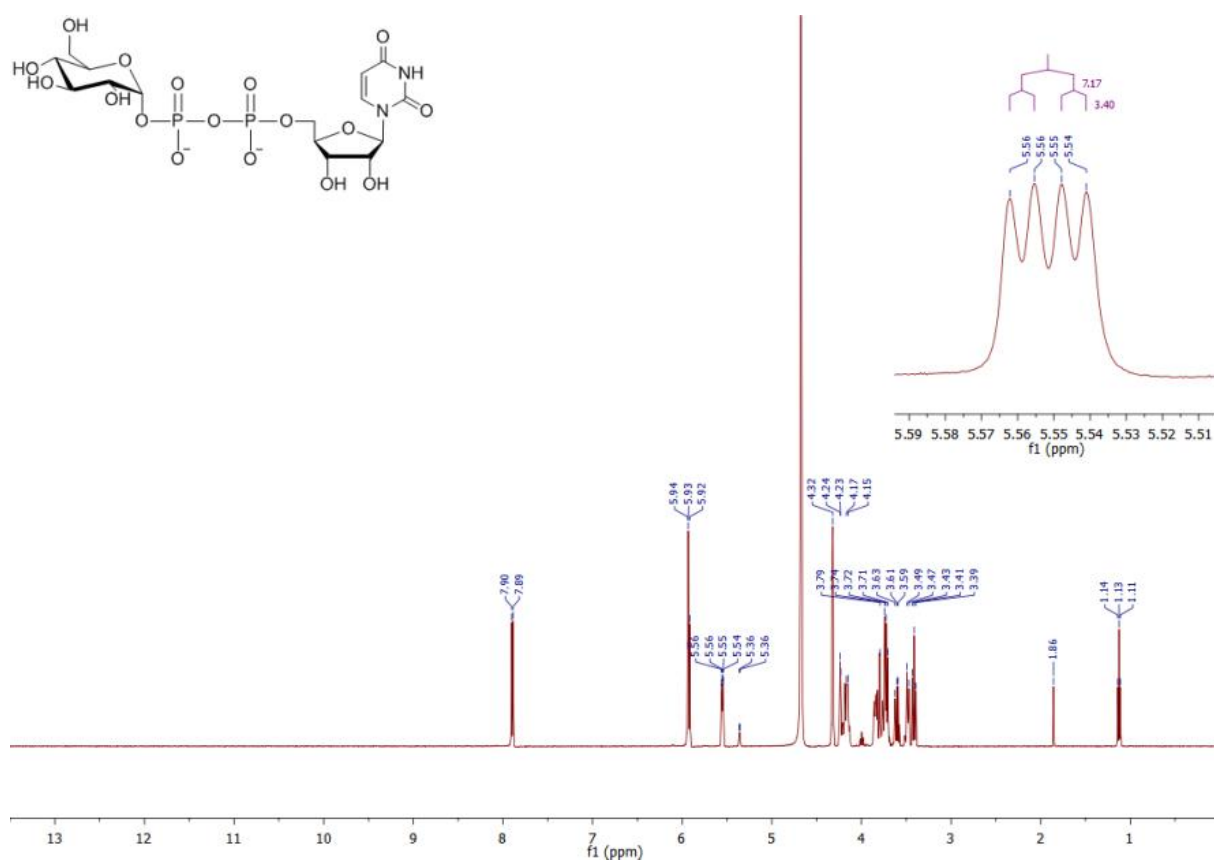


Figure S10. <sup>1</sup>H NMR spectrum of UDP-glc after chromatography-free DSP (Scheme 2C). UDP-glc was dissolved in D<sub>2</sub>O. Spectrum is in accordance with previously published data.<sup>[4]</sup>

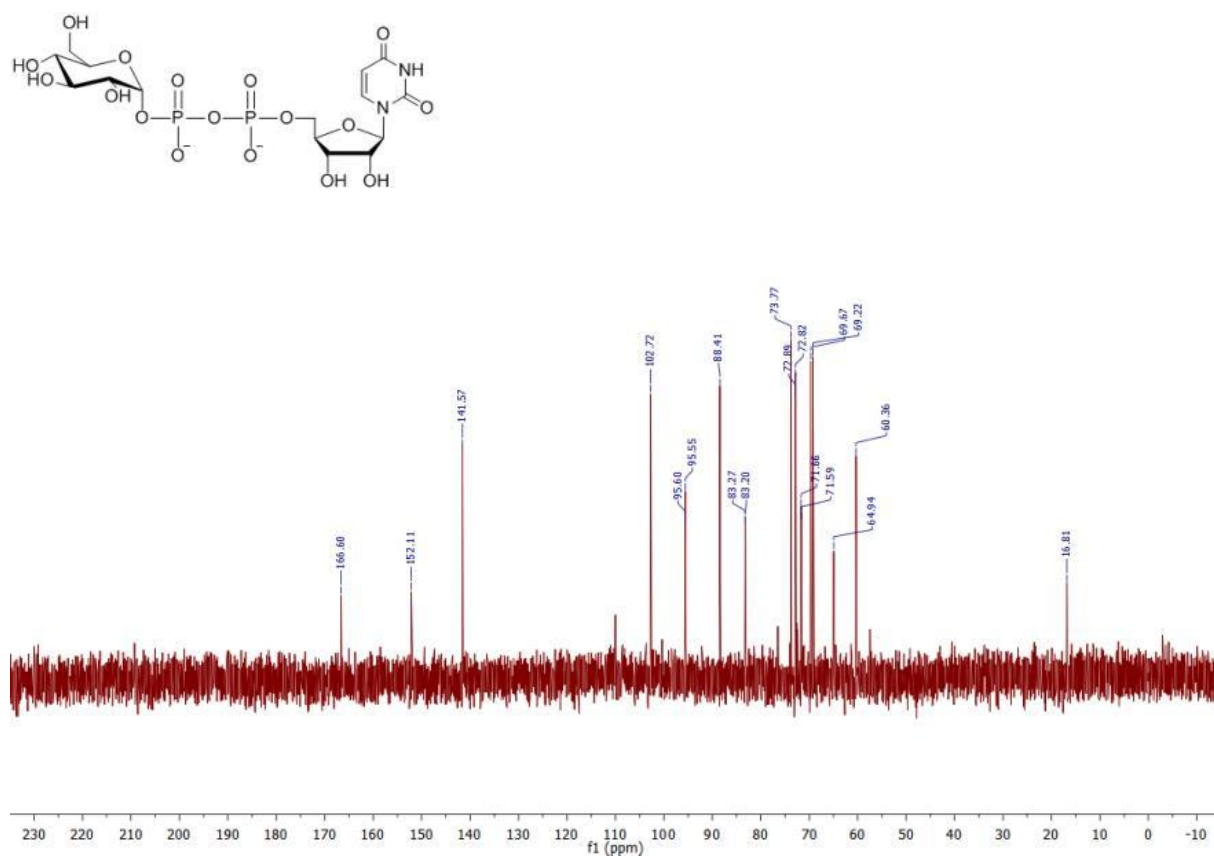


Figure S11.  $^{13}\text{C}$  NMR spectrum of UDP-glc after chromatography-free DSP (Scheme 2C). UDP-glc was dissolved in  $\text{D}_2\text{O}$ . Spectrum is in accordance with previously published data.<sup>[4]</sup>

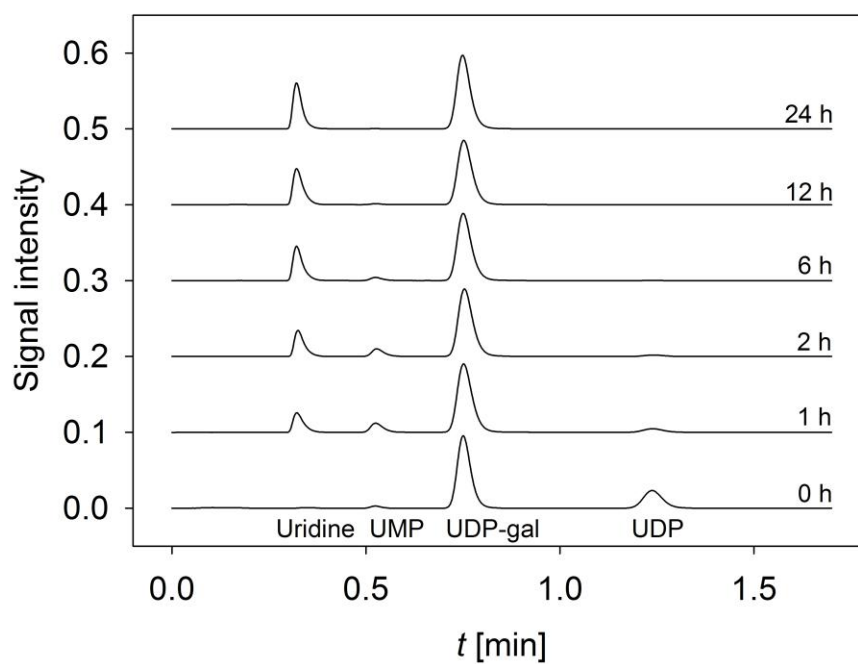


Figure S12. CIAP treatment for chromatography-free DSP of UDP-gal (Scheme 2C). Reversed-phase ion pairing HPLC analysis showing selective hydrolysis of nucleotides by CIAP ( $10 \text{ U mL}^{-1}$ ) at pH 7.0 and  $30^\circ\text{C}$ . The test solution contained 16 mM UDP-gal, 7 mM UDP, 1 mM uridine and 10 mM  $\text{MgCl}_2$ . UV-detection at 262 nm was used.

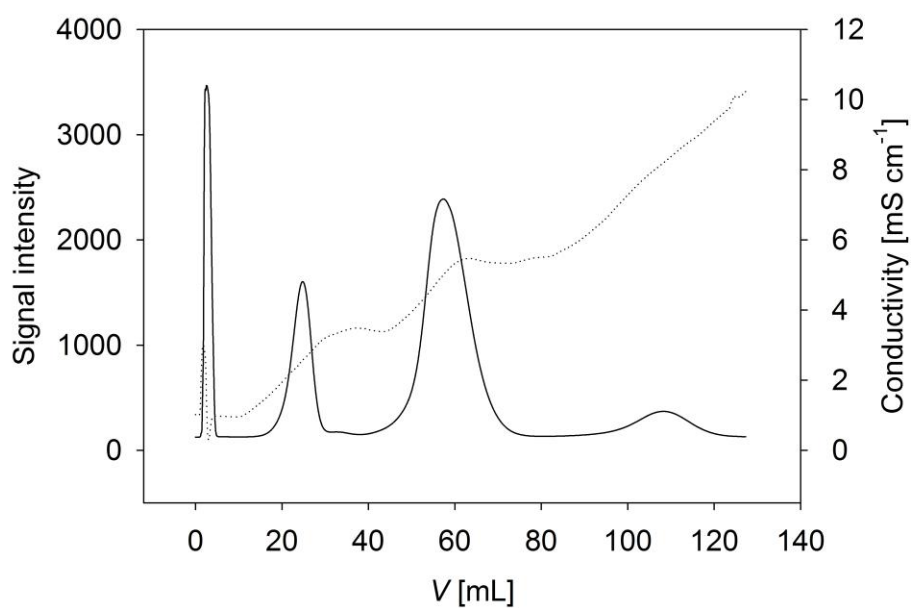


Figure S13. DSP of ADP-glc by AEC (Scheme 2B) on a Toyopearl SuperQ-650M 1 mL column. The loaded sample contained ~10 mg of ADP-glc. An optimized step gradient in sodium acetate (pH 4.3) was used for elution at 3.3 cm min<sup>-1</sup>. Solid line, UV signal (254 nm); dotted line, conductivity (mS cm<sup>-1</sup>). First peak, adenosine; second peak, AMP; third peak, ADP-glc; last peak, ADP.

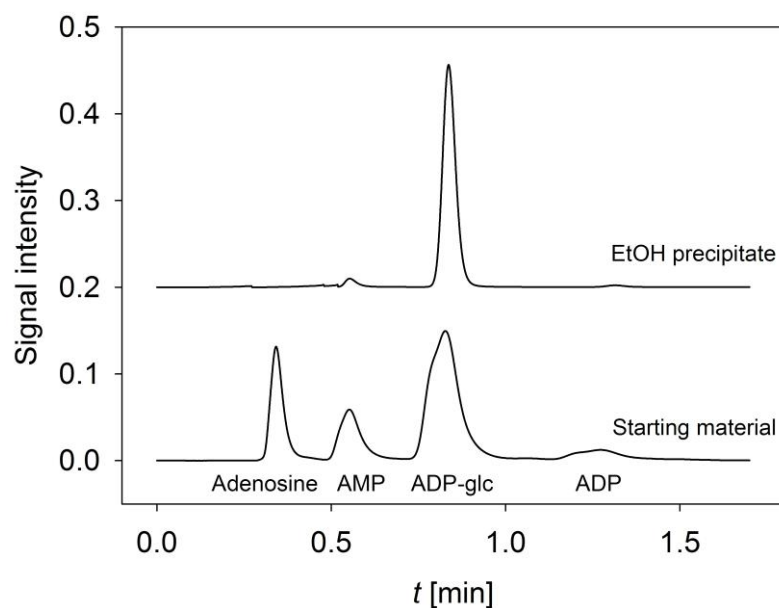


Figure S14. SEC-free DSP of ADP-glc (Scheme 2B). Superposition of ion-pair reversed phase HPLC elution profiles of the samples from different process steps. The ADP-glc containing AEC eluate (see Figure S13) was concentrated and used for EtOH precipitation. For details see the Methods. Authentic AMP and ADP elute with retention times of 0.52 min and 1.3 min. UV-detection at 262 nm was used.

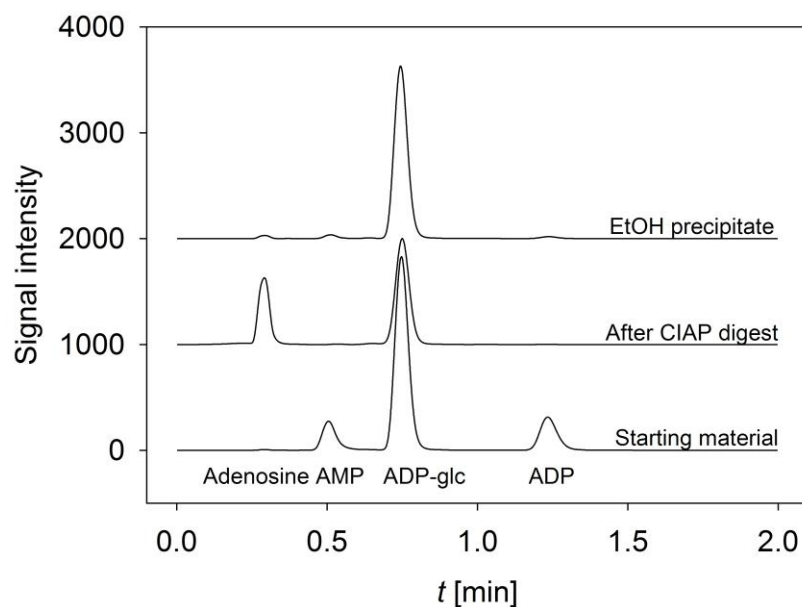


Figure S15. Chromatography-free DSP of ADP-glc (Scheme 2C). Superposition of ion-pair reversed phase HPLC elution profiles of samples from different process steps. Authentic AMP and ADP elute with retention times of 0.52 min and 1.3 min. UV-detection at 262 nm was used.

## References for Supporting Information

- [1] B. Petschacher, B. Nidetzky, *Microb. Cell Fact.* **2008**, *7*, 9.
- [2] M. Diricks, F. De Bruyn, P. Van Daele, M. Walmagh, T. Desmet, *Appl. Microbiol. Biotechnol.* **2015**, *99*, 8465-8474.
- [3] C. Ó'Fágáin, P. M. Cummins, B. F. O'Connor, in *Protein Chromatography: Methods and Protocols, Vol. 681* (Eds.: D. Walls, T. S. Loughran), Humana Press, New York, **2011**, pp. 25-33.
- [4] S. Hanessian, P.-P. Lu, H. Ishida, *J. Am. Chem. Soc.* **1998**, *120*, 13296-13300.

Integrated process design for biocatalytic synthesis  
by a Leloir Glycosyltransferase: UDP-glucose  
production with sucrose synthase



# Integrated Process Design for Biocatalytic Synthesis by a Leloir Glycosyltransferase: UDP-Glucose Production With Sucrose Synthase

Katharina Schmölzer,<sup>1</sup> Martin Lemmerer,<sup>1</sup> Alexander Gutmann,<sup>2</sup> Bernd Nidetzky<sup>1,2</sup>

<sup>1</sup>Austrian Centre of Industrial Biotechnology, Petersgasse 14, 8010 Graz, Austria

<sup>2</sup>Institute of Biotechnology and Biochemical Engineering, Graz University of Technology,

NAWI Graz, Petersgasse 12/I, 8010 Graz, Austria; telephone: +43 316 873 8400;

fax: +43 316 873 8434; e-mail: bernd.nidetzky@tugraz.at

**ABSTRACT:** Nucleotide sugar-dependent (“Leloir”) glycosyltransferases (GTs), represent a new paradigm for the application of biocatalytic glycosylations to the production of fine chemicals. However, it remains to be shown that GT processes meet the high efficiency targets of industrial biotransformations. We demonstrate in this study of uridine-5'-diphosphate glucose (UDP-glc) production by sucrose synthase (from *Acidithiobacillus caldus*) that a holistic process design, involving coordinated development of biocatalyst production, biotransformation, and downstream processing (DSP) was vital for target achievement at ~100 g scale synthesis. Constitutive expression in *Escherichia coli* shifted the recombinant protein production mainly to the stationary phase and enhanced the specific enzyme activity to a level (~480 U/g<sub>cell dry weight</sub>) suitable for whole-cell biotransformation. The UDP-glc production had excellent performance metrics of ~100 g<sub>product</sub>/L, 86% yield (based on UDP), and a total turnover number of 103 g<sub>UDP-glc</sub>/g<sub>cell dry weight</sub> at a space-time yield of 10 g/L/h. Using efficient chromatography-free DSP, the UDP-glc was isolated in a single batch with ≥90% purity and in 73% isolated yield. Overall, the process would allow production of ~0.7 kg of isolated product/L *E. coli* bioreactor culture, thus demonstrating how integrated process design promotes the practical use of a GT conversion.

Biotechnol. Bioeng. 2016;9999: 1–5.

© 2016 Wiley Periodicals, Inc.

**KEYWORDS:** Leloir glycosyltransferases; integrated process development; nucleotide sugars; sucrose synthase; glycobiotechnology; whole-cell biocatalyst

## Introduction

The carbohydrate chemistry is strongly centered around glycosylation, the formation of glycosidic bonds (Krasnova and Wong, 2016). Core problem in synthetic glycosylations is to combine tight control of selectivity with a suitable enhancement of reactivity. This is difficult to achieve by established routes, including the use of transglycosylases (Boltje et al., 2009; Krasnova and Wong, 2016). Because of their unsurpassed proficiency, nucleotide sugar-dependent (“Leloir”) glycosyltransferases (GTs; EC 2.4) are potential “game-changing” catalysts of synthetic glycosylation, enabling convenient conversions of unprotected substrates in single-step reactions. However, except for occasional applications, mainly for synthesis of selected oligosaccharides (Baumgärtner et al., 2013; Koizumi et al., 1998; Liu et al., 2003), these GTs represent a new paradigm for the biocatalytic production of glycosides as fine chemicals. Process technology for effective use of Leloir GTs is not well established and case studies of complete process analysis are lacking. In this study of uridine-5'-diphosphate glucose (UDP-glc) production by sucrose synthase (SuSy), as shown in Scheme 1, we describe integrated process design for whole-cell GT biocatalysis. Nucleoside-diphospho-sugars (NDP-sugars) are used as speciality carbohydrates and biochemical reagents (Warnock et al., 2005; Zhao et al., 2010). UDP-glc is the substrate of many GTs and also the precursor of various other UDP-sugars, such as UDP-galactose, UDP-glucuronic acid, and UDP-xylose (Eixelsberger and Nidetzky, 2014; Lee et al., 2010; Oka and Jigami, 2006). Therefore, its production was of particular interest.

About 60% of the industrial biocatalytic reactions use whole cells for reasons of time and cost (Straathof et al., 2002; Tufvesson et al., 2011a). Selected GTs were employed in whole-cell conversions (Baumgärtner et al., 2013; Koizumi et al., 1998; Liu et al., 2003; Mao et al., 2006) but typical efficiency targets of industrial

Katharina Schmölzer and Martin Lemmerer contributed equally to this work. Abbreviations: CIAP, calf intestinal alkaline phosphatase; DSP, downstream processing; GT, glycosyltransferase; UDP, uridine-5'-diphosphate; UMP, uridine-5'-monophosphate; SEC, size exclusion chromatography; SuSy, sucrose synthase.

Correspondence to: B. Nidetzky

Contract grant sponsor: Federal Ministry of Science, Research, and Economy (BMWFV)

Contract grant sponsor: Federal Ministry of Traffic, Innovation and Technology (BMVIT)

Contract grant sponsor: Styrian Business Promotion Agency (SFG)

Contract grant sponsor: Standortagentur Tirol

Contract grant sponsor: Government of Lower Austria

Contract grant sponsor: Business Agency Vienna

Contract grant sponsor: FFG-COMET-Funding Program

Contract grant sponsor: EU FP7 project SuSy

Contract grant number: 613633

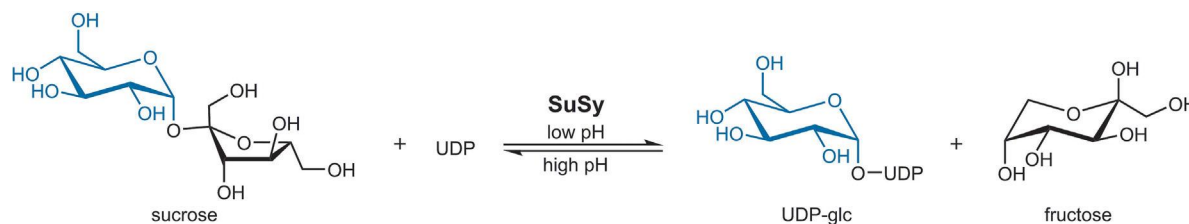
Received 22 August 2016; Revision received 11 October 2016; Accepted 17 October 2016

Accepted manuscript online xx Month 2016;

Article first published online in Wiley Online Library (wileyonlinelibrary.com).

DOI 10.1002/bit.26204

Integrated process design for biocatalytic synthesis by a Leloir Glycosyltransferase:  
UDP-glucose production with sucrose synthase



**Scheme 1.** UDP-glc synthesis from sucrose and UDP by SuSy.

biotransformations were not reached. The total turnover numbers (*TTN*) were fairly low ( $\leq 0.75 \text{ g}_{\text{product}}/\text{g}_{\text{cell wet weight}}$ ) in particular. Despite the high catalyst loadings ( $100\text{--}250 \text{ g}_{\text{CDW}}/\text{L}$ ) used, the space-time yields (*STYs*) were usually below  $1 \text{ g/L/h}$  and never exceeded  $5 \text{ g/L/h}$ . However, an average yield of  $\sim 80\%$ , a final product concentration  $\geq 100 \text{ g/L}$ , a  $STY \geq 15 \text{ g/L/h}$ , and a *TTN* of  $70\text{--}230 \text{ g}_{\text{product}}/\text{g}_{\text{cell dry weight}}$  are usually the minimum requirements set for the fine chemical industry (Straathof et al., 2002; Tufvesson et al., 2011a). Integrated process development is key to the success of industrial biocatalysis (Panke et al., 2000; Tufvesson et al., 2011b). The interrelation of all tasks, including the biocatalyst production, the biocatalytic process, and the downstream processing (DSP) has to be considered right from the beginning. In the process described herein, the SuSy from *Acidithiobacillus caldus* (SuSyAc; Diricks et al., 2015) was used as whole-cell catalyst and UDP-glc production at  $\sim 100 \text{ g}$  scale is demonstrated.

The efficiency of the whole-cell catalyst production is critical to the performance of the biocatalytic process (Eixelsberger et al., 2013; Tufvesson et al., 2011a). As earlier reported in Diricks et al. (2015), SuSyAc was expressed in *Escherichia coli* harboring the expression vector pCXP34h, in which the SuSyAc gene was under the control of a constitutive promoter of intermediate strength (Fig. S1, Aerts et al., 2011). A simple constitutive expression system like this is beneficial for the mass production of the biocatalyst as no

costly chemical inducers are needed (Lee et al., 1997). However, SuSyAc expression under standard conditions yielded only  $\geq 8 \text{ mg/L}$  (based on purification) (Diricks et al., 2015; Schmöler et al., 2016). Thus, the production of recombinant biomass suitable for whole-cell catalysis was a clear requirement. Based on the aforementioned necessary performance metrics of the biotransformation, the maximum catalyst loading is limited to  $\sim 1 \text{ g}_{\text{CDW}}/\text{L}$  in the whole-cell conversion. This results in a specific whole cell activity of  $\sim 450 \text{ U/g}_{\text{CDW}}$  as a target value. To achieve this, we replaced *E. coli* shake flask cultivation previously used for production of SuSyAc (Diricks et al., 2015), by a batch fermentation process using LB medium supplemented with glucose, trace elements, and additional salts (medium C2; see the Supporting Information; Eixelsberger et al., 2013). Full time-courses of glucose utilization, biomass growth, and SuSyAc activity were recorded and the results are shown in Figure 1A. This revealed that the SuSyAc production was mainly shifted to the stationary phase when glucose was depleted. A shift toward the stationary phase is not unusual under these conditions (Kleist et al., 2003). The SuSyAc expression was apparently subject to catabolite repression in response to the glucose availability. This was also observed for a constitutively expressed D-hydantoinase (Lee et al., 1997). The resulting slow SuSyAc expression appeared to have been beneficial for the enzyme production. The final specific and volumetric activities (based on

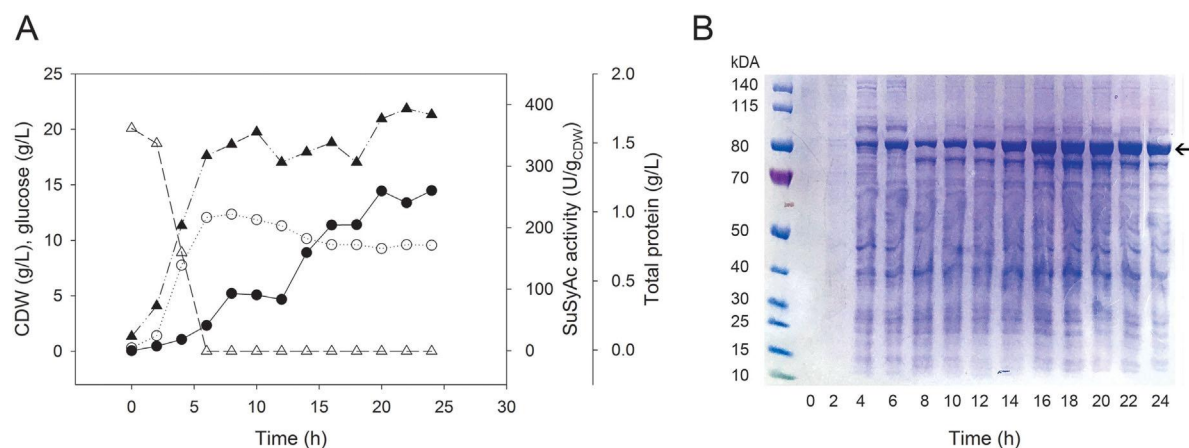


**Figure 1.** Time-course analysis of *E. coli* bioreactor cultivation for production of SuSyAc is shown. (A) Cell dry weight (CDW) (g/L) is shown as open circles, the glucose concentration (g/L) as open triangles, the total protein concentration (g/L) as filled triangles and the SuSyAc activity ( $\text{U/g}_{\text{CDW}}$ ) of the cell-free extract as filled circles. (B) A SDS polyacrylamide gel of the cell-free extract of *E. coli* at different cultivation times is shown. The corresponding protein band of SuSyAc (monomeric subunit) is indicated by an arrow.

## Integrated process design for biocatalytic synthesis by a Leloir Glycosyltransferase: UDP-glucose production with sucrose synthase

whole cells) were  $\sim 480 \text{ U/g}_{\text{CDW}}$  and  $\sim 4600 \text{ U/L}$ , respectively. A rough quantification of SuSyAc in the cell-free extract by size exclusion chromatography (SEC) yielded  $\sim 350 \text{ mg/L}_{\text{medium}}$  (Fig. S2). The SuSyAc amount expressed correlated well with the volumetric activity (Fig. S3). The SDS gel (Fig. 1B) showed a predominant band at an apparent molecular mass of  $>80 \text{ kDa}$ , representing the SuSyAc subunit. The native molecular mass of SuSyAc estimated by SEC was about  $367 \text{ kDa}$ , consistent with a SuSy homotetramer as reported for SuSys from other sources (Schmölzer et al., 2016). Under the conditions described, the target expression level of SuSyAc was clearly reached. Furthermore, the SuSy yield was 10- to 100-fold increased compared to maximum enzyme titers of different SuSys in the literature (3 and  $25 \text{ mg/L}_{\text{medium}}$ , Schmölzer et al., 2016).

In the next step, we applied the whole-cell SuSyAc to the synthesis of UDP-glc (Scheme 1) from UDP (0.21 M) and sucrose (1.5 M). A  $\sim 7$ -fold molar excess of sucrose was applied to maximize the utilization of UDP in the equilibrium-controlled reaction of the SuSy. To overcome mass transfer limitations in the whole-cell conversion, simple cell permeabilization by one freeze-thaw cycle was used (Fig. 2A) (Chen, 2007; Liu et al., 2003). Under the conditions applied, the activity of freeze-thawed cells reached  $\sim 90\%$  of the respective sonicated cell level. The mass transport was therefore not hindered in our whole-cell setup. In comparison to the whole-cell SuSyAc, the cell-free extract showed only  $\sim 53\%$  of the activity. The activity of the insoluble fraction accounted for about 50% of the total activity of the cell lysate. This could result from membrane association of the enzyme, as reported for plant SuSys (Amor et al., 1995). Figure 2B depicts whole-cell synthesis of UDP-glc on  $\sim 50 \text{ g}$  scale. Despite a biocatalyst concentration of only  $1 \text{ g}_{\text{CDW/L}}$ , a high initial UDP-glc production rate of  $55 \text{ mM/h}$  was reached, which remained constant over  $\sim 3 \text{ h}$ . UDP-glc was obtained in high yield (86%; based on UDP) and concentration ( $103 \text{ g/L}$ ,  $181 \text{ mM}$ ) within 10 h, giving a *STY* of  $10 \text{ g/L/h}$  and an excellent *TTN* value of  $103 \text{ g}_{\text{UDP-glc}}/\text{g}_{\text{CDW}}$ . Once formed, the UDP-glc was very stable. Less than 0.1% was degraded within the next 12 h and UDP was not degraded at all under the reaction conditions applied. Considering the final cell density of  $\sim 10 \text{ g}_{\text{CDW/L}}$  of the *E. coli* bioreactor cultivation, it would be possible to synthesize about 1 kg of UDP-glc from 1 L culture medium.

The whole-cell synthesis of UDP-glc met the above-described parameters of process efficiency. Benchmarked against the best NDP-sugar syntheses using whole cells, the UDP-glc concentration of  $181 \text{ mM}$  represents a significant improvement (2.5- to 3.5-fold) (Kawai et al., 1978; Koizumi et al., 1998; Nahalka and Patoprsty, 2009). The *STY* was 2.4- to 4.8-fold enhanced. The *TTN* of  $103 \text{ g}_{\text{UDP-glc}}/\text{g}_{\text{CDW}}$  presents an improvement by one to two orders of magnitude. This *TTN* value already meets the level ( $10^2$ – $10^4 \text{ g}_{\text{product}}/\text{g}_{\text{catalyst}}$ ) of chemical processes and bioprocesses that use immobilized enzymes or immobilized whole cells (Thomas et al., 2002). The high product concentration obtained at low catalyst loading facilitates the subsequent DSP and furthermore is beneficial for the scalability of the GT process (Straathof et al., 2002).

We have recently developed a convenient chromatography-free DSP of NDP-sugars from SuSy reaction mixtures (Lemmerer et al., 2016). The DSP included calf intestinal alkaline phosphatase (CIAP)

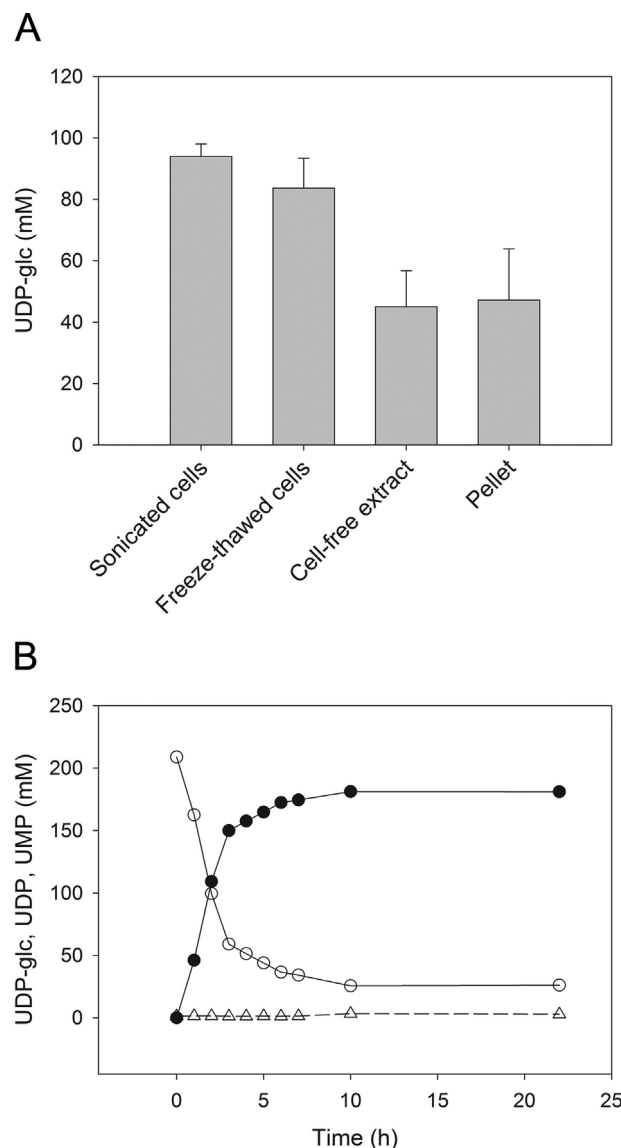


**Figure 2.** UDP-glc synthesis by whole-cell SuSyAc is shown. (A) Different biocatalyst preparations are compared at the same amount of cells used in the reactions. The UDP-glc concentration after 45 min is shown. (B) Production of 41 g UDP-glc in a 400 mL bioreactor using  $1 \text{ g}_{\text{CDW/L}}$  of biocatalyst. The symbols show UDP-glc, filled circle; UDP, open circle; and UMP, open triangle. All reactions contained 0.21 M UDP, 1.5 M sucrose, 10 mM  $\text{MgCl}_2$ , and were carried out at pH 5.0,  $37^\circ \text{C}$ .

treatment for selective hydrolysis of the phosphomonoesters (UMP, UDP) present in the reaction mixture (Fig. 2B) into the nucleoside and inorganic phosphate. Separation from remaining sugars (sucrose, fructose) and nucleosides (uridine) was accomplished by repeated product precipitation with 4-fold excess of ethanol (EtOH). This DSP was adapted here for use with mixtures from whole-cell biotransformation and compared to the earlier study, it was up-scaled by about 100-fold. Results of a single-batch purification of UDP-glc at 30 g scale are summarized in Table I. The product was recovered in 73% yield and  $\geq 90\%$  purity (see also Table I and Fig. S4). UDP-glc was thus prepared from UDP in 63% overall yield.

# Integrated process design for biocatalytic synthesis by a Leloir Glycosyltransferase: UDP-glucose production with sucrose synthase

**Table 1.** The UDP-glc production summarized.

Sample	UDP-glc <sup>e</sup> (g)	Yield (%)
After whole-cell synthesis	40.9	86.0
After filtration <sup>a</sup> and CIAP digest <sup>b</sup>	38.7	81.4
EtOH precipitate 1	38.0	79.9
After filtration <sup>c</sup> and EtOH precipitate 2	32.7	68.7
EtOH precipitate 3 <sup>d</sup>	30.6	64.2
Freeze-dried sample	30.0 <sup>f</sup>	63.0

<sup>a</sup>Whole-cell removal.

<sup>b</sup>CIAP reaction (10 U/mL) was carried out overnight at 30°C, pH 7.0.

<sup>c</sup>CIAP removal.

<sup>d</sup>Precipitate 3 was air-dried at room temperature and dissolved in deionized water to a final concentration of ~90 mg/mL before freeze-drying.

<sup>e</sup>Absolute amount of pure UDP-glc.

<sup>f</sup>Freeze-drying yielded 37.7 g of white powder containing 80% (30.0 g) UDP-glc, 6.1% phosphate, 1.2% EtOH, 0.7% sucrose, 0.6% UMP, and H<sub>2</sub>O.

Product identity was unequivocally confirmed by <sup>1</sup>H and <sup>13</sup>C NMR spectroscopy (Figs. S5 and S6). The UDP-glc thus obtained meets commercial standards of quality (e.g., Carbosynth product MU08960).

In this work, to our knowledge for the first time, a process using a Leloir GT reached the typical efficiency targets of industrial biotransformations. Integrated design was essential to realize UDP-glc production at ~100 g scale. The established process would allow the production of ~0.7 kg of isolated product/L of bioreactor culture. The success of this holistic approach might support the development of other GTs into industrial biocatalysts.

## Materials and Methods

### Chemicals

Media components and chemicals were of reagent grade from Sigma Aldrich/Fluka (Vienna, Austria), Roth (Karlsruhe, Germany) or Merck (Vienna, Austria). UDP disodium salt (purity ≥98%) was from Carbosynth (Compton, Berkshire, UK). CIAP was from New England Biolabs (Ipswich, MA). EtOH (purity 96%) was from Lactan (Graz, Austria).

### Strain and Cell Cultivation

*E. coli* BL21 (DE3) strain harboring the expression vector pCXP34h was used for production of SuSyAc (Diricks et al., 2015). The vector provides ampicillin resistance and target protein expression under the control of a constitutive promoter (P34) (Aerts et al., 2011). LB medium supplemented with 20 g/L glucose · H<sub>2</sub>O, 1 g/L NH<sub>4</sub>Cl; 0.25 g/L MgSO<sub>4</sub> · 7H<sub>2</sub>O; 3 g/L K<sub>2</sub>HPO<sub>4</sub>, 6 g/L KH<sub>2</sub>PO<sub>4</sub>, 0.1 mL/L polypropylene glycol, 115 µg/mL ampicillin, 2 µg/mL thiamine, and trace elements was used (medium C2, Eixelsberger et al., 2013). Pre-cultures (300 mL in 1000 mL baffled shake flasks) were inoculated from glycerol stock. Incubation was overnight at 37°C and 130 rpm (Certomat<sup>®</sup> BS-1; Sartorius, Germany). Fermentation was performed in a Biostat CT 6.9 L bioreactor from Braun Biotech International (Melsungen, Germany). The bioreactor was inoculated to an OD<sub>600</sub> of 0.5. Dissolved oxygen was kept at 40% air saturation by an agitation and airflow cascade. pH was controlled at 7.0 with 2 M potassium hydroxide and 1 M

phosphoric acid. 10% polypropylene glycol was used for foam control. The temperature was kept constant at 37°C. For full details, sampling and sample analysis (CDW, SuSyAc activity, total protein, SEC) see the Supporting information. Biomass was resuspended in deionized water (~100 g<sub>CDW</sub>/L) and stored at -20°C.

### UDP-Glc Synthesis by Different Biocatalyst Preparations

SuSyAc activities of freeze-thawed cells, sonicated cells, cell-free extract, and insoluble fraction (pellet) were compared. Freeze-thawed cell suspension was ultrasonicated. Supernatant (cell-free extract) was collected after centrifugation (21,130 g, 4°C, 30 min, Centrifuge 5424 R; Eppendorf). Pellet was resuspended in deionized water. UDP-glc synthesis by different biocatalyst preparations was carried out for 45 min at pH 5.0, 37°C. The reaction mixtures contained 0.21 M UDP, 1.5 M sucrose, and 10 mM MgCl<sub>2</sub>. Preparations were compared at the same amount of cells. See the Supplementary information for full details.

### Whole-Cell Synthesis of UDP-Glc

It was known from studies using the free enzyme (Gutmann and Nidetzky, 2016), that pH control at 5.0 is crucial for high conversion. The reaction was performed in a total volume of 400 mL using 84.1 mmol UDP disodium salt (38 g), 600 mmol sucrose (205 g), and 4 mmol MgCl<sub>2</sub> (0.38 g) dissolved in water. The pH was adjusted to 5.0 with 1 M sodium hydroxide and the reaction was started by adding 1 g<sub>CDW</sub>/L freeze-thawed whole-cell SuSyAc. The conversion was performed at 37°C in a temperature controlled room in a Duran Schott bottle (diameter 7.5 cm, height 10 cm) under magnetic stirring (stir bar: 50 × 7 mm; 150 rpm). The pH was constantly monitored and manually controlled by adding 100% acetic acid. Incubation was for 22 h. Samples were taken at certain times and analyzed by HPLC.

### Downstream Processing of UDP-Glc

Chromatography-free DSP of UDP-glc was performed according to Lemmerer et al. (2016). Biomass was roughly removed by vacuum filtration through cellulose filter paper discs (Macherey-Nagel, MN 619 EH, particle retention 2–26 µm, thickness 0.17 mm, diameter 150 mm, 1 per 100 mL suspension). The permeate was ultrafiltered using a Vivaflow 50 unit (50 kDa; polyethersulfone; Sartorius, Germany) to remove residual cells. CIAP (10 U/mL) was added to the permeate to hydrolyze all phosphomonoesters (e.g., UDP) while leaving intact the UDP-glc, which contains a phosphodiester linkage. The reaction was carried out at 30°C, pH 7.0 for 24 h. This CIAP sample was supplemented with 200 mM sodium acetate. For product purification, UDP-glc was precipitated three times with five volumes of EtOH at -20°C for 72 h. Precipitates were dissolved in deionized water. After the first precipitation step, CIAP was removed by Vivaspin concentrators (10 kDa; 4000 rpm, 20°C). The final precipitate was air-dried at room temperature, dissolved in deionized water to ~90 mg/mL, frozen at -80°C, and freeze-dried (Christ Alpha 1–4, B. Braun Biotech International, Melsungen, Germany) for 72 h. See Supplementary information for more details.

# Integrated process design for biocatalytic synthesis by a Leloir Glycosyltransferase: UDP-glucose production with sucrose synthase

## Analytical Methods

HPLC analysis is described in Lemmerer et al. (2016). See Supplementary information for details.

This work was supported by the Federal Ministry of Science, Research and Economy (BMWFV), the Federal Ministry of Traffic, Innovation and Technology (BMVIT), the Styrian Business Promotion Agency SFG, the Standortagentur Tirol, the Government of Lower Austria and Business Agency Vienna through the COMET-Funding Program managed by the Austrian Research Promotion Agency FFG. Financial support from the EU FP7 project SuSy (Sucrose Synthase as Effective Mediator of Glycosylation) is gratefully acknowledged. The authors thank Dr. Hansjörg Weber from the Graz University of Technology for NMR analysis and Prof. Tom Desmet, Ghent University (Belgium) for the plasmid expression vector pCXP34h carrying the SuSyAc gene.

## References

- Aerts D, Verhaeghe T, De Mey M, Desmet T, Soetaert W. 2011. A constitutive expression system for high-throughput screening. *Eng Life Sci* 11(1):10–19.
- Amor Y, Haigler CH, Johnson S, Wainwright M, Delmer DP. 1995. A membrane-associated form of sucrose synthase and its potential role in synthesis of cellulose and callose in plants. *Proc Natl Acad Sci USA* 92(20):9353–9357.
- Baumgärtner F, Seitz L, Sprenger GA, Albermann C. 2013. Construction of *Escherichia coli* strains with chromosomally integrated expression cassettes for the synthesis of 2'-fucosyllactose. *Microb Cell Fact* 12(1):1–13.
- Boltje TJ, Buskas T, Boons G-J. 2009. Opportunities and challenges in synthetic oligosaccharide and glycoconjugate research. *Nat Chem* 1(8):611–622.
- Chen RR. 2007. Permeability issues in whole-cell bioprocesses and cellular membrane engineering. *Appl Microbiol Biotechnol* 74(4):730–738.
- Diricks M, De Bruyn F, Van Daele P, Walmagh M, Desmet T. 2015. Identification of sucrose synthase in nonphotosynthetic bacteria and characterization of the recombinant enzymes. *Appl Microbiol Biotechnol* 99(20):8465–8474.
- Eixelsberger T, Nidetzky B. 2014. Enzymatic redox cascade for one-pot synthesis of uridine 5'-diphosphate xylose from uridine 5'-diphosphate glucose. *Adv Synth Catal* 356(17):3575–3584.
- Eixelsberger T, Woodley JM, Nidetzky B, Kratzer R. 2013. Scale-up and intensification of (S)-1-(2-chlorophenyl) ethanol bioproduction: Economic evaluation of whole cell-catalyzed reduction of *o*-chloroacetophenone. *Biotechnol Bioeng* 110(8):2311–2315.
- Gutmann A, Nidetzky B. 2016. Unlocking the potential of Leloir glycosyltransferases for applied biocatalysis: Efficient synthesis of uridine 5'-diphosphate-glucose by sucrose synthase. *Adv Synth Catal* (in press) <http://onlinelibrary.wiley.com/doi/10.1002/adsc.201600754/full>
- Kawai H, Nakajima S, Okuda M, Yano T, Tachiki T, Tochikura T. 1978. Production of UDP-glucose by *Torulopsis candida* IFO 0768: Studies on microbial metabolism of sugar nucleotides (VIII). *J Ferment Technol* 56(6):586–592.
- Kleist S, Miksch G, Hitzmann B, Arndt M, Friehs K, Flaschel E. 2003. Optimization of the extracellular production of a bacterial phytase with *Escherichia coli* by using different fed-batch fermentation strategies. *Appl Microbiol Biotechnol* 61(5):456–462.
- Koizumi S, Endo T, Tabata K, Ozaki A. 1998. Large-scale production of UDP-galactose and globotriose by coupling metabolically engineered bacteria. *Nat Biotechnol* 16(9):847–850.
- Krasnova L, Wong C-H. 2016. Understanding the chemistry and biology of glycosylation with glycan synthesis. *Annu Rev Biochem* 85(1):599–630.
- Lee D-C, Kim G-J, Cha Y-K, Lee C-Y, Kim H-S. 1997. Mass production of thermostable D-hydantoinase by batch culture of recombinant *Escherichia coli* with a constitutive expression system. *Biotechnol Bioeng* 56(4):449–455.
- Lee J-H, Chung S-W, Lee H-J, Jang K-S, Lee S-G, Kim B-G. 2010. Optimization of the enzymatic one pot reaction for the synthesis of uridine 5'-diphosphogalactose. *Bioprocess Biosyst Eng* 33(1):71–78.
- Lemmerer M, Schmörlzer K, Gutmann A, Nidetzky B. 2016. Downstream processing of nucleoside-diphospho-sugars from sucrose synthase reaction mixtures at decreased solvent consumption. *Adv Synth Catal* 358(19):3113–3122.
- Liu Z, Lu Y, Zhang J, Pardee K, Wang PG. 2003. P1 trisaccharide (Gal $\alpha$ 1,4Gal $\beta$ 1,4GlcNAc) synthesis by enzyme glycosylation reactions using recombinant *Escherichia coli*. *Appl Environ Microbiol* 69(4):2110–2115.
- Mao Z, Shin HD, Chen RR. 2006. Engineering the *E. coli* UDP-glucose synthesis pathway for oligosaccharide synthesis. *Biotechnol Prog* 22(2):369–374.
- Nahalka J, Patoprsty V. 2009. Enzymatic synthesis of sialylation substrates powered by a novel polyphosphate kinase (PPK3). *Org Biomol Chem* 7(9):1778–1780.
- Oka T, Jigami Y. 2006. Reconstruction of *de novo* pathway for synthesis of UDP-glucuronic acid and UDP-xylose from intrinsic UDP-glucose in *Saccharomyces cerevisiae*. *FEBS J* 273(12):2645–2657.
- Panke S, Wubbolts MG, Schmid A, Witholt B. 2000. Production of enantiopure styrene oxide by recombinant *Escherichia coli* synthesizing a two-component styrene monooxygenase. *Biotechnol Bioeng* 69(1):91–100.
- Schmörlzer K, Gutmann A, Diricks M, Desmet T, Nidetzky B. 2016. Sucrose synthase: A unique glycosyltransferase for biocatalytic glycosylation process development. *Biotechnol Adv* 34(2):88–111.
- Straathof AJ, Panke S, Schmid A. 2002. The production of fine chemicals by biotransformations. *Curr Opin Biotechnol* 13(6):548–556.
- Thomas SM, DiCosimo R, Nagarajan V. 2002. Biocatalysis: Applications and potentials for the chemical industry. *Trends Biotechnol* 20(6):238–242.
- Tufvesson P, Lima-Ramos J, Nordblad M, Woodley JM. 2011a. Guidelines and cost analysis for catalyst production in biocatalytic processes. *Org Process Res Dev* 15(1):266–274.
- Tufvesson P, Lima-Ramos J, Jensen JS, Al-Haque N, Neto W, Woodley JM. 2011b. Process considerations for the asymmetric synthesis of chiral amines using transaminases. *Biotechnol Bioeng* 108(7):1479–1493.
- Warnock D, Bai X, Autote K, Gonzales J, Kinealy K, Yan B, Qian J, Stevenson T, Zopf D, Bayer RJ. 2005. *In vitro* galactosylation of human IgG at 1kg scale using recombinant galactosyltransferase. *Biotechnol Bioeng* 92(7):831–842.
- Zhao G, Guan W, Cai L, Wang PG. 2010. Enzymatic route to preparative-scale synthesis of UDP-GlcNAc/GalNAc, their analogues and GDP-fucose. *Nat Protoc* 5(4):636–646.

## Supporting Information

Additional supporting information may be found in the online version of this article at the publisher's web-site.

## Supporting Information

# Integrated Process Design for Biocatalytic Synthesis by a Leloir Glycosyltransferase: UDP-Glucose Production with Sucrose Synthase

Katharina Schmölzer<sup>1</sup>, Martin Lemmerer<sup>1</sup>, Alexander Gutmann<sup>2</sup>, Bernd Nidetzky<sup>1,2</sup>

<sup>1</sup>Austrian Centre of Industrial Biotechnology, Petersgasse 14, 8010 Graz, Austria

<sup>2</sup>Institute of Biotechnology and Biochemical Engineering, Graz University of Technology,  
NAWI Graz, Petersgasse 12/I, 8010 Graz, Austria

**Corresponding author:** bernd.nidetzky@tugraz.at; Phone: +43 316 873 8400; FAX: +43  
316 873 8434

Proofs and reprints should be addressed to Bernd Nidetzky.

Authors' contributions: Katharina Schmölzer and Martin Lemmerer contributed equally to  
this work.

### Table of Contents

Analytical Methods	S3
Strain, Cell Cultivation, Sampling and Sample Analysis	S3
UDP-Glc Synthesis by Different Biocatalyst Preparations	S6
Downstream Processing of UDP-Glc	S6
<sup>1</sup> H and <sup>13</sup> C NMR Measurements	S7
Figure S1. Oligonucleotide sequence of the P34 promoter region as in pCXP34h	S8

Figure S2. SEC analysis of SuSyAc	S9
Figure S3. Time-course analysis of <i>E. coli</i> bioreactor cultivation for production of SuSyAc (relative SuSyAc concentration determined by SEC <i>versus</i> relative volumetric SuSyAc activity is shown)	S10
Figure S4. Final purity of UDP-glc after the chromatography-free DSP. Superposition of ion-pair reversed phase and ion exchange HPLC elution profiles	S11
Figure S5. <sup>1</sup> H NMR spectrum of produced UDP-glc	S12
Figure S6. <sup>13</sup> C NMR spectrum of produced UDP-glc	S13
References for Supporting Information	S14

## Methods

### Analytical Methods

UDP-glc, uridine, UMP and UDP were analyzed by reversed phase HPLC using a Kinetex® C18 column (5  $\mu\text{m}$ , 100  $\text{\AA}$ , 50 x 4.6 mm; Phenomenex, Germany) in reversed phase ion-pairing mode (Lemmerer et al. 2016). HPLC analysis was performed at 35°C with a mobile phase of 87.5% 20 mM potassium phosphate buffer, pH 5.9 containing 40 mM tetra-n-butylammonium bromide (TBAB) and 12.5% acetonitrile at an isocratic flow rate of 2 mL/min. UV-detection at 262 nm was used.

Sucrose, fructose, glucose, acetate, phosphate and EtOH were analyzed by HPLC as described by Petschacher et al. (2008). A Merck-Hitachi LaChrome HPLC System equipped with an Aminex HPX-87H (Biorad, Richmond, CA, USA) column, a Merck-Hitachi LaChrome L-7250 autosampler and a Merck L-7490 RI detector was used. The system was operated at 65°C, using a flow rate of 0.6 mL/min for the eluent (5 mM sulfuric acid). Applied conditions caused hydrolysis of sucrose into equimolar concentrations of fructose and glucose. The difference of glucose and fructose gave the remaining fructose.

Authentic standards were used for calibration.

### Strain, Cell Cultivation, Sampling and Sample Analysis

*Strain for Production of SuSyAc.* *E. coli* BL21 (DE3) strain harboring the expression vector pCXP34h was used for production of SuSyAc, as earlier reported in Diricks et al. (2015). The vector provides ampicillin resistance and target protein expression under the control of a constitutive promoter (P34) of intermediate strength (Aerts et al. 2011). The strain was stored in glycerol stocks at -70°C.

*E. coli Bioreactor Cultivation for Production of SuSyAc.* LB medium supplemented with glucose, salts and trace elements was used (medium C2; Eixelsberger et al. 2013). Medium



C2 contains 10 g/L peptone from casein; 5 g/L yeast extract; 5 g/L NaCl; 5.5 g/L (pre-culture) or 20 g/L glucose·H<sub>2</sub>O (main culture); 1 g/L NH<sub>4</sub>Cl; 0.25 g/L MgSO<sub>4</sub>·7H<sub>2</sub>O; 1 mL/L trace element solution (4 g/L FeSO<sub>4</sub>·7H<sub>2</sub>O; 1 g/L MnSO<sub>4</sub>·H<sub>2</sub>O; 0.73 g/L CoCl<sub>2</sub>·6H<sub>2</sub>O; 0.1 g/L H<sub>3</sub>BO<sub>3</sub>; 0.095 g/L CuSO<sub>4</sub>; 0.2 g/L ZnSO<sub>4</sub>·7H<sub>2</sub>O; 0.2 g/L Na<sub>2</sub>MoO<sub>4</sub>·7H<sub>2</sub>O; 0.55 g/L AlCl<sub>3</sub>·6H<sub>2</sub>O); 0.1 mL/L polypropylene glycol, 3 g/L K<sub>2</sub>HPO<sub>4</sub> and 6 g/L KH<sub>2</sub>PO<sub>4</sub>. Filter-sterilized ampicillin (115 µg/mL) and thiamine (2 µg/mL) were added. Pre-cultures (300 mL in 1000 mL baffled shake flasks) were inoculated from glycerol stock (100 µL). Incubation was overnight at 37°C and 130 rpm (Certomat<sup>®</sup> BS-1; Sartorius, Germany). Main cultivation was carried out in a Biostat CT bioreactor (Braun Biotech International; Melsungen, Germany) with 5 L working volume (for dimensions see Eixelsberger et al. 2013). The bioreactor was inoculated to an OD<sub>600</sub> of 0.5. Dissolved oxygen was kept at 40% air saturation by an agitation (150 to 1000 rpm) and airflow (7.5 L pressurized air per min) cascade. The pH was maintained at 7.0 by an automated addition of 2 M potassium hydroxide and 1 M phosphoric acid. 10% polypropylene glycol was used for foam control. The temperature was kept constant at 37°C. The cell growth was recorded as increase in OD<sub>600</sub>. Samples (2 mL; 50 mL) were collected by centrifugation at 4°C for 30 min (for details see ‘Determination of Cell Dry Weight’ and ‘SuSyAc activity’). Pellets were used for determination of CDW or stored at -20°C for further analysis. The glucose concentration in the supernatant was determined by ion exchange HPLC and RI detection. Cells were harvested after 24 h by 30 min centrifugation (Sorvall RC-5B) at 4°C, 4420 g, resuspended in deionized water to a concentration of ~100 g<sub>CDW</sub>/L and stored at -20°C for further analysis and UDP-glc synthesis.

*Determination of Cell Dry Weight.* 2 mL of cell suspension were transferred in pre-weighed Eppendorf tubes and harvested by centrifugation (21,130 g, 4°C, 30 min, Centrifuge 5424 R;

Eppendorf). Pellets were dried to constant weight at 105°C. Experiments were carried out in duplicate.

*Determination of SuSyAc Activity and Total Protein Concentration.* 50 mL samples were centrifuged at 4500 g, 4°C for 30 min in an Eppendorf 5804 R centrifuge (Eppendorf, Germany). SuSyAc activity of whole cells (after freeze-thawing) or cell-free extracts was determined as indicated in the text. Cell-free extracts were prepared by sonication followed by centrifugation (21,130 g, 4°C, 30 min, Centrifuge 5424 R; Eppendorf). One unit of sucrose cleavage activity by SuSyAc was defined as the amount of catalyst producing at 45°C 1 µmol UDP-glc per min from 500 mM sucrose and 10 mM UDP. As buffer 100 mM MES, pH 5.5 containing 10 mM MgCl<sub>2</sub> was used. 0.01% BSA was added to reactions with cell-free extract. Reactions were performed in a volume of 200 µL in 1.5 mL Eppendorf tubes on a thermomixer comfort (Eppendorf, Germany) at 150 rpm (whole cells) or without agitation (cell-free extract). Samples (10 µL) were taken at certain times and reactions were stopped adding 90 µL of 1:2 diluted acetonitrile. Cells or precipitated proteins were removed by centrifugation (21,130 g, 4°C, 15 min, Centrifuge 5424 R; Eppendorf). Supernatant was analyzed by reverse phase ion-pair HPLC. Initial reaction rates were calculated. Total protein concentration of the cell-free extract was determined using the Pierce<sup>TM</sup> BCA Protein Assay Kit from Thermo Scientific (Waltham, MA, US).

*Characterization of SuSyAc by Size Exclusion Chromatography.* In order to determine the oligomerization state of SuSyAc and for rough enzyme quantification, 50 µL of 10-fold diluted cell-free extract were fractionated by size exclusion chromatography (SEC) on a G3000SWXL column (300 mm × 7.8 mm, inner diameter 5 µm; Tosoh Bioscience, Tokyo, Japan). The column was operated at room temperature and a flow rate of 0.4 mL/min with 150 mM potassium phosphate, pH 6.5. The detection was performed at three different wavelengths (214, 260 and 280 nm) to distinguish between peptides/proteins and nucleic

acids. The HMW Native Marker Kit (GE Healthcare, Austria) was used for calibration. Activities of different fractions were determined as described above. Purified SuSyAc was used as authentic standard (Diricks et al. 2015).

### **UDP-Glc Synthesis by Different Biocatalyst Preparations**

SuSyAc activities of freeze-thawed cells, sonicated cells, cell-free extract and insoluble fraction (pellet) were compared. 5 mL of freeze-thawed cell suspension were ultrasonicated on ice bath at 30% amplitude for 5 min (1 s pulse on and 2 s pulse off) using a Sonic Dismembrator (Ultrasonic Processor FB-505; Fisher Scientific, Austria) equipped with a 3.1 mm microtip. Supernatant (cell-free extract) from 1 mL sample was collected after centrifugation at 21,130 g and 4°C for 30 min (Centrifuge 5424 R; Eppendorf). Volume of the supernatant was about 0.7 mL. The Pellet was resuspended in deionized water (final volume 1 mL). UDP-glc synthesis by different biocatalyst preparations, derived from the same amount of cells, was carried out at pH 5.0, 37°C. The reaction mixtures contained 0.21 M UDP, 1.5 M sucrose and 10 mM MgCl<sub>2</sub>. Reactions were run for 45 min.

### **Downstream Processing of UDP-Glc**

Chromatography-free DSP of UDP-glc was performed according to Lemmerer et al. (2016). After completion of the biotransformation, biomass was roughly removed by vacuum filtration through cellulose filter paper discs (Macherey-Nagel, MN 619 EH, particle retention 2 – 26 µm, thickness 0.17 mm, diameter 150 mm, 1 per 100 mL suspension). The permeate was ultrafiltered using a Vivaflow 50 unit (50 kDa; polyethersulfone; Sartorius, Germany) to remove residual cells. Then CIAP was used to hydrolyze all phosphomonoesters (UMP, UDP) in the sample while leaving intact the UDP-glc, which contains a phosphodiester linkage. CIAP (10 U/mL) was added to the permeate and the reaction was carried out at 30°C for 24 h, controlling the pH at 7.0 using 1 M sodium hydroxide. This

CIAP sample was supplemented with 200 mM sodium acetate. For product purification, UDP-glc was precipitated 3 times with 5 volumes of EtOH at -20°C for 72 h. The first EtOH precipitation step was performed before CIAP removal to reduce viscosity for improved filterability. The precipitate was dissolved in deionized water to give the initial UDP-glc concentration and CIAP (molecular mass of 69 kDa) was removed by Vivaspin concentrators (10 kDa; 4000 rpm, 20 °C). The permeate was 3-fold diluted to further reduce viscosity. A 3-fold dilution presented a compromise between viscosity reduction for better separation of UDP-glc from remaining sugars in EtOH precipitation steps and final volume of the sample. Two additional EtOH precipitation steps were performed as described above. The final precipitate was air-dried at room temperature, dissolved in deionized water to a final concentration of ~90 mg/mL, frozen at -80°C and freeze-dried (Christ Alpha 1-4, B. Braun Biotech International, Melsungen, Germany) for 72 h. Samples were taken at each step and analyzed by HPLC.

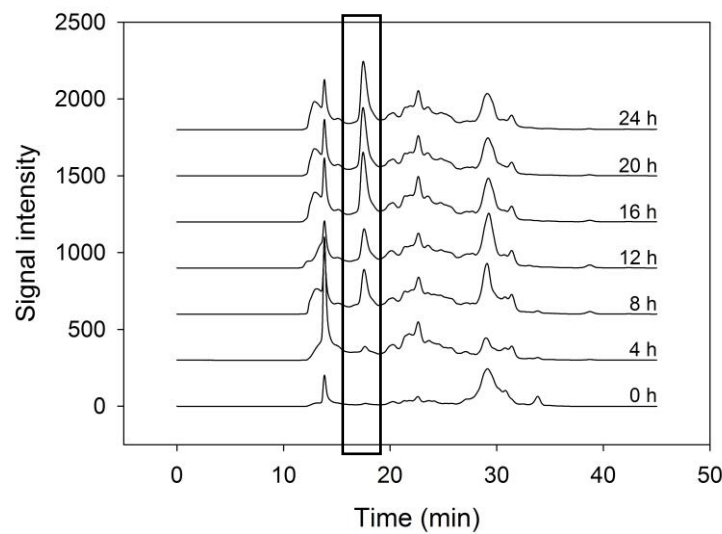
### **<sup>1</sup>H and <sup>13</sup>C NMR Measurements**

~10 mg of UDP-glc were dissolved in 600 µL D<sub>2</sub>O. A Varian (Agilent) INOVA 500-MHz NMR spectrometer (Agilent Technologies, Santa Clara, California, USA) and the VNMRJ 2.2D software were used for all measurements. <sup>1</sup>H NMR spectra (499.98 MHz) were measured on a 5 mm indirect detection PFG-probe, while a 5 mm dual direct detection probe with z-gradients was used for <sup>13</sup>C NMR spectra (125.71 MHz). Standard pre-saturation sequence was used: relaxation delay 2 s; 90° proton pulse; 2.048 s acquisition time; spectral width 8 kHz; number of points 32 k. <sup>13</sup>C NMR spectra were recorded with the following pulse sequence: standard <sup>13</sup>C pulse sequence with 45° carbon pulse, relaxation delay 2 s, Waltz decoupling during acquisition, 2 s acquisition time. ACD/NMR Processor Academic Edition 12.0 (Advanced Chemistry Development Inc.) was used for evaluation of spectra.

5' -CCGGGAGAGCTCGATATCCCGGGCGGCCGCTTTGAGGACAAAAGGTTCTT**GACA**TGTTTC  
-35  
TAATGTTTATGC**TATAAT**TTTTTCGGTATCCATGGCGGCCGCTCTAGAAGAAGCTTGGGATCC  
-10  
GTCGACCTCGAATTC**GGAGGA**AACAAAG**ATG**-3'  
RBS SuSyAc start codon

Figure S1. Oligonucleotide sequence of the P34 promoter region as in pCXP34h (Aerts et al. 2011; De Mey et al. 2007). The -35 and -10 boxes are underlined and in bold. The ribosome binding site (RBS) is boxed in black and the start codon of the SuSyAc gene is indicated by an arrow.

(A)



(B)

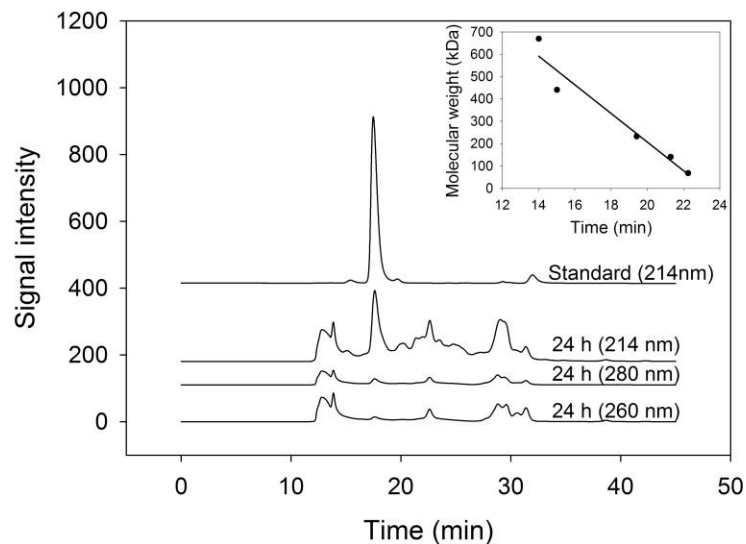


Figure S2. SEC analysis of SuSyAc. (A) Analysis of the cell-free extract of *E. coli* at different cultivation times is shown. The peak inside the black box is SuSyAc. (B) Molecular weight estimation. Elution profile of sample (24 h) in comparison to authentic SuSyAc standard (purified SuSyAc; Diricks et al. 2015). The detection was at three different wavelengths (214, 260 and 280 nm) to distinguish between peptides/proteins and nucleic acids. Sample was fractionated and activities of fractions were determined. For details see the Methods. Inset: The calibration curve was determined using the HMW Native Marker Kit (GE Healthcare, Austria), containing thyroglobulin (669 kDa), ferritin (440 kDa), catalase (232 kDa), lactate dehydrogenase (140 kDa), and bovine serum albumin (66 kDa).

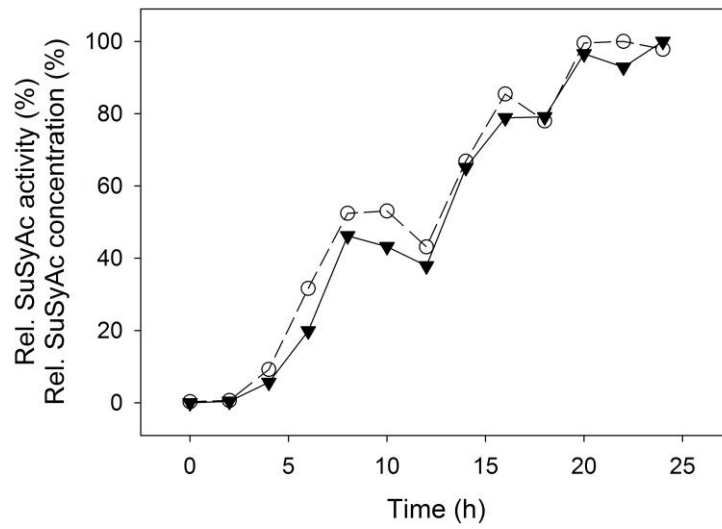


Figure S3. Time-course analysis of *E. coli* bioreactor cultivation for production of SuSyAc. Relative SuSyAc concentration determined by SEC (closed reverse triangle) *versus* the relative volumetric SuSy activity (open circle) in the cell-free extract is shown.

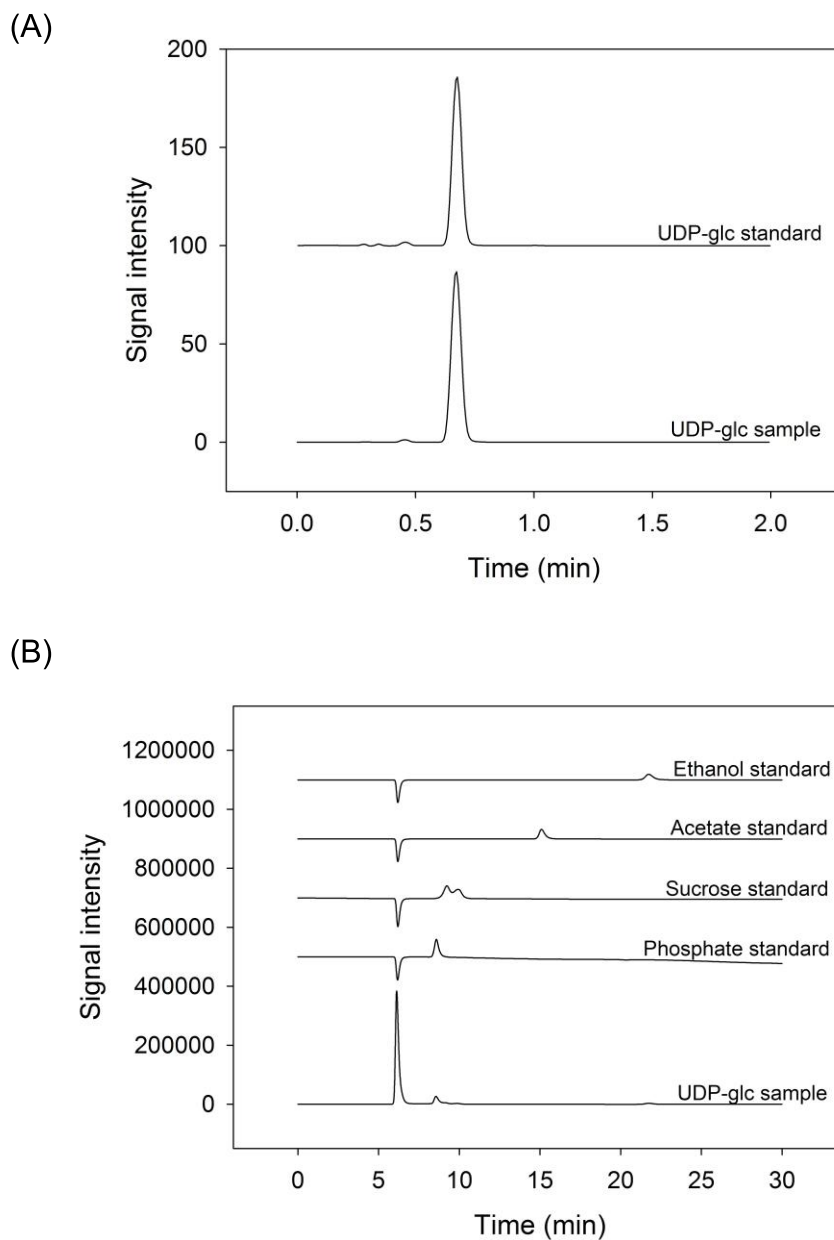


Figure S4. Final purity of UDP-glc after the chromatography-free DSP. Superposition of (A) ion-pair reversed phase and (B) ion exchange HPLC elution profiles. Note that the identity of UDP-glc was additionally confirmed by NMR.



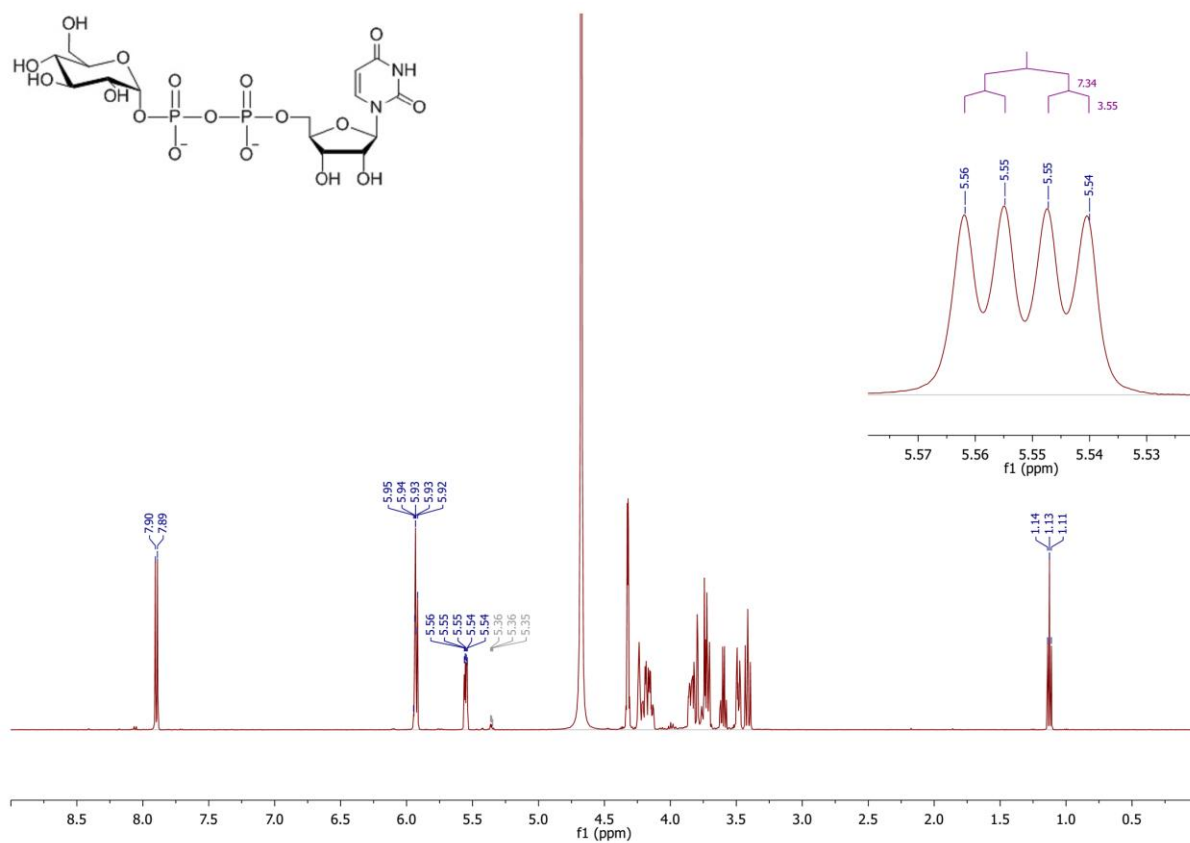


Figure S5. <sup>1</sup>H NMR spectrum of UDP-glc obtained from whole-cell synthesis and chromatography-free DSP. UDP-glc was dissolved in D<sub>2</sub>O. Spectrum is in accordance with previously published data (Hanessian et al. 1998).

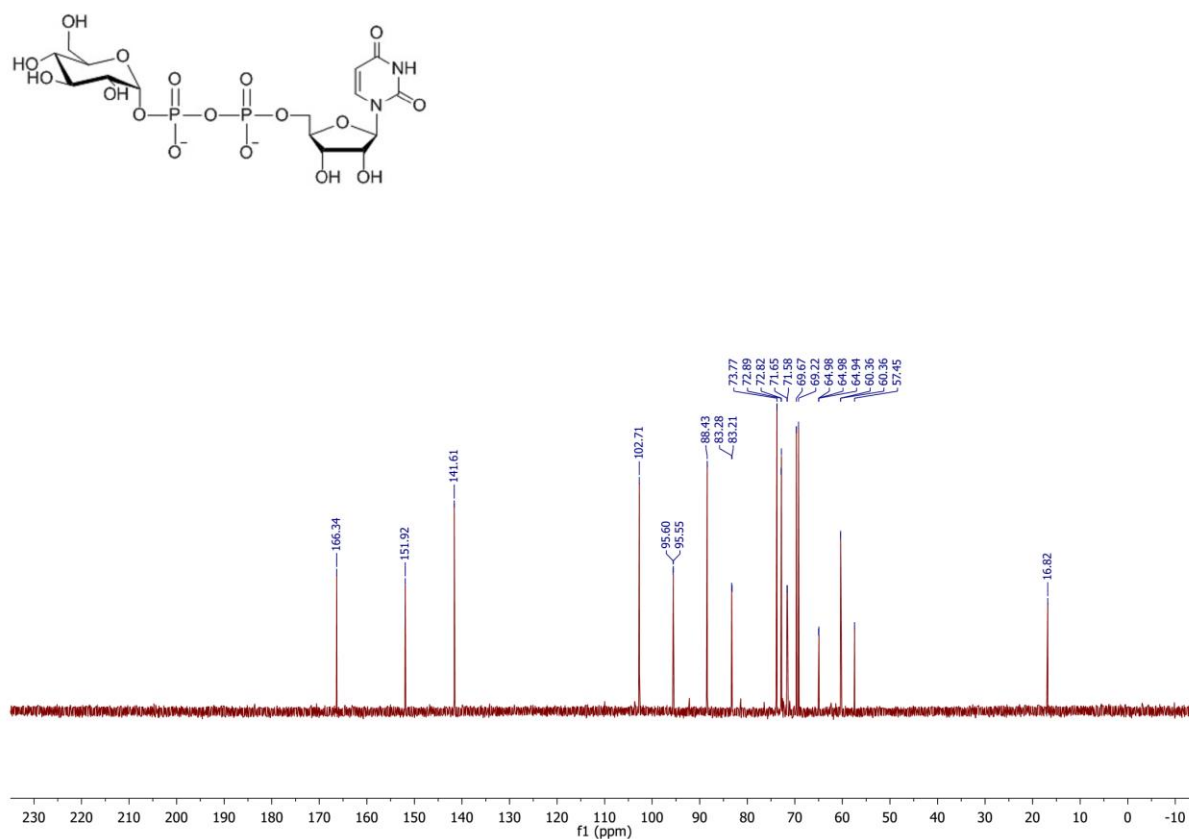


Figure S6. <sup>13</sup>C NMR spectrum of UDP-glc obtained from whole-cell synthesis and chromatography-free DSP. UDP-glc was dissolved in D<sub>2</sub>O. Spectrum is in accordance with previously published data (Hanessian et al. 1998).

## References for Supporting Information

- Aerts D, Verhaeghe T, De Mey M, Desmet T, Soetaert W. 2011. A constitutive expression system for high-throughput screening. *Eng Life Sci* 11(1):10-19.
- De Mey M, Maertens J, Lequeux GJ, Soetaert WK, Vandamme EJ. 2007. Construction and model-based analysis of a promoter library for *E. coli*: An indispensable tool for metabolic engineering. *BMC Biotechnol* 7(1):1-14.
- Diricks M, De Bruyn F, Van Daele P, Walmagh M, Desmet T. 2015. Identification of sucrose synthase in nonphotosynthetic bacteria and characterization of the recombinant enzymes. *Appl Microbiol Biotechnol* 99(20):8465-8474.
- Eixelsberger T, Woodley JM, Nidetzky B, Kratzer R. 2013. Scale-up and intensification of (*S*)-1-(2-chlorophenyl) ethanol bioproduction: Economic evaluation of whole cell-catalyzed reduction of *o*-chloroacetophenone. *Biotechnol Bioeng* 110(8):2311-2315.
- Hanessian S, Lu P-P, Ishida H. 1998. One-step, stereocontrolled synthesis of glycosyl 1-phosphates, uridine-5'-diphosphogalactose, and uridine-5'-diphosphoglucose from unprotected glycosyl donors. *J Am Chem Soc* 120(51):13296-13300.
- Lemmerer M, Schmölzer K, Gutmann A, Nidetzky B. 2016. Downstream processing of nucleoside-diphospho-sugars from sucrose synthase reaction mixtures at decreased solvent consumption. *Adv Synth Catal* 358(19):3113-3122.
- Petschacher B, Nidetzky B. 2008. Altering the coenzyme preference of xylose reductase to favor utilization of NADH enhances ethanol yield from xylose in a metabolically engineered strain of *Saccharomyces cerevisiae*. *Microb Cell Fact* 7:9.

Biocatalytic Cascade of Polyphosphate Kinase and  
Sucrose Synthase for Synthesis of Nucleotide-  
Activated Derivatives of Glucose

# Biocatalytic Cascade of Polyphosphate Kinase and Sucrose Synthase for Synthesis of Nucleotide-Activated Derivatives of Glucose

Sandra T. Kulmer,<sup>+a</sup> Alexander Gutmann,<sup>+a</sup> Martin Lemmerer,<sup>b</sup>  
and Bernd Nidetzky<sup>a,b,\*</sup>

<sup>a</sup> Institute of Biotechnology and Biochemical Engineering, Graz University of Technology, NAWI Graz, Petersgasse 12, 8010 Graz, Austria

Fax: (+43)-316-873-8434; phone: (+43)-316-873-8400; e-mail: bernd.nidetzky@tugraz.at

<sup>b</sup> Austrian Centre of Industrial Biotechnology, Petersgasse 14, 8010 Graz, Austria

<sup>+</sup> These authors contributed equally to this work.

Received: September 28, 2016; Revised: November 9, 2016; Published online: January 12, 2017



Supporting information for this article is available on the WWW under <http://dx.doi.org/10.1002/adsc.201601078>.

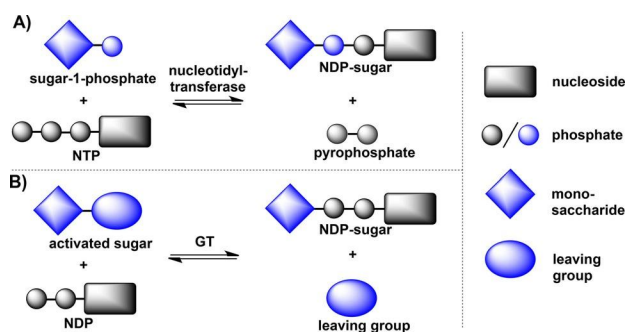
**Abstract:** Sucrose synthase (SuSy) catalyzes in the presence of a pyrimidine or purine nucleoside diphosphate (NDP) the conversion of sucrose to the corresponding nucleotide-activated derivative of glucose (NDP-glucose). To realize the potential of SuSy for NDP-glucose synthesis fully, a nucleoside monophosphate (NMP) should be employed in the reaction, for it is a much more cost-effective substrate than NDP. Therefore we explored in this study the use of polyphosphate kinases (PPK) from class II and III of family 2 which catalyze in the presence of polyphosphate (polyP) the conversion of NMP into NDP. A biocatalytic cascade of PPK (from *Meiothermus ruber*) and SuSy (from *Acidithiobacillus caldus*) was established for NDP-glucose production. The synthetic efficiency of the cascade reflected the NMP substrate specificity of the PPK, following the order of nucleoside monophosphate: adenosine (AMP) > guanosine (GMP) > cytidine (CMP) > uridine (UMP) > deoxy-thymidine (dTMP). The efficiency

was also influenced by the concentrations of magnesium ( $Mg^{2+}$ ) and polyphosphate (polyP) as well as by the pH. An optimized synthesis at 45 °C and pH 5.5 gave 81 mM ( $48\text{ g L}^{-1}$ ) ADP-glucose from 100 mM AMP and 132 mM polyP in the presence of an excess of sucrose (1 M) and 25 mM  $Mg^{2+}$ . The productivity was  $2.0\text{ g L}^{-1}\text{ h}^{-1}$  despite using an enzyme concentration of only  $150\text{ }\mu\text{g mL}^{-1}$ . Isolation of ADP-glucose (~99% purity) by anion-exchange chromatography required prior removal of the polyP, which was achieved by fractional precipitation with ethanol. The herein developed coupling with PPK, to form the NDP substrate from NMP *in situ*, could be generally useful to advance NDP-sugar synthesis by Leloir glycosyltransferases.

**Keywords:** biocatalysis; glycosylation; NDP-glucose; nucleoside diphosphate (NDP); nucleotides; phosphorylation

## Introduction

For common sugars, such as glucose, galactose, mannose and several others, NDP-derivatives represent the naturally activated molecular forms used in cellular biosynthesis.<sup>[1]</sup> NDP-sugars are the substrates of Leloir glycosyltransferases (EC 2.4), a large class of enzymes catalyzing the glycosidic attachment of sugars during assembly of a variety of glycostructures, including oligo- and polysaccharides as well as glycosylated natural products, glycoproteins and glycolipids.<sup>[2]</sup> NDP-sugars are important high-value biochemicals and reagents with broad use in glycobiology, to assay glycosyltransferase activity, for example, as well as in the synthesis of specialty carbohydrates.<sup>[3]</sup> NDP-sugars are prepared naturally, and also in biomimetic synthesis, through transformations by multi-enzyme cascades.<sup>[1a,4]</sup> Typically, sugar phosphorylation from a nucleoside triphosphate (NTP) is followed by nucleotidyl transfer from a second NTP (Scheme 1A).<sup>[4,5]</sup> To cope with product inhibition and an unfavorable reaction equilibrium, pyrophosphate is usually



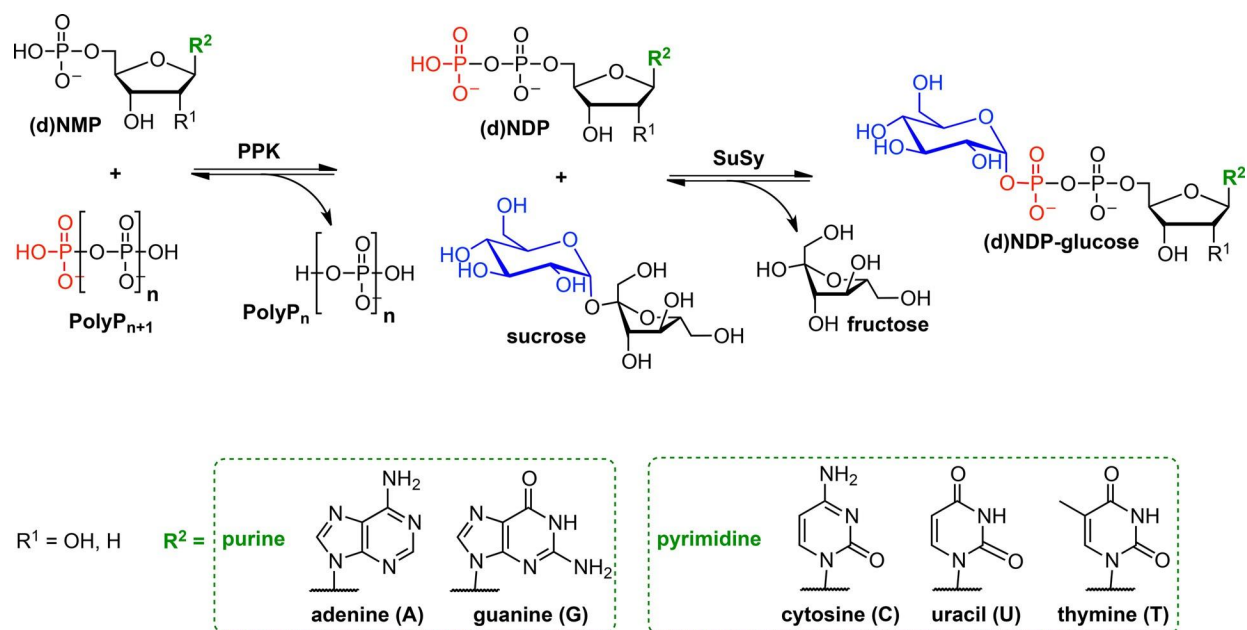
**Scheme 1.** Enzymatic synthesis of NDP-sugars involves A) a nucleotidyltransferase (EC 2.7.7) or B) the reverse reaction of a glycosyltransferase (EC 2.4).

cleaved by an inorganic pyrophosphatase.<sup>[5b,6]</sup> The reverse reaction of glycosyltransferases represents an alternative direct (single-step) route towards NDP-sugars (Scheme 1B). A suitable glycoside serves as the “donor” substrate converted in the presence of NDP.<sup>[7]</sup> However, convenient availability of a donor sufficiently high in energy to drive glycosylation of NDP can be a problem.<sup>[8]</sup>

In the synthesis of NDP-glucose, sucrose appears to be an ideal donor, for it comprises an exceptionally energy-rich disaccharide structure and is furthermore a highly expedient substrate.<sup>[7b,9]</sup> The work of Elling and colleagues has shown that sucrose synthase (SuSy; EC 2.4.1.13) utilizes different NDP acceptors (UDP, ADP, GDP, CDP, dTDP) to convert sucrose into the corresponding NDP-glucoses, therefore raising considerable interest in the synthetic use of this enzyme.<sup>[10]</sup> More recently, we have shown that, based

on a detailed evaluation of kinetic and thermodynamic constraints of the biocatalytic process, the performance metrics of UDP-glucose synthesis with SuSy could be pushed to meet the typical requirements of fine chemicals production in industry.<sup>[11]</sup> However, it was also recognized that the high potential of SuSy could be realized far more effectively if, instead of the costly NDP substrate, the around 20- to 150-fold less expensive NMP (see the Supporting Information, Table S1) was employed in the reaction.<sup>[7b,10c,12]</sup> In a study of the gram-scale production of ADP-glucose by SuSy, Elling and co-workers used the adenylate kinase (EC 2.7.4.3)-catalyzed conversion of AMP and ATP to prepare the ADP substrate *in situ*.<sup>[10c]</sup> However, the nucleoside phosphates were utilized only partially in a process that is furthermore restricted to adenosine phosphates and requires ATP. Therefore, the formation of NDP *via* direct enzymatic phosphorylation of NMP from the expedient phosphate donor polyP seemed to be a more promising approach. The present study describes the development of a cascade of polyphosphate kinase (PPK; EC 2.7.4.1) and SuSy for an efficient synthesis of NDP-glucoses (Scheme 2).

PPKs are categorized according to sequence similarity into families 1 and 2.<sup>[13]</sup> Within family 2, PPKs are further subdivided according to specificity for the substrate phosphorylated from polyP: NDP (class I), NMP (class II) or both (class III).<sup>[13a,14]</sup> Family 1 PPKs use ATP to produce polyP.<sup>[15]</sup> For the purpose of this study, only family 2 PPKs of class II and III were suitable, and a member of each class was therefore examined.



**Scheme 2.** One-pot synthesis of NDP-glucose starts from the inexpensive substrates NMP, polyP and sucrose. NMP is phosphorylated by PPK to NDP, which is then glucosylated by SuSy.

Reports about the application of PPKs in biocatalysis are relatively scarce and their use was so far mainly restricted to regenerate ATP from ADP.<sup>[16]</sup> Applying the phosphorylation-nucleotidyl transfer route (Scheme 1A) to the synthesis of UDP-galactose,<sup>[16b,17]</sup> UDP-glucose<sup>[17]</sup> and CMP-*N*-acetylneuraminic acid,<sup>[18]</sup> the PPK-polyphosphate system was used to form the NTPs needed as nucleotidyltransferase substrate or as phosphate donor of additionally required kinases. Up to 7 enzymes were needed in multi-enzyme cascade transformations performed in one pot.<sup>[16b]</sup> Therefore, in order to telescope the *formation* and the *glucosylation* of NDP into a single overall conversion (Scheme 2), the NDP should be directly produced from NMP which, in the context of a biocatalytic cascade, is reported here for the first time. Five NDP derivatives of glucose (ADP, UDP, GDP, CDP, dTDP) were synthesized using coupled PPK and SuSy. Optimized production at high yield and productivity was demonstrated for ADP-glucose.

## Results and Discussion

### Enzyme Production and Nucleotide Quantification

Enzymes were recombinantly expressed in *Escherichia coli* and purified by Strep- (*GmSuSy*) or His-tag (*AjPPK*, *MrPPK*, *AcSuSy*) affinity chromatography (see the Supporting Information, Figure S1). The typical yields of purified enzyme from one liter of shaking flask cultivation were 39 mg *AjPPK*, 7 mg *MrPPK*, 12 mg *GmSuSy* and 9 mg *AcSuSy*. Enzyme production can be boosted by bioreactor cultivations as we recently demonstrated by improving *AcSuSy* expression to roughly 350 mg L<sup>-1</sup>.<sup>[19]</sup> Enzyme activities were determined using a reversed-phase ion-pairing HPLC assay for nucleotide quantification (see the Supporting Information, Figure S2).

### Selecting a PPK for NMP Phosphorylation

The family 2 PPKs from *Acinetobacter johnsonii* (class II; *AjPPK*)<sup>[20]</sup> and *Meiothermus ruber* (class III; *MrPPK*)<sup>[14]</sup> were compared. Basic biochemical properties of the two PPKs were known from earlier publications,<sup>[14,20]</sup> but their utility in forming NDP from NMP needed to be assessed. Figure 1 shows results of the phosphorylation of different NMP substrates. Both enzymes preferred reaction with the purine-type NMPs (AMP, GMP). Among the pyrimidine NMPs, CMP was preferably used. Only small activities were observed with UMP and dTMP, especially when using *AjPPK*, which was inactive with UMP. Consistent with their class II or III placement, *AjPPK* only formed NDP as product while *MrPPK* continued

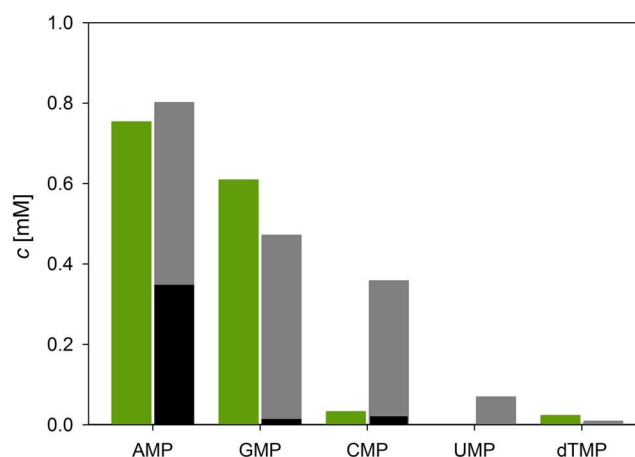


**Figure 1.** Phosphorylation of different NMP acceptors by *AjPPK* (green, NDP) and *MrPPK* (grey, NDP; black, NTP) is shown. Reaction conditions: 1 mM NMP, 6.6 mM polyP, 10 mM MgCl<sub>2</sub>, 50 μg mL<sup>-1</sup> PPK, pH 7.2, 6 h, 30 °C; standard deviation < 0.04 mM.

phosphorylation on NDP to also synthesize NTP.<sup>[13a,14]</sup> The relative amount of NTP in the total product varied with the NMP substrate used. It was particularly significant in the reaction of AMP. Overall, *MrPPK* appeared to be better suited to provide a broad range of NDPs. Partial conversion of NDP to NTP was potentially problematic, for it would compete with the SuSy reaction. However, we show later that advantageously it did not interfere with the NDP-glucose production.

We considered that accumulation of large amounts of NDP-glucose in simple batch conversions necessitates that the PPK used tolerates the required high concentrations of polyP in the reaction. Results in the Supporting Information (Figure S3) show that both PPKs were inhibited at elevated polyP levels, however, *MrPPK* much less so than *AjPPK*. At 100 mM polyP, ADP formation with *MrPPK* was more than 10 times faster than it was with *AjPPK*. Furthermore, because of the strong pH dependence of its reaction equilibrium, SuSy cannot be applied above pH 5.5.<sup>[11]</sup> However, *AjPPK* was reported to be inactive at pH 5.5 and lower,<sup>[20a]</sup> while *MrPPK* lost its activity only below pH 4.0. Finally, the far superior thermostability was recognized as another advantage of *MrPPK*.<sup>[14,20a]</sup> In conclusion, therefore, *MrPPK* was the enzyme of choice to be used in combination with SuSy.

### Establishing the Biocatalytic Cascade

To select a SuSy suitable for coupling with *MrPPK*, we evaluated an enzyme from *Glycine max* (soybean; *GmSuSy*)<sup>[21]</sup> and another one from *Acidithiobacillus caldus* (*AcSuSy*),<sup>[22]</sup> representing the two main evolu-

tionary lineages of SuSy which are in plants and in bacteria. Both SuSys have previously been characterized in the synthesis of UDP-glucose from sucrose and UDP.<sup>[11]</sup> Coupled reactions to convert AMP (10 mM) into ADP-glucose were performed applying *MrPPK* (200  $\mu\text{g mL}^{-1}$ ) in 4-fold excess over SuSy to make the SuSy activity (partly) limiting. PolyP (33 mM) and sucrose (250 mM) were applied in excess to drive the product formation. Because *GmSuSy* is less thermostable than *AcSuSy* and *MrPPK*,<sup>[11,14]</sup> the reaction of *GmSuSy* was done at 30 °C, that of *AcSuSy* at 45 °C. Time courses of ADP-glucose production are compared in Figure 2. Although ADP-glucose synthesis was feasible with both SuSys it was much faster when *AcSuSy* was used. The release of 6 mM ADP-glucose took about 10 min with *AcSuSy* and around 5 h with *GmSuSy*.

The difference in rates of the SuSy reactions was also reflected in the course of the ADP concentration. Using *GmSuSy*, ADP accumulated initially to ~2.4 mM, only to decrease afterwards to a stable concentration of around 1.4 mM. Using *AcSuSy*, by contrast, the ADP remained constant at ~1.4 mM throughout the whole conversion. Note that only ~0.2 mM ATP was formed in both reactions, clearly indicating that AMP “overphosphorylation” by *MrPPK* was not a problem. The marked benefit in terms of productivity obtained from the coupling of *MrPPK* with *AcSuSy*, as compared to the coupling with *GmSuSy*, was likely the combined result of the common preference of *MrPPK* and *AcSuSy* for the nucleobase adenine (as compared to the preference of *GmSuSy* for uridine) and the higher applicable reaction temperature.<sup>[14,21b,23]</sup>

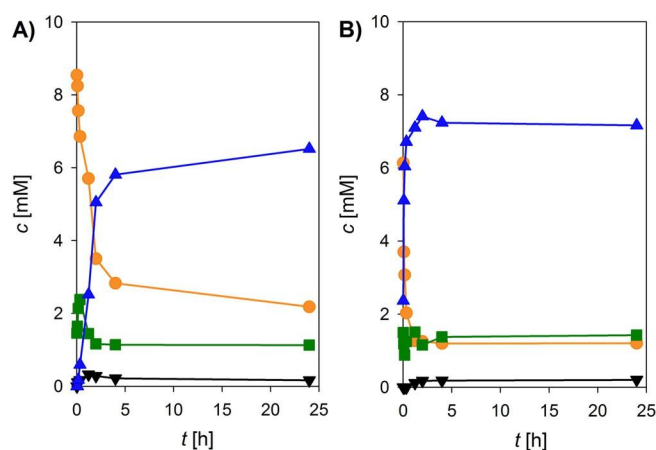


**Figure 2.** Time course analysis of ADP-glucose synthesis from AMP using *MrPPK* in tandem with *GmSuSy* (A) and *AcSuSy* (B) at 30 and 45 °C, respectively, is shown. Reaction conditions: 10 mM AMP, 33 mM polyP, 250 mM sucrose, 10 mM  $\text{MgCl}_2$ , 200  $\mu\text{g mL}^{-1}$  *MrPPK*, 50  $\mu\text{g mL}^{-1}$  SuSy, pH 5.5; standard deviation < 0.3 mM. AMP (orange), ADP (green), ADP-glucose (blue), ATP (black).

In a next step, we evaluated the substrate scope of the *MrPPK*-*AcSuSy* cascade reaction. Yields after 24 h are shown in Figure 3 and the time courses of NMP conversion can be found in the Supporting In-

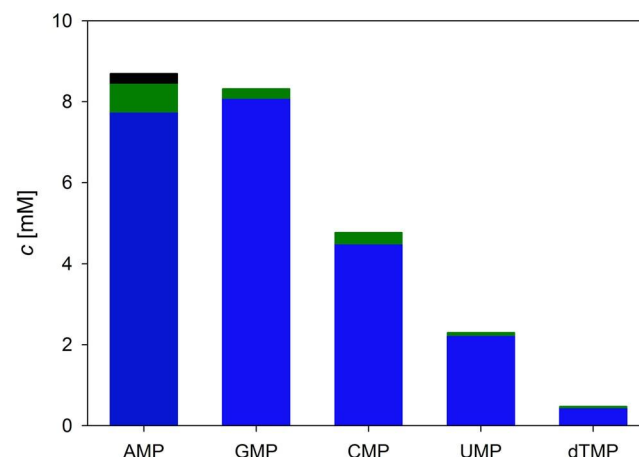


**Figure 3.** Final conversion of 10 mM NMP by 300  $\mu\text{g mL}^{-1}$  *MrPPK* and 50  $\mu\text{g mL}^{-1}$  *AcSuSy* after 24 h incubation at 45 °C (33 mM polyP, 250 mM sucrose, 10 mM  $\text{MgCl}_2$ , pH 5.5; standard deviation < 0.4 mM) is shown. NDP (green), NDP-glucose (blue), NTP (black).

formation (Figure S4). All NMPs were successfully converted to the corresponding NDP-glucoses but there were marked differences in the reaction rates. As anticipated from the substrate preference of *MrPPK* (Figure 1), production of ADP-glucose and GDP-glucose was favored. However, CDP-glucose and UDP-glucose were also synthesized in significant amounts. Even dTMP-glucose was formed to an appreciable extent. We note that the ADP-glucose rate exceeded that of GDP-glucose by at least 7-fold (see the Supporting Information, Figure S4), although the final GDP-glucose concentration (8.1 mM) was slightly higher than the ADP-glucose concentration (7.7 mM). Based on NDP-glucose synthesis rates, therefore, the substrate preference of the cascade conversion was identical to that of the individual *MrPPK* reaction (Figure 1), following the order AMP > GMP > CMP > UMP > dTMP. In all conversions shown in Figure 3, less than 1 mM NDP accumulated during the reaction course. Therefore, this suggested that *MrPPK* was the limiting enzyme in the biocatalytic cascade under the conditions used, despite the fact that it was applied in six-fold excess (by mass) over *AcSuSy*.

To assess the synthetic potential of the cascade reaction and optimize its use for NDP-glucose production, we further on focused on the synthesis of ADP-glucose.



## Optimized Synthesis of ADP-Glucose

Economic constraints of fine chemical production usually dictate that biocatalytic conversions not only utilize inexpensive substrates but also accumulate high final product concentrations, typically  $50 \text{ g L}^{-1}$  or more.<sup>[24]</sup> To obtain such high titers of NDP-glucose, at least 100 mM of NMP substrate need to be applied in the reaction. Effects of the pH and of the concentrations of  $\text{MgCl}_2$  and polyP have to be assessed carefully to enable an efficient conversion under these conditions.

Figure 4A shows that a  $\text{MgCl}_2$  concentration of 25 mM was ideal for ADP-glucose synthesis. At higher  $\text{MgCl}_2$  levels the ADP-glucose concentration decreased but ADP increased. The implied negative effect of  $\text{Mg}^{2+}$  on the equilibrium of the SuSy reaction was recently also observed during synthesis of UDP-glucose.<sup>[11]</sup> Furthermore, high  $\text{MgCl}_2$  concentrations triggered gradual polyP precipitation. Decreased ADP-glucose formation below 25 mM  $\text{MgCl}_2$  was presumably caused by reduced enzyme activities. The role of  $\text{Mg}^{2+}$  is likely complex and it was beyond the scope of the current work to analyze it in detail. It seemed sufficient to have identified a 25 mM concentration of  $\text{MgCl}_2$  as the optimum for ADP-glucose formation.

The polyP concentration was a key factor of reaction optimization, not only for its effect by mass action on the conversion of AMP but also because of its potential impact on PPK kinetics. Besides the substrate inhibition discussed earlier, *MrPPK* was known to gradually lose activity when the polyP chain length decreases below the optimum of 25 phosphate units.<sup>[14]</sup> Figure 4B shows that the ADP-glucose titer

dropped significantly on increasing the polyP concentration from 132 mM to 265 mM. The molar ratio of ADP-glucose and ADP in final reaction mixtures was however constant at a value of  $\sim 13$ , showing that *AcSuSy* was not affected by the change in the polyP concentration. The trend of the results in Figure 4B implies that polyP chain length did not limit the ADP-glucose yield. The decrease in ADP-glucose formation at higher polyP concentrations was probably caused by substrate inhibition of *MrPPK*. To minimize this effect, a polyP concentration of 132 mM was used in all further conversions.

Finally, the effect of pH in the range 5.0–7.0 was examined (Figure 4C). The ADP-glucose titer dropped sharply above and below an optimum pH of 5.5. The cause for decreased product formation is different at high and low pH, as revealed clearly by comparing the levels of ADP-glucose and ADP in the final product mixture. The drop in the ADP-glucose concentration at high pH was paralleled by an increase in the ADP concentration, suggesting that the observed pH dependence reflects the influence of the pH on the equilibrium of the SuSy reaction. We have shown in a recent study on UDP-glucose production by SuSy that the conversion of sucrose and UDP proceeded most efficiently at low pH ( $\leq 5.0$ ) and that the pH dependence of the reaction equilibrium reflected the protonation of UDP below an apparent  $\text{pK}_a$  of around 6.<sup>[11]</sup> Figure S5 in the Supporting Information shows that ADP-glucose formation from ADP exhibited a similar pH dependence. The decrease in the ADP-glucose concentration at a pH smaller than 5.5 was due to a substantially lowered activity ( $\geq 80\%$  loss) of *MrPPK*. Therefore, when working below pH 5.5, it was impossible to benefit from favorable effects on the SuSy equilibrium. In summary therefore, a pH of 5.5 represented the best compromise between a high reaction rate and suitable reaction equilibrium.

Reaction conditions considered optimal from Figure 4 (25 mM  $\text{MgCl}_2$ , 132 mM polyP and pH 5.5) were applied to ADP-glucose synthesis from 100 mM AMP. ADP-glucose formation was characterized by rapid accumulation of product to a concentration of  $69 \text{ mM}$  ( $41 \text{ g L}^{-1}$ ) in the first 5 h of reaction (Figure 5). This corresponds to a space-time-yield (STY) of about  $14 \text{ mM h}^{-1}$  ( $8.1 \text{ g L}^{-1} \text{ h}^{-1}$ ). The maximum amount of ADP-glucose released after 24 h was  $81 \text{ mM}$  ( $48 \text{ g L}^{-1}$ ), corresponding to a yield of 81% based on the AMP initially added to the reaction. Because of the strongly declined reaction rate the STY after 24 h was reduced to  $2.0 \text{ g L}^{-1} \text{ h}^{-1}$ . Evidence that only little ADP accumulated during the conversion indicates its efficient utilization in the *AcSuSy* reaction and shows that the overall conversion was limited by the *MrPPK* reaction. The activity of *AcSuSy* was sufficient to maintain the ratio of ADP-glucose to ADP throughout the conversion at an apparent equi-

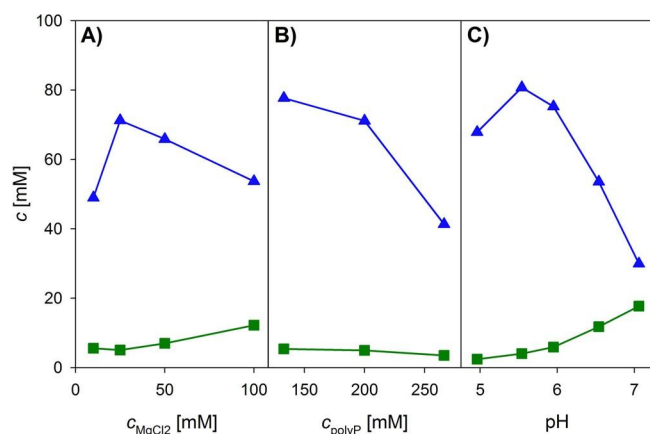


**Figure 4.** The effects of  $\text{MgCl}_2$  concentration (A), polyP concentration (B) and pH (C) on ADP-glucose yields in the *MrPPK-AcSuSy* cascade reaction were analyzed. *Standard reaction conditions:* 100 mM AMP, 132 mM polyP, 1 M sucrose, 25 mM  $\text{MgCl}_2$ ,  $100 \mu\text{g mL}^{-1}$  *MrPPK*,  $50 \mu\text{g mL}^{-1}$  *AcSuSy*, pH 5.5,  $45^\circ\text{C}$ , 48 (A) or 24 h (B, C)); standard deviation  $< 3 \text{ mM}$ . ADP (green), ADP-glucose (blue).

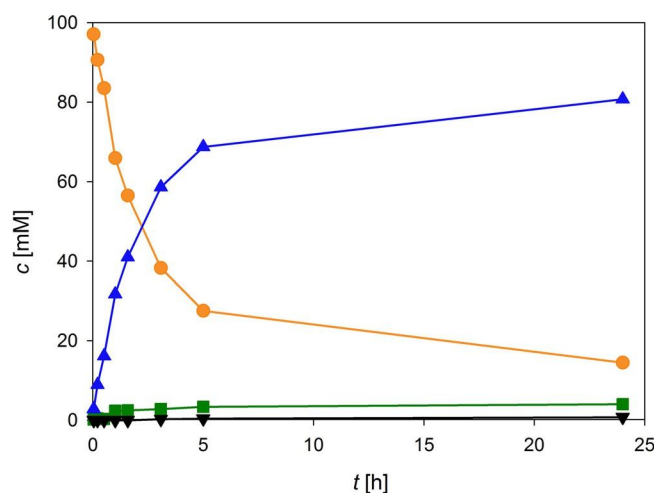


**Figure 5.** A time course of ADP-glucose synthesis by the *MrPPK-AcSuSy* cascade reaction under optimized conditions is shown: 100 mM AMP, 1 M sucrose, 132 mM polyP, 25 mM  $\text{MgCl}_2$ ,  $100 \mu\text{g mL}^{-1}$  *MrPPK*,  $50 \mu\text{g mL}^{-1}$  *AcSuSy*, pH 5.5; standard deviation  $< 2$  mM. AMP (orange), ADP (green), ADP-glucose (blue), ATP (black).

librium around 20:1. Even at the end of the conversion only 4 mM ADP was present and phosphorylation of ADP to ATP was negligible ( $< 0.75$  mM). Interestingly the cascade reaction was nevertheless competitive with direct ADP-glucose formation from ADP (see the Supporting Information, Figure S6). Single step conversion by *GmSuSy* was more than 3-fold slower than the *MrPPK-AcSuSy* cascade reaction. Despite rate enhancement in direct ADP-glucose formation by *AcSuSy*, the final ADP-glucose concentration of  $\sim 80$  mM was identical to that of the coupled reaction. Based on synthesis of 62 mM ADP-glucose (the highest concentration obtained with *GmSuSy*) the STY of the cascade reaction was 2.8 times lower than that of the single step reaction with *AcSuSy* but 6-fold higher than that achieved with *GmSuSy*.

The herein described synthetic route represents a significant advancement over previous reports on ADP-glucose production.<sup>[10a,c,12,25]</sup> Most notably, Elling and co-workers isolated 2.2 g of ADP-glucose from a coupled reaction of adenylate kinase (from rabbit muscle) and SuSy (from potato).<sup>[10c]</sup> However, the main drawback of the approach was the moderate final ADP-glucose concentration of just 4.4 mM. Although AMP was used, the reaction still required ATP (4.0 mM) to form ADP and the yield based on total adenine phosphates added to the reaction was 55%. By substituting the adenylate kinase reaction with the PPK reaction we fully avoided use of expensive substrates like ATP or ADP and achieved a significant boost in the ADP-glucose concentration (18-fold) and increased the yield by 26%.

The final ADP-glucose concentration, 41–48  $\text{g L}^{-1}$  depending on when one is prepared to stop the reaction in Figure 5, roughly matched the broadly defined target value for industrial fine chemical synthesis.<sup>[24]</sup> Similar product concentrations were obtained in biocatalytic syntheses of NDP-sugars using the phosphorylation-nucleotidyl transfer route in Scheme 1A: UDP-galactose ( $44 \text{ g L}^{-1}$ ),<sup>[26]</sup> CMP-*N*-acetylneuraminic acid ( $34 \text{ g L}^{-1}$ ),<sup>[18]</sup> UDP-glucose ( $34 \text{ g L}^{-1}$ )<sup>[27]</sup> and GDP-fucose ( $18 \text{ g L}^{-1}$ ).<sup>[28]</sup> In the field of NDP-glucose production, the current synthesis was only outmatched by the direct conversion of sucrose and UDP into UDP-glucose ( $144 \text{ g L}^{-1}$ ) catalyzed by *AcSuSy*, as recently reported by Gutmann and Nidetzky.<sup>[11]</sup> However, use of the costly UDP was a clear limitation. The STY of the *MrPPK-AcSuSy* reaction was 3- to 12-fold lower than that of the direct UDP-glucose synthesis ( $25 \text{ g L}^{-1} \text{ h}^{-1}$ ),<sup>[11]</sup> but there was clearly a favorable trade-off between STY and substrate costs on moving from the direct conversion to the coupled reaction with PPK. The STY obtained here was comparable or exceeded the STYs from the alternative synthesis of UDP-glucose ( $4.3 \text{ g L}^{-1} \text{ h}^{-1}$ ),<sup>[27]</sup> CMP-*N*-acetylneuraminic acid ( $2.9 \text{ g L}^{-1} \text{ h}^{-1}$ )<sup>[18]</sup> and UDP-galactose ( $2.1 \text{ g L}^{-1} \text{ h}^{-1}$ ).<sup>[26]</sup> It should be noted, however, that the current ADP-glucose synthesis was achieved with a low enzyme loading of only  $50 \mu\text{g mL}^{-1}$  *AcSuSy* and  $100 \mu\text{g mL}^{-1}$  *MrPPK*. Previous cascade reactions, by contrast, relied on high enzyme loading, typically in the form of whole cells (up to  $215 \text{ g L}^{-1}$ ).<sup>[26–28]</sup> We therefore achieved an excellent mass-based turnover number ( $\text{TTN}_{\text{mass}}$  in  $\text{g product/g enzyme}$ ) of  $320 \text{ g g}^{-1}$  which already approached the typical industrial requirement of  $1000 \text{ g g}^{-1}$ .<sup>[24]</sup> Altogether the *MrPPK-AcSuSy* cascade reaction represents a significant advance in ADP-glucose synthesis and emphasizes the large potential of PPKs to facilitate cost-efficient synthesis of further NDP-glucoses and NDP-sugars in general.

### Establishing Purification of ADP-Glucose

NDP-sugars are rather unstable molecules which makes their isolation from reaction mixtures a problem requiring special attention.<sup>[29]</sup> Here in particular, it was important to evaluate the unknown impact of polyP on the recovery of ADP-glucose. To obtain sufficient amounts of ADP-glucose, the enzymatic synthesis was performed in a 150-mL magnetically stirred reactor (see the Supporting Information, Figure S7).

Considering evidence from our previous study that phosphatase-catalyzed dephosphorylation of nucleoside phosphates followed by selective precipitation with ethanol constitutes a convenient method of chromatography-free isolation of NDP-glucoses from SuSy reaction mixtures,<sup>[29]</sup> we initially examined the

same for the sample from the *MrPPK-AcSuSy* conversion. Unfortunately, the calf intestinal alkaline phosphatase (CIAP) used was strongly inhibited by polyP so that even after prolonged incubation of 24 h large amounts of AMP and ADP remained intact (see the Supporting Information, Figure S8). Another problem was that, at pH 7.3 (which was required for the action of the phosphatase) and in presence of 25 mM  $\text{MgCl}_2$ , a substantial amount of the ADP-glucose (17%) was degraded chemically during the dephosphorylation step.<sup>[10c]</sup> It was known that alternatively ADP-glucose could be separated from AMP and ADP by anion-exchange chromatography (AEC).<sup>[29]</sup> However, in strong contrast to our previous study in the absence of polyP, all compounds co-eluted from a 1 mL SuperQ-650M column, in spite of using a shallow sodium acetate gradient for optimal separation (Figure 6A). Therefore, this indicated the need to remove polyP from the reaction mixture in order to take advantage of the established methods for NDP-sugar isolation.

Employing fractional precipitation with ethanol at 4 °C (see the Supporting Information, Figure S9), it was possible to separate polyP as a glassy solid from ADP-glucose and residual AMP and ADP. The polyP precipitated on adding between 0.5 and 1.5 sample volumes of ethanol while the product and the adenosine phosphates remained fully soluble under these conditions. The beneficial effect of having removed the polyP on AEC efficiency in separating ADP-glucose from AMP and ADP is shown in Figure 6B. Despite using a 20-fold increased sample loading compared to Figure 6A, all compounds were baseline separated by the same AEC protocol, so enabling convenient isolation of the ADP-glucose. It is worth em-

phasizing that the simple, yet efficient strategy of removing polyP by precipitation with ethanol could be generally applicable in the isolation of NDP-sugars obtained in syntheses involving PPK-catalyzed phosphorylations.

Using the protocol just established, ADP-glucose was isolated after polyP removal at preparative scale from a 10-mL sample containing 334 mg product. In the Supporting Information Table S2 summarizes the results and Figure S10 shows performance of the AEC for a 40-mL column. Sodium acetate in the product was removed by ethanol precipitation and ADP-glucose (155 mg) was obtained as a white powder by freeze drying from solution in water. The isolation yield of 51% is due to ~10% product loss in each step, primarily as a (well-known) consequence of the relatively small scale used. Employing a similar procedure for the isolation of UDP-glucose at the gram scale, lacking the precipitation of polyP however, we obtained a product recovery of 81%.<sup>[29]</sup> Considering the reduced ADP-glucose concentration of 59 mM in the up-scaled conversion the isolated yield was therefore around 30%. It should be recognized therefore that the main interest here was not maximizing the isolated yield but demonstrating that the overall process is feasible for the production of highly pure ADP-glucose.

Analysis of the final product by HPLC,  $^1\text{H}$  and  $^{13}\text{C}$  NMR (see the Supporting Information, Figures S11–S13) confirmed its identity and revealed an excellent ADP-glucose purity with a mass percentage of 98.5% or greater. Around 1% ethanol remained in the product and additionally small amounts of AMP ( $\leq 0.25\%$ ), ADP ( $\leq 0.1\%$ ) and acetate ( $\leq 0.1\%$ ) were detected. Therefore, these results show that the PPK-SuSy cascade reaction combined with a suitable downstream procedure offers a straightforward synthesis of highly pure ADP-glucose and other NDP-glucoses (Figure 3) from inexpensive substrates.

## Conclusions

In this study we have evaluated PPKs, and demonstrated their synthetic use, for phosphorylation of NMP from polyP in the context of a bi-enzymatic linear cascade of PPK and a Leloir glycosyltransferase applied to the preparation of NDP-sugars. *In situ* formation of NDP by the PPK reaction is shown to present a highly efficient and cost-effective way of supplying the NDP substrate to the glycosyltransferase reaction. The concept of the PPK-glycosyltransferase cascade appears to be quite general in its possible synthetic applicability. By exploiting the reversibility of promiscuous glycosyltransferases a broad variety of NDP-sugars is accessible.<sup>[8a,30]</sup> However, NDP-sugar synthesis is thermodynamically disfavored unless high

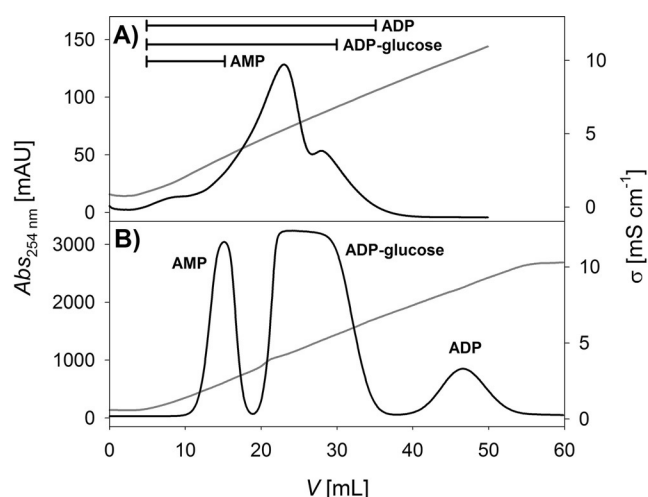


**Figure 6.** Separation of ADP-glucose from AMP and ADP by AEC before (A) and after (B) removal of polyP is shown. A sodium acetate gradient (20–510 mM, pH 4.3) was applied on a 1-mL SuperQ-650M column. UV absorbance at 254 nm (black), conductivity (grey).

energy sugar donors like sucrose are used.<sup>[7a,b,11]</sup> To compensate for the lacking diversity of naturally abundant activated donors Thorson and co-workers introduced synthetic nitrophenyl glycosides to drive the formation of a broad variety of NDP-sugars.<sup>[8a]</sup>

However, as demonstrated for the system of PPK and SuSy, in order to make NDP-glucose synthesis from the expedient substrates NMP, polyP and sucrose truly efficient, careful attention had to be paid not only to the optimization of the coupled biotransformations but also to the downstream processing of the product. The example of ADP-glucose production demonstrates the successful development and implementation of the biocatalytic process across all steps. It also provides a strong case for process intensification in the enzymatic NDP-sugar synthesis. Considering the clear preference of almost all currently known PPKs for reaction with pyrimidine as compared to purine nucleobases,<sup>[13a,18]</sup> enzyme engineering for increased activity towards the purine substrates seems important to enable full realization of the high synthetic potential that PPK-glycosyltransferase cascades offer.

## Experimental Section

### Materials

PolyP (115% H<sub>3</sub>PO<sub>4</sub> basis) was obtained from Sigma-Aldrich (Vienna, Austria) and nucleotides were purchased from Carbosynth (Berkshire, UK). CIAP was from New England Biolabs (Ipswich, MA, US) and SuperQ-650M was from Tosoh Bioscience (Tokyo, Japan).

### Enzyme Preparation

*Aj*PPK (GenBank: BAC76403.1), *Mr*PPK (GenBank: AGK05310.1), *Gm*SuSy (GenBank: AAC39323.1) and *Ac*SuSy (GenBank: AIA55343.1) were recombinantly expressed in *E. coli* and purified by His- or Strep-tag affinity chromatography as described in detail in the Supporting Information.

### HPLC-Based Activity Assay

NMP, NDP, NTP and NDP-glucose were quantified by reversed-phase ion-pairing HPLC. Typically 5  $\mu$ L of solutions containing an overall nucleoside concentration of 1 mM were loaded on a Kinetex™ C18 column (5  $\mu$ m, 100  $\text{\AA}$ , 50  $\times$  4.6 mm). Compounds with the same nucleobase were baseline separated by 6.5 min long isocratic runs using 20 mM phosphate buffer, pH 5.9 containing 40 mM tetra-*n*-butylammonium bromide (TBAB) and 12.5% acetonitrile. The flow rate was 2 mL min<sup>-1</sup> and the temperature was controlled to 35 °C. Depending on the nucleobase, quantifications were made by UV-detection at 253 (guanine), 259 (adenine), 262 (uracil), 267 (thymine) or 271 nm (cytosine).

To follow enzymatic conversions aliquots were withdrawn from reaction mixtures and enzymatic conversions were

stopped by adding an equal volume of acetonitrile. Precipitated proteins were removed by centrifugation (13,200 rpm, 10 min) and appropriately diluted supernatant was applied to HPLC analysis.

### Kinetic Characterization of PPKs

All conversions contained 0.1 mg mL<sup>-1</sup> BSA and were performed in 1.5 mL reaction tubes under agitation at 450 rpm. The pH of polyP stock solutions was set to the pH of the respective conversion. The pH of reaction mixtures was controlled before starting conversions by enzyme addition and at the end of each reaction. The pH change was typically below 0.1 units. Note that polyP concentrations correspond to the total phosphate residues not the number of polyP chains.

The acceptor spectrum of *Aj*PPK and *Mr*PPK was tested by phosphorylating 1 mM AMP, GMP, CMP, UMP or dTMP. Reaction mixtures contained 6.6 mM polyP, 10 mM MgCl<sub>2</sub>, 50 mM Tris, pH 7.2 and 50  $\mu$ g mL<sup>-1</sup> PPK. Conversions at 30 °C were stopped after 6 h. The influence of the polyP concentration was evaluated in the range of 6.6–660 mM in reactions containing 1 mM AMP, 10 mM MgCl<sub>2</sub>, 50 mM Tris, pH 7.1 and 50  $\mu$ g mL<sup>-1</sup> PPK. Conversions at 30 °C were stopped after 6 h. Phosphorylation of 1 mM AMP by 10  $\mu$ g mL<sup>-1</sup> *Mr*PPK was studied at 45 °C in the pH range of 4.0–8.5. Reactions contained 10 mM MnCl<sub>2</sub> and were buffered by 50 mM Tris and 33 mM polyP.

### Establishing PPK-SuSy Cascade Reactions

Reactions were performed as described above. 10 mM AMP was converted with *Gm*SuSy and *Ac*SuSy at 30 and 45 °C, respectively. Reaction mixtures contained 33 mM polyP, 250 mM sucrose, 10 mM MgCl<sub>2</sub>, 50 mM MES, pH 5.5, 50  $\mu$ g mL<sup>-1</sup> SuSy and 200  $\mu$ g mL<sup>-1</sup> *Mr*PPK. ADP-glucose formation was followed for 24 h. Under identical conditions conversion of 10 mM AMP, GMP, CMP, UMP and dTMP was tested with 300  $\mu$ g mL<sup>-1</sup> *Mr*PPK and 50  $\mu$ g mL<sup>-1</sup> *Ac*SuSy.

To optimize conversion of 100 mM AMP we varied the concentration of MgCl<sub>2</sub> and polyP as well as the pH. All reactions were performed at 45 °C and contained 1 M sucrose, 50 mM MES, 50  $\mu$ g mL<sup>-1</sup> *Ac*SuSy and 100  $\mu$ g mL<sup>-1</sup> *Mr*PPK. MgCl<sub>2</sub> was varied from 10 to 100 mM in 48 h long conversions with 132 mM polyP at pH 5.5. Reactions with 132–265 mM polyP and 25 mM MgCl<sub>2</sub> were stopped after 24 h at pH 5.5. Finally pH was varied from 5.0 to 7.0 in 24 h long conversions with 132 mM polyP and 25 mM MgCl<sub>2</sub>. Eq. (1) was used to approximate the equilibrium constant ( $K_{\text{eq}}$ ) of the SuSy reaction, whereby the concentrations of ADP and ADP-glucose were directly measured and those of fructose and sucrose were inferred from ADP-glucose formation and reaction stoichiometry.

$$K_{\text{eq}} = \frac{c_{\text{ADP-glucose}} \cdot c_{\text{fructose}}}{c_{\text{ADP}} \cdot c_{\text{sucrose}}} \quad (1)$$

### Optimized Synthesis of ADP-Glucose from ADP

Conversion of 100 mM AMP by 50  $\mu$ g mL<sup>-1</sup> *Ac*SuSy and 100  $\mu$ g mL<sup>-1</sup> *Mr*PPK was monitored under optimized condi-

tions for 24 h. Reactions performed at pH 5.5 and 45 °C contained 1 M sucrose, 132 mM polyP and 25 mM MgCl<sub>2</sub>. ADP-glucose synthesis was also upscaled to 150 mL and performed in a double-walled glass reactor with a diameter of 6.5 cm and a height of 6.4 cm. Throughout the 30 h long conversion agitation was applied by a magnetic stirrer (65 rpm). The reaction was terminated by removing enzymes through ultrafiltration by Vivaspin concentrators (10 kDa cut-off, Sartorius, Germany). The obtained mixture containing 59 mM ADP-glucose, 20 mM AMP, 6 mM ADP and polyP was used to isolate ADP-glucose.

### SuSy Catalyzed ADP-Glucose Synthesis from AMP

ADP-glucose was formed in single step conversions using 50 µg mL<sup>-1</sup> SuSy. *GmSuSy* and *AcSuSy* were applied at 30 and 45 °C, respectively. Reaction mixtures contained 100 mM ADP, 1 M sucrose, 25 mM MgCl<sub>2</sub> and 0.1% BSA. To maintain a constant pH of 5.5 it was adjusted throughout the 22 h long conversion by addition of 4 M HCl.

### Establishing Isolation of ADP-Glucose

To cleave phosphomonoesters 10 U mL<sup>-1</sup> CIAP were added to the reaction mixture after setting the pH to 7.3. Dephosphorylation at 30 °C was monitored over 24 h by HPLC analysis.

AEC was optimized with self-packed 1 mL SuperQ-650M columns at room temperature. Samples were loaded and separated with flow rates of 0.2 and 1 mL min<sup>-1</sup>, respectively. After unbound compounds were washed off with 20 mM sodium acetate (pH 4.3), a 50 column-volume-long gradient to 510 mM sodium acetate was applied for separation of AMP, ADP-glucose and ADP. If required for complete release of ADP, an isocratic run at 510 mM sodium acetate was added.

All precipitations involved overnight incubation at the specified temperature and ethanol content. Precipitate and soluble fraction were separated by centrifugation (10 min, 5,000 rpm, 4 °C). To find conditions for selective polyP precipitation, the enzyme-free reaction solution was incubated overnight at 4 and -20 °C in presence of 0.5 to 2.5 equivalents of ethanol. The amounts of soluble and insoluble AMP, ADP-glucose and ADP were determined by HPLC.

### Preparative Isolation of ADP-Glucose

Initially polyP was precipitated with 1.5 volumes of ethanol at 4 °C. Before AEC dissolved nucleosides were precipitated at -20 °C in presence of 5 equivalents of ethanol and redissolved in 10 mL water. AEC was performed as described above but on a 40 mL column with flow rates of 1 and 10 mL min<sup>-1</sup> during sample loading and compound separation, respectively. ADP-glucose containing fractions were pooled and concentrated to 20 mL. To remove acetate, ADP-glucose was precipitated with 4 volumes of ethanol at -20 °C. After dissolving the insoluble fraction in 5 mL water a final precipitation of ADP-glucose was performed with 5 volumes of ethanol at -20 °C. The precipitate was dissolved in 1 mL water and after freeze drying ADP-glucose was obtained as a white powder. It was analyzed by HPLC and NMR spectroscopy using a Varian Unity Inova 500 MHz spectrometer. The results of <sup>1</sup>H and <sup>13</sup>C NMR were in agree-

ment with literature data.<sup>[12,25c]</sup> <sup>1</sup>H NMR (500 MHz, D<sub>2</sub>O): δ = 8.53 (s, 1H), 8.26 (s, 1H), 6.18 (d, *J* = 5.7 Hz, 1H), 5.65 (dd, *J* = 7.3, 3.5 Hz, 1H), ~4.8 (overlapping with H<sub>2</sub>O signal), 4.60 (t, *J* = 4.4 Hz, 1H), 4.46 (q, *J* = 3.0 Hz, 1H), 4.30 (dd, *J* = 5.3, 3.1 Hz, 2H), 3.99–3.76 (m, 4H), 3.58 (dt, *J* = 9.8, 3.2 Hz, 1H), 3.50 (t, *J* = 9.7 Hz, 1H); <sup>13</sup>C NMR (126 MHz, D<sub>2</sub>O): δ = 156.18, 153.48, 149.68, 140.41, 119.22, 96.22, 87.55, 84.47, 74.95, 73.50, 72.32, 72.25, 71.02, 69.90, 65.92, 61.03.


### Acknowledgements

*Financial Support from the EU FP7 project SuSy (Sucrose Synthase as Cost-Effective Mediator of Glycosylation Reactions) is gratefully acknowledged. The plasmid for expression of AcSuSy was received from Prof. Tom Desmet (Centre for Industrial Biotechnology and Biocatalysis, Ghent University, Belgium) and Prof. Jennifer Alexander (Institute of Pharmaceutical Sciences, University of Freiburg, Germany) kindly provided the plasmids for expression of AjPPK and MrPPK. B. N. acknowledges the EU COST action BioSysCat.*

### References

- [1] a) M. Bar-Peled, M. A. O'Neill, *Annu. Rev. Plant Biol.* **2011**, *62*, 127–155; b) C. J. Thibodeaux, C. E. Melançon III, H.-W. Liu, *Angew. Chem.* **2008**, *120*, 9960–10007; *Angew. Chem. Int. Ed.* **2008**, *47*, 9814–9859.
- [2] a) L. L. Lairson, B. Henrissat, G. J. Davies, S. G. Withers, *Annu. Rev. Biochem.* **2008**, *77*, 521–555; b) D. Bowles, E.-K. Lim, B. Poppenberger, F. E. Vaistij, *Annu. Rev. Plant Biol.* **2006**, *57*, 567–597; c) L. Krasnova, C.-H. Wong, *Annu. Rev. Biochem.* **2016**, *85*, 599–630; d) K. Ohtsubo, J. D. Marth, *Cell* **2006**, *126*, 855–867.
- [3] a) P. Bubner, T. Czabany, C. Luley-Goedl, B. Nidetzky, *Anal. Biochem.* **2015**, *490*, 46–51; b) C. A. G. M. Weijers, M. C. R. Franssen, G. M. Visser, *Biotechnol. Adv.* **2008**, *26*, 436–456; c) D. Warnock, X. Bai, K. Autote, J. Gonzales, K. Kinealy, B. Yan, J. Qian, T. Stevenson, D. Zopf, R. J. Bayer, *Biotechnol. Bioeng.* **2005**, *92*, 831–842; d) H. Yu, X. Chen, *Org. Biomol. Chem.* **2016**, *14*, 2809–2818.
- [4] T. Bülter, L. Elling, *Glycoconjugate J.* **1999**, *16*, 147–159.
- [5] a) J. Liu, Y. Zou, W. Guan, Y. Zhai, M. Xue, L. Jin, X. Zhao, J. Dong, W. Wang, J. Shen, P. G. Wang, M. Chen, *Bioorg. Med. Chem. Lett.* **2013**, *23*, 3764–3768; b) M. M. Muthana, J. Qu, Y. Li, L. Zhang, H. Yu, L. Ding, H. Malekan, X. Chen, *Chem. Commun.* **2012**, *48*, 2728–2730; c) J. Fang, M. Xue, G. Gu, X.-w. Liu, P. G. Wang, *Bioorg. Med. Chem. Lett.* **2013**, *23*, 4303–4307; d) S. C. Timmons, R. H. Mosher, S. A. Knowles, D. L. Jakeman, *Org. Lett.* **2007**, *9*, 857–860.
- [6] a) T. Ohashi, N. Cramer, T. Ishimizu, S. Hase, *Anal. Biochem.* **2006**, *352*, 182–187; b) B. A. Wagstaff, M. Rejzek, T. Pesnot, L. M. Tedaldi, L. Caputi, E. C. O'Neill, S. Benini, G. K. Wagner, R. A. Field, *Carbohydr. Res.* **2015**, *404*, 17–25.

- [7] a) C. Zhang, B. R. Griffith, Q. Fu, C. Albermann, X. Fu, I.-K. Lee, L. Li, J. S. Thorson, *Science* **2006**, *313*, 1291–1294; b) K. Schmölzer, A. Gutmann, M. Diricks, T. Desmet, B. Nidetzky, *Biotechnol. Adv.* **2016**, *34*, 88–111; c) A. Gutmann, C. Krump, L. Bungaruang, B. Nidetzky, *Chem. Commun.* **2014**, *50*, 5465–5468.
- [8] a) R. W. Gantt, P. Peltier-Pain, W. J. Cournoyer, J. S. Thorson, *Nat. Chem. Biol.* **2011**, *7*, 685–691; b) J. Seibel, H.-J. Jördening, K. Buchholz, *Biocatal. Bio-transform.* **2006**, *24*, 311–342.
- [9] E. F. Neufeld, W. Z. Hassid, *Adv. Carbohydr Chem.* **1963**, *18*, 309–356.
- [10] a) L. Elling, M. Grothus, M.-R. Kula, *Glycobiology* **1993**, *3*, 349–355; b) L. Elling, M.-R. Kula, *Enzyme Microb. Technol.* **1995**, *17*, 929–934; c) A. Zervosen, U. Römer, L. Elling, *J. Mol. Catal. B* **1998**, *5*, 25–28.
- [11] A. Gutmann, B. Nidetzky, *Adv. Synth. Catal.* **2016**, *358*, 3600–3609.
- [12] A. Zervosen, A. Stein, H. Adrian, L. Elling, *Tetrahedron* **1996**, *52*, 2395–2404.
- [13] a) J. N. Andexer, M. Richter, *ChemBioChem* **2015**, *16*, 380–386; b) B. Nocek, S. Kochinyan, M. Proudfoot, G. Brown, E. Evdokimova, J. Osipiuk, A. M. Edwards, A. Savchenko, A. Joachimiak, A. F. Yakunin, *Proc. Natl. Acad. Sci. USA* **2008**, *105*, 17730–17735.
- [14] K. Motomura, R. Hirota, M. Okada, T. Ikeda, T. Ishida, A. Kuroda, *Appl. Environ. Microbiol.* **2014**, *80*, 2602–2608.
- [15] a) K. Ahn, A. Kornberg, *J. Biol. Chem.* **1990**, *265*, 11734–11739; b) L. Achbergerová, J. Nahálka, *Microb. Cell Fact.* **2011**, *10*, 1–14.
- [16] a) K. Murata, T. Uchida, J. Kato, I. Chibata, *Agric. Biol. Chem.* **1988**, *52*, 1471–1477; b) Z. Liu, J. Zhang, X. Chen, P. G. Wang, *ChemBioChem* **2002**, *3*, 348–355; c) S. Iwamoto, K. Motomura, Y. Shinoda, M. Urata, J. Kato, N. Takiguchi, H. Ohtake, R. Hirota, A. Kuroda, *Appl. Environ. Microbiol.* **2007**, *73*, 5676–5678; d) M. Sato, Y. Masuda, K. Kirimura, K. Kino, *J. Biosci. Bioeng.* **2007**, *103*, 179–184; e) E. Restiawaty, Y. Iwasa, S. Maya, K. Honda, T. Omasa, R. Hirota, A. Kuroda, H. Ohtake, *Process Biochem.* **2011**, *46*, 1747–1752.
- [17] a) T. Noguchi, T. Shiba, U.S. Patent 6,022,713, **2000**; b) T. Noguchi, T. Shiba, *Biosci. Biotechnol. Biochem.* **1998**, *62*, 1594–1596.
- [18] J. Nahálka, V. Pätöprstý, *Org. Biomol. Chem.* **2009**, *7*, 1778–1780.
- [19] K. Schmölzer, M. Lemmerer, A. Gutmann, B. Nidetzky, *Biotechnol. Bioeng.* **2016**, doi: 10.1002/bit.26204.
- [20] a) C. F. C. Bonting, G. J. J. Kortstee, A. J. B. Zehnder, *J. Bacteriol.* **1991**, *173*, 6484–6488; b) T. Shiba, H. Itoh, A. Kameda, K. Kobayashi, Y. Kawazoe, T. Noguchi, *J. Bacteriol.* **2005**, *187*, 1859–1865.
- [21] a) L. Bungaruang, A. Gutmann, B. Nidetzky, *Adv. Synth. Catal.* **2013**, *355*, 2757–2763; b) M. Morell, L. Copeland, *Plant Physiol.* **1985**, *78*, 149–154.
- [22] M. Diricks, F. De Bruyn, P. Van Daele, M. Walmagh, T. Desmet, *Appl. Microbiol. Biotechnol.* **2015**, *99*, 8465–8474.
- [23] M. Diricks, A. Gutmann, S. Debacker, G. Dewitte, B. Nidetzky, T. Desmet, *Protein Eng. Des. Sel.* **2016**, doi: 10.1093/protein/gzw048.
- [24] a) D. J. Pollard, J. M. Woodley, *Trends Biotechnol.* **2007**, *25*, 66–73; b) A. J. J. Straathof, S. Panke, A. Schmid, *Curr. Opin. Biotechnol.* **2002**, *13*, 548–556.
- [25] a) H. Kawai, M. Kaneko, K. Maejima, I. Kato, M. Yamasaki, *Agric. Biol. Chem.* **1985**, *49*, 2905–2911; b) M. E. Baroja-Fernández, F. J. Muñoz Perez, F. J. Pozueta-Romero, M. T. Morán-Zorzano, N. A. Casajus, U.S. Patent 8,168,856 B2, **2009**; c) J. Bae, K.-H. Kim, D. Kim, Y. Choi, J. S. Kim, S. Koh, S.-I. Hong, D.-S. Lee, *ChemBioChem* **2005**, *6*, 1963–1966; d) S.-I. Ryu, J.-E. Kim, E.-J. Kim, S.-K. Chung, S.-B. Lee, *Process Biochem.* **2011**, *46*, 128–134; e) S.-I. Ryu, S.-B. Lee, *Enzyme Microb. Technol.* **2013**, *53*, 359–363.
- [26] S. Koizumi, T. Endo, K. Tabata, A. Ozaki, *Nat. Biotechnol.* **1998**, *16*, 847–850.
- [27] H. Kawai, S. Nakajima, M. Okuda, T. Yano, T. Tachiki, T. Tochikura, *J. Ferment. Technol.* **1978**, *56*, 586–592.
- [28] S. Koizumi, T. Endo, K. Tabata, H. Nagano, J. Ohnishi, A. Ozaki, *J. Ind. Microbiol. Biotechnol.* **2000**, *25*, 213–217.
- [29] M. Lemmerer, K. Schmölzer, A. Gutmann, B. Nidetzky, *Adv. Synth. Catal.* **2016**, *358*, 3113–3122.
- [30] a) R. Chen, H. Zhang, G. Zhang, S. Li, G. Zhang, Y. Zhu, J. Liu, C. Zhang, *J. Am. Chem. Soc.* **2013**, *135*, 12152–12155; b) C. Zhang, E. Bitto, R. D. Goff, S. Singh, C. A. Bingman, B. R. Griffith, C. Albermann, G. N. Phillips, J. S. Thorson, *Chem. Biol.* **2008**, *15*, 842–853.

*Advanced*   
**Synthesis &  
Catalysis**

Supporting Information

## SUPPORTING INFORMATION

# Biocatalytic Cascade of Polyphosphate Kinase and Sucrose Synthase for Synthesis of Nucleotide-activated Derivatives of Glucose

Sandra T. Kulmer,<sup>+a</sup> Alexander Gutmann,<sup>+a</sup> Martin Lemmerer,<sup>b</sup> and Bernd Nidetzky<sup>a,b\*</sup>

<sup>a</sup> Institute of Biotechnology and Biochemical Engineering, Graz University of Technology, NAWI Graz, Petersgasse 12, 8010 Graz, Austria  
Fax: (+43)-316-873-8434; phone:(+43)-316-873-8400; e-mail: bernd.nidetzky@tugraz.at

<sup>b</sup> Austrian Centre of Industrial Biotechnology, Petersgasse 14, 8010 Graz, Austria

<sup>+</sup> These authors contributed equally to this work.

### Table of contents

<b>1 Methods</b>	<b>S3</b>
<b>2 Results</b>	<b>S5</b>
<b>3 References</b>	<b>S12</b>



## 1. Methods

### Construction of *E. coli* expression strains

The pET-28a vectors for expression of *Aj*PPK (GenBank: BAC76403.1) and *Mr*PPK (GenBank: AGK05310.1) were kindly received from Prof. Jennifer Andexer (Institute of Pharmaceutical Sciences, University of Freiburg, Germany). The coding genes were inserted into *Nde*I and *Hind*III sites for expression as fusion proteins with N-terminal His-tag. Construction of the pET-STRP3 vector for expression of *Gm*SuSy (GenBank: AAC39323.1) with N-terminally fused *Strep*-tag II was described elsewhere in detail.<sup>[1]</sup> The pCXP34h vector for constitutive expression of *Ac*SuSy (GenBank: AIA55343.1) as a fusion proteins with N-terminal His-tag was obtained from Prof. Tom Desmet (Centre for Industrial Biotechnology and Biocatalysis, Ghent University, Belgium).<sup>[2]</sup> Expression strains were created by transformation of electro-competent *E. coli* BL21-Gold (DE3) cells. The correct sequences were verified by sequencing the complete genes.

### Enzyme expression

*Aj*PPK, *Mr*PPK and *Gm*SuSy were cultivated in lysogeny broth (LB) medium (10 g L<sup>-1</sup> tryptone, 10 g L<sup>-1</sup> NaCl and 5 g L<sup>-1</sup> yeast extract) supplemented with 50 µg mL<sup>-1</sup> kanamycin. *E. coli* strains were grown overnight in 250 mL baffled shake flasks containing 50 mL medium on a rotary shaker at 37°C and 120 rpm. Overnight cultures were used to inoculate 300 mL of main culture to an optical density at 600 nm (OD<sub>600</sub>) of 0.05. Cells were grown in 1 L baffled shake flasks on a rotary shaker at 37°C and 120 rpm until an OD<sub>600</sub> of 0.8 – 1.0 was reached. Then enzyme expression was induced by addition of 500 µM isopropyl β-D-1-thiogalactopyranoside (IPTG) and the temperature was lowered for *Gm*SuSy and PPKs to 25 and 18°C, respectively. After overnight expression cells were harvested by centrifugation (5000 rpm, 30 min, 4°C). Cell pellets were resuspended with an equal volume of deionized water and stored at -20°C.

*Ac*SuSy was cultivated similarly in LB medium supplemented with 100 µg mL<sup>-1</sup> ampicillin. However, by using a constitutive promoter IPTG induction was omitted and the temperature remained constant at 37°C throughout the 24 h long incubation of the main culture.

### Enzyme purification

Thawed cells were lysed by repeated passage through a cooled French press at 100 bar. Cell debris was removed by centrifugation (35 min, 15,000 rpm, 4°C) and the cell extract was filtrated through a 1.2 µm cellulose-acetate filter prior to enzyme purification.

For His-tag affinity purification of *Aj*PPK, *Mr*PPK and *Ac*SuSy derived from 1 – 2 L of shaking flask cultivation two 5 mL His Trap FF columns (GE Healthcare; Vienna, Austria) were connected in series on an ÄktaPrime plus system (GE Healthcare). A constant flow rate of 2 mL min<sup>-1</sup> was applied. A 50 mM Tris buffer (pH 7.4) containing 500 mM NaCl and 20 mM imidazole was used to equilibrate the columns and to wash off unbound proteins. Enzymes were eluted in a single peak during a 100 mL long gradient from 20 to 250 mM imidazole.

*Gm*SuSy was purified by *Strep*-tag affinity chromatography. Typically a 3 mL gravity flow *Strep*-Tactin<sup>®</sup> Sepharose<sup>®</sup> column (IBA GmbH, Göttingen, Germany) was used per 300 mL of shaking flask culture. Columns were equilibrated with 3 column volumes (CV) of washing buffer (100 mM Tris pH 8, 150 mM NaCl, 1 mM EDTA) before loading the cell extract which was twofold diluted with washing buffer. A 5 CVs long wash with washing buffer was followed by elution of *Gm*SuSy with 3 CVs of elution buffer (100 mM Tris pH 8, 150 mM NaCl, 1 mM EDTA, 2.5 mM desthiobiotin) whereas the first 0.5 CVs were discarded and

the rest was pooled. Columns were regenerated with 15 CVs of regeneration buffer (100 mM Tris pH 8, 150 mM NaCl, 1 mM EDTA, 1 mM hydroxy-azophenyl-benzoic acid) and equilibrated with 10 CVs of washing buffer.

Enzymes were concentrated and buffer exchanged to 25 mM HEPES, pH 7.0 using centrifugal concentrators with a molecular weight cut off of 10 kDa. *AcSuSy*, *MrPPK* and *AjPPK* were stored at 4°C and *GmSuSy* was kept at -20°C. Protein concentrations were determined photometrically at 280 nm and protein purities were assessed by SDS-PAGE.

## 2. Results

**Table S1.** Prices of nucleoside phosphates [ $\$ \text{g}^{-1}$ ] as listed by Carbosynth Limited (Berkshire, UK)<sup>[a]</sup>

nucleoside	monophosphate	diphosphate	triphosphate
adenosine	0.55 <sup>[b,c]</sup>	12.00 <sup>[f,c]</sup>	1.50 <sup>[e,j]</sup>
guanosine	0.18 <sup>[d]</sup>	30.00	55.00
cytidine	1.50 <sup>[e]</sup>	30.00 <sup>[g]</sup>	30.00 <sup>[g]</sup>
uridine	1.00 <sup>[e]</sup>	65.00	13.00 <sup>[f]</sup>
deoxy-thymidine	50.00	1420.00 <sup>[h,i]</sup>	725.00 <sup>[i]</sup>

<sup>[a]</sup> Based on 1 g of the least expensive salt available on November 11<sup>th</sup> 2016 (disodium salt unless mentioned otherwise)

<sup>[b]</sup> Based on the smallest listed amount of 100 g

<sup>[c]</sup> Acid form

<sup>[d]</sup> Based on the smallest listed amount of 250 g

<sup>[e]</sup> Based on the smallest listed amount of 50 g

<sup>[f]</sup> Based on the smallest listed amount of 5 g

<sup>[g]</sup> Based on the smallest listed amount of 2 g

<sup>[h]</sup> Based on the largest listed amount of 0.5 g

<sup>[i]</sup> Trisodium salt

<sup>[j]</sup> Disodium salt hydrate

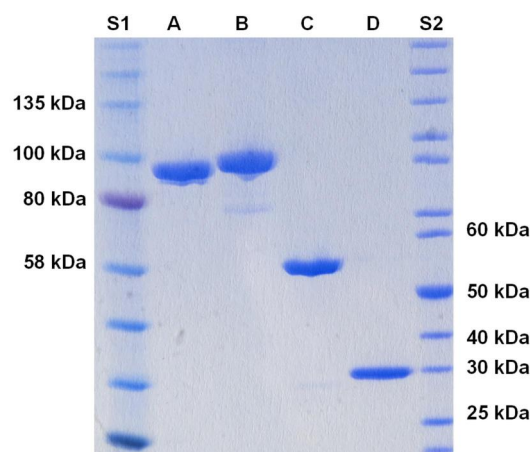


**Figure S1.** SDS-PAGE of *Mr*PPK, *Aj*PPK, *Gm*SuSy and *Ac*SuSy purified from *E. coli* overexpression cultures. *Gm*SuSy was purified by *Strep*-tag affinity chromatography while all other enzymes were purified by His-tag affinity chromatography. S1: Color Prestained Protein Standard, Broad Range (New England BioLabs) A: *Ac*SuSy (monomeric molecular mass: 92.0 kDa); B: *Gm*SuSy (monomeric molecular mass: 94.1 kDa); C: *Aj*PPK (monomeric molecular mass: 55.8 kDa); D: *Mr*PPK (monomeric molecular mass: 31.6 kDa); S2: PageRuler<sup>TM</sup> Unstained Protein Ladder (Thermo Scientific).

Biocatalytic Cascade of Polyphosphate Kinase and Sucrose Synthase  
for Synthesis of Nucleotide-Activated Derivatives of Glucose

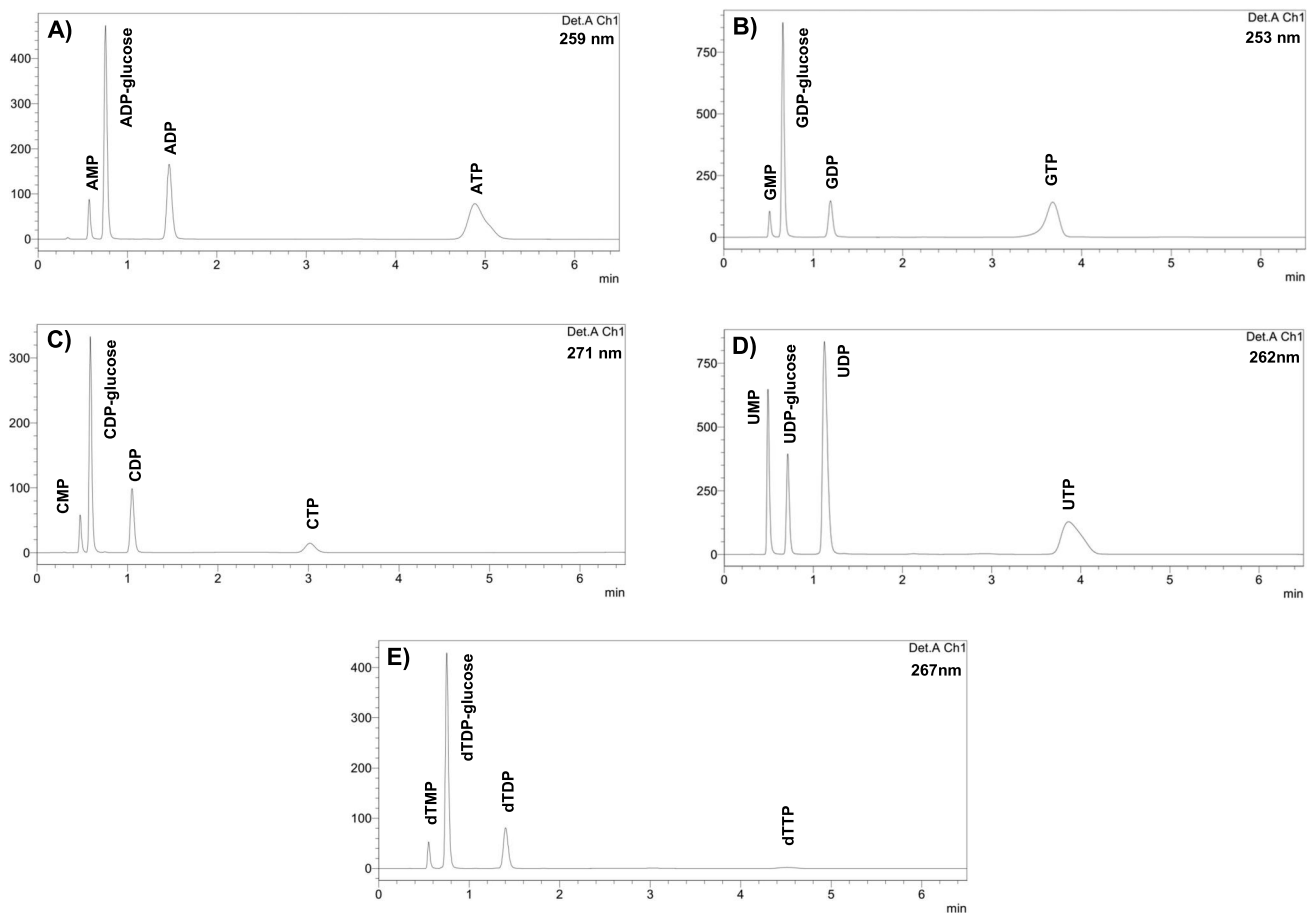


**Figure S2.** Nucleoside phosphates and NDP-glucose were quantified by reversed-phase C-18 HPLC using a TBAB based ion-pairing protocol with UV-detection at the absorption maximum of the respective nucleobase. Compounds with the same nucleobase were baseline separated. A) adenine (259 nm), B) guanine (253 nm), C) cytosine (271 nm), D) uracil (262 nm), E) thymine (267 nm).

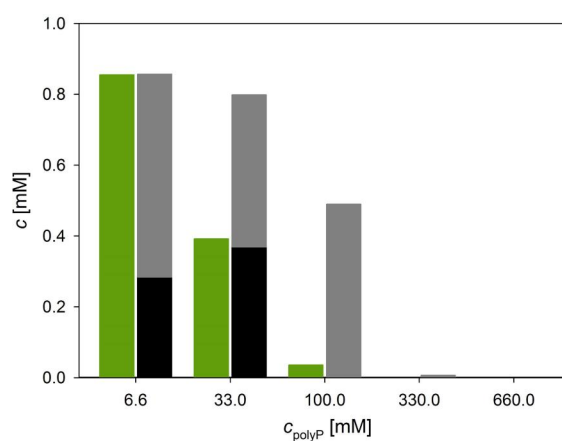


**Figure S3.** Phosphorylation of AMP by *Aj*PPK and *Mr*PPK was tested at various polyP concentrations (1 mM AMP, 50  $\mu\text{g mL}^{-1}$  PPK, 10 mM  $\text{MgCl}_2$ , pH 7.1, 6 h, 30°C). *Aj*PPK formed exclusively ADP (green) but *Mr*PPK partially converted ADP (grey) further to ATP (black).

Biocatalytic Cascade of Polyphosphate Kinase and Sucrose Synthase  
for Synthesis of Nucleotide-Activated Derivatives of Glucose

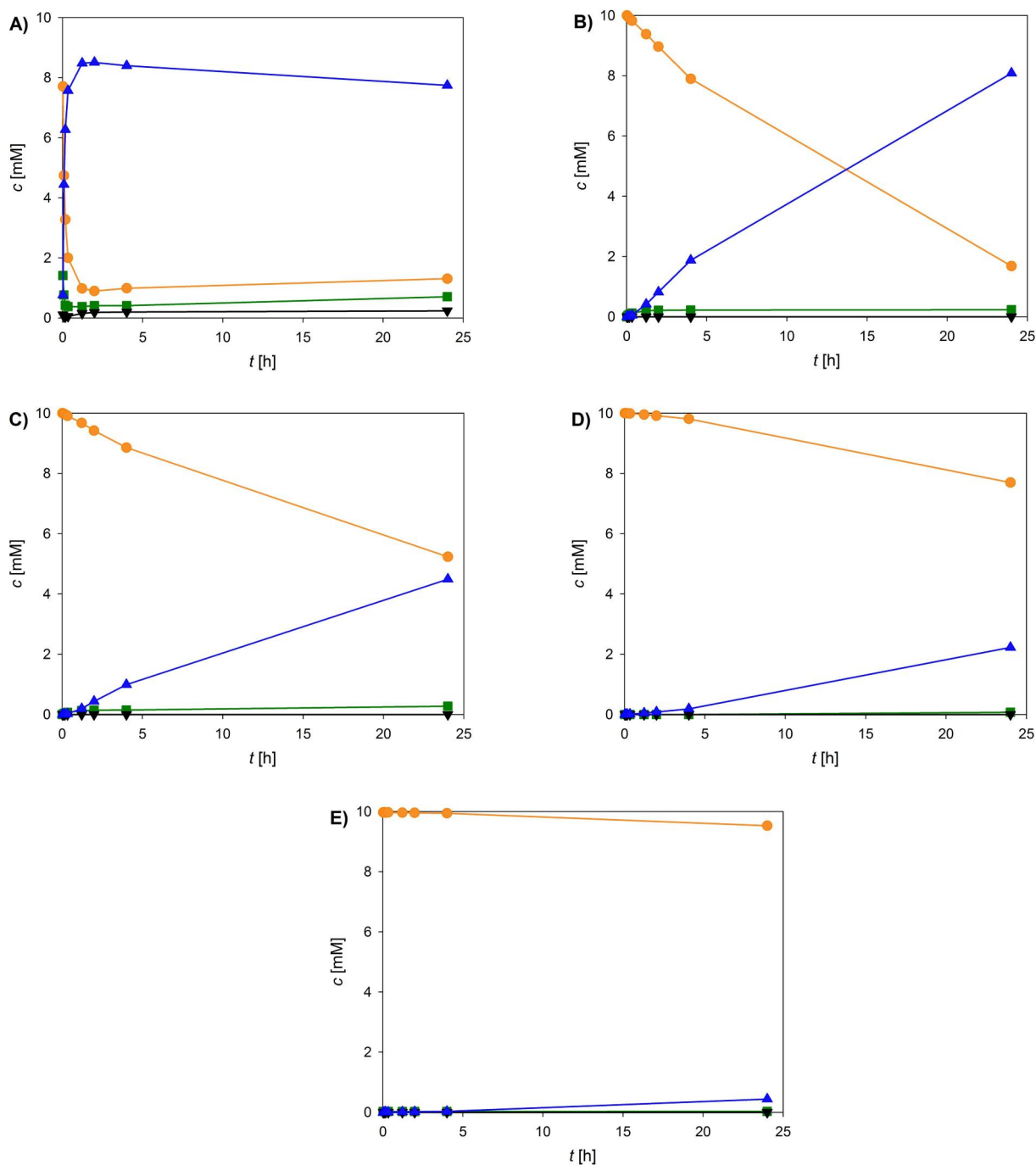


**Figure S4.** AMP (A), GMP (B), CMP (C), UMP (D) and dTMP (E) were used to synthesize NDP-glucose by the *Mr*PPK-*Ac*SuSy cascade reaction at 45°C. Reaction mixtures contained 10 mM NMP, 33 mM polyP, 250 mM sucrose, 10 mM MgCl<sub>2</sub>, 300 μg mL<sup>-1</sup> *Mr*PPK, 50 μg mL<sup>-1</sup> *Ac*SuSy and 50 mM MES, pH 5.5. NMP (orange), NDP (green), NDP-glucose (blue), NTP (black).

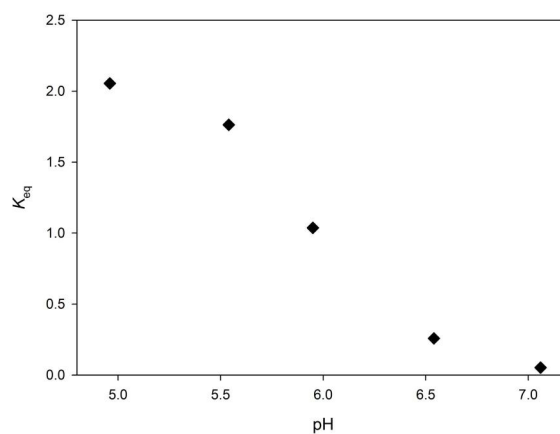


**Figure S5.** The equilibrium constant ( $K_{eq}$ ) of ADP-glucose formation by SuSy showed a strong pH-dependence. The final ADP and ADP-glucose concentrations from AMP conversions in the *MrPPK-AcSuSy* cascade reactions (Figure 4C) were used to calculate the respective  $K_{eq}$ . Reaction conditions: 100 mM AMP, 132 mM polyP, 1 M sucrose, 25 mM  $MgCl_2$ , 100  $\mu g\ mL^{-1}$  *MrPPK*, 50  $\mu g\ mL^{-1}$  *AcSuSy*, 45°C.

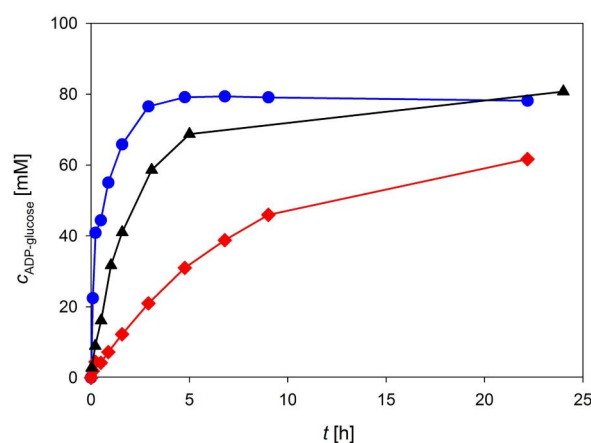


**Figure S6.** ADP-glucose formation from AMP by the *MrPPK-AcSuSy* cascade reaction (45°C, black) was compared to single step ADP-glucose synthesis from ADP using either *GmSuSy* (30°C, red) or *AcSuSy* (45°C, blue). Conversions were performed at pH 5.5 whereby only in uncoupled SuSy conversions pH control by addition of 4 M HCl was required for pH maintenance. All reactions contained 1 M sucrose, 25 mM  $MgCl_2$  and 50  $\mu g\ mL^{-1}$  SuSy. Single step SuSy conversions were supplemented with 100 mM ADP. The coupled conversion additionally contained 100 mM AMP, 132 mM polyP and 100  $\mu g\ mL^{-1}$  *MrPPK*.

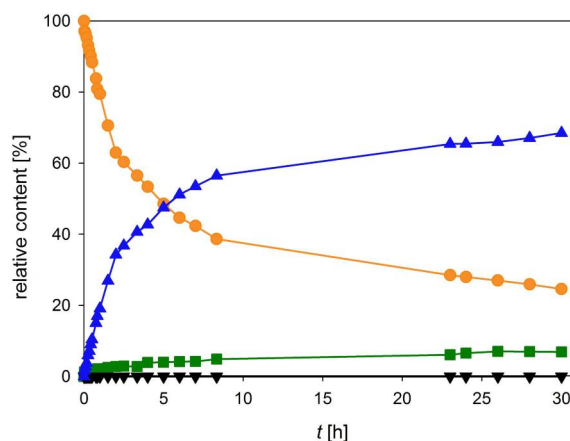


**Figure S7.** ADP-glucose synthesis by the *Mr*PPK-*Ac*SuSy cascade reaction was upscaled to a working volume of 150 mL (100 mM AMP, 1 M sucrose, 132 mM polyP, 25 mM MgCl<sub>2</sub>, pH 5.5). The relative content of soluble AMP (orange), ADP (green), ADP-glucose (blue), ATP (black) is shown. The final ADP-glucose yield of 68% (based on soluble AMP) was somewhat lower than in the small-scale reaction. This was likely due to a depletion of the polyP substrate caused by compound precipitation under the conditions used. Periodic feeding of polyP is an approach to overcome the problem of substrate solubility.

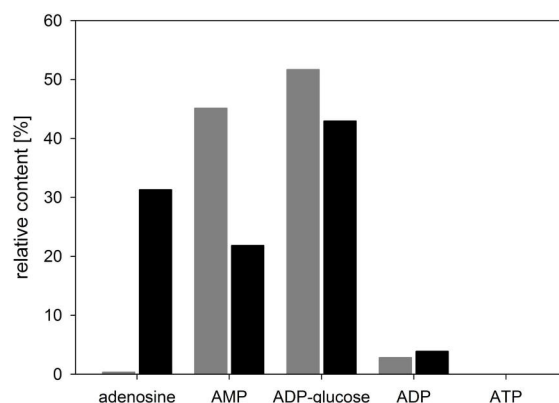


**Figure S8.** The relative content of adenine containing compounds is shown before (grey) and after (black) dephosphorylating a reaction mixture from an *Mr*PPK-*Ac*SuSy cascade reaction (10 U mL<sup>-1</sup> CIAP, 25 mM MgCl<sub>2</sub>, 24 h, 30°C, pH 7.3). Inhibition of CIAP by polyP prevented complete conversion of AMP and ADP to adenosine. Reduced stability under conditions ideal for dephosphorylation resulted in partial ADP-glucose loss through chemical degradation.

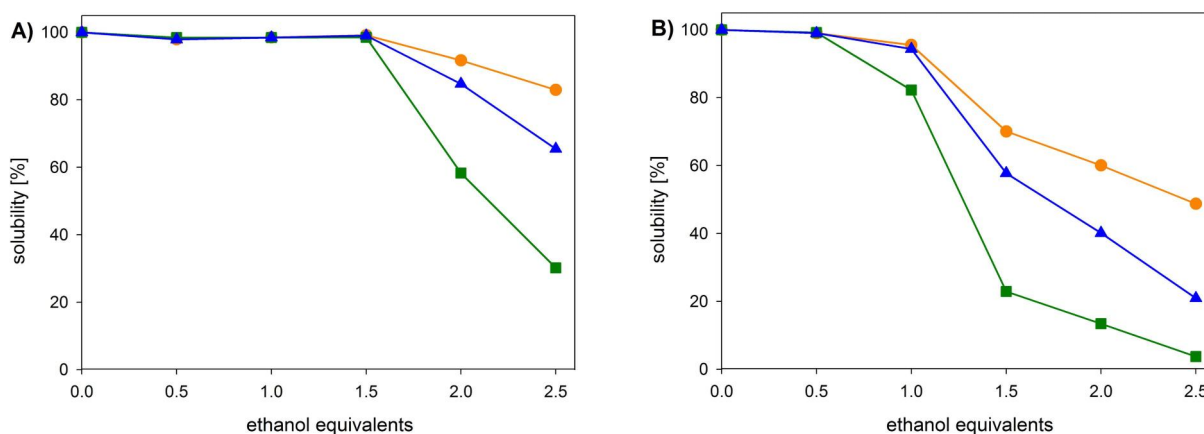


**Figure S9.** The solubility of ADP-glucose (blue), AMP (orange) and ADP (green) was tested in presence of various ethanol concentrations at A) 4 and B) -20°C. A protein free reaction mixture containing 57 mM ADP-glucose, 20 mM AMP, 6 mM ADP and polyP was used. Samples were incubated overnight and centrifuged to separate soluble fraction and precipitate, which were analyzed separately by HPLC.

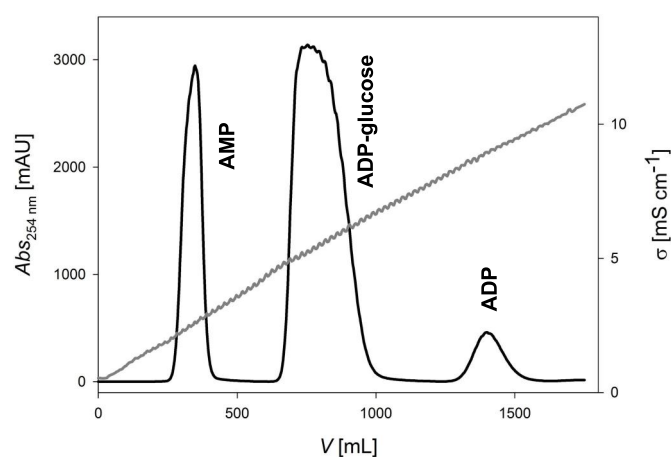


**Figure S10.** ADP-glucose (259 mg) was separated from AMP (51 mg) and ADP (15 mg) by preparative AEC on a 40 mL Toyopearl SuperQ-650M column (inner diameter 1.6 cm, length 20 cm) using a sodium acetate gradient (20 - 510 mM, pH 4.3). A flow rate of 5 cm min<sup>-1</sup> (10 mL min<sup>-1</sup>) was used. UV absorbance at 254 nm (black), conductivity (grey).

**Table S2.** Purification of ADP-glucose by AEC after fractionated polyP precipitation

step	T [°C]	ethanol equivalents	recovery [%]		ADP-glucose content <sup>[a]</sup> [%]	<i>m</i> <sub>ADP-glucose</sub> [mg]
			step	total		
end of reaction					68.5	334
polyP precipitation	4	1.5	83.3	83.3	66.4	278
1 <sup>st</sup> ADP-glucose precipitation	-20	5	93.1	77.6	70.7	259
AEC			81.9	63.5	99.7	212
2 <sup>nd</sup> ADP-glucose precipitation	-20	4	84.4	53.6	99.7	179
3 <sup>rd</sup> ADP-glucose precipitation	-20	5	95.5	51.2	99.7	171

<sup>[a]</sup> Based on nucleoside quantification by HPLC measurement.



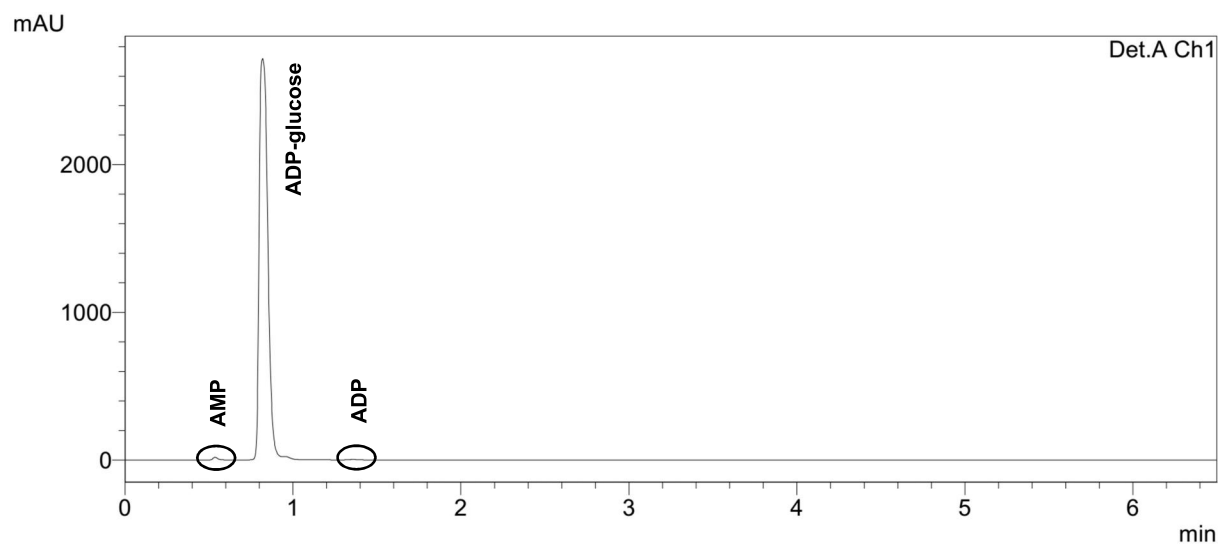


**Figure S11.** Using HPLC analysis with UV-detection at 259 nm the very high purity of ADP-glucose was shown. AMP ( $\leq 0.25\%$ ) and ADP ( $\leq 0.10\%$ ) were hardly detectable in the purified product.

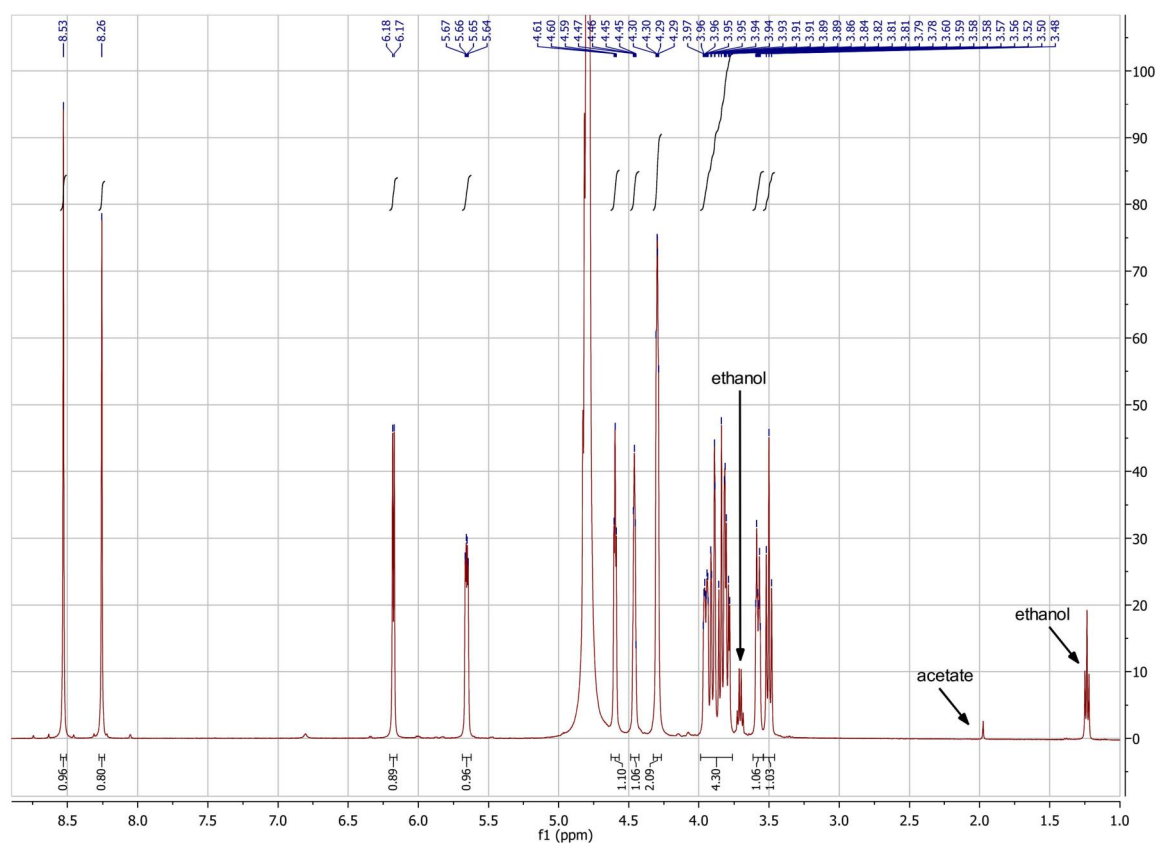


**Figure S12.**  $^1\text{H-NMR}$  of purified ADP-glucose was consistent with literature reports.<sup>[3]</sup> The only detectable impurities were ethanol ( $\sim 1\%$ ) and acetate ( $\sim 0.1\%$ ).

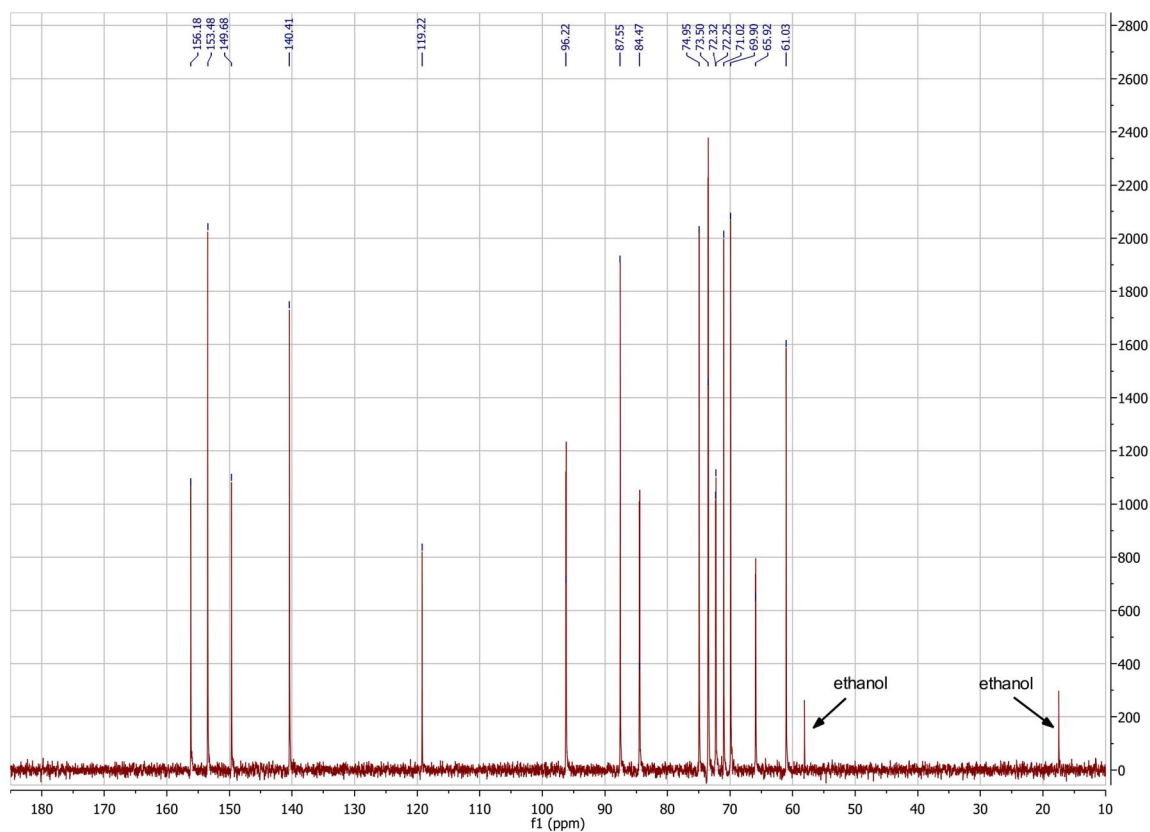


**Figure S13.** <sup>13</sup>C-NMR of purified ADP-glucose was consistent with literature reports.<sup>[3]</sup> Ethanol was the only detectable impurity.

### 3. References

- [1] L. Bungaruang, A. Gutmann, B. Nidetzky, *Adv. Synth. Catal.* **2013**, *355*, 2757-2763.
- [2] M. Diricks, F. De Bruyn, P. Van Daele, M. Walmagh, T. Desmet, *Appl. Microbiol. Biotechnol.* **2015**, *99*, 8465-8474.
- [3] a) J. Bae, K.-H. Kim, D. Kim, Y. Choi, J. S. Kim, S. Koh, S.-I. Hong, D.-S. Lee, *ChemBioChem* **2005**, *6*, 1963-1966; b) A. Zervosen, A. Stein, H. Adrian, L. Elling, *Tetrahedron* **1996**, *52*, 2395-2404.

Glycosyltransferase Cascades Made Fit for  
Chemical Production: Integrated Biocatalytic  
Process for the Natural Polyphenol C-Glucoside  
Nothofagin

ARTICLE

# Glycosyltransferase cascades made fit for chemical production: Integrated biocatalytic process for the natural polyphenol C-glucoside nothofagin

Katharina Schmölzer<sup>1</sup> | Martin Lemmerer<sup>1</sup> | Bernd Nidetzky<sup>1,2</sup> 

<sup>1</sup> Austrian Centre of Industrial Biotechnology, Graz, Austria

<sup>2</sup> Institute of Biotechnology and Biochemical Engineering, Graz University of Technology, NAWI Graz, Graz, Austria

## Correspondence

Bernd Nidetzky, Institute of Biotechnology and Biochemical Engineering, Graz University of Technology, NAWI Graz, Petersgasse 12/I, Graz 8010, Austria.  
Email: bernd.nidetzky@tugraz.at

## Funding information

The Federal Ministry of Science, Research and Economy (BMWFW); The Federal Ministry of Traffic, Innovation and Technology (BMVIT); The Styrian Business Promotion Agency, SFG; The Standortagentur Tirol; The Government of Lower Austria and Business Agency Vienna through the COMET-Funding Program managed by the Austrian Research Promotion Agency FFG; EU FP7 project SuSy (Sucrose Synthase as Effective Mediator of Glycosylation)

## Abstract

Glycosyltransferase cascades are promising tools of biocatalysis for natural product glycosylation, but their suitability for actual production remains to be shown. Here, we demonstrate at a scale of 100 g isolated product the integrated biocatalytic production of nothofagin, the natural 3'-C-β-D-glucoside of the polyphenol phloretin. A parallel reaction cascade involving coupled C-glycosyltransferase and sucrose synthase was optimized for the one-pot glycosylation of phloretin from sucrose via an UDP/UDP-glucose shuttle. Inclusion complexation with the highly water soluble 2-hydroxypropyl-β-cyclodextrin pushed the phloretin solubility to its upper practical limit (~120 mM) and so removed the main bottleneck on an efficient synthesis of nothofagin. The biotransformation thus intensified had excellent performance metrics of 97% yield and ~50 g<sub>product</sub>/L at a space-time yield of 3 g/L/hr. The UDP-glucose was regenerated up to ~220 times. A scalable downstream process for efficient recovery of nothofagin (≥95% purity; ≥65% yield) was developed. A tailored anion-exchange chromatography at pH 8.5 was used for capture and initial purification of the product. Recycling of the 2-hydroxypropyl-β-cyclodextrin would also be possible at this step. Product precipitation at a lowered pH of 6.0 and re-dissolution in acetone effectively replaced desalting by size exclusion chromatography in the final step of nothofagin purification. This study therefore, reveals the potential for process intensification in the glycosylation of polyphenol acceptors by glycosyltransferase cascades. It demonstrates that, with up- and downstream processing carefully optimized and suitably interconnected, a powerful biocatalytic technology becomes available for the production of an important class of glycosides difficult to prepare otherwise.

## KEYWORDS

C-glycosides, cyclodextrin inclusion complex, glycosyltransferase cascade, natural product glycosylation, solubility enhancement, up- and downstream processing

**Abbreviations:** AEC, anion-exchange chromatography; AEX, anion-exchange; CD, cyclodextrin; DSP, downstream processing; GT, glycosyltransferase; SEC, size-exclusion chromatography; SuSy, sucrose synthase; UDP, uridine-5'-diphosphate; USP, upstream processing.

Proofs and reprints should be addressed to Bernd Nidetzky.

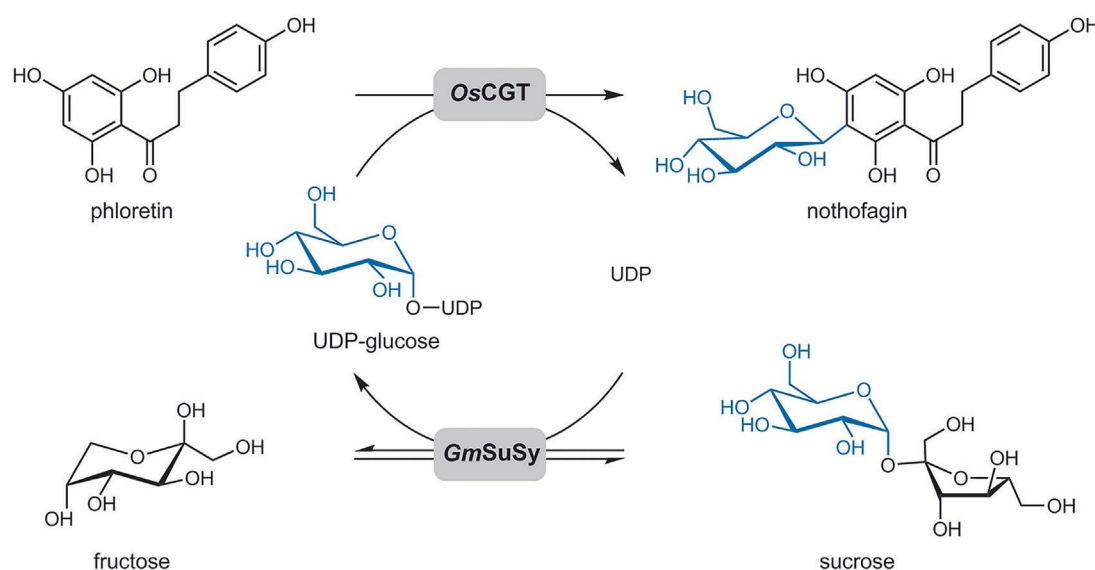
## 1 | INTRODUCTION

Flavonoids are plant-derived polyphenols widely known for their important roles in the human diet related to health (Andersen & Markham, 2005; Rodriguez-Mateos et al., 2014). Many flavonoids occur naturally as glycosides, having one or more sugars covalently attached to them. The glycosylation profoundly impacts the solubility, stability, and bioactivity of flavonoids, thus making their glycosides attractive as food additives, therapeutics, and nutraceuticals (De Bruyn, Maertens, Beauprez, Soetaert, & De Mey, 2015; Kren & Martinkova, 2001). Nothofagin, the 3'-C- $\beta$ -D-glucoside of the dihydrochalcone phloretin (Scheme 1), is a prominent example of a unique class of flavonoid glycosides featuring a rare-in-nature C-glycosidic structure (Veitch & Grayer, 2011). Unlike the naturally widespread flavonoid O-glycosides, the corresponding C-glycosides cannot be degraded via canonical hydrolysis of the glycosidic linkage (Bililign, Hyun, Williams, Czisny, & Thorson, 2004; Härle et al., 2011). They therefore excel in biological stability and so, generally, in long-term efficacy during application (Lee et al., 2010; Meng et al., 2008). Nothofagin is almost exclusively found in rooibos plant (*Aspalathus linearis*) and linked to various health-promoting effects of its herbal tea (Joubert et al., 2012; McKay & Blumberg, 2007). Nothofagin has attracted considerable interest due to its antioxidative and antithrombotic activities (Ku, Lee, Kang, & Bae, 2014; Snijman et al., 2009), antimutagenic properties (Snijman, Swanevelder, Joubert, Green, & Gelderblom, 2007), influences on steroid levels (Schloms, Storbeck, Swart, Gelderblom, & Swart, 2012), and positive effects in diabetes treatment (Ku, Kwak, Kim, & Bae, 2015).

Despite recent progress in isolating nothofagin from rooibos (de Beer et al., 2015), natural scarcity severely restricts the application of the C-glucoside in food and pharmaceutical products. Also, the chemical synthesis of nothofagin is difficult and not suitable for large

scale production (Yepremyan, Salehani, & Minehan, 2010). These problems are not just relevant for nothofagin, but concern the flavonoid glycoside production in general (Chen et al., 2015; Lim, Ashford, Hou, Jackson, & Bowles, 2004; Zhang et al., 2017). The biocatalytic synthesis, via enzymatic glycosylation of the flavonoid core, was often found useful in preparing, and so enhancing the availability of the corresponding flavonoid O-glycosides (Bertrand et al., 2006; De Bruyn, Van Brempt et al., 2015; Gao, Mayon, MacManus, & Vulfson, 2000; Ono et al., 2005; Xia & Eiteman, 2017). The specific problem of nothofagin is that the glycosylation strategies established for O-glycosides are inappropriate for C-glycosides. Installing the intricate C-glycosidic linkage necessitates special enzymes from the class of nucleoside diphospho (NDP)-sugar dependent (Leloir) glycosyltransferases, clearly distinct from the enzymes able, and used previously, to form flavonoid O-glycosides (Brazier-Hicks et al., 2009; Chen et al., 2015; Ito, Fujimoto, Shimosaka, & Taguchi, 2014). These Leloir glycosyltransferases are not well established for application in biocatalytic synthesis. A C-glucosyltransferase from rice (*Oryza sativa*) catalyzes the site- and chemo-selective 3'-C- $\beta$ -D-glucosylation of phloretin from uridine 5'-diphospho (UDP)-glucose (Brazier-Hicks et al., 2009). Promising design of a biocatalytic process for nothofagin involves a parallel reaction cascade of C-glucosyltransferase and sucrose synthase, as depicted in Scheme 1 (Bungaruang, Gutmann, & Nidetzky, 2013). The one-pot glucosylation of phloretin thus occurs from sucrose via an UDP/UDP-glucose shuttle (Schmölzer, Gutmann, Diricks, Desmet, & Nidetzky, 2016). Sucrose is a highly expedient donor substrate for (enzymatic) glucosylation processes (Desmet et al., 2012; Rupprath, Kopp, Hirtz, Müller, & Elling, 2007).

Nothofagin synthesis according to Scheme 1 was demonstrated in principle (Bungaruang et al., 2013) and some optimizations on it were made (Bungaruang, Gutmann, & Nidetzky, 2016; Gutmann, Lepak,



**SCHEME 1** One-pot synthesis of nothofagin by enzymatic C-glycosylation of phloretin from sucrose via UDP-glucose is shown. C-glucosyltransferase from rice (OsCGT) and sucrose synthase from soybean (*GmSuSy*) are used. Catalytic amounts of UDP are used

Diricks, Desmet, & Nidetzky, 2017), but its suitability for actual production remains to be shown. Phloretin solubility was identified as a major bottleneck on the biotransformation efficiency. Organic cosolvents (e.g., Bertrand et al., 2006; De Winter et al., 2013; Meulenbeld & Hartmans, 2000) were of limited use because in amounts needed to boost the soluble phloretin concentration to 10 mM or greater (e.g.,  $\geq 20\%$  DMSO), they were not tolerated by the enzymes (Bungaruang et al., 2016). Unlike free phloretin when present insoluble, a  $\beta$ -cyclodextrin inclusion complex of the phloretin did not cause inactivation of the enzymes (Bungaruang et al., 2016). A suspension of this complex (50 mM) was converted in 88% yield ( $19 \text{ g}_{\text{product}}/\text{L}$ ; 44 mM). The space-time yield (STY) was 1 g/L/hr and the recycling number ( $RC_{\text{max}}$ ) for UDP-glucose was 88 (Bungaruang et al., 2016). Despite these promising characteristics, the biocatalytic synthesis was considered not yet fit for process scale-up to enable nothofagin production at demonstration scale ( $\sim 100 \text{ g}$ ). In this line, the phloretin complexation with  $\beta$ -cyclodextrin required attention in particular, for it involved a slow and labor-intensive processing in multiple steps (Bungaruang et al., 2016). Moreover,  $\beta$ -cyclodextrin has limited solubility in water ( $\sim 16 \text{ mM}$ ), creating mixing issues in suspension and restricting the nothofagin concentration attainable in a batch conversion to about 40–50 mM at maximum. Immediately related to the problem of phloretin solubility, isolation of nothofagin from the liquid–solid reaction slurry appeared complicated.

The current study was performed to address these critical issues of nothofagin production. A systematic approach of process “debottlenecking” was applied. The approach is widely recognized for its importance in facilitating process development in industrial biocatalysis (Kratzer, Woodley, & Nidetzky, 2015; Panke, Wubbolts, Schmid, & Witholt, 2000; Schmölzer, Lemmerer, Gutmann, & Nidetzky, 2016; Tufvesson et al., 2011), yet it is novel to glycosyltransferase cascade transformations of the type represented in Scheme 1. An integrated process design, featuring strong interconnection between the upstream and downstream processing steps of the process, was the key to unlock the full potential of the biocatalytic flavonoid glycosylation. Phloretin complexation with the highly water-soluble 2-hydroxypropyl- $\beta$ -cyclodextrin (Szente & Szejtli, 1999; Wei, Zhang, Memon, & Liang, 2017) succeeded in pushing the limits of enzymatic synthesis. Besides significant intensification of biocatalysis, the development of innovative downstream processing was vital to the success of the overall process: nothofagin production is demonstrated at 100 g scale. Thus, a powerful biocatalytic technology based on glycosyltransferase cascades is introduced for the production of an important class of natural glycosides difficult to prepare otherwise. The results for nothofagin are broadly relevant for flavonoid glycosides and methods of their enzymatic production.

## 2 | MATERIALS AND METHODS

### 2.1 | Chemicals and materials

2-Hydroxypropyl- $\beta$ -cyclodextrin ( $\geq 96\%$ ), 2,6-dimethyl- $\beta$ -cyclodextrin ( $\geq 98\%$ ), sulfobutyl ether- $\beta$ -cyclodextrin sodium salt

( $\geq 98\%$ ),  $\beta$ -cyclodextrin crosslinked with epichlorohydrin (50–70%), phloretin ( $>98\%$ ), and UDP disodium salt ( $\geq 98\%$ ) were from Carbosynth (Compton, Berkshire, UK). Toyopearl SuperQ-650M resin was from Tosoh Bioscience (Tokyo, Japan). Acetone ( $\geq 99\%$ ) and isopropanol ( $\geq 99\%$ ) were from Roth (Karlsruhe, Germany).

### 2.2 | Enzyme preparation

Production of the enzymes and their purification were done according to protocols from literature (Bungaruang et al., 2013). Briefly, each enzyme was expressed separately in *Escherichia coli* BL21-Gold (DE3), using reported plasmid vectors for the expression of OsCGT (GenBank: CAQ77160.1; Brazier-Hicks et al., 2009; Gutmann & Nidetzky, 2012) and GmSuSy (GenBank: AAC39323.1; Bungaruang et al., 2013). Each enzyme was produced as N-terminal *Strep*-tag II fusion protein. Enzyme purification was by single-step *Strep*-tag affinity chromatography. The enzyme preparations used were (almost) pure by the criterion of migration as single protein band in SDS PAGE (Figure S1) and exhibited specific activities consistent with the literature (Bungaruang et al., 2013). Purified enzymes were stored in 50 mM HEPES, pH 7.5, at  $-20^\circ\text{C}$ .

### 2.3 | Inclusion complex formation using chemically modified $\beta$ -cyclodextrins

#### 2.3.1 | Phloretin solubilization with $\beta$ -cyclodextrin derivatives

$\beta$ -Cyclodextrin derivatives (200–300 mM) were dissolved in HEPES buffer (50 mM, pH 7.5) containing 50 mM KCl, 0.5 mM UDP, 13 mM  $\text{MgCl}_2$ , and 300 mM sucrose. Samples were incubated overnight at  $30^\circ\text{C}$  and agitation at 1400 rpm (Thermomixer comfort; Eppendorf, Germany). Phloretin (200 mM) was added and samples were incubated overnight. Insoluble phloretin was removed (30 min, 15,000 rpm) and the obtained supernatant centrifuged once again. Samples were diluted with 80% DMSO and analyzed by HPLC.

#### 2.3.2 | Formation of liquid inclusion complex

Protocol adapted from literature was used (Giordano & Bettini, 2011; Wei et al., 2017). The 2-hydroxypropyl- $\beta$ -cyclodextrin (300 mM; 500 ml) was dissolved in water by microwave heating (Micro-Chef V98, Moulinex, Austria; 20 s at 750 W) and incubation in a drying chamber ( $70^\circ\text{C}$  for 1 hr). The Duran Schott bottle used was inverted every 15 min for mixing. For inclusion complex formation, phloretin (240 mM) was added and the suspension microwave heated and incubated in the drying chamber as described above. Insoluble phloretin was centrifuged (5,000 rpm, 5 min, room temperature). The liquid inclusion complex (supernatant) was used for nothofagin synthesis.

## 2.4 | Nothofagin synthesis from phloretin/ 2-hydroxypropyl- $\beta$ -cyclodextrin complex

### 2.4.1 | Standard reactions for inclusion complex evaluation

Phloretin and 2-hydroxypropyl- $\beta$ -cyclodextrin were used in equimolar amounts for preparation of solid and liquid inclusion complexes (see the Supporting Information). Inclusion complexes (85 mM) were used as substrate. Reactions were performed in water (1 ml) using 0.5 mM UDP, 500 mM sucrose, 50 mM KCl, 10 mM MgCl<sub>2</sub>, 0.5 mg/ml OsCGT, and 0.25 mg/ml GmSuSy. Reactions were carried out at pH 6.5, 30°C and an agitation rate of 300 rpm using a Thermomixer comfort. Samples were taken at certain times and analyzed by HPLC.

### 2.4.2 | Optimization of the biotransformation

Liquid phloretin/2-hydroxypropyl- $\beta$ -cyclodextrin inclusion complex (95–150 mM) was used. Enzymatic conversions were carried out at pH 6.5–7.5 and 30–50°C as described above. OsCGT and GmSuSy were used at 0.3–0.5 mg/ml and 0.15–0.25 mg/ml, respectively. Under optimized conditions in 1-L scale reactions, liquid phloretin/2-hydroxypropyl- $\beta$ -cyclodextrin inclusion complex was used at ~115 mM. The enzymatic conversion was carried out as described above at pH 6.5 (adjusted with 1 M NaOH) and 40°C in a total volume of 1 L (3 batches). Reaction was started by adding 0.5 mg/ml (~1.6 U/ml) of OsCGT and 0.25 mg/ml (~0.5 U/ml) of GmSuSy. The conversion was performed in a Duran Schott bottle (diameter 10 cm, height 20 cm) under magnetic stirring (stir bar: 50 × 7 mm; 100 rpm). For temperature control, the bottle was placed in a water bath. Samples were taken at certain times and analyzed by HPLC.

## 2.5 | Downstream processing of nothofagin

### 2.5.1 | Anion-exchange chromatography

AEC was performed at pH 8.5, adjusted with 1 M NaOH. Enzymes were precipitated with 0.25 volumes of cold isopropanol and removed after 10 min incubation by centrifugation (5,000 rpm). Different AEX resins were evaluated in batch experiments. A 10 mM potassium phosphate buffer pH 8.5 (mobile phase A) and 0.8 M sodium chloride in the same buffer (mobile phase B) were used for binding and elution, respectively. Isopropanol (20%) was added to prevent precipitation of nothofagin, caused by dissociation of cyclodextrin complexes upon dilution (Loftsson, 2015). The resins (100 mg) were incubated with 0.5 ml of sample containing ~17 mg nothofagin. Two desorption steps were performed. Incubation was for 30 min on an end-over-end rotator (SB3 from Stuart) at 30 rpm and room temperature. Samples were centrifuged after each step (500g, 30 min). Samples were analyzed by HPLC. For further details, see the Supporting Information.

Preparative AEC was performed on Äkta FPLC system (GE Healthcare, Germany) at room temperature. A self-packed XK 50/30 column (GE Healthcare, Austria) containing about 500 ml of Toyopearl

SuperQ-650M was applied. Sample was loaded at a flow rate of 0.25 cm/min using mobile phase A. Mobile phase B was used at 0.51 cm/min. Eluting nothofagin was detected at 280 nm and relevant fractions were pooled. In total, 12 runs were performed.

### 2.5.2 | Nothofagin precipitation and extraction

This was used mainly for desalting of nothofagin, but gave an additional purification of the product. To remove isopropanol, the typical AEC sample from SuperQ-650M was approximately threefold concentrated under reduced pressure (40 °C, 20 mbar). The product was precipitated at pH 6, adjusted with 0.1 M HCl. After centrifugation (5,000 rpm, 30 min), the product was frozen at –80°C and freeze-dried (Christ Alpha 1-4, B. Braun Biotech International, Melsungen, Germany) overnight. For removal of 2-hydroxypropyl- $\beta$ -cyclodextrin, nothofagin was extracted from the homogenized sample using acetone (~50 ml/g; vortexing for 5 min). Remaining pellet was removed by centrifugation. Acetone was evaporated under reduced pressure to dryness (40 °C, 20 mbar) before freeze-drying overnight. Evaporated acetone was recycled. The final product was analyzed by HPLC and its chemical identity confirmed by <sup>1</sup>H NMR.

## 2.6 | Analytical methods

Nothofagin and phloretin were analyzed by reversed phase HPLC using a Kinetex<sup>®</sup> EVO C18 column (5  $\mu$ m, 100 Å, 150 × 4.6 mm; Phenomenex, Germany). HPLC analysis was performed at 35°C with water and acetonitrile as mobile phases, each containing 0.1% formic acid. The flow rate was 1 ml/min. Samples were eluted with a linear gradient from 25% to 80% acetonitrile in 4 min and detected by UV absorbance at 288 nm.

A Varian Unity Inova 400 MHz spectrophotometer (Bruker, Germany) and the VNMRJ 2.2D software were used for <sup>1</sup>H NMR measurements. About 10 mg of nothofagin or phloretin were dissolved in 600  $\mu$ l of pyridine. <sup>1</sup>H NMR spectra were measured on a 5 mm indirect detection PFG-probe (Seebacher, Simic, Weis, Saf, & Kunert, 2003). Mnova 9.0 was used for evaluation of spectra.

## 3 | RESULTS AND DISCUSSION

### 3.1 | Phloretin solubility enhancement through improved inclusion complex formation

Several studies show that in terms of size and polarity, the central cavity of the  $\beta$ -cyclodextrin ring is well suitable to accommodate different flavonoids, including phloretin, as guest molecules for inclusion complex formation (Bungaruang et al., 2016; Pinho, Grootveld, Soares, & Henriques, 2014; Wei et al., 2017). Besides its low water solubility compared to synthetic derivatives (Brewster & Loftsson, 2007), the native  $\beta$ -cyclodextrin was not convenient for phloretin complexation. Precipitation from aqueous solution, which is the most commonly used method of cyclodextrin complex preparation, at least in the laboratory, was inefficient. The solvent consumption was

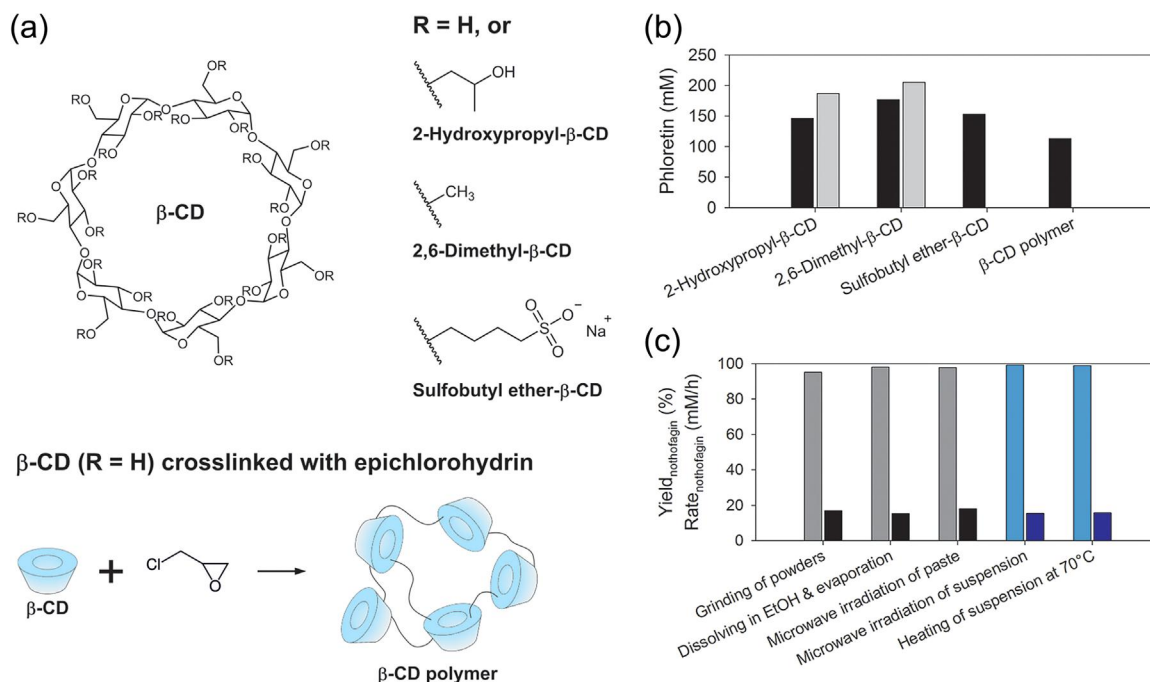
high (Hedges, 1998) and processing in multiple slow steps was required. As an example, to form the phloretin complex in solution prior to precipitation necessitated a full day of stirring. We therefore considered the highly water-soluble synthetic derivatives of  $\beta$ -cyclodextrin, such as 2-hydroxypropyl-, 2,6-dimethyl-, and sulfobutyl ether- $\beta$ -cyclodextrins or a cross-linked  $\beta$ -cyclodextrin polymer (Figure 1a; Brewster & Loftsson, 2007; Szente & Szejtli, 1999) as alternatives for phloretin complexation. Thus, inclusion complex preparation might be simplified and efficiency, hence scalability, of the biocatalytic synthesis enhanced.

Figure 1b shows phloretin solubility in solutions of the modified  $\beta$ -cyclodextrins (200–300 mM). Besides the phloretin concentration solubilizable, fluid viscosity was an additional criterion for application. The effect of the concentration of  $\beta$ -cyclodextrin derivatives on the viscosity of aqueous solutions has been extensively described in the literature (Häusler & Müller-Goymann, 1993; Loftsson, Másson, & Sigurjónsdóttir, 1999; Puskás et al., 2015). 2-Hydroxypropyl- $\beta$ -cyclodextrin and 2,6-dimethyl- $\beta$ -cyclodextrin solutions had comparable viscosities at corresponding concentrations, with 300 mM (~45%, w/w) representing a practical upper limit regarding the viscosity (Figure S2; Häusler & Müller-Goymann, 1993; Loftsson et al., 1999). This critical concentration was experimentally verified (Figure S2). Sulfobutyl ether- $\beta$ -cyclodextrin was shown to increase the viscosity significantly more, by about 20% at 30% (w/w; ~170 mM sulfobutyl

ether- $\beta$ -cyclodextrin; ~200 mM 2-hydroxypropyl- $\beta$ -cyclodextrin) cyclodextrin concentration, than 2-hydroxypropyl- $\beta$ -cyclodextrin (Puskás et al., 2015). The  $\beta$ -cyclodextrin polymer used at 200 mM formed a highly viscous gel. Overall, 2-hydroxypropyl- $\beta$ -cyclodextrin was the preferred choice for nothofagin synthesis. It was best at solubilizing phloretin ( $\geq 145$  mM;  $\geq 40$  g/L) (Figure 1b). It is comparably inexpensive and exhibits manageable effects on fluid viscosity. A highly water-soluble phloretin/2-hydroxypropyl- $\beta$ -cyclodextrin inclusion complex was reported recently (Wei et al., 2017).

### 3.2 | Optimization of inclusion complex formation with 2-hydroxypropyl- $\beta$ -cyclodextrin

Next, we examined methods of phloretin/2-hydroxypropyl- $\beta$ -cyclodextrin complex preparation and analyzed their compatibility with enzymatic nothofagin synthesis. Considering the literature (Bertacche, Lorenzi, Nava, Pini, & Sinico, 2006; Giordano & Bettini, 2011; Lin, Hsu, & Sheu, 2010; Loftsson, 1995; Ranpise, Kulkarni, Mair, & Ranade, 2010), co-grinding, solvent evaporation, microwave irradiation, and heating were used. Figure 1c (see also Figure S3) compares production rate and final nothofagin yield for inclusion complexes prepared differently. The method of substrate solubilization had no effect on the biotransformation efficiency. Microwave-assisted formation of a liquid inclusion complex was considered



**FIGURE 1**  $\beta$ -Cyclodextrin derivatives are used for phloretin solubility enhancement in nothofagin production. (a) Chemical structures of  $\beta$ -cyclodextrin derivatives used. (b) Phloretin solubility at 30°C in aqueous solution containing  $\beta$ -cyclodextrin derivatives. Black bars, 200 mM phloretin, 200 mM  $\beta$ -cyclodextrin derivative; gray bars, 200 mM phloretin, 300 mM  $\beta$ -cyclodextrin derivative. (c) Compatibility of inclusion complexation methods with nothofagin synthesis. Phloretin and 2-hydroxypropyl- $\beta$ -cyclodextrin were used in equimolar amounts. Nothofagin was synthesized from 85 mM phloretin using 0.5 mg/ml of OsCGT and 0.25 mg/ml of GmSuSy. Solid complexes: gray bars, yield after 23 hr; black bars, average production rate within first 3 hr. Liquid complexes: light blue bars, yield after 23 hr; blue bars, average production rate within first 3 hr. Reaction conditions: 0.5 mM UDP, 500 mM sucrose, pH 6.5 and 30°C



suitable, for it was simple, fast and did not require recovery of the solid complex in dried form. Upstream processing of the substrate was optimized with respect to soluble phloretin concentration and yield of total phloretin solubilized (Figure S4). A 2-hydroxypropyl- $\beta$ -cyclodextrin concentration of 300 mM was suitable. 255 mM of phloretin (85%) were soluble under these conditions. For quantitative solubilization of the flavonoid, phloretin, and 2-hydroxypropyl- $\beta$ -cyclodextrin were used at a molar ratio of 1:1.25.

Inclusion complexation with 2-hydroxypropyl- $\beta$ -cyclodextrin strongly improved phloretin solubilization compared to the literature (Bungarung et al., 2016). Phloretin solubility was enhanced 16-fold (=255 mM/16 mM), solvent consumption was reduced 16-fold, preparation time was shortened  $\geq 24$ -fold to about 2 hr, and the number of processing steps was reduced to essentially mixing and heating. Since flavonoid solubility enhancement is a problem generally relevant to the different approaches of their biocatalytic glycosylation, the complexation with 2-hydroxypropyl- $\beta$ -cyclodextrin could become broadly useful. Its demand on enzyme robustness is clearly smaller than when using organic solvents (Bertrand et al., 2006; Bungarung et al., 2016), ionic liquids (De Winter et al., 2013), supersaturated substrate solutions (Gao et al., 2000), or high pH and temperature (Weignerová, Marhol, Gerstorferová, & Křen, 2012) for solubility enhancement. Feeding of flavonoid acceptor substrate (Bungarung et al., 2013; Dai et al., 2017; Ito et al., 2014) can also deteriorate the enzyme stability. Using Leloir glycosyltransferases, which are notorious for their low resistance to nonconventional reaction conditions, a "mild" way of substrate solubilization is critical.

### 3.3 | Systematic step-by-step optimization of biocatalytic synthesis of nothofagin

The basic conditions for nothofagin synthesis were established in previous studies (Bungarung et al., 2013; Bungarung et al., 2016). At the pH 7.5 and 30°C used earlier, OsCGT and GmSuSy both were well active and reasonably stable. However, the pH profiles of the two enzymes show a suitable overlap in a broader pH range, namely between pH 6.5 and 7.5 (Figure S5) (Bungarung et al., 2013). Considering change in substrate conditions due to 2-hydroxypropyl- $\beta$ -cyclodextrin instead of  $\beta$ -cyclodextrin, we evaluated the entire suitable pH range (Figures 2a and S6). Nothofagin synthesis was best at pH 6.5, giving about 12% more product after 22 hr than at pH 7.5. The initial conversion rate was about 1.5-fold increased under these conditions.

Gutmann et al. (2017) showed the OsCGT-GmSuSy cascade to be operational at a temperature as high as 50 °C. We therefore analyzed nothofagin synthesis at 30, 40, and 50°C (Figure 2a). Temperature increase from 30 to 40°C reduced the time to complete conversion ( $\geq 90\%$ ) by fivefold. A further increase in temperature to 50°C had no effect on the conversion rate. Time courses of nothofagin production at 40 and 50°C were superimposable and about 95 mM phloretin ( $\geq 95\%$  conversion) were released within 5 hr. Considering that the final process might involve longer reaction times due higher phloretin

concentrations applied, we compared the stabilities of OsCGT (Figure 2b) and GmSuSy (Figure 2c) at 30 and 40°C. Increase in temperature enhanced the initial activity of both enzymes, that of GmSuSy substantially more than that of OsCGT. Both enzymes lost activity over time, GmSuSy faster than OsCGT. The stability of OsCGT was affected more strongly by temperature increase than the stability of GmSuSy. Enzyme comparison (Figures 2b and 2c) reveals the activity of GmSuSy to be limiting for nothofagin synthesis at both 30 and 40°C. As the initial and 5 hr residual activities of GmSuSy were substantially (approximately threefold) higher at 40°C compared to 30°C and the activity remaining after 16 hr was independent of the two temperatures used, we no longer considered 30°C for further reaction optimization.

Different concentrations of the phloretin/2-hydroxypropyl- $\beta$ -cyclodextrin complex in the range 95–150 mM were used and their conversion analyzed at 40 (Figure 2d) and 50°C (Figure 2e). Although the enzyme stability was likely lowered at 50°C, viscosity decrease at elevated temperature might be beneficial to the reaction. An effect of temperature was noted at high phloretin concentration (125 and 150 mM) where synthesis at 40°C clearly outperformed synthesis at 50°C. At 50°C, the relevant time courses showed a relatively fast phloretin conversion initially, but slowed down after about 4 hr and gradually leveled off, so that after about 8 hr constant nothofagin concentrations were reached although up to 50% of the initial phloretin was still available (Figures 2e and S7). At 40°C, by contrast, the phloretin conversion proceeded to completion ( $\geq 85\%$  within 24 hr) at all concentrations used (Figures 2d and S7). The comparably slow reaction of 150 mM phloretin/2-hydroxypropyl- $\beta$ -cyclodextrin probably reflects increasing difficulty of proper mixing of the highly viscous fluid. The additional presence of 500 mM sucrose in the reaction mixtures should be noted, causing an about 2.5-fold increase in the viscosity. From these results, a maximum in phloretin concentration of about 120 mM was suggested. In terms of the nothofagin concentration achievable, the enzymatic process was thus pushed to its practical upper limits. Under the conditions applied (40°C), the reaction mixture presented an approximate Newton fluid behavior ( $\eta = \sim 3.5$  mPa s). The temperature of 40°C balanced well between enzyme activity and stability (Figure 2) for a single batch conversion ( $\sim 24$  hr) without enzyme recycling.

We finally analyzed the role of catalyst loading, using conditions from Bungarung et al. (2016) as a reference (0.33 mg<sub>OsCGT</sub>/ml, 0.13 mg<sub>GmSuSy</sub>/ml). The mass ratio of the two enzymes was kept constant and their concentrations were varied in the range 0.3–0.5 mg<sub>OsCGT</sub>/ml and 0.15–0.25 mg<sub>GmSuSy</sub>/ml. Reaction time courses are shown in Figure S8. The use of 0.5 mg/ml of OsCGT and 0.25 mg/ml of GmSuSy gave a suitable balance between high conversion rate and moderate catalyst loading. Almost full conversion of  $\sim 120$  mM phloretin was achieved within 21 hr. By way of comparison, the reference showed 85% conversion after 45 hr.

In summary, therefore, the evidence presented sets the optimum conditions for nothofagin synthesis as follows:  $\sim 120$  mM of liquid phloretin inclusion complex with 2-hydroxypropyl- $\beta$ -cyclodextrin,

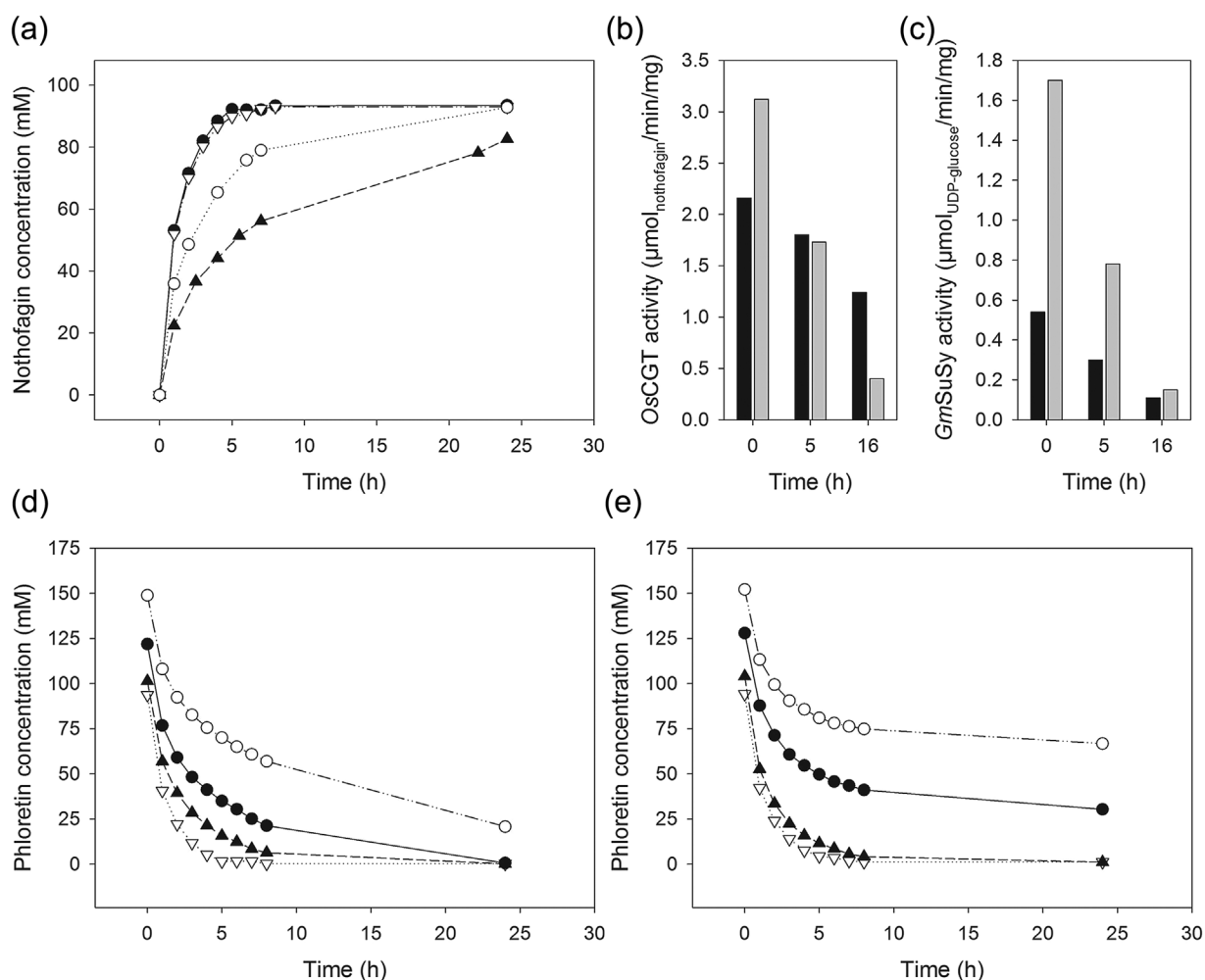


**FIGURE 2** Establishing the key operational parameters of OsCGT-GmSuSy cascade for nothofagin production from liquid phloretin/ 2-hydroxypropyl- $\beta$ -cyclodextrin inclusion complex. (a) Time courses of nothofagin formation from 95 mM phloretin at different temperatures and pH values. pH 6.5: 30°C, filled triangles; 40°C, filled circles; 50°C, open reverse triangles; pH 7.0: 40°C, open circles. Activities and stabilities of OsCGT (b) and GmSuSy (c) under process conditions. Black bars, 30°C; gray bars, 40°C. Time-courses of nothofagin formation from various phloretin concentrations at 40°C (d) and 50°C (e). Reaction conditions: 0.5 mM UDP, 500 mM sucrose. 0.5 mg/ml OsCGT, 0.25 mg/ml GmSuSy, pH 6.5

pH 6.5, 40°C, 0.5 mg/ml ( $\sim 1.6$  U/ml) of OsCGT and 0.25 mg/ml ( $\sim 0.5$  U/ml) of GmSuSy.

### 3.4 | Scale-up of nothofagin synthesis

Figure 3a shows synthesis of  $\sim 50$  g of nothofagin in a single batch (1 L) under the optimized conditions. The initial nothofagin production rate was 20 g/L/hr. Nothofagin was obtained in excellent yield (97%; based on the phloretin used) and concentration (50 g/L, 110 mM) within 16 hr of reaction. The STY of the biotransformation overall was 3 g/L/hr. The high product concentration was vital for efficient downstream processing, as is shown later and is generally recognized as important (Straathof, Panke, & Schmid, 2002). Compared to the experiments described above or reported previously (Bungaruang et al., 2013; Bungaruang et al., 2016), nothofagin synthesis was up-scaled by 500-fold. Synthesis of different quantities of nothofagin

gave almost identical yields and STYs (Figure 3b), indicating a highly successful scale-up. In contrast to the enzymatic reaction using the native  $\beta$ -cyclodextrin (Bungaruang et al., 2016), phloretin precipitation was prevented effectively in the process and none of the nothofagin formed was lost as insoluble. The UDP-glucose was regenerated up to  $\sim 220$  times ( $RC_{max}$ ), representing a 2.5-fold improvement in recycling efficiency compared to the reference reaction using  $\beta$ -cyclodextrin. With efficiency parameters of the batch conversion largely pushed to their respective limits, further intensification of nothofagin synthesis could only be realized by changing to a continuous or semi-continuous process mode. This would however necessitate improvement of enzyme activities and stabilities (Figures 2b and 2c), especially the stability of the GmSuSy. However, even as it stands, the current nothofagin synthesis is performance-wise without precedent in preparative glycosyltransferase-catalyzed glycosylations of flavonoids and other polyphenols (e.g., Bungaruang et al., 2013;

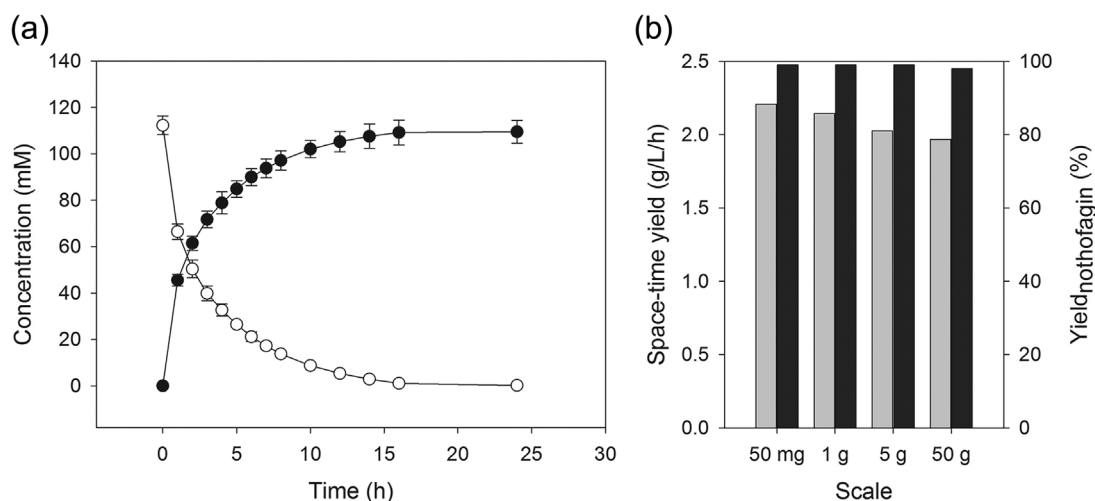


**FIGURE 3** Scale-up of nothofagin synthesis from liquid phloretin/2-hydroxypropyl- $\beta$ -cyclodextrin inclusion complex is shown. Phloretin and 2-hydroxypropyl- $\beta$ -cyclodextrin were used at a molar ratio of 1:1.25. Nothofagin was produced from 112 mM phloretin using 1.6 U/ml of OsCGT and 0.5 U/ml of *GmSuSy*. (a) Time course of nothofagin production at 50 g scale. Nothofagin, filled circles; phloretin, open circles. (b) Space-time yields and nothofagin yields after 24 hr obtained at different scales. Gray bars, space-time yield; black bars, nothofagin yield. Reaction conditions: 0.5 mM UDP, 500 mM sucrose, pH 6.5 and 40°C

Bungaruang et al., 2016; Dai et al., 2017; De Bruyn, De Paep et al., 2015; De Bruyn, Van Brempt et al., 2015; Dewitte et al., 2016; Ito et al., 2014; Lepak, Gutmann, Kulmer, & Nidetzky, 2015; Michlmayr et al., 2015; Shen et al., 2017; Xia & Eiteman, 2017).

### 3.5 | Downstream processing of nothofagin

The downstream processing had to remove sugars (390 mM sucrose; 110 mM fructose) and ~140 mM 2-hydroxypropyl- $\beta$ -cyclodextrin from the nothofagin (110 mM). Tiny amounts of phloretin ( $\leq 0.5$  mM) and unidentified glycosylation products ( $\leq 2.5\%$  based on HPLC peak area) were also present.

### 3.6 | Tailored AEC for initial purification of nothofagin

We considered AEC to be promising for capture and initial purification of the product. For this an effective AEX resin was needed. The pH was set to 8.5. Sugars and the cyclodextrin are not ionized at this pH and can so be removed in the flow-through (Rocklin & Pohl, 1983). The phenolic groups of flavonoids have  $pK_a$  values ranging from 7.2 to ~10 (Gutmann, Krump, Bungaruang, & Nidetzky, 2014), thus supporting AEC-based separation at basic pH. After removal of enzymes by precipitation with isopropanol, adsorption/desorption characteristics of different AEX resins were evaluated in batch experiments (Figure 4a). The binding capacity and the desorption efficiency for nothofagin varied broadly across the resins examined. Dowex 1  $\times$  2 (Cl<sup>-</sup>-form, 50–100 mesh) showed by far the highest binding capacity of ~120 mg<sub>nothofagin</sub>/g<sub>resin</sub>, but also a very poor desorption efficiency. Only 14% of the nothofagin bound was released in two desorption steps. The Toyopearl SuperQ-650M was the most effective resin among those examined. It showed a good binding capacity of

~50 mg<sub>nothofagin</sub>/g<sub>resin</sub> and allowed almost quantitative desorption of nothofagin in two steps. However, a batch adsorption/desorption process was not possible due to difficult phase separation after each step by centrifugation and high solvent consumption of ~2.2 L/g<sub>nothofagin</sub>. By contrast, preparative AEC on a SuperQ-650M column (~500 ml bed volume) enabled isolation of about 11 g of nothofagin in a single AEC run with a run time of 11 h (Figure 4b). The total solvent used was only ~0.6 L/g<sub>nothofagin</sub>. A low solvent consumption is vital for the scalability of AEC. About 80% of the 2-hydroxypropyl- $\beta$ -cyclodextrin was removed with the flow through. Recycling of the 2-hydroxypropyl- $\beta$ -cyclodextrin would thus be possible at this process step by extraction (Pitha, Szabo, & Fales, 1987) or chromatography (Szathmary, 1989). The SuperQ-650M was described previously as the most effective material for AEC of NDP-glucoses (Kulmer, Gutmann, Lemmerer, & Nidetzky, 2017; Lemmerer, Schmölzer, Gutmann, & Nidetzky, 2016).

### 3.7 | Efficient SEC-free isolation of nothofagin

Precipitation of nothofagin was used as alternative to size exclusion chromatography (SEC) for desalting. SEC is difficult to scale up because its throughput is low and highly diluted product is obtained (Lemmerer et al., 2016; Ó'Fágáin et al., 2011). The AEC eluate was concentrated (approximately threefold), paying attention to not exceed the solubility limit of sodium chloride (~6 M in water). A pH of 6 was used to precipitate the non-ionic nothofagin from solution (Gutmann et al., 2014). The precipitate had its residual water removed by freeze-drying and nothofagin was then extracted with acetone, which we found to be an excellent solvent for the C-glucoside (~100 g/L at 20 °C). The 2-hydroxypropyl- $\beta$ -cyclodextrin still present in the solid sample (~20% of total) was removed at this step due to its low solubility in dry acetone (<0.1 g/L at 20°C). Note:

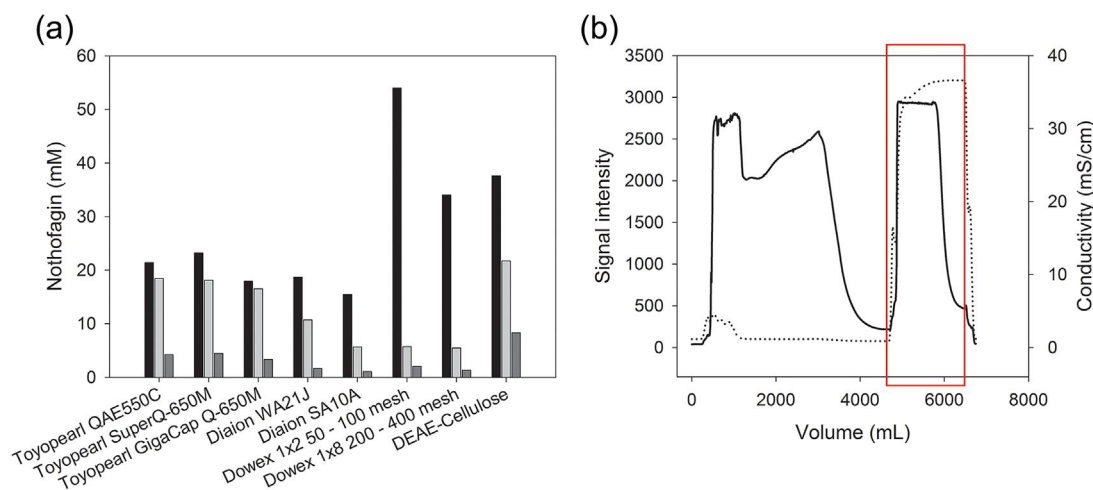


**FIGURE 4** DSP of nothofagin by tailored AEC at pH 8.5. (a) Selection of an AEX resin by batch adsorption/desorption of nothofagin, using 10 mM potassium phosphate, pH 8.5 for binding and 0.8 M sodium chloride for desorption. Black bars, bound nothofagin; light gray bars, nothofagin released in 1st desorption step; dark gray bars, nothofagin released in 2nd desorption step. (b) Preparative AEC run on a Toyopearl SuperQ-650M 500 ml column. Approximately 13 g of nothofagin were loaded. A total of 0.8 M of sodium chloride was used for elution at 0.51 cm/min. Solid line, UV signal (280 nm); dotted line, conductivity (mS/cm). First peak, injection peak; second peak, nothofagin. Pooled fractions are indicated by the red box (~11 g nothofagin)

since 2-hydroxypropyl- $\beta$ -cyclodextrin is well soluble in water, drying of the solid sample was important for selective acetone extraction of the nothofagin. Isopropanol was not a suitable solvent, due to a 2-hydroxypropyl- $\beta$ -cyclodextrin solubility of ~15 g/L (at 20°C).

The results of nothofagin purification are summarized in Table 1. About 9 g of nothofagin were obtained in a single batch. We were able to isolate 102 g of nothofagin in 12 batches with constant quality. Nothofagin was obtained as a yellowish powder in  $\geq 65\%$  yield and  $\geq 95\%$  purity (see also Table 1 and Figs. S9–S11).

**TABLE 1** Production of 102 g of nothofagin (12 batches, S.D. was  $\leq 10\%$ )

Sample	Nothofagin <sup>e</sup> (g/batch)	Yield (%)
After synthesis	13.4	100
After enzyme removal <sup>a</sup>	13.0	97.0
AEC <sup>b</sup>	10.6	79.1
After concentration and nothofagin precipitation <sup>c</sup>	10.4	77.6
After freeze-drying and acetone extraction <sup>d</sup>	8.8	65.7
Freeze-dried sample	8.6 <sup>f</sup>	64.2

<sup>a</sup>Enzyme precipitation by isopropanol.

<sup>b</sup>AEC at pH 8.5. Eluate (1800 ml) from SuperQ-650M column, containing, 0.8 M sodium chloride.

<sup>c</sup>Product precipitation at pH 6.

<sup>d</sup>Nothofagin extraction with acetone (~50 ml/g).

<sup>e</sup>Absolute amount of pure nothofagin.

<sup>f</sup>Freeze-drying yielded 9.1 g of yellowish powder containing 94% (8.6 g) nothofagin,  $\leq 5\%$  acetone,  $< 1\%$  phloretin and unidentified products. No 2-hydroxypropyl- $\beta$ -cyclodextrin was detected in the final product.

Downstream processing of polyphenol glycosides from glycosyltransferase reactions mixtures was previously realized mostly at small preparative scale ( $\leq 100$  mg) and involved procedures (e.g., reversed phase HPLC/FPLC, SEC) difficult to scale up (Bungaruang et al., 2016; Dai et al., 2017; Dewitte et al., 2016; Ito et al., 2014; Lepak et al., 2015; Terasaka, Mizutani, Nagatsu, & Mizukami, 2012; Zhang et al., 2017). Nothofagin recovery at the 100 g demonstration scale is therefore novel and broadly relevant in the field. Also significant, the downstream processing herein used is likely applicable to other flavonoid glycosides (e.g., quercetin glucosides; Son et al., 2009; Terasaka et al., 2012), after minor adaption of the process conditions, due to similar properties of the target molecules ( $pK_a$ , hydrophobicity).

## 4 | CONCLUSIONS

The biocatalytic C-glycosylation of phloretin to produce nothofagin was demonstrated at a scale of 100 g isolated product. This presents an important, and we believe paradigmatic, example for the practical use of Leloir glycosyltransferases in flavonoid glycosylation for chemical production. The main bottlenecks on nothofagin process efficiency, and the strategies developed herein for their removal, extend to biocatalytic systems for flavonoid glycoside synthesis (e.g., trans-glycosidases) different from the Leloir glycosyltransferases (Bertrand et al., 2006; Masada et al., 2007; Son et al., 2009; Terasaka et al., 2012; Woo et al., 2012). They are therefore relevant, and should draw interest, broadly in the field of flavonoid, and more generally, natural product glycosylation. Inclusion complexation with 2-hydroxypropyl- $\beta$ -cyclodextrin is efficient, and highly biocompatible, by means of flavonoid solubility enhancement to a point (~150 mM, assuming a 1:1 complex) where viscous fluid mixing becomes a physical boundary on the process operation. The SEC-free isolation of nothofagin provides a

strong case for efficient recovery of glycosidic products from biotransformation mixtures with relatively simple, scalable procedures at low solvent consumption. The successful nothofagin process involves upstream and downstream processing optimized for efficient interconnected performance. The idea of a holistic process development in glycosyltransferase biocatalysis is thus supported. In the production of flavonoid glycosides, building up the product by glycosylation presents a conceptually important alternative to trimming down a natural diglycoside substrate. The kg scale preparation of quercetin glucoside via rhamnosidase-catalyzed hydrolysis of rutin is a notable example (Weignerová et al., 2012).

## ACKNOWLEDGMENTS

This work was supported by the Federal Ministry of Science, Research and Economy (BMWFV), the Federal Ministry of Traffic, Innovation and Technology (BMVIT), the Styrian Business Promotion Agency, SFG, the Standortagentur Tirol, the Government of Lower Austria and Business Agency Vienna through the COMET-Funding Program managed by the Austrian Research Promotion Agency FFG. Financial support from the EU FP7 project SuSy (Sucrose Synthase as Effective Mediator of Glycosylation) is gratefully acknowledged. The authors thank Prof. O. Kunert from Karl Franzens University of Graz for NMR analysis. The authors thank colleagues from the Austrian Centre of Industrial Biotechnology and Graz University of Technology for excellent support.

## CONFLICT OF INTEREST

The authors have no conflict of interest to declare.

## ORCID

Bernd Nidetzky  <http://orcid.org/0000-0002-5030-2643>

## REFERENCES

- Andersen, O. M., & Markham, K. R. (2005). *Flavonoids: Chemistry, biochemistry and applications*. Boca Raton: CRC Press.
- Bertacche, V., Lorenzi, N., Nava, D., Pini, E., & Sinico, C. (2006). Host-guest interaction study of resveratrol with natural and modified cyclodextrins. *Journal of Inclusion Phenomena and Macrocyclic Chemistry*, 55(3–4), 279–287.
- Bertrand, A., Morel, S., Lefoulon, F., Rolland, Y., Monsan, P., & Remaud-Simeon, M. (2006). *Leuconostoc mesenteroides* glucansucrase synthesis of flavonoid glucosides by acceptor reactions in aqueous-organic solvents. *Carbohydrate Research*, 341(7), 855–863.
- Billign, T., Hyun, C.-G., Williams, J. S., Czisny, A. M., & Thorson, J. S. (2004). The hedamycin locus implicates a novel aromatic PKS priming mechanism. *Chemistry & Biology*, 11(7), 959–969.
- Brazier-Hicks, M., Evans, K. M., Gershtater, M. C., Puschmann, H., Steel, P. G., & Edwards, R. (2009). The C-glycosylation of flavonoids in cereals. *The Journal of Biological Chemistry*, 284(27), 17926–17934.
- Brewster, M. E., & Loftsson, T. (2007). Cyclodextrins as pharmaceutical solubilizers. *Advanced Drug Delivery Reviews*, 59(7), 645–666.
- Bungaruang, L., Gutmann, A., & Nidetzky, B. (2013). Leloir glycosyltransferases and natural product glycosylation: Biocatalytic synthesis of the C-glucoside nothofagin, a major antioxidant of redbush herbal tea. *Advanced Synthesis and Catalysis*, 355(14–15), 2757–2763.
- Bungaruang, L., Gutmann, A., & Nidetzky, B. (2016).  $\beta$ -cyclodextrin improves solubility and enzymatic C-glycosylation of the flavonoid phloretin. *Advanced Synthesis and Catalysis*, 358(3), 486–493.
- Chen, D., Chen, R., Wang, R., Li, J., Xie, K., Bian, C., ... Dai, J. (2015). Probing the catalytic promiscuity of a regio- and stereospecific C-glycosyltransferase from *Mangifera indica*. *Angewandte Chemie-International Edition*, 54(43), 12678–12682.
- Dai, L., Li, J., Yao, P., Zhu, Y., Men, Y., Zeng, Y., ... Sun, Y. (2017). Exploiting the aglycon promiscuity of glycosyltransferase Bs-YjC from *Bacillus subtilis* and its application in synthesis of glycosides. *Journal of Biotechnology*, 248, 69–76.
- de Beer, D., Malherbe, C. J., Beelders, T., Willenburg, E. L., Brand, D. J., & Joubert, E. (2015). Isolation of aspalathin and nothofagin from rooibos (*Aspalathus linearis*) using high-performance countercurrent chromatography: Sample loading and compound stability considerations. *Journal of Chromatography A*, 1381, 29–36.
- De Bruyn, F., De Paepe, B., Maertens, J., Beauprez, J., De Cocker, P., Mincke, S., ... De Mey, M. (2015). Development of an in vivo glycosylation platform by coupling production to growth: Production of phenolic glucosides by a glycosyltransferase of *Vitis vinifera*. *Biotechnology and Bioengineering*, 112(8), 1594–1603.
- De Bruyn, F., Maertens, J., Beauprez, J., Soetaert, W., & De Mey, M. (2015). Biotechnological advances in UDP-sugar based glycosylation of small molecules. *Biotechnology Advances*, 33(2), 288–302.
- De Bruyn, F., Van Brempt, M., Maertens, J., Van Belleghem, W., Duchi, D., & De Mey, M. (2015). Metabolic engineering of *Escherichia coli* into a versatile glycosylation platform: Production of bio-active quercetin glycosides. *Microbial Cell Factories*, 14(1), 138.
- De Winter, K., Verlinden, K., Kren, V., Weignerová, L., Soetaert, W., & Desmet, T. (2013). Ionic liquids as cosolvents for glycosylation by sucrose phosphorylase: Balancing acceptor solubility and enzyme stability. *Green Chemistry*, 15(7), 1949–1955.
- Desmet, T., Soetaert, W., Bojarová, P., Křen, V., Dijkhuizen, L., Eastwick-Field, V., & Schiller, A. (2012). Enzymatic glycosylation of small molecules: Challenging substrates require tailored catalysts. *European Journal of Chemistry*, 18(35), 10786–10801.
- Dewitte, G., Walmagh, M., Diricks, M., Lepak, A., Gutmann, A., Nidetzky, B., & Desmet, T. (2016). Screening of recombinant glycosyltransferases reveals the broad acceptor specificity of stevia UGT-76G1. *Journal of Biotechnology*, 233, 49–55.
- Gao, C., Mayon, P., MacManus, D. A., & Vulfson, E. N. (2000). Novel enzymatic approach to the synthesis of flavonoid glycosides and their esters. *Biotechnology and Bioengineering*, 71(3), 235–243.
- Giordano, F., & Bettini, R. 2011. Process for preparation of inclusion compounds between a non-steroidal anti-inflammatory drug and betacyclodextrin by microwave treatment. Patent US 7935685 B2.
- Gutmann, A., Krump, C., Bungaruang, L., & Nidetzky, B. (2014). A two-step O- to C-glycosidic bond rearrangement using complementary glycosyltransferase activities. *Chemical Communications*, 50(41), 5465–5468.
- Gutmann, A., Lepak, A., Diricks, M., Desmet, T., & Nidetzky, B. (2017). Glycosyltransferase cascades for natural product glycosylation: Use of plant instead of bacterial sucrose synthases improves the UDP-glucose recycling from sucrose and UDP. *Biotechnology Journal*, 12(7), 1600557.
- Gutmann, A., & Nidetzky, B. (2012). Switching between O- and C-glycosyltransferase through exchange of active-site motifs. *Angewandte Chemie-International Edition*, 51(51), 12879–12883.
- Härle, J., Günther, S., Lauinger, B., Weber, M., Kammerer, B., Zechel, D. L., ... Bechthold, A. (2011). Rational design of an aryl-C-glycoside catalyst from a natural product O-glycosyltransferase. *Chemistry & Biology*, 18(4), 520–530.

- Häusler, O., & Müller-Goymann, C. C. (1993). Properties and structure of aqueous solutions of hydroxypropyl-beta-cyclodextrin. *Starch-Stärke*, 45(5), 183–187.
- Hedges, A. R. (1998). Industrial applications of cyclodextrins. *Chemical Reviews*, 98(5), 2035–2044.
- Ito, T., Fujimoto, S., Shimosaka, M., & Taguchi, G. (2014). Production of C-glucosides of flavonoids and related compounds by *Escherichia coli* expressing buckwheat C-glucosyltransferase. *Plant Biotechnology*, 31(5), 519–524.
- Joubert, E., Beelders, T., de Beer, D., Malherbe, C. J., de Villiers, A. J., & Sigge, G. O. (2012). Variation in phenolic content and antioxidant activity of fermented rooibos herbal tea infusions: Role of production season and quality grade. *Journal of Agriculture and Food Chemistry*, 60(36), 9171–9179.
- Kratzer, R., Woodley, J. M., & Nidetzky, B. (2015). Rules for biocatalyst and reaction engineering to implement effective, NAD(P)H-dependent, whole cell bioreductions. *Biotechnology Advances*, 33(8), 1641–1652.
- Kren, V., & Martinkova, L. (2001). Glycosides in medicine: The role of glycosidic residue in biological activity. *Current Medicinal Chemistry*, 8(11), 1303–1328.
- Ku, S. K., Kwak, S., Kim, Y., & Bae, J. S. (2015). Aspalathin and nothofagin from rooibos (*Aspalathus linearis*) inhibits high glucose-induced inflammation in vitro and in vivo. *Inflammation*, 38(1), 445–455.
- Ku, S. K., Lee, W., Kang, M., & Bae, J. S. (2014). Antithrombotic activities of aspalathin and nothofagin via inhibiting platelet aggregation and FIIa/FXa. *Archives of Pharmaceutical Research*, 38(6), 1080–1089.
- Kulmer, S. T., Gutmann, A., Lemmerer, M., & Nidetzky, B. (2017). Biocatalytic cascade of polyphosphate kinase and sucrose synthase for synthesis of nucleotide-activated derivatives of glucose. *Advanced Synthesis and Catalysis*, 359(2), 292–301.
- Lee, J., Lee, S.-H., Seo, H. J., Son, E.-J., Lee, S. H., Jung, M. E., ... Lee, J. (2010). Novel C-aryl glucoside SGLT2 inhibitors as potential antidiabetic agents: 1,3,4-thiadiazolylmethylphenyl glucoside congeners. *Bioorganic and Medicinal Chemistry*, 18(6), 2178–2194.
- Lemmerer, M., Schmölzer, K., Gutmann, A., & Nidetzky, B. (2016). Downstream processing of nucleotide-diphospho-sugars from sucrose synthase reaction mixtures at decreased solvent consumption. *Advanced Synthesis and Catalysis*, 358(19), 3113–3122.
- Lepak, A., Gutmann, A., Kulmer, S. T., & Nidetzky, B. (2015). Creating a water-soluble resveratrol-based antioxidant by site-selective enzymatic glucosylation. *Chembiochem*, 16(13), 1870–1874.
- Lim, E. K., Ashford, D. A., Hou, B., Jackson, R. G., & Bowles, D. J. (2004). *Arabidopsis* glycosyltransferases as biocatalysts in fermentation for regioselective synthesis of diverse quercetin glucosides. *Biotechnology and Bioengineering*, 87(5), 623–631.
- Lin, S.-Y., Hsu, C.-H., & Sheu, M.-T. (2010). Curve-fitting FTIR studies of loratadine/hydroxypropyl-β-cyclodextrin inclusion complex induced by co-grinding process. *Journal of Pharmaceutical and Biomedical Analysis*, 53(3), 799–803.
- Loftsson, T. 1995; Cyclodextrin complexation. Patent US 5472954 A.
- Loftsson, T., (2015). Formulation of drug-cyclodextrin complexes. In N. Dragicevic, & H. I. Maibach (Eds.), *Percutaneous penetration enhancers chemical methods in penetration enhancement: Drug manipulation strategies and vehicle effects* (pp. 189–205). Berlin, Heidelberg: Springer Berlin Heidelberg.
- Loftsson, T., Másson, M., & Sigurjónsdóttir, J. F. (1999). Methods to enhance the complexation efficiency of cyclodextrins. *STP Pharma Sciences*, 9(3), 237–242.
- Masada, S., Kawase, Y., Nagatoshi, M., Oguchi, Y., Terasaka, K., & Mizukami, H. (2007). An efficient chemoenzymatic production of small molecule glucosides with in situ UDP-glucose recycling. *FEBS Letters*, 581(13), 2562–2566.
- McKay, D. L., & Blumberg, J. B. (2007). A review of the bioactivity of south African herbal teas: Rooibos (*Aspalathus linearis*) and honeybush (*Cyclopia intermedia*). *Phytotherapy Research*, 21(1), 1–16.
- Meng, W., Ellsworth, B. A., Nirschl, A. A., McCann, P. J., Patel, M., Girotra, R. N., ... Washburn, W. N. (2008). Discovery of dapagliflozin: A potent, selective renal sodium-dependent glucose cotransporter 2 (SGLT2) inhibitor for the treatment of type 2 diabetes. *Journal of Medicinal Chemistry*, 51(5), 1145–1149.
- Meulenbeld, G. H., & Hartmans, S. (2000). Transglycosylation by *Streptococcus mutans* GS-5 glucosyltransferase-D: Acceptor specificity and engineering of reaction conditions. *Biotechnology and Bioengineering*, 70(4), 363–369.
- Michlmayr, H., Malachová, A., Varga, E., Kleinová, J., Lemmens, M., Newmister, S., ... Adam, G. (2015). Biochemical characterization of a recombinant UDP-glucosyltransferase from rice and enzymatic production of deoxynivalenol-3-O-β-D-glucoside. *Toxins*, 7(7), 2685.
- ÓFágáin, C., Cummins, P. M., & O'Connor, B. F., (2011). Gel-filtration chromatography. In D. Walls, & T. S. Loughran (Eds.), *Protein chromatography: Methods and protocols* (pp. 25–33). New York: Humana Press.
- Ono, Y., Tomimori, N., Tateishi, N., Moriwaki, M., Emura, K., & Okuyama, S. 2005. Quercetin glycoside composition and method of preparing the same. Patent WO 2006/070883 A1.
- Panke, S., Wubboldts, M. G., Schmid, A., & Witholt, B. (2000). Production of enantiopure styrene oxide by recombinant *Escherichia coli* synthesizing a two-component styrene monooxygenase. *Biotechnology and Bioengineering*, 69(1), 91–100.
- Pinho, E., Grootveld, M., Soares, G., & Henriques, M. (2014). Cyclodextrins as encapsulation agents for plant bioactive compounds. *Carbohydrate Polymers*, 101, 121–135.
- Pitha, J., Szabo, L., & Fales, H. M. (1987). Reaction of cyclodextrins with propylene oxide or with glycidol: Analysis of product distribution. *Carbohydrate Research*, 168(2), 191–198.
- Puskás, I., Varga, E., Tuza, K., Szemán, J., Fenyvesi, S., Sohajda, T., & Sente, L., (2015). Sulfobutylether-cyclodextrins: structure, degree of substitution and functional performance. In F. G. Ramirez (Ed.), *Cyclodextrins: Synthesis, chemical applications and role in drug delivery*. (pp. 293–320). New York: Nova Science Publishers.
- Ranpise, N. S., Kulkarni, N. S., Mair, P. D., & Ranade, A. N. (2010). Improvement of water solubility and in vitro dissolution rate of aceclofenac by complexation with β-cyclodextrin and hydroxypropyl-β-cyclodextrin. *Pharmaceutical Development and Technology*, 15(1), 64–70.
- Rocklin, R. D., & Pohl, C. A. (1983). Determination of carbohydrates by anion exchange chromatography with pulsed amperometric detection. *Journal of Liquid Chromatography*, 6(9), 1577–1590.
- Rodríguez-Mateos, A., Vauzour, D., Krueger, C. G., Shanmuganayagam, D., Reed, J., Calani, L., ... Crozier, A. (2014). Bioavailability, bioactivity and impact on health of dietary flavonoids and related compounds: An update. *Archives of Toxicology*, 88(10), 1803–1853.
- Rupprath, C., Kopp, M., Hirtz, D., Müller, R., & Elling, L. (2007). An enzyme module system for in situ regeneration of deoxythymidine 5'-diphosphate (dTDP)-activated deoxy sugars. *Advanced Synthesis and Catalysis*, 349(8–9), 1489–1496.
- Schloms, L., Storbeck, K.-H., Swart, P., Gelderblom, W. C. A., & Swart, A. C. (2012). The influence of *Aspalathus linearis* (rooibos) and dihydrochalcones on adrenal steroidogenesis: Quantification of steroid intermediates and end products in H295R cells. *The Journal of Steroid Biochemistry and Molecular Biology*, 128(3–5), 128–138.
- Schmölzer, K., Gutmann, A., Diricks, M., Desmet, T., & Nidetzky, B. (2016). Sucrose synthase: A unique glycosyltransferase for biocatalytic glycosylation process development. *Biotechnology Advances*, 34(2), 88–111.
- Schmölzer, K., Lemmerer, M., Gutmann, A., & Nidetzky, B. (2016). Integrated process design for biocatalytic synthesis by a Leloir glycosyltransferase: UDP-glucose production with sucrose synthase. *Biotechnology and Bioengineering*, 114(4), 924–928.

- Seebacher, W., Simic, N., Weis, R., Saf, R., & Kunert, O. (2003). Complete assignments of  $^1\text{H}$  and  $^{13}\text{C}$  NMR resonances of oleanolic acid,  $18\alpha$ -oleanolic acid, ursolic acid and their 11-oxo derivatives. *Magnetic Resonance in Chemistry*, 41(8), 636–638.
- Shen, X., Wang, J., Wang, J., Chen, Z., Yuan, Q., & Yan, Y. (2017). High-level de novo biosynthesis of arbutin in engineered *Escherichia coli*. *Metabolic Engineering*, 42, 52–58.
- Snijman, P. W., Joubert, E., Ferreira, D., Li, X. C., Ding, Y., Green, I. R., & Gelderblom, W. C. (2009). Antioxidant activity of the dihydrochalcones aspalathin and nothofagin and their corresponding flavones in relation to other rooibos (*Aspalathus linearis*) flavonoids, epigallocatechin gallate, and Zrolox. *Journal of Agriculture and Food Chemistry*, 57(15), 6678–6684.
- Snijman, P. W., Swanevelder, S., Joubert, E., Green, I. R., & Gelderblom, W. C. (2007). The antimutagenic activity of the major flavonoids of rooibos (*Aspalathus linearis*): Some dose-response effects on mutagen activation-flavonoid interactions. *Mutation Research*, 631(2), 111–123.
- Son, M. H., Kim, B.-G., Kim, D. H., Jin, M., Kim, K., & Ahn, J.-H. (2009). Production of flavonoid O-glucoside using sucrose synthase and flavonoid O-glucosyltransferase fusion protein. *Journal of Microbiology and Biotechnology*, 19(7), 709–712.
- Straathof, A. J., Panke, S., & Schmid, A. (2002). The production of fine chemicals by biotransformations. *Current Opinion in Biotechnology*, 13(6), 548–556.
- Szathmary, S. C. (1989). Determination of hydroxypropyl- $\beta$ -cyclodextrin in plasma and urine by size-exclusion chromatography with post-column complexation. *Journal of Chromatography B: Biomedical Sciences and Applications* 487, 99–105.
- Szente, L., & Szejtli, J. (1999). Highly soluble cyclodextrin derivatives: Chemistry, properties, and trends in development. *Advanced Drug Delivery Reviews*, 36(1), 17–28.
- Terasaka, K., Mizutani, Y., Nagatsu, A., & Mizukami, H. (2012). In situ UDP-glucose regeneration unravels diverse functions of plant secondary product glycosyltransferases. *FEBS Letters*, 586(24), 4344–4350.
- Tufvesson, P., Lima-Ramos, J., Jensen, J. S., Al-Haque, N., Neto, W., & Woodley, J. M. (2011). Process considerations for the asymmetric synthesis of chiral amines using transaminases. *Biotechnology and Bioengineering*, 108(7), 1479–1493.
- Veitch, N. C., & Grayer, R. J. (2011). Flavonoids and their glycosides, including anthocyanins. *Natural Product Reports*, 28(10), 1626–1695.
- Wei, Y., Zhang, J., Memon, A. H., & Liang, H. (2017). Molecular model and in vitro antioxidant activity of a water-soluble and stable phloretin/hydroxypropyl- $\beta$ -cyclodextrin inclusion complex. *Journal of Molecular Liquids*, 236, 68–75.
- Weignerová, L., Marhol, P., Gerstorferová, D., & Křen, V. (2012). Preparatory production of quercetin-3- $\beta$ -D-glucopyranoside using alkali-tolerant thermostable  $\alpha$ -L-rhamnosidase from *Aspergillus terreus*. *Bioresource Technology*, 115, 222–227.
- Woo, H.-J., Kang, H.-K., Nguyen, T. T. H., Kim, G.-E., Kim, Y.-M., Park, J.-S., ... Kim, D. (2012). Synthesis and characterization of ampelopsin glucosides using dextransucrase from *Leuconostoc mesenteroides* B-1299C B4: Glucosylation enhancing physicochemical properties. *Enzyme and Microbial Technology*, 51(6), 311–318.
- Xia, T., & Eiteman, M. A. (2017). Quercetin glucoside production by engineered *Escherichia coli*. *Applied Biochemistry and Biotechnology*, 182(4), 1358–1370.
- Yepremyan, A., Salehani, B., & Minehan, T. G. (2010). Concise total syntheses of aspalathin and nothofagin. *Organic Letters*, 12(7), 1580–1583.
- Zhang, T.-J., Liang, J.-Q., Wei, X.-Y., Wang, P.-X., Xu, Y., Pen, S., & Fan, M.-T. (2017). Development of an enzymatic synthesis approach to produce phloridzin using *Malus x domestica* glycosyltransferase in engineered *Pichia pastoris* GS115. *Process Biochemistry*, 59, 187–193.

## SUPPORTING INFORMATION

Additional Supporting Information may be found online in the supporting information tab for this article.

**How to cite this article:** Schmölder K, Lemmerer M, Nidetzky B. Glycosyltransferase cascades made fit for chemical production: Integrated biocatalytic process for the natural polyphenol C-glucoside nothofagin. *Biotechnology and Bioengineering*. 2018;115:545–556.  
<https://doi.org/10.1002/bit.26491>

## Supporting Information

### **Glycosyltransferase Cascades Made Fit for Chemical Production: Integrated Biocatalytic Process for the Natural Polyphenol C- Glucoside Nothofagin**

Katharina Schmölzer<sup>1</sup>, Martin Lemmerer<sup>1</sup>, Bernd Nidetzky<sup>1,2</sup>

<sup>1</sup>Austrian Centre of Industrial Biotechnology, Petersgasse 14, 8010 Graz, Austria

<sup>2</sup>Institute of Biotechnology and Biochemical Engineering, Graz University of Technology, NAWI Graz, Petersgasse 12/I, 8010 Graz, Austria

**Corresponding author:** bernd.nidetzky@tugraz.at; Phone: +43 316 873 8400; FAX: +43 316 873 8434

Proofs and reprints should be addressed to Bernd Nidetzky.

#### **Table of Contents**

Chemicals and Materials	S3
Analytical Methods	S3
Viscosity Measurements	S4
Preparation of Phloretin/2-Hydroxypropyl- $\beta$ -Cyclodextrin Inclusion Complexes	S4
Optimization of Phloretin Solubilization With 2-Hydroxypropyl- $\beta$ -Cyclodextrin	S5
Determination of Enzyme Activities and Stabilities Under Process Conditions	S5
Downstream Processing of Nothofagin by Batch Anion-Exchange	
Adsorption/Desorption	S5



Figure S1. SDS PAGE of enzymes purified by <i>Strep</i> -tag affinity chromatography.	S7
Figure S2. Viscosity of aqueous 2-hydroxypropyl- $\beta$ -cyclodextrin solutions.	S8
Figure S3. Phloretin/2-hydroxypropyl- $\beta$ -cyclodextrin complexation methods.	S9
Figure S4. Optimization of phloretin solubilization with 2-hydroxypropyl- $\beta$ -cyclodextrin inclusion complex.	S10
Figure S5. pH profiles for nothofagin synthesis by <i>OsCGT</i> , UDP-glucose synthesis and UDP-glucose degradation by <i>GmSuSy</i> .	S11
Figure S6. Optimization of reaction pH.	S12
Figure S7. Optimization of substrate concentration and reaction temperature.	S13
Figure S8. Optimization of catalyst loading.	S14
Figure S9. HPLC analysis of nothofagin after the SEC-free DSP.	S15
Figure S10. $^1\text{H}$ NMR spectrum of nothofagin after the SEC-free DSP.	S16
Figure S11. $^1\text{H}$ NMR spectrum of phloretin (acceptor substrate).	S17
References for Supporting Information	S18

## Methods

### Chemicals and Materials

Media components and chemicals were of reagent grade from Sigma Aldrich/Fluka (Vienna Austria), Roth (Karlsruhe, Germany) or Merck (Vienna, Austria). 2-Hydroxypropyl- $\beta$ -cyclodextrin ( $\geq 96\%$ ), 2,6-dimethyl- $\beta$ -cyclodextrin ( $\geq 98\%$ ), sulfobutyl ether- $\beta$ -cyclodextrin sodium salt ( $\geq 98\%$ ),  $\beta$ -cyclodextrin crosslinked with epichlorohydrin (50 - 70%), phloretin ( $>98\%$ ) and UDP disodium salt ( $\geq 98\%$ ) were from Carbosynth (Compton, UK). *Strep-Tactin*<sup>®</sup> Sepharose<sup>®</sup> and D-desthiobiotin were from IBA (Goettingen, Germany). Toyopearl QAE550C, SuperQ-650M and GigaCap Q-650M resins were from Tosoh Bioscience (Tokyo, Japan). Diaion<sup>™</sup> WA21J and SA10A resins were from Mitsubishi Chemical Corporation (Tokyo, Japan). Dowex 1 $\times$ 2 (Cl<sup>-</sup>-form, 50 - 100 mesh) and Dowex 1 $\times$ 8 (Cl<sup>-</sup>-form, 200 - 400 mesh) resins were from Dow Chemical (Midland, MI, US). DEAE-cellulose was from Sigma Aldrich (Vienna, Austria). Minisart<sup>®</sup> NML syringe membrane filter (1.2  $\mu$ m, 0.2  $\mu$ m) and Vivaspin<sup>®</sup> Turbo 15 centrifugal concentrators (10 kDa) were from Sartorius (Goettingen, Germany). Acetone ( $\geq 99\%$ ) and isopropanol ( $\geq 99\%$ ) were from Roth (Karlsruhe, Germany).

### Analytical Methods

UDP-glucose, uridine, UMP and UDP were analyzed by reversed phase HPLC using a Kinetex<sup>®</sup> C18 column (5  $\mu$ m, 100 Å, 50 x 4.6 mm; Phenomenex, Germany) in reversed phase ion-pairing mode (Lemmerer et al. 2016). HPLC analysis was performed at 35°C with a mobile phase of 87.5% 20 mM potassium phosphate buffer, pH 5.9 containing 40 mM tetra-n-butylammonium bromide (TBAB) and 12.5% acetonitrile at an isocratic flow rate of 2 mL/min. UV-detection at 262 nm was used.

## Viscosity Measurements

The viscosities of the aqueous 2-hydroxypropyl- $\beta$ -cyclodextrin solutions, with and without 500 mM sucrose, were measured with an automated SVM 3000 Anton Paar (Austria) rotational Stabinger viscometer at 20°C and 40°C, respectively.

## Preparation of Phloretin/2-Hydroxypropyl- $\beta$ -Cyclodextrin Inclusion Complexes

Solid and liquid inclusion complexes of phloretin with 2-hydroxypropyl- $\beta$ -cyclodextrin were prepared by various methods described in literature (Bertacche et al. 2006; Giordano and Bettini 2011; Lin et al. 2010; Loftsson 1995; Ranpise et al. 2010; Wei et al. 2017). Phloretin and 2-hydroxypropyl- $\beta$ -cyclodextrin were weighed at a molar ratio of 1:1 (1 mmol).

*Preparation of Solid Inclusion Complexes.* (1) Preparation of inclusion complex by co-grinding. The physical mixture of phloretin and 2-hydroxypropyl- $\beta$ -cyclodextrin was prepared by grinding powders in a mortar for 15 min. (2) Preparation of inclusion complex by solvent evaporation. Phloretin and 2-hydroxypropyl- $\beta$ -cyclodextrin were dissolved in 10 mL ethanol (EtOH). EtOH was evaporated under reduced pressure (40°C, 20 mbar) to obtain the isolated inclusion complex as a powder. (3) Preparation of inclusion complex by microwave irradiation. A homogenous paste was prepared by mixing phloretin and 2-hydroxypropyl- $\beta$ -cyclodextrin with 1 mL of EtOH in a mortar. The paste formed was irradiated in a microwave oven (Micro-Chef V98, Moulinex, Austria) for 20 s at 750 W.

*Preparation of Liquid Inclusion Complexes.* Phloretin and 2-hydroxypropyl- $\beta$ -cyclodextrin were suspended in 5 mL deionized water. The suspension was irradiated in a microwave oven for 20 s at 750 W. Alternatively, the suspension was heated in a drying chamber at 70°C for 1 h. Remaining phloretin particles were removed by centrifugation (5000 rpm, 5 min, room temperature). Liquid inclusion complexes (supernatant) were used for nothofagin synthesis.

### **Optimization of Phloretin Solubilization With 2-Hydroxypropyl- $\beta$ -Cyclodextrin**

Liquid phloretin/2-hydroxypropyl- $\beta$ -cyclodextrin inclusion complex was prepared at a 1:1 molar ratio under microwave-assisted conditions (Giordano and Bettini 2011; Wei et al. 2017). First, 2-hydroxypropyl- $\beta$ -cyclodextrin (200 mM – 400 mM) was completely dissolved in water by irradiation in a microwave oven (Micro-Chef V98, Moulinex, Austria) for 20 s at 750 W and subsequent incubation in a drying chamber at 70°C for 1 h. Samples were inverted every 15 min to mix the solution. For complex formation, phloretin was added. The suspension was irradiated in the microwave and then allowed to equilibrate in the drying chamber as described above. Remaining phloretin particles were removed by centrifugation (5000 rpm, 5 min, room temperature). Supernatant was analyzed by HPLC.

### **Determination of Enzyme Activities and Stabilities Under Process Conditions**

The activity and stability of *OsCGT* was determined at 30°C and 40°C, pH 6.5. The reaction mixtures (1 mL; in water) contained phloretin/2-hydroxypropyl- $\beta$ -cyclodextrin inclusion complex (112 mM), 500 mM sucrose, 50 mM KCl, 10 mM MgCl<sub>2</sub> and *OsCGT*. Conversions were started by addition of 2 mM UDP-glucose either immediately for activity measurements or after 5 h and 16 h of incubation for stability measurements. The activity and stability of *GmSuSy* was determined as described for *OsCGT* but 2 mM UDP were used as substrate. All experiments were carried out in duplicate.

### **Downstream Processing of Nothofagin by Batch Anion-Exchange Adsorption/Desorption**

Binding capacity and desorption characteristics of different (anion-exchange) AEX resins were evaluated in batch experiments. 100 mg resin were washed with 1 mL elution buffer (10 mM potassium phosphate, 0.8 M sodium chloride, pH 8.5) containing 20% of isopropanol (mobile phase B). Isopropanol was added to prevent precipitation of nothofagin, caused by

dissociation of cyclodextrin complexes upon dilution (Loftsson 2015). After equilibration with 1 mL binding buffer (mobile phase A = mobile phase B without sodium chloride) the resins were incubated with 0.5 mL of sample containing ~17 mg of nothofagin. Desorption was with 0.5 mL mobile phase B. Two desorption steps were performed. Incubation was for 30 min on an end-over-end rotator (SB3 from Stuart) at 30 rpm and room temperature. For phase separation samples had to be centrifuged after each step (500 g, 30 min). Supernatants after binding and desorption steps were analyzed by HPLC.

For preparative isolation of ~0.15 g nothofagin by batch adsorption/desorption, 10 g of SuperQ-650M were washed and equilibrated with 40 mL of mobile phase B and A, respectively. Incubation was for 15 min. The equilibration step with mobile phase A was repeated once to ensure efficient binding. 3.8 mL sample (containing ~0.2 g nothofagin) and 6.2 mL mobile phase A were added to the pretreated resin. Incubation was for 30 min. To remove impurities, the resin was washed with 10 mL mobile phase A. For nothofagin desorption 40 mL mobile phase B were used. Three desorption steps were performed. Incubation was for 10 min on an end-over-end rotator (SB3 from Stuart) at 30 rpm and room temperature. For phase separation samples had to be centrifuged after each step (500 g, 1 h). Sampling and sample analysis were carried out as described above. Nothofagin containing eluates were pooled.

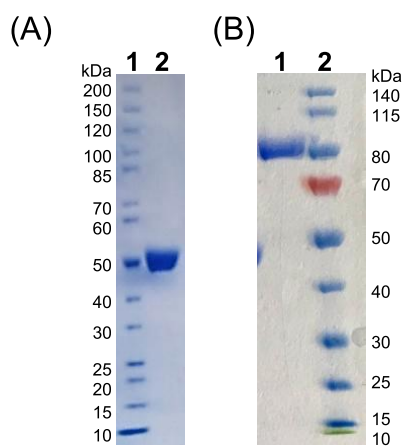


Figure S1. SDS PAGE of enzymes purified by *Strep*-tag affinity chromatography. (A) Lane 1, PageRuler™ Unstained Protein Ladder (Thermo Scientific); lane 2, *OsCGT*. (B) Lane 1, *GmSuSy* (monomeric subunit); lane 2, PageRuler™ Prestained Protein Ladder (Thermo Scientific).

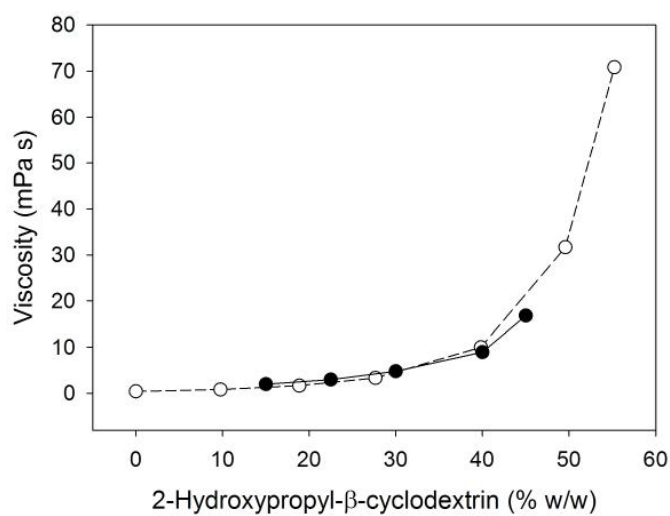


Figure S2. Viscosity of aqueous 2-hydroxypropyl- $\beta$ -cyclodextrin solutions at room temperature. Filled circle, experimental data; open circle, data from Loftsson et al. (1999).

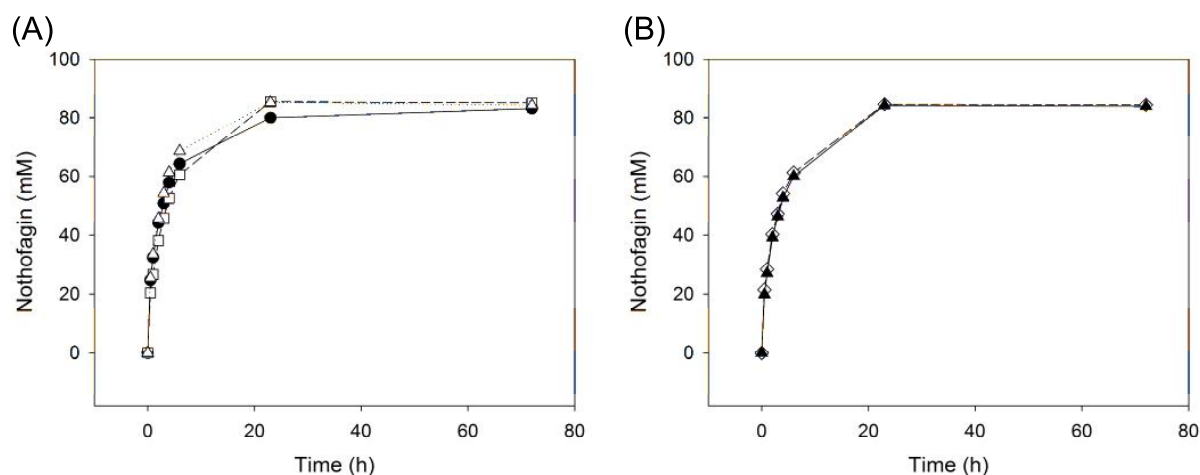


Figure S3. Phloretin/2-hydroxypropyl- $\beta$ -cyclodextrin complexation methods. (A) Solid and (B) liquid inclusion complexes were prepared by different methods and compared for nothofagin synthesis. Phloretin and 2-hydroxypropyl- $\beta$ -cyclodextrin were used at a molar ratio of 1:1. (A) Preparation of inclusion complex by grinding (physical mixture), filled circle; by dissolving in EtOH and subsequent solvent evaporation, open square; by microwave irradiation of a homogenous paste prepared by mixing with a small amount of EtOH, open triangle. (B) Microwave irradiation (20 s, 750 W) of aqueous suspension, filled triangle; heating in drying chamber (70°C, 1 h) of aqueous suspension, open diamond. Phloretin/2-hydroxypropyl- $\beta$ -cyclodextrin inclusion complexes (85 mM) were used as substrate. Reactions contained 0.5 mM UDP, 500 mM sucrose, 50 mM KCl, 10 mM MgCl<sub>2</sub>, 0.5 mg/mL *OsCGT*, 0.25 mg/mL *GmSuSy* and were carried out at pH 6.5, 30°C and 300 rpm.



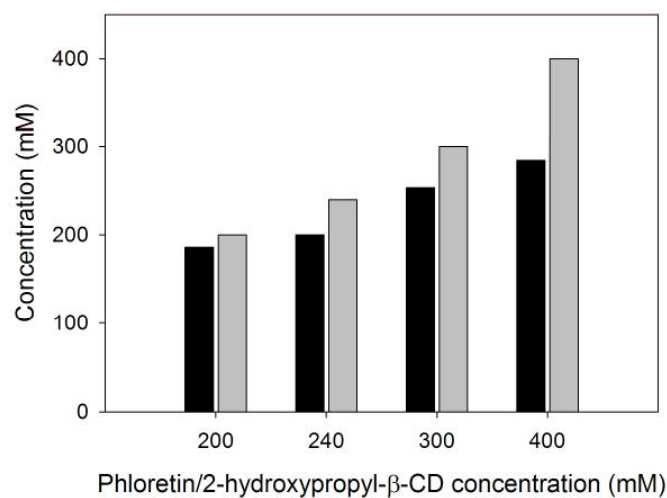


Figure S4. Optimization of phloretin solubilization with 2-hydroxypropyl-β-cyclodextrin inclusion complex. Phloretin and 2-hydroxypropyl-β-cyclodextrin were used at a molar ratio of 1:1 for liquid inclusion complex formation under microwave-assisted conditions. For details see the Methods. Black bars, soluble phloretin concentration; grey bars, applied concentration of phloretin/2-hydroxypropyl-β-cyclodextrin.

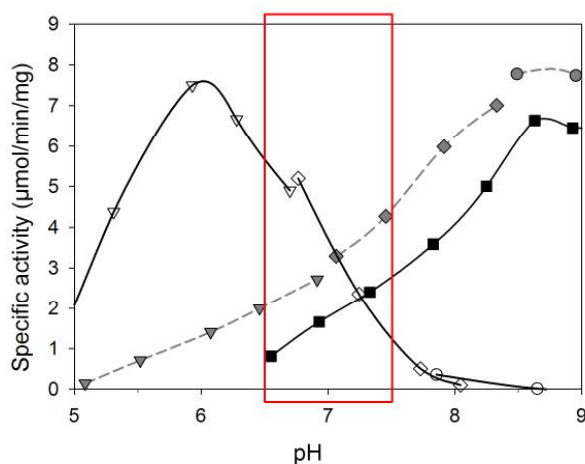


Figure S5. pH profiles for nothofagin synthesis by *OsCGT* (full line, filled squares), UDP-glucose synthesis (full line, open symbols) and UDP-glucose degradation (dashed line, filled symbols) by *GmSuSy*, using a mixture of HEPES, Tris and CAPS (filled squares), MES (reverse triangles), HEPES (diamonds) or CHES (circles) as buffer. Adapted from Bungaruang et al. (2013). Reaction conditions: 5 mM phloretin, 0.6 mM UDP-glucose, 20% (v/v) DMSO (nothofagin synthesis by *OsCGT*); 100 mM sucrose, 2 mM UDP (UDP-glucose synthesis by *GmSuSy*); 15 mM fructose, 2 mM UDP-glucose (UDP-glucose degradation by *GmSuSy*). Measurements were performed at 30°C.

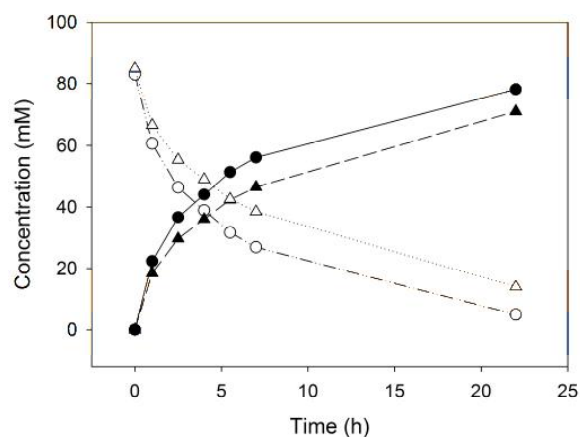


Figure S6. Optimization of reaction pH. Nothofagin was synthesized at pH 6.5 (circles) and 7.5 (triangles) from liquid phloretin/2-hydroxypropyl- $\beta$ -cyclodextrin inclusion complex (85 mM). Reactions (1 mL) contained 0.5 mM UDP, 500 mM sucrose, 50 mM KCl, 10 mM MgCl<sub>2</sub>, 0.5 mg/mL *OsCGT*, 0.25 mg/mL *GmSuSy* and were carried out at 30°C and 300 rpm. Nothofagin, filled symbols; phloretin, open symbols.

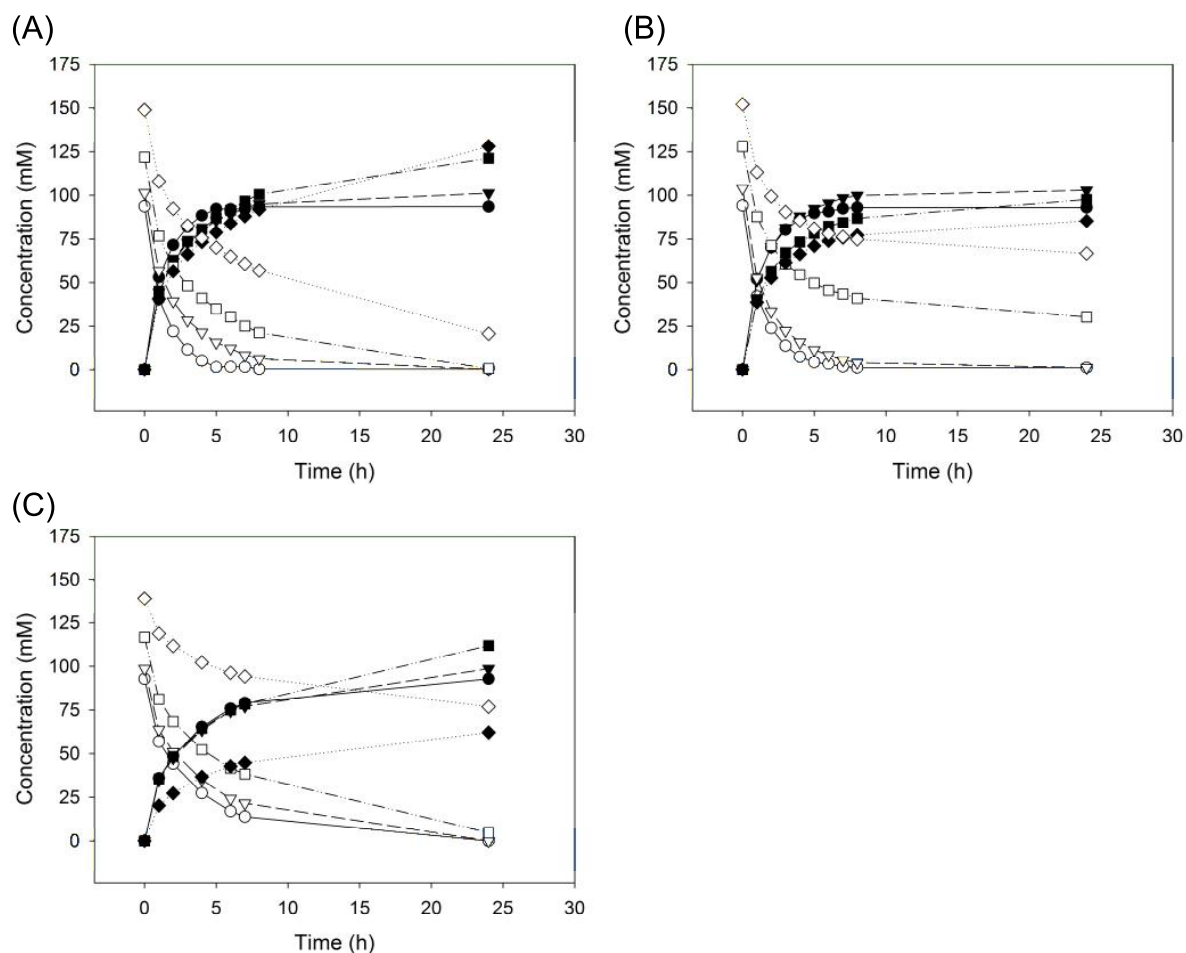


Figure S7. Optimization of substrate concentration and reaction temperature. Nothofagin was synthesized at (A) 40°C, pH 6.5, (B) 50°C, pH 6.5 and (C) 40°C, pH 7.0 from liquid phloretin/2-hydroxypropyl- $\beta$ -cyclodextrin inclusion complex as substrate: 95 mM, circles; 105 mM, reverse triangles; 125 mM, squares; 150 mM, diamonds. Reactions (1 mL) contained 0.5 mM UDP, 500 mM sucrose, 50 mM KCl, 10 mM MgCl<sub>2</sub>, 0.5 mg/mL *OsCGT*, 0.25 mg/mL *GmSuSy* and were carried out at 300 rpm. Nothofagin, filled symbols; phloretin, open symbols.

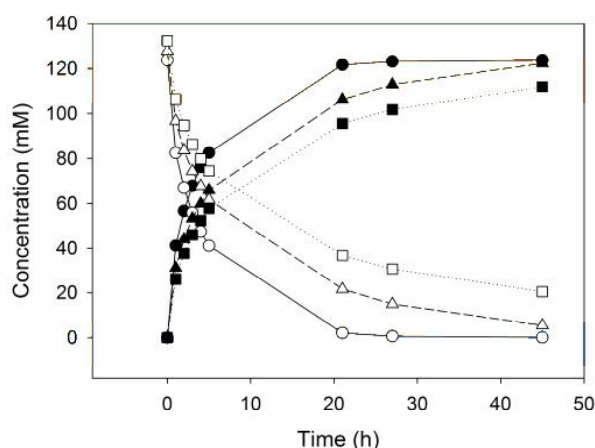


Figure S8. Optimization of catalyst loading. Liquid phloretin/2-hydroxypropyl- $\beta$ -cyclodextrin inclusion complex ( $\sim 120$  mM) was used as substrate. Reactions contained 0.5 mM UDP, 500 mM sucrose, 50 mM KCl, 10 mM MgCl<sub>2</sub>, varying amounts of enzymes and were carried out at pH 6.5, 40°C and 300 rpm. 0.5 mg/mL ( $\sim 1.6$  U/mL) *OsCGT*, 0.25 mg/mL ( $\sim 0.5$  U/mL) *GmSuSy*, circles; 0.4 mg/mL *OsCGT*, 0.2 mg/mL *GmSuSy*, triangles; 0.3 mg/mL *OsCGT*, 0.15 mg/mL *GmSuSy*, squares. Nothofagin, filled symbols; phloretin, open symbols.

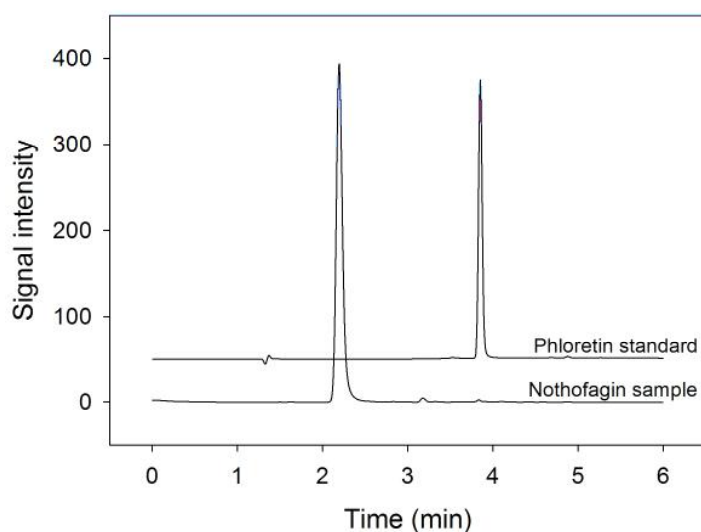


Figure S9. HPLC analysis of nothofagin after the SEC-free DSP. Superposition of ion-pair reversed phase HPLC elution profiles of produced nothofagin and an authentic phloretin (substrate) standard is shown. Retention time of nothofagin is 2.2 min, of phloretin 3.8 min. Purity was  $\geq 99\%$ .  $<1\%$  remaining impurities (phloretin, unidentified products) were detected in the final product (based on HPLC peak area). UV detection at 288 nm was used. Note that the identity of nothofagin was additionally confirmed by NMR.

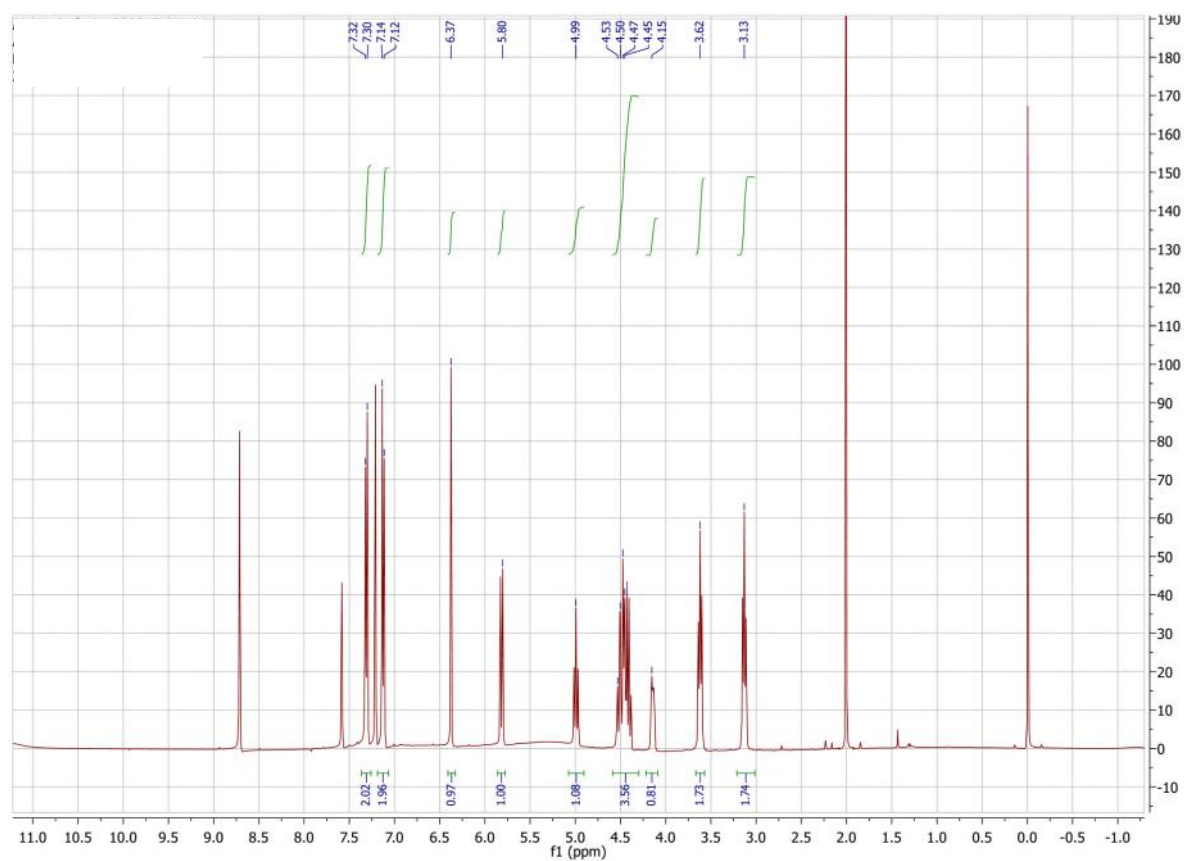


Figure S10. <sup>1</sup>H NMR spectrum of nothofagin after the SEC-free DSP. Nothofagin was dissolved in pyridine. Spectrum is in accordance with previously published data (Bungaruang et al. 2013; Bungaruang et al. 2016). ≤5% of residual acetone was detected. No residual 2-hydroxypropyl-β-cyclodextrin was detected.

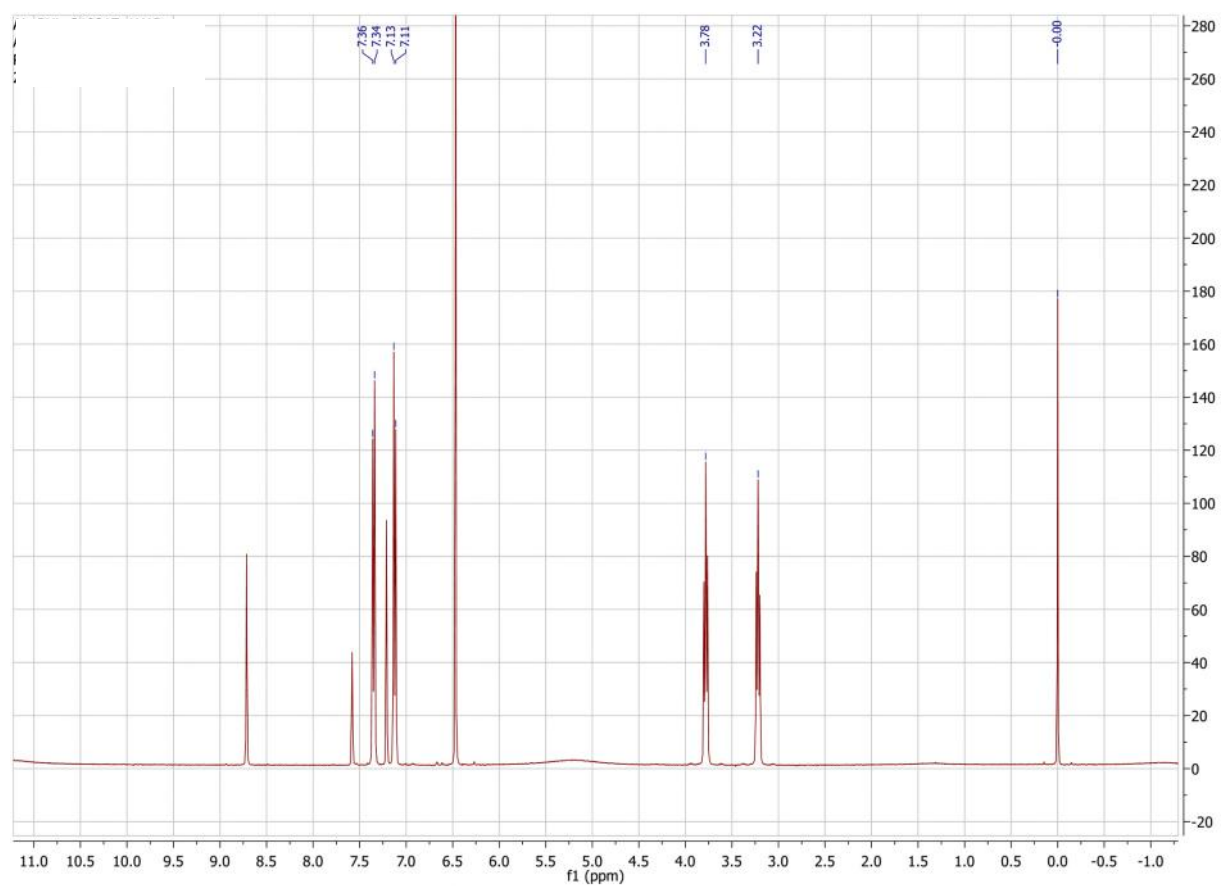


Figure S11. <sup>1</sup>H NMR spectrum of phloretin (acceptor substrate). Phloretin was dissolved in pyridine.



## References for Supporting Information

- Bertacche V, Lorenzi N, Nava D, Pini E, Sinico C. 2006. Host-guest interaction study of resveratrol with natural and modified cyclodextrins. *J Incl Phenom Macrocycl Chem* 55(3-4):279-287.
- Bungaruang L, Gutmann A, Nidetzky B. 2013. Leloir glycosyltransferases and natural product glycosylation: biocatalytic synthesis of the C-glucoside nothofagin, a major antioxidant of redbush herbal tea. *Adv Synth Catal* 355(14-15):2757-2763.
- Bungaruang L, Gutmann A, Nidetzky B. 2016.  $\beta$ -cyclodextrin improves solubility and enzymatic C-glucosylation of the flavonoid phloretin. *Adv Synth Catal* 358(3):486-493.
- Giordano F, Bettini R. 2011. Process for preparation of inclusion compounds between a non-steroidal anti-inflammatory drug and betacyclodextrin by microwave treatment. Patent US 7935685 B2.
- Lemmerer M, Schmölzer K, Gutmann A, Nidetzky B. 2016. Downstream processing of nucleotide-diphospho-sugars from sucrose synthase reaction mixtures at decreased solvent consumption. *Adv Synth Catal*. 358(19):3113-3122.
- Lin S-Y, Hsu C-H, Sheu M-T. 2010. Curve-fitting FTIR studies of loratadine/hydroxypropyl- $\beta$ -cyclodextrin inclusion complex induced by co-grinding process. *J Pharm Biomed Anal* 53(3):799-803.
- Loftsson T. 1995. Cyclodextrin complexation. Patent US 5472954 A.
- Loftsson T. 2015. Formulation of drug-cyclodextrin complexes. In: Dragicevic N, Maibach HI, editors. *Percutaneous Penetration Enhancers Chemical Methods in Penetration Enhancement: Drug Manipulation Strategies and Vehicle Effects*. Berlin, Heidelberg: Springer Berlin Heidelberg. p 189-205.
- Loftsson T, Másson M, Sigurjónsdóttir JF. 1999. Methods to enhance the complexation efficiency of cyclodextrins. *STP Pharma Sci* 9(3):237-242.
- Ranpise NS, Kulkarni NS, Mair PD, Ranade AN. 2010. Improvement of water solubility and *in vitro* dissolution rate of aceclofenac by complexation with  $\beta$ -cyclodextrin and hydroxypropyl- $\beta$ -cyclodextrin. *Pharm Dev Technol* 15(1):64-70.
- Wei Y, Zhang J, Memon AH, Liang H. 2017. Molecular model and *in vitro* antioxidant activity of a water-soluble and stable phloretin/hydroxypropyl- $\beta$ -cyclodextrin inclusion complex. *J Mol Liq* 236:68-75.

Decoupling of recombinant protein production from  
*E. coli* growth enhances functional expression of  
plant Leloir glycosyltransferases

## **Decoupling of recombinant protein production from *Escherichia coli* cell growth enhances functional expression of plant Leloir glycosyltransferases**

Martin Lemmerer<sup>1</sup>, Jürgen Mairhofer<sup>2</sup>, Alexander Lepak<sup>3</sup>, Karin Longus<sup>3</sup>, Rainer Hahn<sup>4</sup>, Bernd Nidetzky<sup>1,3,\*</sup>

<sup>1</sup>Austrian Centre of Industrial Biotechnology (acib), Petersgasse 14, 8010 Graz, Austria

<sup>2</sup>enGenes Biotech GmbH, Mooslackengasse 17, 1190 Vienna, Austria

<sup>3</sup>Institute of Biotechnology and Biochemical Engineering, Graz University of Technology, NAWI Graz, Petersgasse 12/I, 8010 Graz, Austria

<sup>4</sup>Department of Biotechnology, University of Natural Resources and Life Sciences Vienna, Muthgasse 18, 1190 Vienna, Austria

**\*Corresponding author:** Bernd Nidetzky; e-mail: bernd.nidetzky@tugraz.at; phone: +43 316 873 8400; FAX: +43 316 873 8434

**Abbreviations:** cdm, cell dry mass; GmSuSy, sucrose synthase from soybean (*Glycine max*); GT, glycosyltransferase; UGT71A15, UDP-glycosyltransferase 71A15; SEC, size exclusion chromatography; UDP-glc, uridine 5'-diphospho- $\alpha$ -D-glucose

**Abstract.** Sugar nucleotide-dependent (Leloir) glycosyltransferases from plants are important catalysts for the glycosylation of small molecules and natural products. Limitations on their applicability for biocatalytic synthesis arise due to low protein expression ( $\leq 10$  mg/L culture) in standard microbial hosts. Here, we show for two representative glycosyltransferases (sucrose synthase from soybean; UGT71A15 from apple) that a synthetic biology-based strategy of decoupling the enzyme expression from *E. coli* BL21(DE3) cell growth was effective in enhancing their individual (~5-fold) or pairwise (~2-fold) production as correctly folded, biologically active proteins. The T7 phage-derived Gp2 protein, which inhibits the *E. coli* endogenous RNA polymerase, was used for growth control. Its expression was arabinose-inducible from a genome-integrated site transcribed by T7 RNA polymerase which is unaffected by Gp2. A PET plasmid vector integrated the gene(s) of interest separately inducible by isopropyl- $\beta$ -D-galactoside and also transcribed by the T7 RNA polymerase. Laboratory batch and up-scaled (20 L) fed-batch bioreactor cultivations demonstrated improvements in overall yield of active enzyme by around one magnitude order as result of production under growth-arrested conditions. Sucrose synthase and UGT71A15 were obtained, respectively, at 115 U/g and 2.30 U/g cell dry weight, corresponding to ~5% and ~1% of total intracellular protein. Fed-batch production gave sucrose synthase in a yield of 2,300 U/L of culture (830 mg protein/L). Analyzing the isolated glycosyltransferase, we show that improvement in the enzyme production was due to enhancement of both amount (2.5-fold) and quality (2.4-fold) of the soluble sucrose synthase. Enzyme preparation from decoupled production comprised an increased portion (62% compared with 26%) of the active sucrose synthase homo-tetramer. In summary, therefore, we show that expression in growth-arrested *E. coli* is promising for recombinant production of plant Leloir glycosyltransferases.

Key words: Synthetic biology; Leloir glycosyltransferase; Recombinant protein production; Protein quality; Growth-arrested *E. coli*; Small molecule glycosylation

## 1 INTRODUCTION

Plant metabolisms for natural product biosynthesis and detoxification involve an elaborate enzymatic machinery for attaching sugars onto non-carbohydrate small-molecule structures (Bowles, Lim, Poppenberger, & Vaistij, 2006). This glycosylation machinery is comprised of a large set of sugar nucleotide glycosyltransferases. The enzymes, also referred to collectively as Leloir glycosyltransferases, transfer glycosyl residues from sugar nucleotide donors to specific position(s) on acceptor substrates (Liang et al., 2015). Compared with other enzymes (e.g., glycoside hydrolases; glycoside phosphorylases) also able to glycosylate small molecules, the glycosyltransferases often present a unique combination of high chemo/regioselectivity and relatively flexible substrate specificity (Desmet et al., 2012; Thuan & Sohng, 2013; Chen, 2018). The plant glycosyltransferases are therefore promising catalysts for glycoside production (for reviews, see: Lim, 2005; Nidetzky, Gutmann, & Zhong, 2018). Glycosylated derivatives of small molecules (e.g., flavonoids, terpenoids, peptides) with important applications in the food, fragrance, cosmetic and chemical industries are synthesized efficiently using glycosyltransferases (Desmet et al., 2012; Xiao, Muzashvili, & Georgiev, 2014; De Bruyn, Maertens, Beauprez, Soetaert, & De Mey, 2015; Kim, Yang, Kim, Cha, & Ahn, 2015; Schwab, Fischer, & Wüst, 2015; Schwab, Fischer, Giri, & Wüst, 2015; Hofer, 2016; Olsson et al., 2016; Hsu et al., 2018; Nidetzky, Gutmann, & Zhong, 2018; Schmölzer, Lemmerer, & Nidetzky, 2018).

Limitation on the applicability of plant glycosyltransferases arises from their difficult expression in standard microbial hosts (Lim, 2005; Desmet et al., 2012; Nidetzky, Gutmann, & Zhong, 2018). *Escherichia coli* is mostly used. Expression is low ( $\leq 10$  mg/L) in general (e.g., Arend, Warzecha, Hefner, & Stöckigt, 2001; Schmölzer, Gutmann, Diricks, Desmet, & Nidetzky, 2016), poor ( $\leq 1$  mg/L) in various instances (e.g., Cai et al., 2017; Weiner et al., 2017). With notable exceptions (Arend et al., 2001; Dewitte et al., 2016; Schmideder et al.,

2016; Priebe, Daschner, Schwab, & Weuster-Botz, 2018), the enzyme production has received relatively little attention for systematic process development. The main bottlenecks on production efficiency thus remain largely unknown. Besides specific requirements an individual glycosyltransferase may have, it seems probable that there are also important factors of a more general, if not universal relevance. Discovery of such factors, and process optimization along the lines thus suggested, would present important advance for the biocatalytic application of glycosyltransferases.

In a recent study of a bacterial Leloir glycosyltransferase (sucrose synthase from *Acidithiobacillus caldus*; Diricks, de Bruyn, van Daele, Walmagh, & Desmet, 2015) we showed that constitutive expression in *E. coli* BL21 shifted the production of recombinant protein mainly to the stationary growth phase (Schmölzer, Lemmerer, Gutmann, & Nidetzky, 2017). Once the glucose carbon source had been depleted, active enzyme was accumulated gradually to a substantial titer of ~350 mg/L of culture. This result gave rise to the working hypothesis for this study, namely that expression in growth-arrested *E. coli* might constitute a general strategy for efficiency-enhanced production of (plant) glycosyltransferases.

Here, we used a synthetic biology-based approach to decouple *E. coli* BL21(DE3) cell growth from target gene overexpression (Mairhofer, Striedner, Grabherr, & Wilde, 2016). The underlying concept is built upon the Gp2 protein from the bacteriophage T7. Gp2 inhibits the *E. coli* endogenous RNA polymerase (Mekler, Minakhin, Sheppard, Wigneshweraraj & Severinov, 2011) while it leaves T7 RNA polymerase unaffected (Mairhofer, Striedner, Grabherr, & Wilde, 2016). An inducible, T7 RNA polymerase-based expression of the Gp2 gene thus allows for a constant supply of the inhibitor. This enables the *E. coli* transcription to be shut off, hence the cell growth to be arrested, in a controllable fashion. Under conditions managed by Gp2, therefore, the *E. coli* protein synthesis machinery is taken over for recombinant production of the target protein(s). The practical design embodied in enGenes

technology involves genome integration of the Gp2 coding gene under control of the *araB* promoter inducible by L-arabinose. Within this strain background, a pET plasmid vector is used that contains the gene(s) of interest inducible by isopropyl- $\beta$ -D-galactoside. This design provides flexibility and temporal control for cell proliferation to be switched off and protein production to be induced (Mairhofer, Striedner, Grabherr, & Wilde, 2016; Mairhofer et al., 2016). It presents a new approach toward quiescent *E. coli* cells applied to recombinant protein production (for alternative approaches, see: Chen, Walia, Mukherjee, Mahalik, & Summers, 2015; Gosh, Gupta, & Mukherjee, 2012; Mahalik, Sharma, & Mukherjee, 2014)

We demonstrate application of the outlined approach to individual and pairwise production of two representative glycosyltransferases, the sucrose synthase from soybean (*Glycine max*; GmSuSy) (Bungaruang, Gutmann, & Nidetzky, 2013) and the flavonoid glycosyltransferase UGT71A15 from apple (*Malus domestica*) (Lepak, Gutmann, Kulmer, & Nidetzky, 2015). The glycosyltransferase reactions are shown in Scheme 1. Enzyme co-expression reflects the idea of a glycosylation cascade in which the sugar nucleotide donor substrate is formed in situ and continuously regenerated (Scheme 1; Nidetzky, Gutmann, & Zhong, 2018). We show that enzyme production in growth-arrested *E. coli* gives significant improvements in the amount and quality of the recombinant glycosyltransferase as compared to the exactly comparable production in the growing *E. coli* reference. We also show transferability of the production strategy to a high-cell density fed-batch culture of *E. coli* at 20 L operating scale and obtain up to 830 mg glycosyltransferase protein/L of culture in that way.

## 2 MATERIALS AND METHODS

### 2.1 Microbial strains

The *E. coli* strain referred to as enGenes-X-press is a BL21(DE3) derivative with the genotype *E. coli* B F<sup>-</sup> *ompT gal dcm lon hsdSB*( $\tau_B^-$   $m_B^-$ )  $\lambda$ (DE3 [*lacI lacUV5-T7p07 ind1 sam7 nin5*])

[*malB*<sup>+</sup>]<sub>K-12</sub>( $\lambda$ S) attTn7::*araC-p<sub>araB</sub>-gp2*> $\Delta$ *araABCD*::CAT<sup>R</sup> (Mairhofer, Striedner, Grabherr, & Wilde, 2016). enGenes-X-press has the Gp2 coding sequence integrated in the genome at the Tn7 attachment (attTn7) site. Gp2 gene expression is controlled by the L-arabinose inducible *araB* promoter. The inserted sequence additionally involves a regulator, an optimized terminator (Mairhofer, Wittwer, Cserjan-Puschmann, & Striedner, 2015) and a chloramphenicol resistance gene. The strain furthermore features knock-out of the complete L-arabinose degrading operon *araABCD*. The strain enGenes-X-press is proprietary material of enGenes Biotech GmbH. Its construction was reported elsewhere (Mairhofer, Striedner, Grabherr, & Wilde, 2016). The reference *E. coli* strain BL21(DE3) was from the Coli Genetic Stock Center (CGSC#: 12504). To compare performance of the two *E. coli* strains, both were transformed with the relevant expression plasmids, as described below. It was shown (Mairhofer, Striedner, Grabherr, & Wilde, 2016) that in the absence of induction by L-Ara enGenes-X-press exhibits growth behavior not different from that of *E. coli* BL21(DE3); and that the presence of L-Ara does not affect growth of the host strain as such.

## 2.2 Enzyme expression

The previously described pET-STRP3 expression vector was used (Lepak, Gutmann, Kulmer, & Nidetzky, 2015). Enzymes are thus produced as fusion proteins harboring N-terminal Strep-Tag II. For single enzyme expression, the coding genes were inserted via NdeI and XhoI restriction sites. The GmSuSy gene (GenBank: AF030231) was codon optimized for expression in *E. coli* (Bungaruang, Gutmann, & Nidetzky, 2013). The UGT71A15 gene (GenBank: DQ103712) was used.

For enzyme co-expression, the vector referred to as pETduo was derived from pET-STRP3 by inserting the UGT71A15 gene into the plasmid harboring the GmSusy gene. Suitable oligonucleotide primers (pDUO\_Ins\_fwd, pDUO\_Ins\_rev; Supporting Information) were used to amplify the introduced expression cassette by specific binding upstream of the promoter



region and downstream of the terminator sequence. The receiving vector was linearized by amplification using pETduo\_BB\_fwd and pETduo\_BB\_rev (Supporting Information) as forward and reverse primer, respectively. The F1 ORI was eliminated in this step (Supporting Information, Figures S1 and S2). The resulting DNA fragments were purified on agarose gel and fused by homologous recombination. The sequences of both glycosyltransferase coding genes were verified in the final expression vector.

Expression strains were obtained by transforming the respective expression vector into electro-competent cells of *E. coli* BL21(DE3) (reference) and enGenes-X-press.

### **2.3 Batch bioreactor cultivations**

With exceptions noted, the strains *E. coli* BL21(DE3) and enGenes-X-press were cultivated under exactly comparable conditions. Each strain harbored the pET expression vector for production of GmSuSy, UGT71A15 or both. Pre-cultures (250 mL in 1000 mL baffled shaken flasks) were inoculated from glycerol stocks (100  $\mu$ L) and incubated overnight at 37°C and 130 rpm (Certomat<sup>®</sup> BS-1; Sartorius, Germany). LB medium supplemented with sterile filtered antibiotics (*E. coli* BL21(DE3): 50  $\mu$ g/mL kanamycin; enGenes-X-press: 50  $\mu$ g/mL kanamycin; 34  $\mu$ g/mL chloramphenicol) was used.

Bioreactor cultivations were performed in parallel in two Labfors III 3.6 L bioreactors from Infors HT (Bottmingen, Switzerland). A semi-synthetic medium (Table S1) prepared from separately autoclaved components was used. To this, 0.4 mL/L of a sterile filtered trace element solution was added (Table S2). A value of 40% air saturation was maintained using an agitation and airflow cascade. Polypropylene glycol (10%) was used for foam control. The pH was maintained at 7.0 using automated addition of 2 M KOH and 1 M H<sub>3</sub>PO<sub>4</sub>. Bioreactors were inoculated to an OD<sub>600nm</sub> of 0.5 at a temperature of 37°C. Temperature was lowered as per Table 1 prior to induction and initiated at an OD<sub>600nm</sub> of 5. The *E. coli* BL21(DE3) strain was induced with filter-sterilized IPTG solution to a final concentration of 0.1 mM. The enGenes-X-press

strain was induced with IPTG (0.1 mM) and L-arabinose (100 mM). Samples (10 mL) were taken at certain times and analyzed for cell dry mass and glycerol (see later).

## 2.4 Up-scaled fed-batch bioreactor cultivations

The strains *E. coli* BL21(DE3) and enGenes-X-press harboring the pET expression vector for production of GmSuSy were used. Fed-batch cultivations were performed in a Bioengineering AG bioreactor (Type NLF22; Wald, Switzerland) with 20 L total working volume (10 L batch volume). The bioreactor was equipped with standard computer-controlled units (Siemens Symantic S7; WinCC). Semi-synthetic medium was used (see the Supporting Information). Its composition was adjusted for total production of 1580 g dry cell mass.

Pre-cultures (250 mL in 2000 mL baffled shaken flasks) were inoculated from cell bank vials (500  $\mu$ L) and incubated at 37°C and 180 rpm (INFORS<sup>®</sup> HT Multitron) until an OD<sub>600nm</sub> of 3.0 to 3.5 was reached. An amount of 1000 OD<sub>600nm</sub> units was transferred into 400 mL of 0.9% (by weight) NaCl solution and added to the bioreactor. Air saturation was kept at 30% through stirrer speed and aeration rate control. The O<sub>2</sub> and CO<sub>2</sub> contents in the outlet air were measured with a BlueSens (Herten, Germany) BlueInOne Gas analyzer. The pH was controlled at 7.0 ( $\pm$  0.05) using 25% (by weight) NH<sub>4</sub>OH solution. During the batch phase the temperature was 37°C  $\pm$  0.5°C. Polypropylene glycol PPG-2000 was added as antifoam (1.5 mL/L batch culture). Before starting the feeding when the culture had reached stationary phase (after ~10 h; ~8 g dry cell mass/L), the temperature was lowered to 30°C. Initially, an exponential substrate feed was used to provide a constant specific growth rate of 0.17 h<sup>-1</sup> over 11 h. Then, a linear substrate feed (9.54 g glucose/min) over 4 h and another linear substrate feed (4.35 g glucose/min) over 15 h were applied (see the Supporting information). The substrate feed involved superimposed feedback control of weight loss in the substrate tank. Protein expression was induced after 15 h of substrate feed. It involved the addition of 31.6 mmol IPTG (= 20  $\mu$ mol/g cell dry mass) and 0.1 M L-Ara based on the final volume of ~20 L. The induction

solution contained 79 mM of  $(\text{NH}_4)_2\text{SO}_4$  based on end volume. Polypropylene glycol PPG-2000 (500 mL in total) was used for foam control. Samples were taken at certain times and the cell growth was recorded as increase in  $\text{OD}_{600\text{nm}}$ . Cells were harvested after 40 h by centrifugation (30 min at  $4^\circ\text{C}$  and 4420 g; Sorvall RC-5B, ThermoFisher Scientific, Waltham, MA, USA) and stored at  $-20^\circ\text{C}$ .

Cell dry mass was determined from 10 mL samples. The cells were centrifuged, washed with 20 mL distilled water, re-suspended and transferred to a dried and weighed beaker, which was then dried at  $105^\circ\text{C}$  for 24 h and re-weighed. Cells were disrupted by high pressure homogenizer (Supporting Information) to obtain cell extract for activity measurement and purification.

## **2.5 Protein purification and characterization**

*Strep-Tag purification.* Pre-packed 1-mL or 5-mL Strep-Tactin Sepharose columns (IBA Life Sciences, Göttingen, Germany) were used on an ÄKTA Explorer 100 system (GE Healthcare, Pasching, Austria) and operated at a flow rate of 1 and 5 mL/min, respectively. Tris/HCl buffer (100 mM, pH 8.0, 150 mM NaCl, 1 mM EDTA) was used. Cell extract filtered through 1.2- $\mu\text{m}$  cellulose-acetate syringe filter was loaded onto the column. After loading, the column was flushed with buffer until the UV signal (280 nm) signal reached baseline level. Elution was done with two column volumes of desthiobiotin (2.5 mM). The columns were regenerated with hydroxy-azophenyl-benzoic acid (1 mM) and equilibrated again with buffer.

*Size-exclusion chromatography.* This was performed using a Superdex 200 increase 10/300 GL column (GE Healthcare) operated on ÄKTA Explorer 100 system. All runs were performed in 10 mM phosphate buffer (pH 7.4) containing 2.7 mM KCl, 0.14 mM NaCl. The flow rate was 0.5 mL/min and UV detection (280 nm) was used. Strep-Tactin eluate (200  $\mu\text{L}$ ) was applied to the column. For analytical SEC, a G3000SWXL column (300 mm  $\times$  7.8 mm, inner diameter 5  $\mu\text{m}$ ; Tosoh Bioscience, Tokyo, Japan) was used.

## 2.6. Enzymatic activity measurements

Assays were performed at 30°C in 1.5 mL tubes on an Eppendorf (Vienna, Austria) Thermomixer comfort at 300 rpm. Enzyme was added as *E. coli* cell extract or in purified form to start the reaction. Product release was measured in samples (20 µL) taken at four different times. Samples were diluted into acetonitrile (180 µL) to stop the reaction. Precipitated protein was removed by centrifugation for 20 min at room temperature and 13200 rpm. Between 5 – 10 µL of supernatant were used for further analysis. Enzymatic rates were determined from linear time courses of product formation. One Unit (U) of enzyme activity is the amount of enzyme producing 1 µmol product/min under the assay conditions.

*GmSuSy*. Sucrose (500 mM) and uridine 5'-diphosphate (10 mM) were used as substrates in HEPES buffer (100 mM; pH 7.5) containing 13 mM MgCl<sub>2</sub> and 0.13% BSA (Bungaruang et al., 2013). The released UDP-glucose was measured by HPLC.

*UGT71A15*. Ferulic acid (1 mM) and UDP-glucose (2 mM) were used as substrates in HEPES buffer (50 mM; pH 7.5) containing 50 mM KCl, 13 mM MgCl<sub>2</sub>, 0.13% BSA and 2% DMSO. The released ferulic acid-4-O-β-D-glucoside (Scheme 1) was measured by HPLC.

## 2.7 Analytical HPLC methods

*Glycerol*. This was analyzed on a Merck-Hitachi LaChrome HPLC System equipped with an Aminex HPX-87H column (BioRad, Richmond, CA, USA), a Merck-Hitachi LaChrome L-7250 autosampler and a Merck L-7490 RI detector. The system was operated at 65°C, using a flow rate of 0.6 mL/min with 5 mM sulfuric acid as the eluent.

*Reaction of GmSuSy*. UDP-glucose and UDP were analyzed by reversed phase HPLC using a Kinetex® C18 column (5 µm, 100 Å, 50 × 4.6 mm; Phenomenex, Torrance, CA, USA) in reversed phase ion-pairing mode. The analysis was performed at 35°C with a mobile phase of 87.5% 20 mM potassium phosphate buffer (pH 5.9) containing 40 mM tetra-*n*-butylammonium

bromide and 12.5% acetonitrile. An isocratic flow rate of 2 mL/min was used and detection was at 262 nm.

*Reaction of UGT71A15.* Ferulic acid and ferulic acid-4-O- $\beta$ -glucoside were analyzed by reversed phase HPLC using the above described Kinetex® C18 column in reversed phase mode. The analysis was performed at 35°C using a gradient separation (mobile phase A: H<sub>2</sub>O + 0.1% formic acid, mobile phase B: acetonitrile + 0.1% formic acid) at a flow rate of 1 mL/min. Gradient conditions were as follows: 0.00 min 10% B; 0.50 min 10% B; 4.00 min 70% B; 4.30 min 70% B; 4.31 min 10% B; 7.00 min 10% B. Detection was at 320 nm. Authentic standards were used for calibration.

### **3 RESULTS AND DISCUSSION**

The enzymes used are representative for plant glycosyltransferases applied to biocatalytic glycosylation of small molecules (Nidetzky, Gutmann, & Zhong, 2018). UGT71A15 shows broad acceptor substrate specificity and has previously been used for the glycosylation of flavonoids (Lepak, Gutmann, Kulmer, & Nidetzky, 2015). It is a member of the glycosyltransferase family GT-1, a large enzyme family comprising numerous plant glycosyltransferases involved in small molecule glycosylation (Liang et al., 2015). UGT71A15 is a 50.2 kDa protein that functions as a monomer. GmSuSy belongs to glycosyltransferase family GT-4. It is a functional homo-tetramer composed of 92.2 kDa subunits. GmSuSy has previously been used for UDP-glucose recycling in glycosylation reactions by coupled glycosyltransferases, including UGT71A15 (Scheme 1) (Lepak, Gutmann, Kulmer, & Nidetzky, 2015; Schmölder, Gutmann, Diricks, Desmet, & Nidetzky, 2016; Schmölder, Lemmerer, & Nidetzky, 2018).

#### **3.1 Single gene expression for production of GmSuSy**

We performed controlled batch bioreactor cultivations at 25°C and 30°C to compare enzyme production in enGenes-X-press under growth arrest to enzyme production in the normally growing *E. coli* BL21(DE3). The different temperatures were chosen to examine their effect on enzyme production and cell growth. The results are shown in Figure 1 (panels A and B; 30°C) and in the Supporting Information (Figure S3; 25°C). At 30°C, enGenes-X-press and *E. coli* BL21(DE3) showed similar growth until the time of induction (8 h). Whereas *E. coli* BL21(DE3) continued exponential growth afterwards (Figure 1B), the growth of enGenes-X-press was reduced to a very small amount, hence effectively switched off, at this point (Figure 1A). Its growth arrest notwithstanding, enGenes-X-press continued consumption of the glycerol carbon source similarly as the growing *E. coli* BL21(DE3) did (Figure 1A,B). The GmSusy production, measured as unit enzyme activity/g dry cell mass, was far superior in enGenes-X-press as compared to *E. coli* BL21(DE3). Both strains started from a similar specific activity of 20 U/g at the time of induction. While in *E. coli* BL21(DE3) the specific activity was constant in the induction phase, it increased almost linearly with time in enGenes-X-press and reached 115 U/g after 24 h. This represents a ~5-fold enhancement of specific activity compared to the reference. Cultivations at 25°C (Figure S3A,B; Supporting Information) gave only poor enzyme production, with an activity of just ~4 U/g in enGenes-X-press and ~1 U/g in *E. coli* BL21(DE3). The strain growth was still switched off reliably in enGenes-X-press through induction, but glycerol consumption was slow compared to *E. coli* BL21(DE3) in the phase post-induction. However, whereas clearly 25°C was not an option for GmSusy production, we show later that it was one for production of UGT71A15.

In Table 1 we summarize production parameters of the different bioreactor cultivations performed. In terms of enzyme activity/culture volume, the production in enGenes-X-press still improved (~2.5-fold) the reference production. However, decreased biomass formation by enGenes-X-press as compared to *E. coli* BL21(DE3) mitigated the effect of growth-arrested

production on the cell mass-based specific enzyme activity. We show later that enzyme production in high cell density fed-batch culture could effectively overcome this problem. Using the specific activity of the purified GmSuSy of 4.5 U/mg protein, comparable to earlier studies (Bungaruang, Gutmann, & Nidetzky, 2013), we calculate that production in enGenes-X-press at 30°C gave an overall enzyme yield of 156 mg/L culture. The corresponding production in *E. coli* BL21(DE3) gave 63 mg/L. These values are used together with measurements of total protein content/g cell dry weight and activity/g cell mass to estimate that the recombinant GmSuSy accounted for roughly ~5% and ~1% of total intracellular protein in enGenes-X-press and *E. coli* BL21(DE3), respectively.

### **3.3 Single gene expression for production of UGT71A15**

UGT71A15 was previously noted to be quite difficult to produce. In shake flask culture of *E. coli* BL21(DE3) about 1 - 5 mg protein/L was obtained (Lepak, Gutmann, Kulmer, & Nidetzky, 2015). The same series of bioreactor cultivations described above for GmSuSy were carried out with UGT71A15. The results are shown in Figure 1 (panels C and D; 25°C) and the Supporting Information (Figure S4, 30°C). Overall trends in biomass growth and glycerol consumption were similar as noted before. Production at 25°C was strongly preferred over production at 30°C, probably because UGT71A15 was not stable at the higher temperature. As observed for GmSuSy, the UGT71A15 was produced poorly in the growing *E. coli* BL21(DE3) (Figure 1D). There was only a small increase in specific enzyme activity in the phase after the induction. By contrast, UGT71A15 was formed efficiently in enGenes-X-press after the induction (Figure 1C). We note that the arrest of growth of enGenes-X-press was less clear-cut at 25°C (Figure 1C) than it was at 30°C (Figure 1A). A marked slow-down of growth was however observed after the induction (Figure 1C). Nonetheless, the effect of growth reduction on enzyme production was pronounced, as evident from comparing panels C and D in Figure 1. A ~4-fold increase in specific activity was thus achieved. The activity of 2.3 U/g cell mass obtained for

UGT71A15 was 50-fold lower than that obtained GmSuSy, reflecting roughly the differences in specific activity of the two enzymes as purified proteins. Parameters of the enzyme production are found in Table 1. The volumetric enzyme titer was 11 U/L culture when using enGenes-X-press, a 2.5-fold improvement compared to the reference strain. The specific activity of purified UGT71A15 is 0.5 U/mg. Translated into functionally expressed recombinant protein, therefore, the production yield was 21 mg/L of enGenes-X-press culture which can be compared to 8 mg/L of *E. coli* BL21(DE3) culture. In terms of abundance relative to total intracellular protein, values of ~1.0% and ~0.2% are calculated for enGenes-X-press and *E. coli* BL21(DE3), respectively.

### 3.3 Gene co-expression for production of UGT71A15 and GmSuSy

Considering the temperature requirements of UGT71A15 revealed in the single gene expression studies, co-expression of the GmSuSy and UGT71A15 genes was performed at 25°C. Time courses from bioreactor cultivations of enGenes-X-press and *E. coli* BL21(DE3) are shown in Figure S5 (Supporting Information). The profiles of growth and glycerol consumption of both strains producing the two glycosyltransferases (Figure S5) were highly similar as compared to their production of only UGT71A15 (Figure 1C,D). Upon induction, enGenes-X-press showed slow accumulation of both enzyme activities. The final specific activity (Table 1) was substantially lower (UGT71A15: 5-fold; GmSuSy: 8-fold) than in single gene expression cultures. Interestingly, the production of GmSuSy next to UGT71A15 was hardly detectable in *E. coli* BL21(DE3). Gene co-expression interfered with functional production of the individual enzymes and it did so in both enGenes-X-press and *E. coli* BL21(DE3). The volumetric titer of GmSuSy was decreased from 3.7 mg/L to 0.8 mg/L for enGenes-X-press and from 1.9 mg/L to 0.8 mg/L in the reference. For UGT71A15, titers dropped from 21.2 mg/L to 6.6 mg/L in enGenes-X-press and from 7.8 mg/L to 3.7 mg/L in the reference. At this stage, therefore, enzyme production through single gene expression would be preferable. Irrespective of the



possible incompatibility of GmSuSy and UGT71A15 for joint production in a single host, production under growth arrest in enGenes-X-press proved superior to production in growing *E. coli* BL21(DE3) under all conditions used (Table 1).

### 3.4 Downstream processing and characterization of GmSuSy

Protein quality is key in recombinant protein production. Although activity is the quintessential parameter of functional expression of the enzyme, it alone is not sufficient to inform about the overall quality of the recombinant glycosyltransferase production. We therefore isolated with Strep-Tactin affinity purification the GmSuSy produced in enGenes-X-press and *E. coli* BL21(DE3). The cell mass (~1 g dry matter each) from bioreactor cultures run for 24 h at 30°C (Figure 1A,B) was used. Target protein was recovered in a single sharp protein peak (Figure S6, Supporting Information). The protein yield after purification was 26.7 mg/g for enGenes-X-press and 5.6 mg/g for *E. coli* BL21(DE3). The specific activity of isolated GmSuSy (enGenes-X-press: 5.1 U/mg; *E. coli* BL21(DE3): 4.8 U/mg) was in line with previous report for GmSuSy produced in shaken flask culture of *E. coli* BL21(DE3) (Bungaruang, Gutmann, & Nidetzky, 2013). Analysis with SDS-PAGE (Figure S6) showed a low abundance of GmSuSy in the soluble fraction from cell disruption. Based on semiquantitative densitometry, ~10% of GmSuSy was present in the soluble fraction in enGenes-X-press while it was only ~2% in the reference.

### 3.5 Up-scaled fed-batch cultivation for production of GmSuSy

It was mentioned that, if volumetric enzyme titer is the parameter used for evaluation, the ~2-fold lower biomass yield in enGenes-X-press cultivations as compared to *E. coli* BL21(DE3) cultivations reduce the benefit of enzyme production under conditions of arrested growth. We addressed this problem for the case of GmSuSy concomitantly with assessing the translatability of the enzyme production in enGenes-X-press to a high cell density fed-batch cultivation at one

magnitude order larger scale (20 L). The important question was whether under these conditions the advantage of a ~5-fold higher enzyme activity/g cell mass would be retained without compromising the total biomass formation.

The fed-batch protocol (Figure S7, Supporting Information) gave a final biomass concentration of 56.0 g dry mass/L for enGenes-X-press and 67.5 g dry mass/L for *E. coli* BL21(DE3), a difference of just ~20% (Table 2). Based on protein purified from cell material (~1 g dry matter) thus received, we obtained 14.8 mg/g for enGenes-X-press and 5.0 mg/g for *E. coli* BL21(DE3), also qualitatively in line with SDS-PAGE (Figure S8). These numbers allow one to calculate a volumetric titer of GmSuSy which was 830 mg/L for the enGenes-X-press culture and 337 mg/L for the *E. coli* BL21(DE3) culture. The recombinant GmSuSy thus accounted for 1.5% of total intracellular protein in enGenes-X-press, for only 0.5% in the reference. The specific activity of the GmSuSy isolated from fed-batch production was in the range 0.5 – 2.1 U/mg, between 3 and 10-fold lower than the specific activities of enzyme isolated from batch bioreactor cultures.

We therefore subjected the enzyme obtained from Strep-Tactin purification to an additional step of size exclusion chromatography (SEC) on a Sephadex 200 column, as shown in Figure 2. Samples from both productions showed a protein peak corresponding in molecular size (350 – 400 kDa) to the functional GmSuSy tetramer. However, there was also material of larger size that represented protein agglomerates of an undefined degree. The two samples analyzed differed considerably regarding the relative content of such agglomerates. While in the sample from the *E. coli* BL21(DE3) culture the agglomerated protein exceeded in abundance by far the protein in its native size, the sample from the enGenes-X-press culture contained the GmSuSy tetramer as its main constituent.

Since the protein peaks in the SEC of the *E. coli* BL21(DE3) sample were baseline separated, they were collected as fraction I and II and further analyzed analytical SEC, as shown in Figure

S9 (Supporting Information). The fraction I did not elute from the column, probably because the agglomerates had already reached size limit for the SEC matrix. The analytical SEC of fraction II showed the expected tetrameric GmSuSy. We also determined the specific activity of the protein in each fraction and found none in fraction I and 4.7 U/mg in fraction II. By integrating the absorbance traces from the preparative SEC (Figure 2) we calculate after normalization that the portion of native tetramer in the enGenes-X-press sample was 65% whereas that in the *E. coli* BL21(DE3) was only 25% (Table 2).

Considering both the specific protein production/g cell mass and the quality of the protein thus made, we find that GmSuSy production in growth-arrested enGenes-X-press outperforms the reference production in growing *E. coli* BL21(DE3) by more than one magnitude order (12.2-fold; Table 2). In terms of improvement from batch to fed-batch culture, GmSuSy activity was increased from 285 U/L to 390 U/L for *E. coli* BL21(DE3). In enGenes-X-press, however, the increase was far more significant (3.3-fold), 700 U/L to 2300 U/L, in consequence of the enhanced biomass formation in the fed-batch as compared to the batch culture.

#### **4 CONCLUSION**

To advance bio-catalysis for small molecule glycosylation with plant glycosyltransferases, better process technologies for the recombinant production of these enzymes are required (e.g., Priebe, Daschner, Schwab, & Weuster-Botz, 2018; Schmieder et al., 2016). The problem is difficult due to the involvement of multiple process variables and the complex interrelationship these variables have with each other. A modularized approach able to interconnect molecular engineering strategies at the levels of the gene, the protein and the host organism is promising to make the development more predictable and faster. Focusing on *E. coli* as the production host, we show here that gene expression under arrested cell growth was highly effective for glycosyltransferase synthesis in enhanced yield and improved quality. Compared to the growing *E. coli* reference, the overall boost of enzyme production in enGenes-X-press exceeded

one order of magnitude. The total amount of functional enzyme (GmSuSy) produced in high-cell-density fed-batch culture at 20 L scale was 830 mg/L, surpassing common titers of plant glycosyltransferases in *E. coli* productions by 100-fold or more. The outstanding titer of 5.5 g/L for the glycosyltransferase from *Vitis vinifera* expressed in *E. coli* BL21(DE3) is clearly noted at this point (Priebe, Daschner, Schwab, & Weuster-Botz, 2018). With its effectiveness and scalability demonstrated in principle, the approach of enzyme production decoupled from cell growth might find further uses with different glycosyltransferases, and potentially other difficult-to-express proteins (see also: Chen, Walia, Mukherjee, Mahalik, & Summers, 2015; Gosh, Gupta, & Mukherjee, 2012; Mahalik, Sharma, & Mukherjee, 2014). Practical realization of approach in the strain enGenes-X-press thus represents a validated platform technology that offers flexible interconnection with gene and protein design strategies for enhanced recombinant protein production.

## **ACKNOWLEDGEMENTS**

This work was supported by the Federal Ministry of Economy, Family and Youth (BMWFJ), the Federal Ministry of Traffic, Innovation and Technology (BMVIT), the Styrian Business Promotion Agency, SFG, the Standortagentur Tirol and ZIT-Technology Agency of the City of Vienna through the COMET-Funding Programme managed by the Austrian Research Promotion Agency FFG. Financial support from the EU FP7 project SuSy (Sucrose Synthase as Effective Mediator of Glycosylation) is gratefully acknowledged. This work was also supported by the FFG “Basisprogramm” grant (No: 853135).

## **Conflict of interest statement**

J.M. is CEO of enGenes Biotech GmbH with an interest in the commercial exploitation of enGene-X-press technology for recombinant protein production.

## References

- Arend, J., Warzecha, H., Hefner, T., & Stöckigt, J. (2001). Utilizing genetically engineered bacteria to produce plant-specific glucosides. *Biotechnology and Bioengineering*, *76*, 126-131. doi:10.1002/bit.1152
- Bowles, D., Lim, E.-K., Poppenberger, B., & Vaistij, F. E. (2006). Glycosyltransferases of lipophilic molecules. *Annual Review of Plant Biology*, *57*, 567-597. doi:10.1146/annurev.arplant.57.032905.105429
- Bungaruang, L., Gutmann, A., & Nidetzky, B., (2013). Leloir glycosyltransferases and natural product glycosylation: biocatalytic synthesis of the C-glucoside nothofagin, a major antioxidant of redbush herbal tea. *Advanced Synthesis and Catalysis*, *355*, 2757–2763. doi:10.1002/adsc.201300251
- Cai, R., Chen, C., Li, Y., Sun, K., Zhou, F., Chen, K., & Jia, H. (2017). Improved soluble bacterial expression and properties of the recombinant flavonoid glucosyltransferase UGT73G1 from *Allium cepa*. *Journal of Biotechnology*, *255*, 9-15. doi:10.1016/j.jbiotec.2017.06.011
- Chen, R. (2018). Enzyme and microbial technology for synthesis of bioactive oligosaccharides: an update. *Applied Microbiology and Biotechnology*, *102*, 3017–3026. doi:10.1007/s00253-018-8839-2
- Chen, C.-C., Walia, R., Mukherjee, K. J., Mahalik, S., & Summers, D. K. (2015). Indole generates quiescent and metabolically active *Escherichia coli* cultures. *Biotechnology Journal*, *10*, 636-646. doi:10.1002/biot.201400381
- De Bruyn, F., Maertens, J., Beauprez, J., Soetaert, W., & De Mey, M. (2015). Biotechnological advances in UDP-sugar based glycosylation of small molecules. *Biotechnology Advances*, *33*, 288–302. doi:10.1016/j.biotechadv.2015.02.005
- Desmet, T., Soetaert, W., Bojarová, P., Křen, V., Dijkhuizen, L., Eastwick-Field, V. & Schiller, A. (2012). Enzymatic glycosylation of small molecules: challenging substrates require tailored catalysts. *Chemistry – A European Journal*, *18*, 10786-10801. doi:10.1002/chem.201103069
- Dewitte, G., Walmagh, M., Diricks, M., Lepak, A., Gutmann, A., Nidetzky, B., & Desmet, T. (2016). Screening of recombinant glycosyltransferases reveals the broad acceptor specificity of stevia UGT-76G1. *Journal of Biotechnology*, *233*, 49-55. doi:10.1016/j.jbiotec.2016.06.034
- Diricks, M., de Bruyn, F., van Deale, P., Walmagh, M., & Desmet, T. (2015). Identification of sucrose synthase in non-photosynthetic bacteria and characterization of the recombinant enzymes. *Applied Microbiology and Biotechnology*, *99*, 8465-8474. doi:10.1007/s00253-015-6548-7

- Gosh, C., Gupta, R., & Mukherjee, K. J. (2012). An inverse metabolic engineering approach for the design of an improved host platform for over-expression of recombinant proteins in *Escherichia coli*. *Microbial Cell Factories*, *11*, 93. doi:10.1186/1475-2859-11-93
- Hofer, B. (2016). Recent developments in the enzymatic O-glycosylation of flavonoids. *Applied Microbiology and Biotechnology*, *100*, 4269-4281. doi:10.1007/s00253-016-7465-0
- Hsu, T.M., Welner, D.H., Russ, Z.N., Cervantes, B., Prathuri, R.L., Adams, P.D., & Dueber, J.E. (2018). Employing a biochemical protecting group for a sustainable indigo dyeing strategy. *Nature Chemical Biology* *14*, 256-261. doi:10.1038/NCHEMBIO.2552
- Kim, B.G., Yang, S.M., Kim, S.Y., Cha, M.N., & Ahn, J.H. (2015). Biosynthesis and production of glycosylated flavonoids in *Escherichia coli*: current state and perspectives. *Applied Microbiology and Biotechnology*, *99*, 2979-2988. doi:10.1007/s00253-015-6504-6
- Lepak, A., Gutmann, A., Kulmer, S. T., & Nidetzky, B. (2015). Creating a water-soluble resveratrol-based antioxidant by site-selective enzymatic glucosylation. *ChemBioChem*, *16*, 1870–1874. doi:10.1002/cbic.201500284
- Liang, D-M., Liu, J.-H., Wu, H., Wang, B.-B., Zhu, H.-J., & Qiao, J.-J. (2015). Glycosyltransferases: mechanisms and applications in natural product development. *Chemical Society Reviews*, *44*, 8350-8374. doi:10.1039/c5cs00600g
- Lim, E.-K. (2005). Plant glycosyltransferases: their potential as novel biocatalysts. *Chemistry – A European Journal*, *11*, 5486-5494. doi:10.1002/chem.200500115
- Mairhofer, J., Wittwer, A., Cserjan-Puschmann, M., & Striedner, G. (2015). Preventing T7 RNA polymerase read-through transcription: a synthetic termination signal capable of improving bioprocess stability. *ACS Synthetic Biology* *4*, 265-273. doi:10.1021/sb5000115
- Mairhofer, J., Stargardt, P., Feuchtenhofer, L., Pontiller, J., Cserjan-Puschmann, M., Grabherr, R., & Striedner, G. (2016). Innovation without growth: non-growth associated recombinant protein production in *Escherichia coli*. *New Biotechnology*, *33*, Supplement, Page S26
- Mairhofer, J., Striedner, G., Grabherr, R., & Wilde, M. (2016). Uncoupling growth and protein production. WO2016/174195 A1
- Mahalik, S., Sharma, A. K., & Mukherjee, K. J. (2014). Genome engineering for improved recombinant protein expression in *Escherichia coli*. *Microbial Cell Factories*, *13*, 177. doi:10.1186/s12934-014-0177-1
- Mekler, V., Minakhin, L., Sheppard, C., Wigneshweraraj, S., & Severinov, K. (2011). Molecular mechanism of transcription inhibition by phage T7 gp2 protein. *Journal of Molecular Biology*, *413*, 1016-27. doi:10.1016/j.jmb.2011.09.029
- Nidetzky, B., Gutmann, A., & Zhong, C. (2018). Leloir glycosyltransferases as biocatalysts for chemical production. *ACS Catalysis*, *8*, 6283-6300. doi:10.1021/acscatal.8b00710

- Olsson, K., Carlsen, S., Semmler, A., Simon, E., Mikkelsen, M.D., & Møller, B.L. (2016). Microbial production of next-generation stevia sweeteners. *Microbial Cell Factories* 15, 207. doi:10.1186/s12934-016-0609-1
- Priebe, X., Daschner, M., Schwab, W., & Weuster-Botz, D. (2018). Rational selection of biphasic reaction systems for geranyl glucoside production by *Escherichia coli* whole-cell biocatalysts. *Enzyme and Microbial Technology*, 112, 79-87. doi:10.1016/j.enzmictec.2017.11.003
- Schmideder, A., Priebe, X., Rubenbauer, M., Hoffmann, T., Huang, F-C., Schwab, W., & Weuster-Botz, D. (2016). Non-water miscible ionic liquid improves biocatalytic production of geranyl glucoside with *Escherichia coli* overexpressing a glycosyltransferase. *Bioprocess and Biosystems Engineering*, 39, 1409-1414. doi:10.1007/s00449-016-1617-6
- Schmölzer, K., Gutmann, A., Diricks, M., Desmet, T., & Nidetzky B. (2015). Sucrose synthase: A unique glycosyltransferase for biocatalytic glycosylation process development. *Biotechnology Advances*, 34, 88-111. doi:10.1016/j.biotechadv.2015.11.003
- Schmölzer, K., Lemmerer, M., Gutmann, A., & Nidetzky, B. (2017). Integrated process design for biocatalytic synthesis by a Leloir glycosyltransferase: UDP-glucose production with sucrose synthase. *Biotechnology and Bioengineering*, 114, 924–928. doi:10.1002/bit.26204
- Schmölzer, K., Lemmerer, M., & Nidetzky, B. (2018). Glycosyltransferase cascades made fit for chemical production: integrated biocatalytic process for the natural polyphenol C-glucoside nothofagin. *Biotechnology and Bioengineering*, 115, 545–556. doi:10.1002/bit.26491
- Schwab, W., Fischer, T. & Wüst, M. (2015). Terpene glucoside production: Improved biocatalytic processes using glycosyltransferases. *Engineering in Life Sciences*, 15, 376-386. doi:10.1002/elsc.201400156
- Schwab, W., Fischer, T., Giri, A., & Wüst, M. (2015). Potential applications of glycosyltransferases in terpene glucoside production: impacts on the use of aroma and fragrance. *Applied Microbiology and Biotechnology*, 99, 165-74. doi:10.1007/s00253-014-6229-y
- Thuan, N.H., & Sohng, J.K. (2013). Recent biotechnological progress in enzymatic synthesis of glycosides. *Journal of Industrial Microbiology and Biotechnology*, 40, 1329-1356. doi:10.1007/s10295-013-1332-0
- Weiner, D. H., Shin, D., Tomaleri, G. P., DeGiovanni, A. M., Tsai, A. Y.-L., Tran, H. M., Hansen, S. F., Green, D. T., Scheller, H. V., & Adams, P. D. (2017). Plant cell wall glycosyltransferases: high-throughput recombinant expression screening and general requirements for these challenging enzymes. *PLoS ONE*, 12, e0177591. doi:10.1371/journal.pone.0177591

Xiao, J., Muzashvili, T. S., & Georgiev, M. I. (2014). Advances in the biotechnological glycosylation of valuable flavonoids. *Biotechnology Advances*, 32, 1145-1156.  
*doi:10.1016/j.biotechadv.2014.04.006*



## Tables

**Table 1.** Glycosyltransferase activities from batch bioreactor cultivations of enGenes-X-press and the *E. coli* BL21(DE3) reference

Glycosyltransferase	Construct	Induction temperature °C	Reference		enGenes-X-press		Fold increase <sup>c</sup>
			U/L <sup>a</sup>	U/g <sup>a</sup>	U/L <sup>a</sup>	U/g <sup>a</sup>	
GmSuSy	single	30	285	25	700	115	4.6
UGT71A15	single	30	0.3	0.0	1.4	0.2	8.9
GmSuSy	single	25	8.7	1.1	16.7	4.2	3.9
UGT71A15	single	25	3.9	0.5	10.6	2.3	4.4
GmSuSy <sup>b</sup>	double	25	3.5	0.5	3.7	0.7	1.6
UGT71A15 <sup>b</sup>	double	25	1.8	0.2	3.3	0.6	2.6

<sup>a</sup> Recorded at the end of the bioreactor cultivation; results are from biological duplicates or triplicates and agree within less 10% relative S.D.

<sup>b</sup> Activities measured individually

<sup>c</sup> Refers to U/g data

**Table 2.** Scaled-up production of GmSuSy in fed-batch bioreactor cultivation and recovery of the enzyme

<i>E. coli</i> strain	Biomass yield (g dry cells/L) <sup>a</sup>	Protein content (mg GmSuSy/g dry cells) <sup>a</sup>	Protein recovery (mAU × mL) <sup>b</sup>	SEC active fraction / total active enzyme (%) <sup>e</sup> / -fold <sup>f</sup>
enGenes-X-press	56	14.8	673 <sup>e</sup> (80) <sup>d</sup>	61 / 12.2
BL21(DE3) reference	68	5.0	226 <sup>e</sup> (15) <sup>d</sup>	26 / 1

<sup>a</sup> From the end of the bioreactor cultivation

<sup>b</sup> Relevant peak area (absorbance detection at 280 nm) in chromatography times the volume collected, <sup>c</sup> Strep-Tactin eluate and <sup>d</sup> eluate from preparative SEC

<sup>e</sup> Percentage of enzymatically active protein in eluate from analytical SEC

<sup>f</sup> Enhanced production of total active enzyme in enGenes-X-press as compared to the reference

## Figure legends

**Figure 1.** Time courses of growth, glycerol consumption and enzyme formation in batch bioreactor cultivations of enGenes-X-press (A,C) and *E. coli* BL21(DE3) (B,D) producing GmSuSy (A,B) and the glycosyltransferase UGT71A15 (C,D). The induction temperature was 30°C for GmSuSy production (A,B) and 25°C for UGT71A15 production (C,D). The symbols show: cell dry mass concentration, open triangles; glycerol concentration, full triangles; volumetric enzyme activity, full circles.

**Figure 2.** Protein quality analysis in GmSuSy produced in enGenes-X-press and *E. coli* BL1(DE3) by high cell density fed-batch cultivation. Absorbance traces of protein elution from Strep-Tactin affinity chromatography (A) and subsequent preparative SEC (B). The SEC trace reveals heterogeneity in both enzyme preparations, however, much less so in the preparation from production in enGenes-X-press. The peak at around 11 mL elution volume corresponds to the size expected for the native GmSuSy tetramer.

**Scheme 1.** Reaction of the glycosyltransferase UGT71A15 as used in this study and reaction of sucrose synthase (SuSy). Coupling of the SuSy reaction to the glycosyltransferase reaction allows for a glycoside synthesis with in situ regeneration of the UDP-glucose as donor substrate (for review, see: Nidetzky, Gutmann, & Zhong, 2018; Schmölzer, Gutmann, Diricks, Desmet, & Nidetzky, 2016; for coupled use of UGT71A15 and SuSy, see: Lepak, Gutmann, Kulmer, & Nidetzky, 2015).

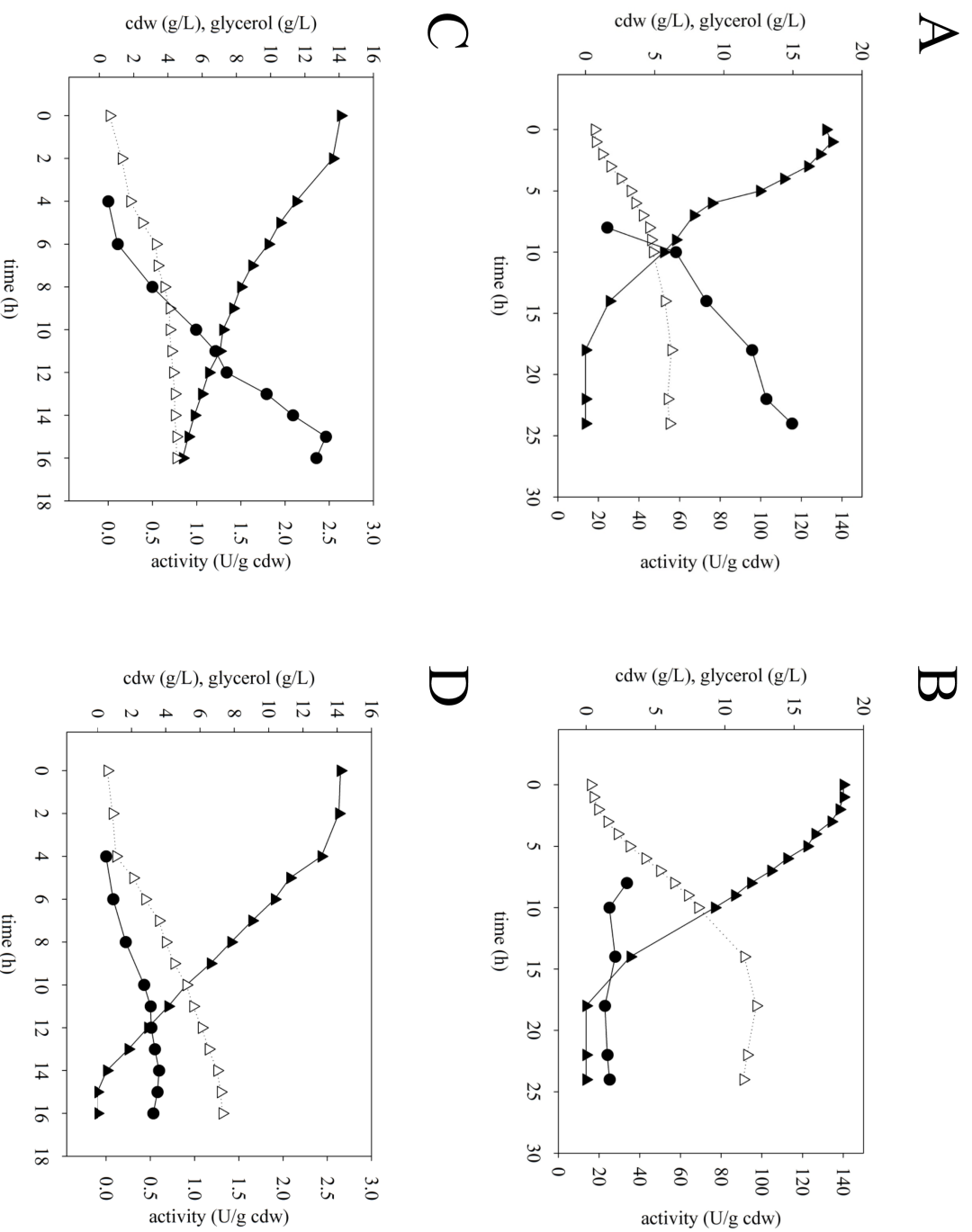


**Figure 1.** Time courses of growth, glycerol consumption and enzyme formation in batch bioreactor cultivations of enGenes-X-press (A,C) and

*E. coli* BL21(DE3) (B,D) producing GmSuSy (A,B) and the glycosyltransferase UGT71A15 (C,D). The induction temperature was 30°C for

GmSuSy production (A,B) and 25°C for UGT71A15 production (C,D). The symbols show: cell dry mass concentration, open triangles; glycerol concentration, full triangles; volumetric enzyme activity, full circles.

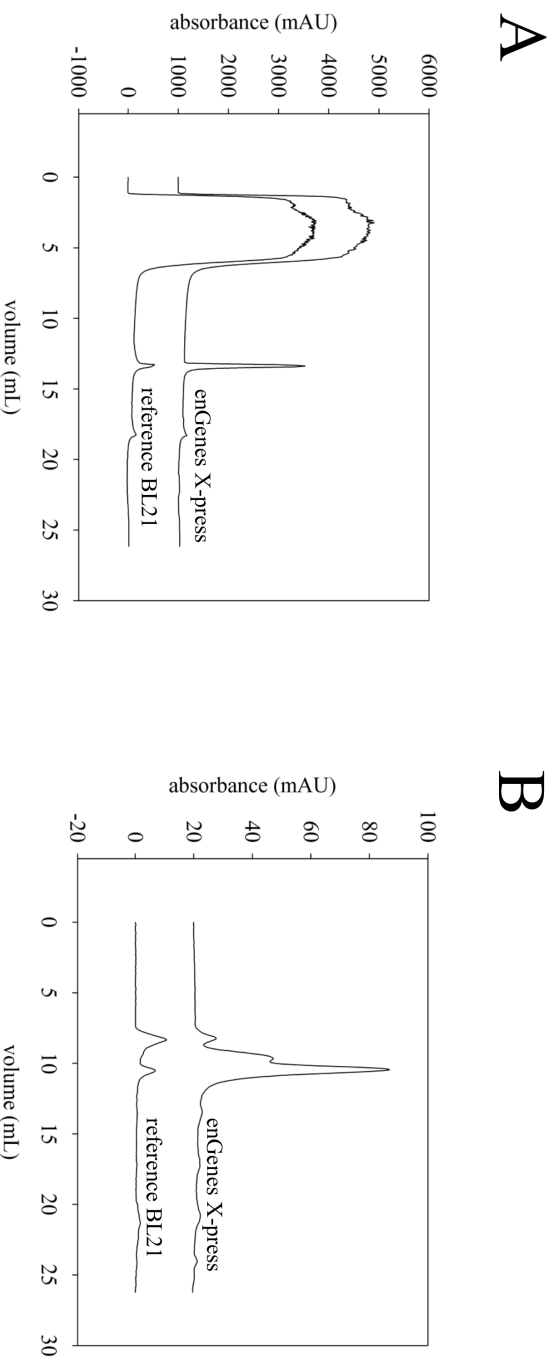
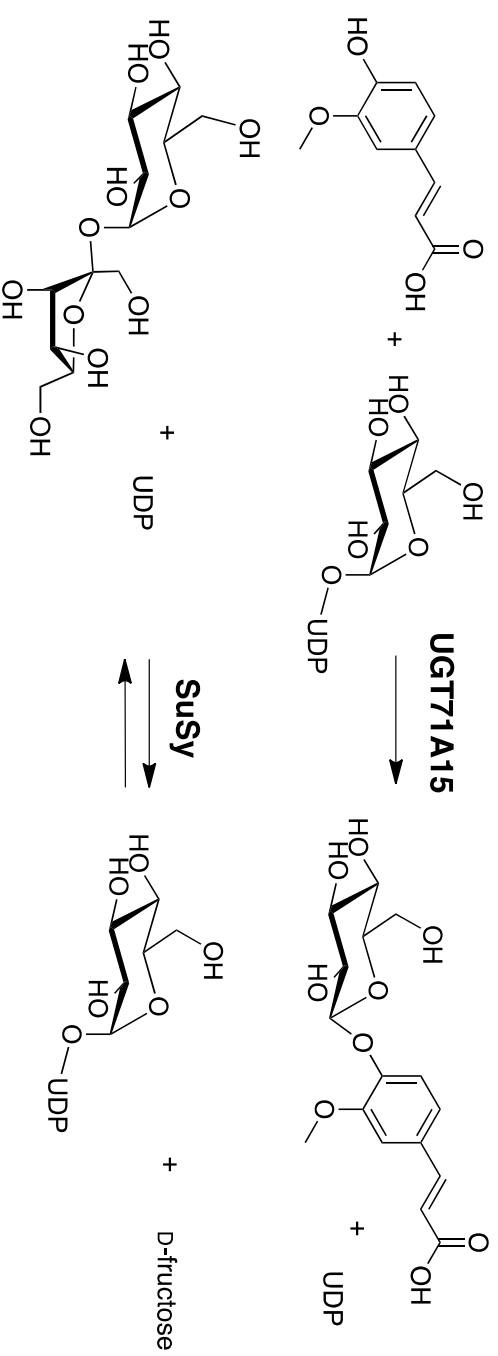


**Figure 2.** Protein quality analysis in GmSuSy produced in enGenes-X-press and *E. coli* BL1(DE3) by high cell density fed-batch cultivation. Absorbance traces of protein elution from Strep-Tactin affinity chromatography (A) and subsequent preparative SEC (B). The SEC trace reveals heterogeneity in both enzyme preparations, however, much less so in the preparation from production in enGenes-X-press. The peak at around 11 mL elution volume corresponds to the size expected for the native GmSuSy tetramer.



**Scheme 1.** Reaction of the glycosyltransferase UGT71A15 as used in this study and reaction of sucrose synthase (SuSy). Coupling of the SuSy reaction to the glycosyltransferase reaction allows for a glycoside synthesis with in situ regeneration of the UDP-glucose as donor substrate (for review, see: Nidetzky, Gutmann, & Zhong, 2018; Schmölzer, Gutmann, Diricks, Desmet, & Nidetzky, 2016; for coupled use of UGT71A15 and SuSy, see: Lepak, Gutmann, Kulmer, & Nidetzky, 2015).

## SUPPORTING INFORMATION

### **Decoupling of recombinant protein production from *Escherichia coli* cell growth enhances functional expression of plant Leloir glycosyltransferases**

Martin Lemmerer<sup>1</sup>, Jürgen Mairhofer<sup>2</sup>, Alexander Lepak<sup>3</sup>, Karin Longus<sup>3</sup>, Rainer Hahn<sup>4</sup>, Bernd Nidetzky<sup>1,3,\*</sup>

<sup>1</sup>Austrian Centre of Industrial Biotechnology (acib), Petersgasse 14, 8010 Graz, Austria

<sup>2</sup>enGenes Biotech GmbH, Mooslackengasse 17, 1190 Vienna, Austria

<sup>3</sup>Institute of Biotechnology and Biochemical Engineering, Graz University of Technology, NAWI Graz, Petersgasse 12/I, 8010 Graz, Austria

<sup>4</sup>Department of Biotechnology, University of Natural Resources and Life Sciences Vienna, Muthgasse 18, 1190 Vienna, Austria

**\*Corresponding author:** Bernd Nidetzky; e-mail: bernd.nidetzky@tugraz.at; phone: +43 316 873 8400; FAX: +43 316 873 8434

## Supporting methods

### Construction of the co-expression plasmid vector

The vector pETduo was derived from pET-STRP3 by inserting the UGT71A15 gene into the plasmid harboring the GmSusy gene. Two oligonucleotide primers (pDUO\_Ins\_fwd, pDUO\_Ins\_rev) were used.

pDUO\_Ins\_fwd: gatctcgatcccgcgaaattaatc

pDUO\_Ins\_rev: cagggcgcgtcccattcg

The receiving vector was linearized by amplification using two oligonucleotide primers, pETduo\_BB\_fwd and pETduo\_BB\_rev. Their use eliminated the F1 ORI in the vector.

pETduo\_BB\_fwd: ggacgcgcctgtggcacttttcggggaaatgt and

pETduo\_BB\_rev: gggatcgagatcttctccttcagcaaaaaaccct

### Fed-batch media and feed composition

*Semi-synthetic medium.* Media were prepared to enable production of 1580 g dry cells. The composition of the feed is given in relation to the unit mass (g) of cell dry mass 94.1 mg  $\text{KH}_2\text{PO}_4$ , 31.8 mg  $\text{H}_3\text{PO}_4$ , 41.2 mg  $\text{C}_6\text{H}_5\text{Na}_3\text{O}_7 \times 2\text{H}_2\text{O}$  (citric acid, trisodium salt), 45.3 mg  $(\text{NH}_4)_2\text{SO}_4$ . Compounds were dissolved in an 8 L feed volume. The other substrate components were added in relation to the grams of cell dry mass to be produced in the batch-phase (80 g): 46.0 mg  $\text{MgCl}_2 \times 6\text{H}_2\text{O}$ , 20.2 mg  $\text{CaCl}_2 \times 2\text{H}_2\text{O}$ , 50  $\mu\text{L}$  trace element solution (Table S2) and 3.3 g glucose  $\times \text{H}_2\text{O}$ . Initially, the batch medium (10 L) also contained yeast extract (0.15 g/g cell dry mass). Filter-sterilized kanamycin (50  $\mu\text{g}/\text{mL}$ ) and chloramphenicol (34  $\mu\text{g}/\text{mL}$ ) were added.

The substrate feed was controlled by increasing pump speed according to an exponential growth algorithm with superimposed feedback control of weight loss in the substrate tank. An



exponential growth rate ( $\mu = 0.111 \text{ h}^{-1}$ ) as held for 15 h. After the first 15 h of feeding, protein expression was induced (see the main text).

### **Sampling, cell disruption, protein purity and concentration**

*Sampling.* The cell growth was recorded as increase in OD<sub>600nm</sub>. Samples ( $2 \times 1 \text{ mL}$ ;  $2 \times 10 \text{ mL}$ ) were collected by centrifugation at 4°C for 30 min. Pellets were used for determination of cell dry mass. For batch cultivation, the residual glycerol concentration in the supernatant as determined by ion exchange HPLC and refractive index detection (see Methods in main text). Cells were harvested after 16 h and 24 h respectively by 30 min centrifugation (Sorvall RC-5B) at 4°C, 4420 g, re-suspended in deionized water to a concentration of  $\sim 100 \text{ g dry cells /L}$  and stored at -20°C.

*Cell disruption batch fermentation and preparation of sample for Strep-Tactin purification.* Cell disruption was performed at 50% amplitude for 1 min (1 s pulse on and 2 s pulse off) using a Sonic dismembrator (Ultrasonic Processor FB-505; Fisher Scientific, Vienna, Austria) equipped with a 3.1 mm micro-tip. Supernatant (cell-free extract) was collected after centrifugation at 21,130 g and 4°C for 30 min (Centrifuge 5424 R; Eppendorf, Vienna, Austria) and used for activity assay. For Strep-Tactin purification the same procedure was used and cell extract was additionally filtered through a 1.2  $\mu\text{m}$  filter prior to loading onto the column.

*Cell disruption fed batch fermentation.* Cell disruption was performed by re-suspending cells at a concentration of 50 g<sub>cdm</sub>/L in 20 mM Tris/HCl, 100 mM NaCl, pH 8.0 buffer and processing the suspension on a Panda 2000 high pressure homogenizer (GEA Westfalia, Oelde, Germany) for two passages at 700 bar. Cell debris was removed by centrifugation at 10,000 g at 4°C for 30 min in an Avanti JXN-26 centrifuge (Beckman Coulter, Vienna, Austria).

*Protein concentration and purity.* The BCA assay was used with bovine serum albumin (BSA) as the standard. Protein purity was determined by SDS-PAGE. Protein bands were stained with Coomassie Brilliant Blue and analyzed by densitometry.

## Supporting Tables

**Table S1. Composition of the medium used in batch bioreactor cultivations**

Component	Concentration (g/L)
K <sub>2</sub> HPO <sub>4</sub>	4.58
KH <sub>2</sub> PO <sub>4</sub>	3
tryptone	0.8
yeast extract	0.4
Na <sub>3</sub> -citrate·2H <sub>2</sub> O	2
MgSO <sub>4</sub> ·7H <sub>2</sub> O	0.8
CaCl <sub>2</sub> ·2H <sub>2</sub> O	0.08
Trace element solution	0.4 <sup>a</sup>
(NH <sub>4</sub> ) <sub>2</sub> SO <sub>4</sub>	3.6
NH <sub>4</sub> Cl	2.96
glycerol 98%	17.36

mL/L

**Table S2. Composition of the trace element solution**

Component <sup>a</sup>	Concentration (g/L)
FeSO <sub>4</sub> ·7H <sub>2</sub> O	40
MnSO <sub>4</sub> ·H <sub>2</sub> O	10
AlCl <sub>3</sub> ·6H <sub>2</sub> O	10
CoCl <sub>2</sub>	4
H <sub>3</sub> BO <sub>3</sub>	0.5
CuCl <sub>2</sub> ·2H <sub>2</sub> O	1
ZnSO <sub>4</sub> ·7H <sub>2</sub> O	2
Na <sub>2</sub> MoO <sub>4</sub> ·2H <sub>2</sub> O	2

<sup>a</sup> All components were dissolved in 5 M HCl.

## Supporting Figures

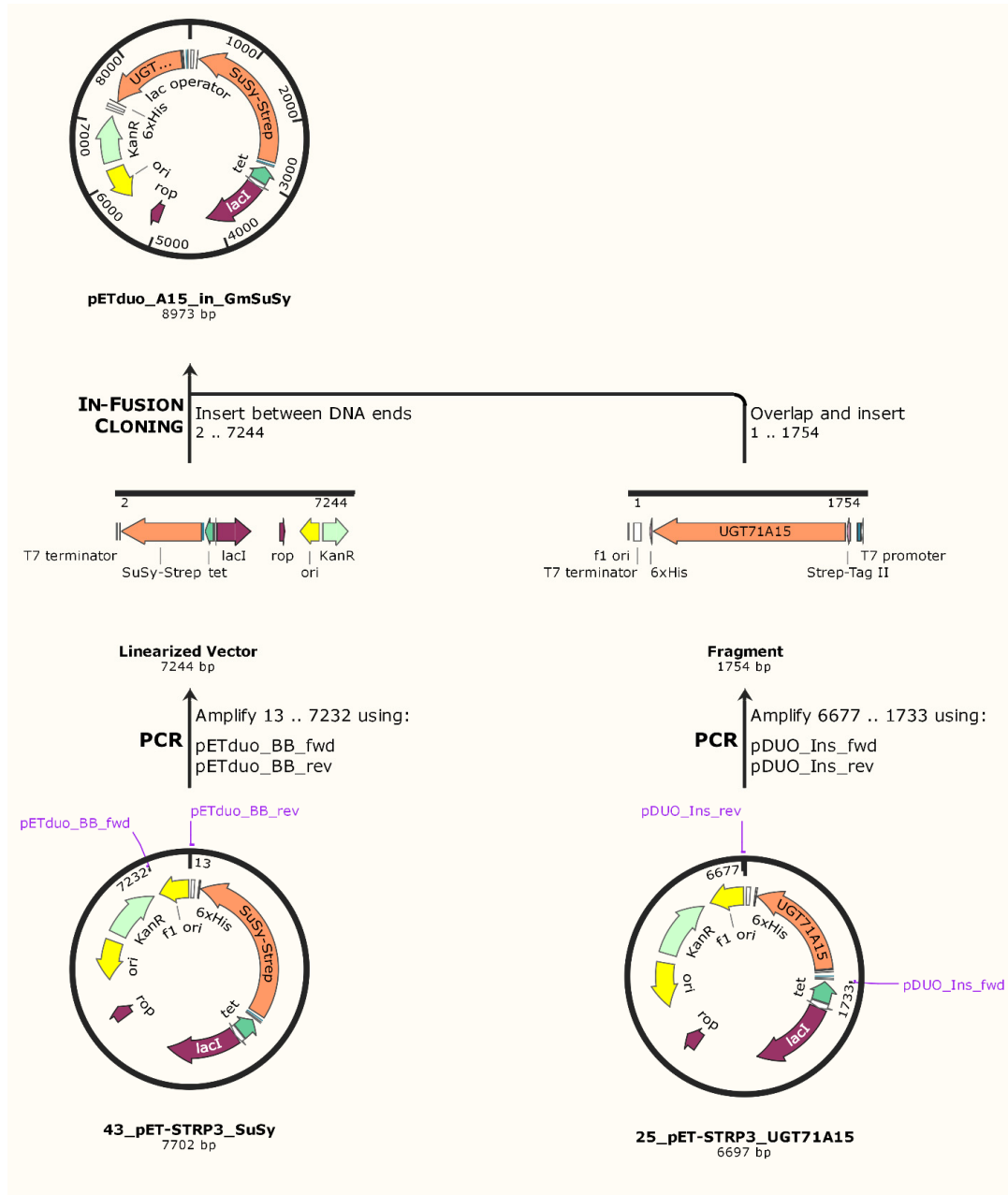


**Figure S1.** Construction of the enzyme co-expression vector by insertion of UGT71A15 gene into the pET plasmid vector harboring the GmSuSy gene.

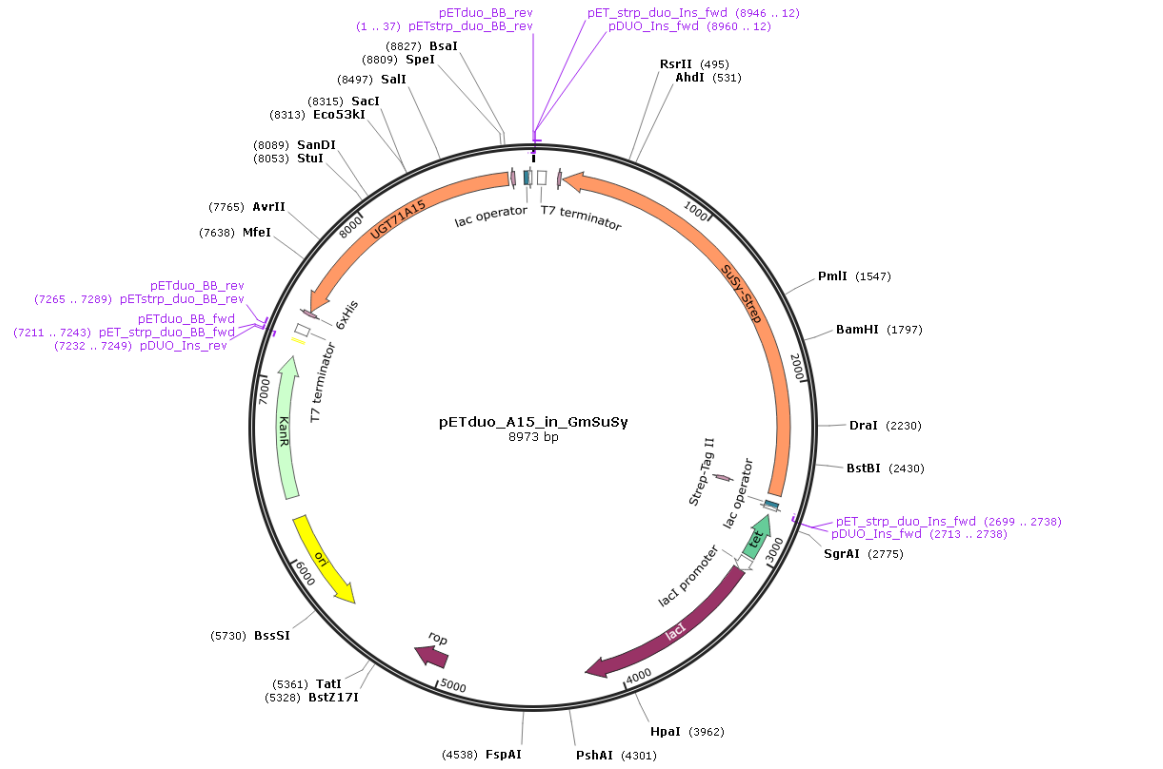
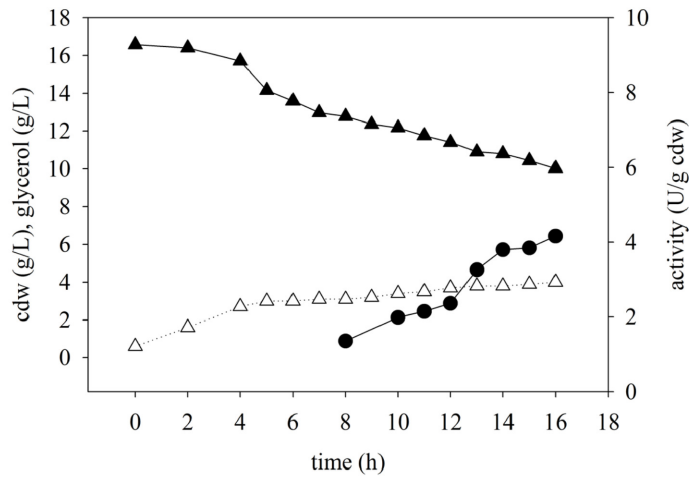


**Figure S2.** Vector map of the pET co-expression vector for production of UGT71A15 and GmSuSy.

A



B

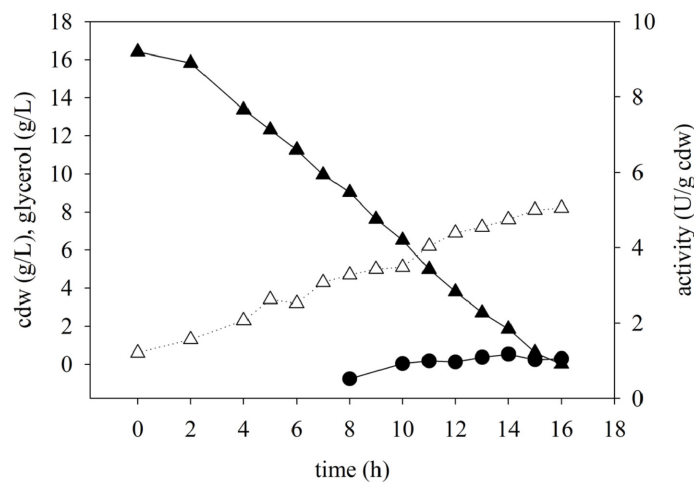
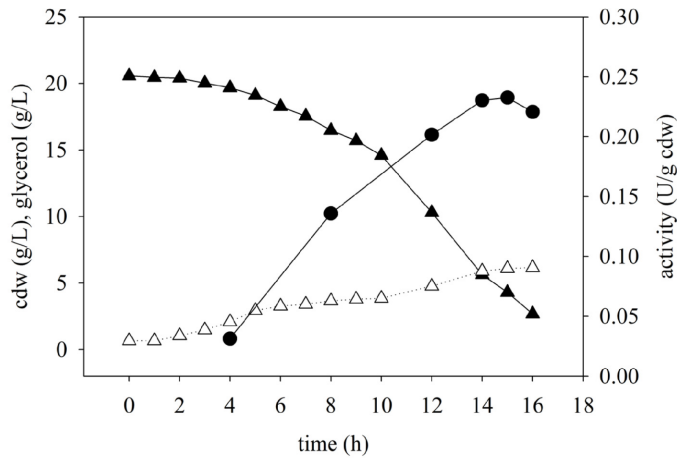


**Figure S3.** Time courses of growth, glycerol consumption and enzyme formation in batch bioreactor cultivations of enGenes-X-press (A) and *E. coli* BL21(DE3) (B) producing GmSuSy. The induction temperature was 25°C. The symbols show: cell dry mass concentration, open triangles; glycerol concentration, full triangles; volumetric enzyme activity, full circles.

A



B

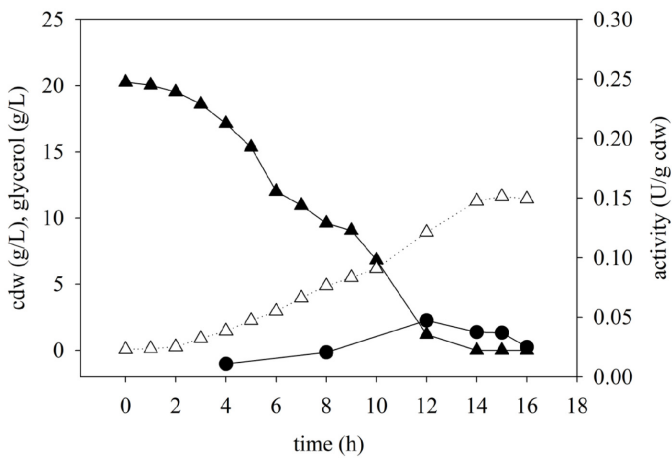
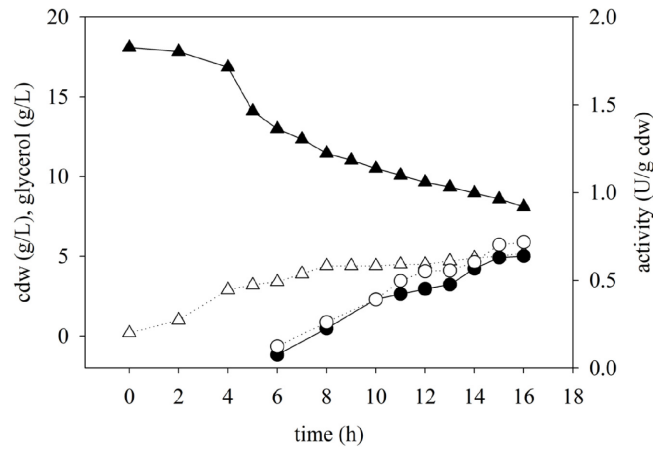


**Figure S4.** Time courses of growth, glycerol consumption and enzyme formation in batch bioreactor cultivations of enGenes-X-press (A) and *E. coli* BL21(DE3) (B) producing UGT71A15. The induction temperature was 30°C. The symbols show: cell dry mass concentration, open triangles; glycerol concentration, full triangles; volumetric enzyme activity, full circles.



A



B

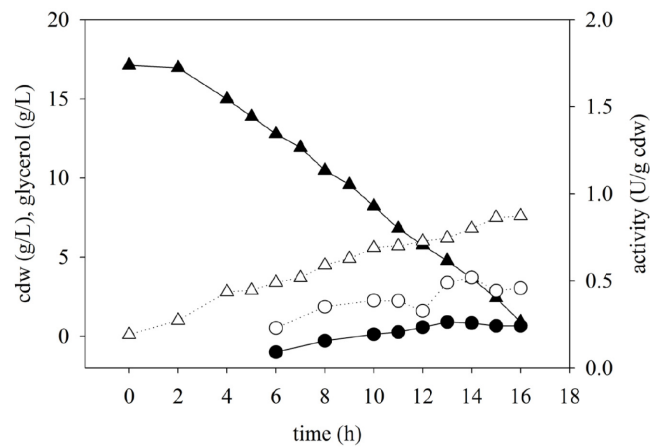
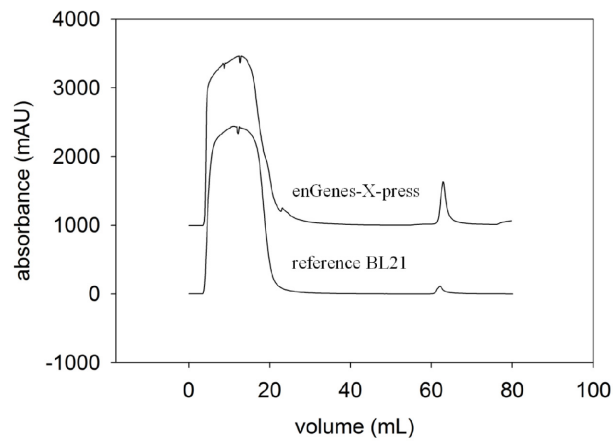


**Figure S5.** Time courses of growth, glycerol consumption and enzyme formation in batch bioreactor cultivations of enGenes-X-press (A) and *E. coli* BL21(DE3) (B) producing GmSuSy and UGT71A15. The induction temperature was 25°C. The symbols show: cell dry mass concentration, open triangles; glycerol concentration, full triangles; volumetric enzyme activity, full circles - UGT71A15, open circles - GmSuSy.

A



B

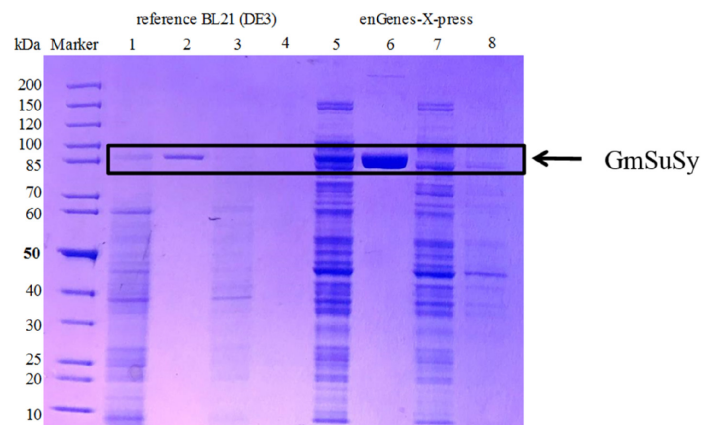


**Figure S6.** Purification of GmSuSy from cell material produced in batch bioreactor cultivations of enGenes-X-press and the *E. coli* BL21(DE3) reference. A: Absorbance traces of protein elution from Strep-Tactin affinity chromatography. B: Analysis by SDS PAGE; lanes 1 - 4 are fractions from purification of BL21(DE3) material, lanes 5 – 8 are from purification of enGenes-X-press material. Lanes 1 and 5, loading fraction; lanes 2 and 6, elution fraction; lanes 3 - 4 and 7 - 8 are flow through fractions.

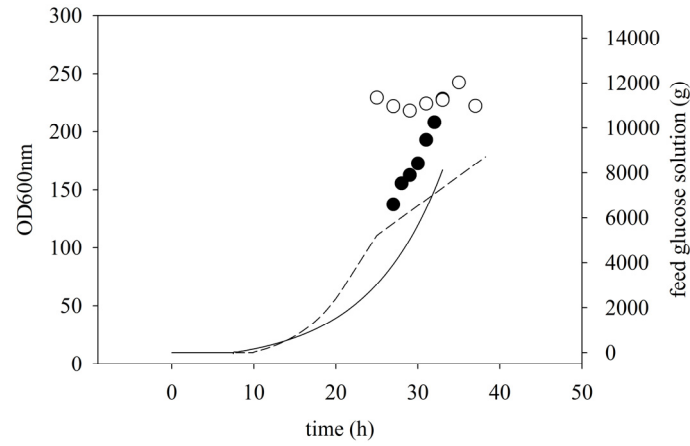


**Figure S7.** Time courses of fed-batch bioreactor cultivations of enGenes-X-press and *E. coli* BL21(DE3) for production of GmSuSy. Symbols show OD<sub>600nm</sub> measurements for enGenes-X-press (empty circles) and the BL21(DE3) reference (full circles) after induction. The dashed and the solid lines show the glucose feed for enGenes-X-press and the BL21(DE3) reference, respectively.

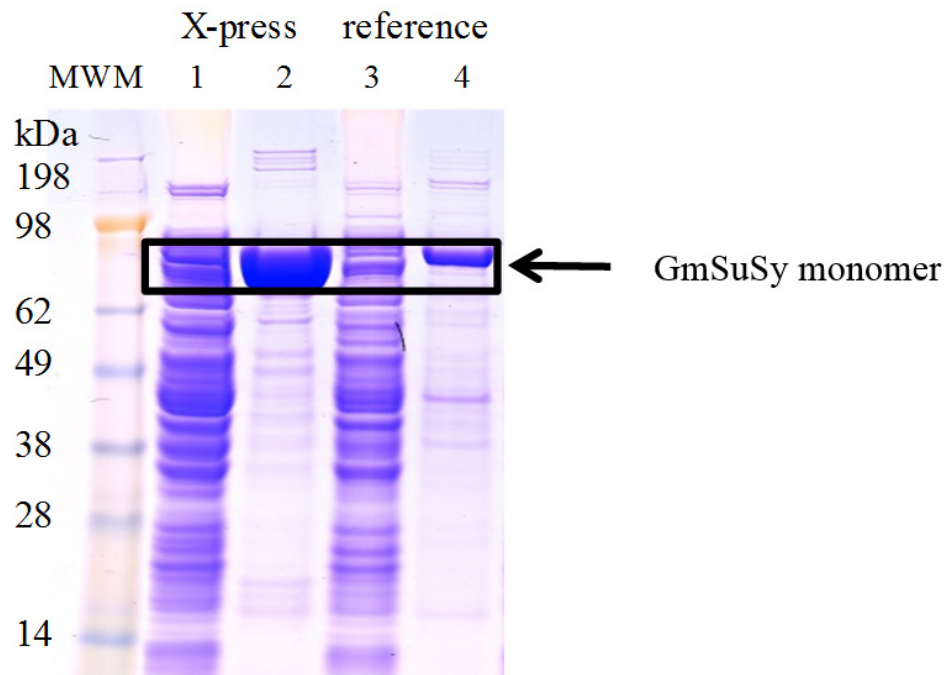
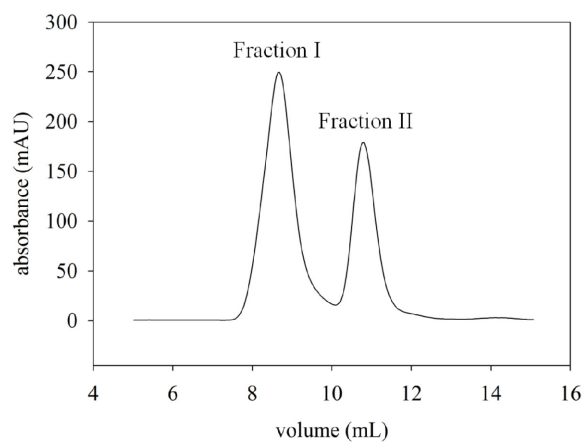


**Figure S8.** Analysis by SDS-PAGE of the Strep-Tactin column load and the eluting fraction derived from material produced with enGene-X-press and *E. coli* BL21(DE3) in fed-batch cultivation. Lanes 1 and 3 are the column loads; lanes 2 and 4 are eluting fractions. The arrow indicates the expected position of the GmSuSy monomer.

A



B

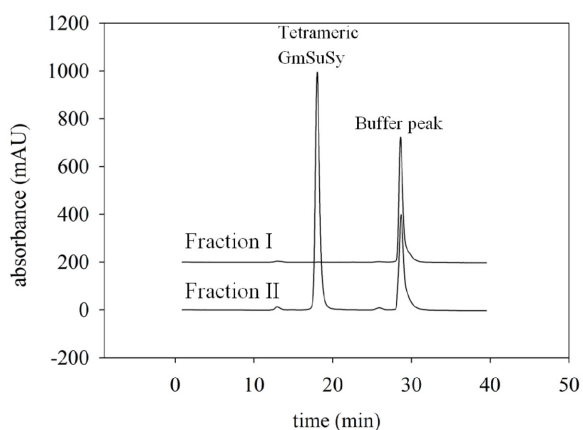


**Figure S9.** Fractionation of the GmSuSy eluate from Strep-Tactin purification using preparative SEC on a SD-200 column (A) and analysis of the SEC fractions thus obtained on an analytical size exclusion column (B). A: fractions I and fraction II represent agglomerated oligomeric and native (tetrameric) species of GmSuSy, respectively. B: Analytical SEC analysis of fractions I and II.

## Scientific record

### Publications

Lemmerer, M., Schmölzer, K., Gutmann, A., Nidetzky, B., 2016. Downstream Processing of Nucleoside-Diphospho-Sugars from Sucrose Synthase Reaction Mixtures at Decreased Solvent Consumption *Adv. Synth. Catal.* 358, 3113.

Schmölzer, K., Lemmerer, M., Gutmann, A., Nidetzky, B., 2017. Integrated process design for biocatalytic synthesis by a Leloir Glycosyltransferase: UDP-glucose production with sucrose synthase. *Biotechnol. Bioeng.* 114, 924–928.

Kulmer, S., Gutmann, A., Lemmerer, M., Nidetzky, B., 2017. Biocatalytic Cascade of Polyphosphate Kinase and Sucrose Synthase for Synthesis of Nucleotide-Activated Derivatives of Glucose. *Adv. Synth. Catal.* 359, 292.

Schmölzer, K., Lemmerer, M., Nidetzky, B., 2018. Glycosyltransferase Cascades Made Fit for Chemical Production: Integrated Biocatalytic Process for the Natural Polyphenol C-Glucoside Nothofagin. *Biotechnol. Bioeng.* 115, 545–556.

### Oral presentations

Lemmerer, M., Schmölzer, K., Gutmann, A., Nidetzky, B., 2017. Integrated process development for nucleotide sugar production. 21st Austrian Carbohydrate Workshop, Graz, Austria

Lemmerer, M., Schmölzer, K., Gutmann, A., Kuballa, J., Nidetzky, B., 2017. Integrated process design for biocatalytic synthesis by Leloir glycosyltransferases. 12th Carbohydrate Bioengineering Meeting, Vienna, Austria

### Poster presentations

Lemmerer, M., Schmölzer, K., Gutmann, A., Lepak, A., Nidetzky, B., 2015. Critical evaluation of different NDP-sugar purification strategies. 12th Biotrans, Vienna, Austria

Lemmerer, M., Schmölzer, K., Gutmann, A., Nidetzky, B., 2016. Downstream-processing of NDP-sugars from sucrose synthase reaction mixtures at decreased solvent consumption. 1<sup>st</sup> European Summit of Industrial Biotechnology, Graz, Austria